

FINAL REPORT

Development of Innovative Passive and Sustainable Treatment Technologies for Energetic Compounds in Surface Runoff on Active Ranges

Mark Fuller

Aptim Federal Sevices, LLC

Pei Chiu
University of Delaware

June 2024

This report was prepared under contract to the Department of Defense Strategic Environmental Research and Development Program (SERDP). The publication of this report does not indicate endorsement by the Department of Defense, nor should the contents be construed as reflecting the official policy or position of the Department of Defense. Reference herein to any specific commercial product, process, or service by trade name, trademark, manufacturer, or otherwise, does not necessarily constitute or imply its endorsement, recommendation, or favoring by the Department of Defense.

REPORT DOCUMENTATION PAGE

Form Approved OMB No. 0704-0188

The public reporting burden for this collection of information is estimated to average 1 hour per response, including the time for reviewing instructions, searching existing data sources, gathering and maintaining the data needed, and completing and reviewing the collection of information. Send comments regarding this burden estimate or any other aspect of this collection of information, including suggestions for reducing the burden, to Department of Defense, Washington Headquarters Services, Directorate for Information Operations and Reports (0704-0188), 1215 Jefferson Davis Highway, Suite 1204, Arlington, VA 22202-4302. Respondents should be aware that notwithstanding any other provision of law, no person shall be subject to any penalty for failing to comply with a collection of information if it does not display a currently valid OMB control number.

PLEASE DO NOT RETURN YOUR FORM TO THE ABOVE ADDRESS.

	t					
1. REPORT DATE (<i>DD-MM-YYYY</i>) 21/06/2024	2. REPORT TYPE SERDP Final Report	3. DATES COVERED (From - To) 7/10/2019 - 7/10/2024				
4. TITLE AND SUBTITLE		5a. CONTRACT NUMBER				
Development of Innovative Passive ar	nd Sustainable Treatment Technologies for Energetic	19-C-0	014			
Compounds in Surface Runoff on Acti		5h G	RANT NUMBER			
		J. 35. 31	ANT NOMBER			
		5c. PF	ROGRAM ELEMENT NUMBER			
6. AUTHOR(S)		5d. Pl	ROJECT NUMBER			
Mark Fuller		ER19-1				
Aptim Federal Sevices, LLC						
Det Obte		5e. TA	ASK NUMBER			
Pei Chiu University of Delaware						
Chiverenty of Belattare		5f. W0	ORK UNIT NUMBER			
7. PERFORMING ORGANIZATION N Aptim Federal Sevices, LLC	IAME(S) AND ADDRESS(ES)		8. PERFORMING ORGANIZATION REPORT NUMBER			
17 PrincessRd.						
Lawrenceville, NJ 08648-2301			ER19-1106			
9. SPONSORING/MONITORING AG			10. SPONSOR/MONITOR'S ACRONYM(S)			
	ry of Defense (Energy Resilience & Optimization)		SERDP			
3500 Defense Pentagon, RM 5C646 Washington, DC 20301-3500						
Washington, 20 2000 1 0000		11. SPONSOR/MONITOR'S REPORT NUMBER(S) ER19-1106				
12. DISTRIBUTION/AVAILABILITY S	STATEMENT					
DISTRIBUTION STATEMENT A. Appr	roved for public release: distribution unlimited.					
13. SUPPLEMENTARY NOTES						
10. 00. 1 222						
14. ABSTRACT						
	to develop a passive technology to treat military contamina	ants in act	ive testing and training range surface runoff.			
This project attempted to more fully cl	haracterize surface runoff from an active range to determi	ne the typ	ical contaminant profile. This was coupled with			
	at have the potential to enhance the sorption and degrada					
	both traditional biofilter materials such as peat moss, as					

15. SUBJECT TERMS

explosives, energetics, HMX, RDX, TNT, DNAN, NQ, NTO, perchlorate, sorption, bioremediation, range, contamination, stormwater

16. SECURITY CLASSIFICATION OF:			17. LIMITATION OF	18. NUMBER	19a. NAME OF RESPONSIBLE PERSON Mark Fuller			
a. REPORT	b. ABSTRACT	c. THIS PAGE	ABSTRACT	OF PAGES	IVIALK FULICI			
UNCLASS	UNCLASS	UNCLASS	UNCLASS	195	19b. TELEPHONE NUMBER (Include area code) 609-895-5348			

The sorbents were combined with slowrelease carbon sources to stimulate biological removal of the MC compounds. Bioaugmentation with known explosive degrading bacteria was also be evaluated. The developed technology was sustainable and compatible with ongoing range activities.

Abstract

Introduction and Objectives: Surface runoff represents a major potential mechanism through which energetics residues and related materials are transported off-site from range soils to groundwater and surface water receptors. This process is particularly important for energetics that are water-soluble (e.g., NTO and NQ) or generate soluble daughter products (e.g., DNAN and TNT). While traditional MC such as RDX and HMX have limited aqueous solubility, they also exhibit recalcitrance under most natural conditions.

The key objective of this project was to develop a passive technology to treat military contaminants in active testing and training range surface runoff. This project attempted to more fully characterize surface runoff from an active range to determine the typical contaminant profile. This was coupled with evaluation of a variety of materials that have the potential to enhance the sorption and degradation of munitions constituents (MC) in surface runoff. Sorbents and reactive media evaluated included both traditional biofilter materials such as peat moss, as well as more novel materials such as biochar, which has unique properties (e.g., high surface area, electron storage and shuttling capabilities) that was hypothesized to allow for more effective treatment of both legacy MC and newer insensitive munition constituents.

The sorbents were combined with slow-release carbon sources to stimulate abiotic and biological removal of the MC compounds. Bioaugmentation with known explosive degrading bacteria was also be evaluated.

Technical Approach: The technical objectives of this project were achieved through initial field sampling of surface runoff. Laboratory experiments conducted at multiple scales allowed identification of appropriate materials, and provided proof-of-concept results demonstrating a passive treatment technology for the effective mitigation of a broad range of range runoff contaminants. The following specific technical tasks were performed:

- Task 1. Characterize range surface runoff.
- Task 2. Batch sorption/degradation experiments.
- Task 3. Column sorption/degradation experiments and modeling.

This project concentrated on legacy energetics (e.g., 1,3,5-hexahydro-1,3,5-trinitro-1,3,5-triazine (RDX), 1,3,5,7-tetranitro-1,3,5,7-tetrazocane (HMX), etc.), insensitive munition constituents (e.g., 2,4-dinitroanisole (DNAN), 3-nitro-1,2,4-triazol-5-one (NTO), and nitroguanidine (NQ)), and ionic energetics (e.g., perchlorate), as well as potential associated non-explosive compounds present in stormwater runoff (e.g., waxes, binders, plasticizers).

Results: This project demonstrated that a combination of peat moss and cationized pine shavings could effectively remove dissolved energetics from solution, with slow-release carbon sources and biochar resulted in sustained (bio)degradation of several of the energetic compounds. Sorption combined with biodegradation was much more effective than sorption alone, with removal enhancement ranging from 2- to 25-fold compared to sorption only. The most recalcitrant energetic was NQ, although biochar appeared to enhance its overall removal.

Benefits: The technology developed during this project could be deployed within existing natural hydrologic features and is capable of sustained treatment of energetics laden runoff, while also complying with both operational range and habitat objectives. This technology could help DoD site managers to effectively address energetic contamination in surface runoff to mitigate off-site impacts to downstream receiving bodies.

Publications:

Fuller, M.E., Thakur, N., Hedman, P.C., Zhao, Y., Chiu, P.C., 2025. Combined sorption-biodegradation for removal of energetic compounds from stormwater runoff. Journal of Hazardous Materials 483, 136595.

Fuller, M.E., Farquharson, E.M., Hedman, P.C., Chiu, P., 2022. Removal of munition constituents in stormwater runoff: Screening of native and cationized cellulosic sorbents for removal of insensitive munition constituents NTO, DNAN, and NQ, and legacy munition constituents HMX, RDX, TNT, and perchlorate. Journal of Hazardous Materials 424, 127335.

Xin, D., Girón, J., Fuller, M.E., Chiu, P.C., 2022. Abiotic reduction of 3-nitro-1,2,4-triazol-5-one (NTO) and other munitions constituents by wood-derived biochar through its rechargeable electron storage capacity. Environmental Science: Processes & Impacts 24, 316-329.

Executive Summary

ES1. Background:

<u>Surface runoff characteristics and treatment approaches.</u> During large precipitation events, the rate of water deposition exceeds the rate of water infiltration, resulting in surface runoff (also called stormwater runoff). Land characteristics, including soil texture, presence of impermeable surfaces (natural and artificial), slope, and density and type of vegetation, all influence the amount of surface runoff from a given land area. The use of passive systems such as retention ponds and biofiltration cells for treatment of surface runoff is well established for urban and roadway runoff. Treatment may be achieved by directing runoff into and through a small constructed wetland, often at the outlet to a retention basin, or via filtration, directing runoff through a more highly engineered channel or vault containing the treatment materials. Filtration-based technologies have proven to be effective for the removal of metals, organics, and suspended solids (Sansalone, 1999; Deletic and Fletcher, 2006; Seelsaen et al., 2006; Grebel et al., 2016).

Surface runoff on ranges. Surface runoff represents a major potential mechanism through which energetics residues and related materials are transported off-site from range soils to groundwater and surface water receptors. This process is particularly important for energetics that are watersoluble (e.g., NTO and NQ) or generate soluble daughter products (e.g., DNAN and TNT). While traditional MC such as RDX and HMX have limited aqueous solubility, they also exhibit recalcitrance under most natural conditions. RDX and perchlorate are frequent groundwater contaminants on military training ranges. In a previous small study, MC were detected in surface runoff from an active live-fire range (Fuller, 2015), and more recent sampling has detected MC in marsh surface water adjacent to the same installation (personal communication). Another recent report from Canada also detected RDX in both surface runoff and surface water at low part per billion levels in a survey of several military demolition sites (Lapointe et al., 2017). However, overall, data regarding the contaminant profile of surface runoff from ranges are very limited, and non-energetic constituents (e.g., metals, binders, plasticizers) in runoff have not been examined. Additionally, while contaminated surface runoff is an important concern, mitigation technologies have not yet been developed or widely deployed. To effectively capture and degrade compounds that are present in surface runoff, novel treatment media are needed to sorb a broad range of energetic materials and to transform the retained compounds through abiotic and/or microbial processes.

Surface runoff of organic and inorganic contaminants from live fire ranges is a challenging issue for the Department of Defense (DoD). Potentially even more problematic is the fact that inputs to surface waters from large testing and training ranges are from multiple sources, often encompassing hundreds of acres. No technologies are currently effective for controlling non-point energetics-laden surface runoff. While numerous technologies exist to treat collected explosives residues, and contaminated soil and groundwater, the decentralized nature and sheer volume of range runoff precludes their use on site.

<u>Innovative range runoff treatment technology.</u> Previous research demonstrated that a peat-based system provided a natural and sustainable sorptive medium for organic explosives such as HMX, RDX, and TNT (Fuller et al., 2004; Hatzinger et al., 2004; Fuller et al., 2005; Schaefer et al., 2005; Fuller et al., 2009), allowing much longer residence times than predicted from hydraulic loading

alone. Peat moss represents a bioactive environment for treatment of the target contaminants. While the bulk microbial reactions are aerobic due to the presence of measurable dissolved oxygen, anaerobic reactions (including methanogenesis) are able to occur in microsites. As noted, the peat-based substrate acts not only as a long term source of reducing equivalents but also as a strong sorbent. This is important in intermittently loaded systems in which a large initial pulse of MC can be temporarily retarded on the peat matrix and then slowly degraded as they desorb (Schaefer et al., 2005; Fuller et al., 2009). This increased residence time enhances the biotransformation of energetics, and promotes the immobilization and further degradation of breakdown products. Abiotic reactions associated with the organic-rich peat are also likely enhanced (e.g., via electron shuttling reactions of humics) (Roden et al., 2010).

During previous work (ESTCP ER-0434), modeling indicated that peat moss amended with crude soybean oil would significantly reduce the flux of dissolved TNT, RDX, and HMX through the vadose zone to groundwater compared to a non-treated soil. The technology was validated in field soil plots, showing a greater than 500-fold reduction in the flux of dissolved RDX from macroscale Composition B detonation residues compared to a non-treated control plot (Fuller et al., 2009). Laboratory testing and modeling indicated that the addition of soybean oil increased the biotransformation rates of RDX and HMX at least 10-fold compared to rates observed with peat moss alone (Schaefer et al., 2005). Subsequent experiments also demonstrated the effectiveness of the amended peat moss material for stimulating perchlorate transformation when added to a highly contaminated soil (Fuller et al., unpublished data). These previous data clearly demonstrate the effectiveness of peat-based materials for mitigating transport of both organic and inorganic energetic compounds through soil to groundwater.

Recent reports have highlighted additional materials that, alone, or in combination with electron donors such as peat moss and soybean oil, may further enhance the sorption and degradation of surface runoff contaminants, including both legacy energetics and IHE. For instance, biochar, a type of black carbon, has been shown to not only sorb a wide range of organic and inorganic contaminants including MCs (Ahmad et al., 2014; Mohan et al., 2014; Xie et al., 2015; Oh et al., 2018), but also facilitate their degradation (Oh et al., 2002b; Ye and Chiu, 2006; Oh and Chiu, 2009; Xu et al., 2010; Oh et al., 2013; Xu et al., 2013). Depending on the source biomass and pyrolysis conditions, biochar can possess a high specific surface area (on the order several hundred m²/g (Zhang and You, 2013; Gray et al., 2014)) and hence a high sorption capacity. Biochar and other black carbon also exhibit especially high affinity for nitroaromatic compounds (NACs) including TNT and 2,4-dinitrotoluene (DNT) (Sander and Pignatello, 2005; Zhu et al., 2005; Zhu and Pignatello, 2005)). This is due to the strong π - π electron donor-acceptor interactions between electron-rich graphitic domains in black carbon and the electron-deficient aromatic ring of the NAC (Zhu et al., 2005; Zhu and Pignatello, 2005). These characteristics make biochar a potentially effective, low-cost, and sustainable sorbent for removing MC and other contaminants from surface runoff and retaining them for subsequent degradation in situ.

Furthermore, black carbon such as biochar can promote abiotic and microbial transformation reactions by facilitating electron transfer. That is, biochar is not merely a passive sorbent for contaminants, but a redox mediator for their degradation. Biochar can promote contaminant degradation through two different mechanisms: electron conduction and electron storage (Sun et al., 2017). First, the microscopic graphitic regions in biochar can sorb contaminants like NACs

strongly, as noted above, and also conduct reducing equivalents such as electrons and atomic hydrogen to the sorbed contaminants, thus promoting their reductive degradation. This catalytic process has been demonstrated for TNT, DNT, RDX, HMX, and nitroglycerin (Oh et al., 2002a; Oh et al., 2004, 2005; Oh and Chiu, 2009; Xu et al., 2010), and is expected to occur also for IHE including DNAN and NTO. This is one of the hypotheses we will test during this project.

Second, biochar contains in its structure abundant redox-facile functional groups such as quinones and hydroquinones, which are known to accept and donate electrons reversibly. Depending on the biomass and pyrolysis temperature, certain biochar can possess a rechargeable electron storage capacity (i.e., reversible electron accepting and donating capacity) on the order of several mmol e⁻/g (Klüpfel et al., 2014; Prévoteau et al., 2016; Xin et al., 2018). This means, when "charged", biochar can provide electrons for either abiotic or biotic degradation of reducible compounds such as MC. The abiotic reduction of DNT and RDX mediated by biochar has been demonstrated (Oh et al., 2013), and we expect similar reactions to occur for DNAN and NTO as well.

Moreover, recent studies have shown that the electron storage capacity of biochar is also accessible to microbes. For example, soil bacteria such as *Geobacter* and *Shewanella* species can utilize oxidized (or "discharged") biochar as an electron acceptor for the oxidation of organic substrates such as lactate and acetate (Kappler et al., 2014; Saquing et al., 2016), and reduced (or "charged") biochar as an electron donor for the reduction of nitrate (Saquing et al., 2016). This is significant because, through microbial access of stored electrons in biochar, contaminants that do not sorb strongly to biochar can still be degraded.

Similar to nitrate, perchlorate and other relatively water-soluble energetic compounds (e.g., NTO and NQ) may also be similarly transformed using reduced biochar as an electron donor. Unlike other electron donors, biochar can be recharged through biodegradation of organic substrates (Saquing et al., 2016) and thus can serve as a long-lasting sorbent and electron repository in soil. Similar to peat moss, the high porosity and surface area of biochar not only facilitate contaminant sorption but creates anaerobic/reducing microsites in its inner pores, where reductive degradation of energetic compounds can take place. The ability/efficacy of biochar to promote both abiotic and biotic reduction of IHE and perchlorate will be evaluated in this proposed study.

Another potential sorbent for range contaminants in surface runoff are modified celluloses. Results presented at the 2017 SERDP Symposium showed that cellulose triacetate evidenced enhanced sorption of both legacy TNT and more water soluble IHE like DNAN (L. Gurtowski, Poster 303) compared to other biopolymers including cellulose, chitin, or chitosan. In contrast, chitin and unmodified cellulose were predicted by Density Function Theory methods to be favorable for absorption NTO and NQ, as well as the legacy explosives (Todde et al., 2018). A substantial body of work has shown that modified cellulosic biopolymers can also be effective sorbents for removing metals from solution (Burba and Willmer, 1983; Brown et al., 2000; O'Connell et al., 2008; Wan Ngah and Hanafiah, 2008), and will likely be applicable for some of the metals that may be found in surface runoff at ranges.

Based on the properties of the target compounds, a combination of materials would yield the best results. This project was undertaken to build on the previous findings, as well as to identify other novel materials, resulting in a practical solution for treating contaminated surface runoff.

During the proposed project, additional and/or alternative components to enhance the attenuation of legacy MC as well as newer IHE constituents (and associated nonenergetic compounds, as applicable) in surface runoff. *The key questions that were addressed during this project include:*

- What are the types and concentrations of range contaminants present in range surface runoff?
- What sustainable and economical materials can be used to sorb and/or degrade range contaminants in surface runoff?
- Can biochar enhance the abiotic and biotic degradation of legacy and insensitive munitions constituents, as well as enhance microbial degradation of more soluble energetics (e.g., perchlorate, NTO, NQ)?
- Can biological degradation of range contaminants in surface runoff be enhanced by bioaugmentation with specific degradative organisms?

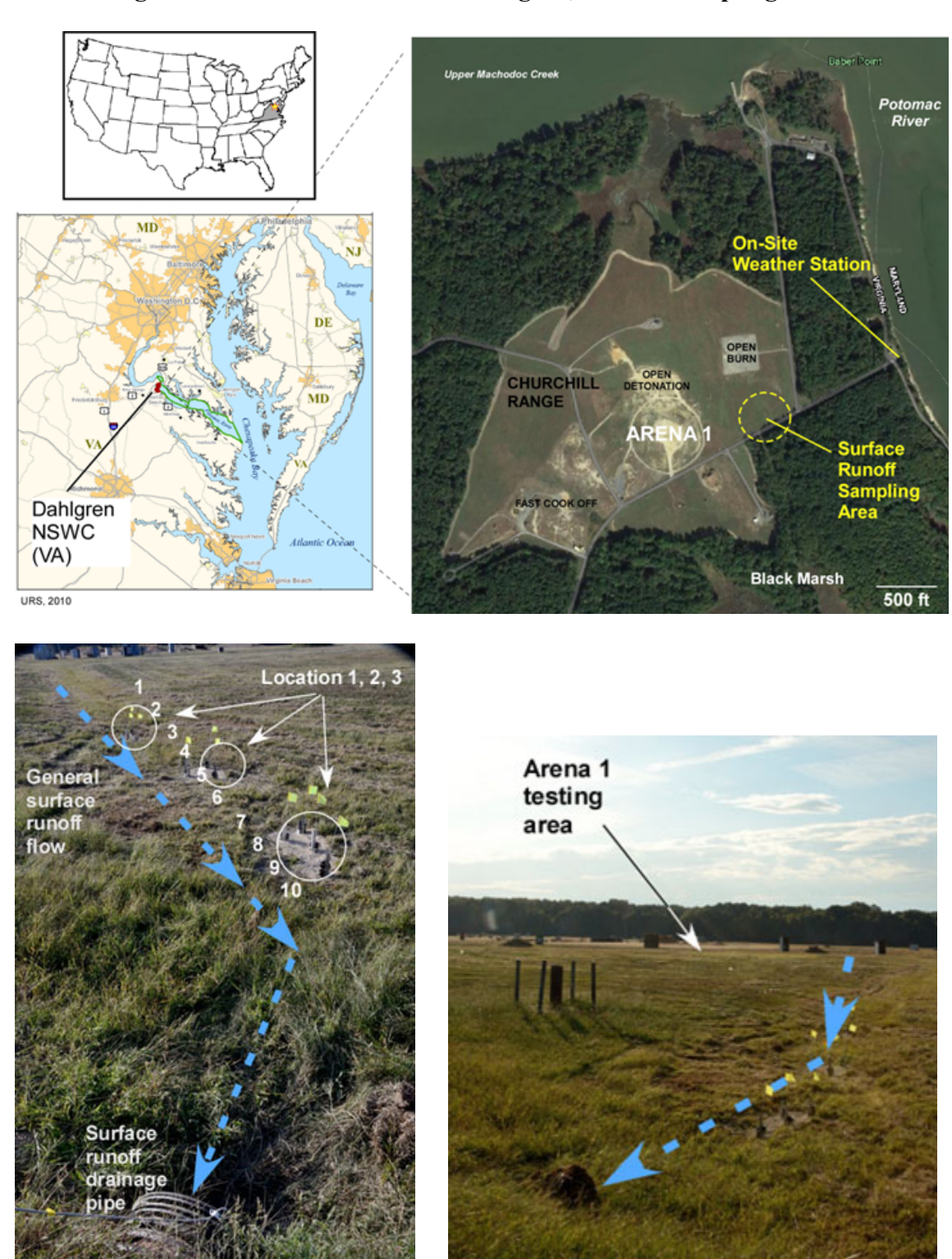
The treatment technology developed during this project could be translated to the field as part of an integrated surface runoff control plan. This would include some means to direct and collect surface runoff from an MC impacted area in a temporary retention basin. The basin would allow settling of undissolved contaminants and other solids. The outflow of the basin would then pass through the treatment material before being released into the receiving body.

ES2. Materials and Methods:

The technical approach for this project consisted of initial field sampling and laboratory experiments at multiple scales to identify, optimize, and provide proof-of-concept results demonstrating a passive treatment technology for the effective mitigation of a broad range of range runoff contaminants. Methods and results are summarized below, with more details provided in the corresponding sections of the full report.

<u>Surface Runoff Characterization</u>. Surface runoff was collected from NSWC Dahlgren's main testing area periodically over three years as precipitation events allowed. The site location and sampling area are shown in Figure E-1. Samples were analyzed for both legacy and insensitive munition constituents, perchlorate, metals, and other non-energetic compounds (e.g., binders, waxes, plasticizers).

Figure E-1. Location of NSWC Dahlgren, VA and sampling area.



<u>Evaluation of Novel Sorbents for Legacy and Insensitive Munition Energetics</u>. Several native and modified materials were examined for their ability to sorb legacy and insensitive munition constituents, as well as perchlorate. Materials included peat moss for the neutral charged organic

explosive compounds, and various amine-modified cellulosic polymers for perchlorate and negatively charged NTO. Batch multipoint isotherms were conducted with peat moss and cationized pine shavings (CAT pine), which consisted of a mixture of seven dissolved energetics (HMX, RDX, TNT, NQ, NTO, DNAN, ClO₄⁻) and the solid sorbent materials. The experiments were sampled over time and analyzed for energetic compounds, and the data was modeled to derive sorption coefficients and sorption capacity estimates.

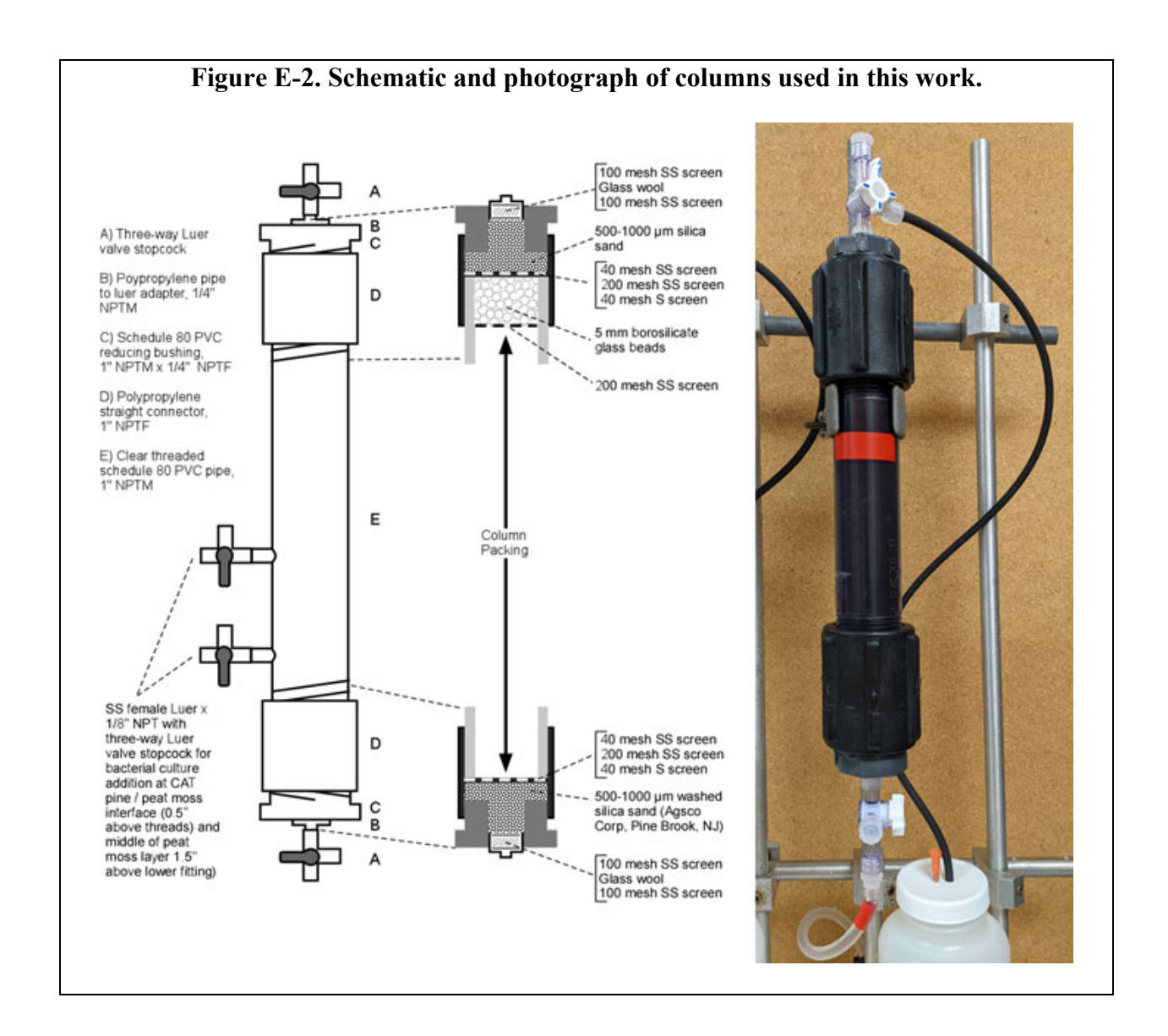
Evaluation of Slow-Release Carbon Sources for Biodegradation of Legacy and Insensitive Munition Energetics. The ability of various biodegradable biopolymers to support the biodegradation of legacy and insensitive munition constituents, as well as perchlorate, was evaluated. Information on the biopolymers examined are listed in Table E-1. The biopolymers were evaluated for their ability to support biodegradation of energetic compounds under both aerobic and anoxic/anaerobic conditions using pure bacterial culture of known explosive-degrading strains as well as anoxic/anaerobic energetics-degrading enrichments. Batch experiments consisted of dissolved energetics in the presence and absence of the various biopolymers, and sterile controls were also included. The experiments were sampled over time and analyzed for energetic compounds.

Table E-1. Slow-release carbon source information.

Material	Description	Source	Notes
PLA6	polylactic acid	Goodfellow	high MW thermoplastic polyester
PLA80	polylactic acid	Goodfellow	low MW thermoplastic polyester
PHB	polyhydroxybutyrate	Goodfellow	bacterial biopolyester
PCL	polycaprolactone	Sarchem Labs	biodegradable polyester
BioPBS	polybutylene succinate	Mitsubishi Chemical Performance Polymers	bio-based product; compostable
SEFA SP10	sucrose ester of fatty acids	Sisterna	food and cosmetic additive
SEFA SP70	sucrose ester of fatty acids	Sisterna	food and cosmetic additive

Evaluation of Biochar for Abiotic and Biotic Degradation of Legacy and Insensitive Munition Energetics. The ability of biochar to sorb and abiotically reduce legacy and insensitive munition constituents, as well as biochar's use as an electron donor for microbial biodegradation of energetic compounds was examined. Batch experiments consisted of dissolved energetics in the presence and absence of biochar, with various experiments focused on air-oxidized, chemically-reduced, and microbially-reduced biochar. The experiments were sampled over time and analyzed for energetic compounds.

Column Study Evaluation of Combined Sorption/Biodegradation of Legacy and Insensitive Munition Energetics. The final phase of the project consisted of column experiments to assess the removal of dissolved energetics via sorption/biodegradation/abiotic transformation under dynamic flow conditions. Columns (PVC, 1" ID x 6" length) were packed with the various materials (sorbents, slow-release biopolymer carbon sources, microbial cultures, biochar) identified in the previous tasks. A schematic and illustration of the columns is shown in Figure E-2. A constant flow of dissolved explosives was introduced into the columns in an upflow direction, and the effluent from each column was directed into a fraction collector. Influent and effluent samples were analyzed for energetic compounds and associated breakdown products. The data was analyzed and modeled to derive sorption capacity estimates.



ES3. Results and Discussion:

<u>Surface Runoff Characterization</u>. A total of six sampling events occurred over the course of the project. The dates of these events were: October 2019, January 2020, June 2020, November 2020, July 2021, and November 2022. The detections of dissolved energetics in surface runoff are shown in Table 2-4. No energetics were detected when filtered solids were extracted. Using the detected concentrations of HMX, RDX, and ClO₄ from the January 2020 sampling event multiplied by the corresponding volume of runoff, the mass loadings into Black Marsh from surface runoff were ~0.1 g for perchlorate, 0.429 g for RDX, and to almost 0.837 g for HMX.

There were no detections of heavy metals above drinking water standards, nor were there any detections of non-energetic compounds (binders, waxes, plasticizers).

These results indicate that there was sporadic detections of energetics in the surface runoff at NSWC Dahlgren, although total loadings could be close to 1 g during a single event.

Table E-2. Summary of energetics concentrations detected in surface runoff.

1	TOTAL (m	g/kg)			
PQL >>	0.04	0.04	0.05	0.5 -	6.5*
Sample Date	HMX	RDX	CIO ₄	HMX	RDX
October 2019	-	-	0.4 ± 0.0	-	-
January 2020	5.9	1.7 ± 1.3	0.8 ± 0.6	-	-
June 2020	-	-	-	-	-
November 2020	-	-	-	-	-
July 2021	-	-	0.4 ± 0.6	-	-
November 2022	-	-	-	-	-

⁻ below PQL

<u>Evaluation of Novel Sorbents for Legacy and Insensitive Munition Energetics</u>. Peat moss proved to be an effective sorbent for DNAN, while various cationized cellulosic materials sorbed NTO to varying degrees (Figure E-3). Sorption isotherm parameters for the full suite of energetics with peat moss and CAT pine are presented in Table E-3. None of the materials tested significantly removed NQ from solution.

These data indicated that a combination of peat moss and CAT pine would be required to effectively remove both insensitive and legacy MC from aqueous solution (excluding NQ).

^{*} PQL varied based on mass of solids > 0.7 µm recovered for extraction

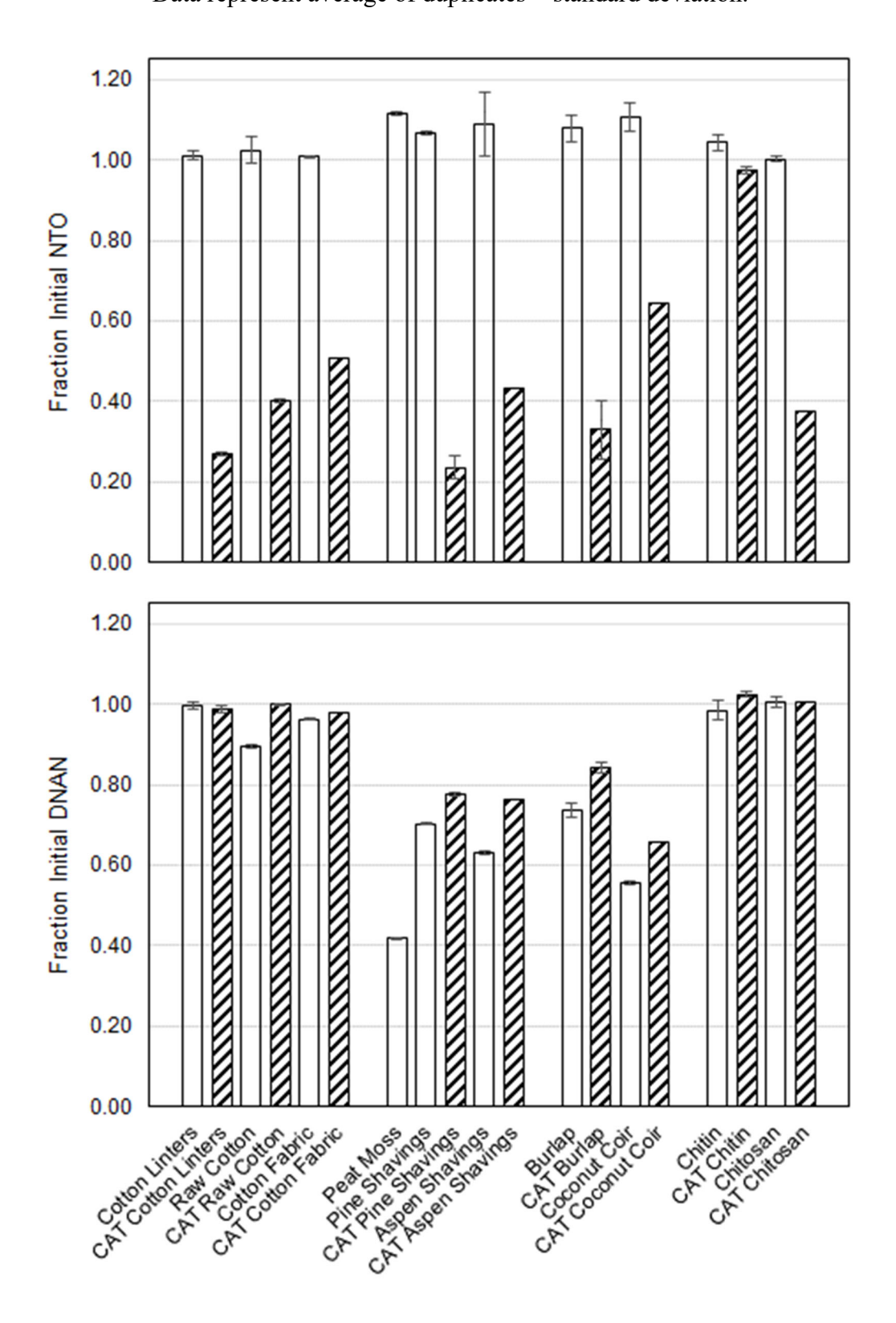
Table E-3. Freundlich and Langmuir adsorption parameters for insensitive and legacy explosives.

		HMX		RDX						
		K _f	n	r ²	K _f	n	r ²	K _f	n	r²
Freundlich	Peat	0.08 ± 0.00	1.70 ± 0.18	0.91	0.11 ± 0.02	2.75 ± 0.63	0.69	1.21 ± 0.15	2.78 ± 0.67	0.81
	CAT Pine	-	-	-	-	-	-	1.02 ± 0.04	4.01 ± 0.44	0.93
	CAT Burlap	-	-	-	-	-	-	0.36 ± 0.02	1.59 ± 0.09	0.98
	CAT Cotton	-	-	-	-	-	-	-	-	-
		q _m (mg/g)	b (L/mg)	r ²	q _m (mg/g)	b (L/mg)	r ²	q _m (mg/g)	b (L/mg)	r ²
Langmuir	Peat	0.29 ± 0.04	0.39 ± 0.09	0.93	0.38 ± 0.05	0.23 ± 0.08	0.69	3.63 ± 0.18	0.89 ± 0.13	0.97
_	CAT Pine	-	-	-	-	-	-	1.26 ± 0.06	0.76 ± 0.10	0.97
	CAT Burlap	-	-	-	-	-	-	-	-	-
	CAT Cotton	-	_	-	-	-	-	-	-	-

a No successful model fit

		NTO			DNAN			CIO4		
		K _f	n	r²	K _f	n	r ²	K _f	n	r ²
Freundlich	Peat	.*			0.38 ± 0.05	1.71 ± 0.20	0.89			-
	CAT Pine	0.94 ± 0.05	1.61 ± 0.11	0.97	0.01 ± 0.01	0.70 ± 0.13	0.76	1.54 ± 0.06	2.42 ± 0.16	0.97
	CAT Burlap	0.41 ± 0.05	2.43 ± 0.41	0.82				0.53 ± 0.03	2.42 ± 0.26	0.92
	CAT Cotton	0.26 ± 0.06	2.53 ± 0.76	0.57			-			-
		q _m (mg/g)	b (L/mg)	r ²	q _m (mg/g)	b (L/mg)	r²	q _m (mg/g)	b (L/mg)	r ²
Langmuir	Peat	-	-	-	2.57 ± 0.33	0.13 ± 0.03	0.92	-	-	-
	CAT Pine	4.07 ± 0.26	0.30 ± 0.04	0.99				3.63 ± 0.18	0.89 ± 0.13	0.97
	CAT Burlap	1.29 ± 0.12	0.36 ± 0.08	0.89	-	-	-	1.26 ± 0.06	0.76 ± 0.10	0.97
	CAT Cotton	0.83 ± 0.15	0.30 ± 0.15	0.58						

Figure E-3. Removal of dissolved NTO (top) and DNAN (bottom). Data represent average of duplicates \pm standard deviation.



<u>Evaluation of Slow-Release Carbon Sources for Biodegradation of Legacy and Insensitive Munition Energetics</u>. Aerobic RDX and NQ degradation by pure bacterial cultures was supported by several of the biopolymers (Figures E-4 and E-5).

These results indicated that combining bioaugmentation with these bacterial cultures with addition of the slow-release carbon sources PHB, PCL, and BioPBS would be effective for biodegrading the mixture of energetics that were going to be tested in the column experiments.

Figure E-4. Aerobic RDX degradation by Gordonia KTR9 and Rhodococcus DN22 in the presence of slow-release carbon source biopolymers.

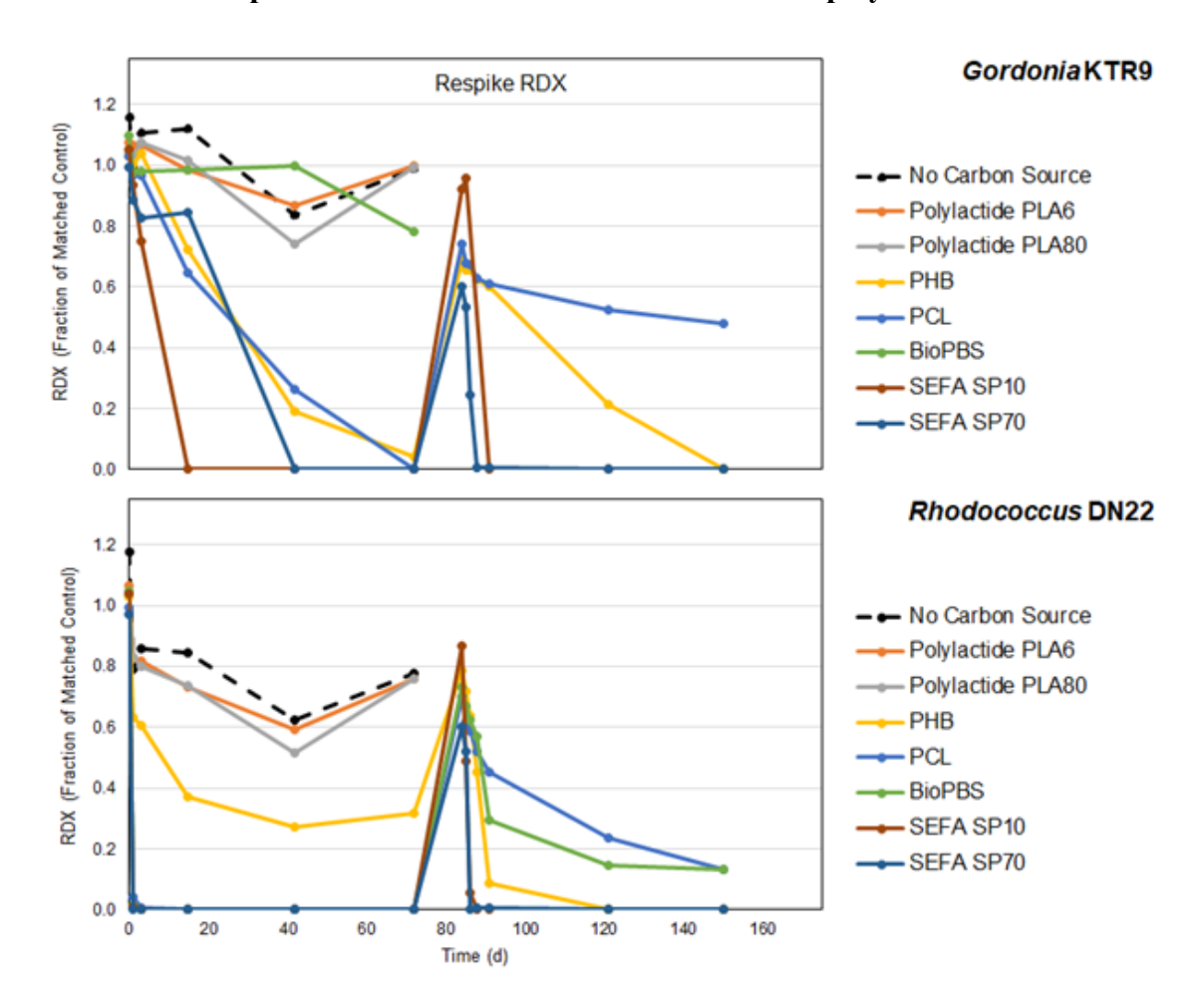


Figure E-5. Aerobic NQ degradation by *Pseudomonas* NQ5 in presence of slow-release carbon source biopolymers.

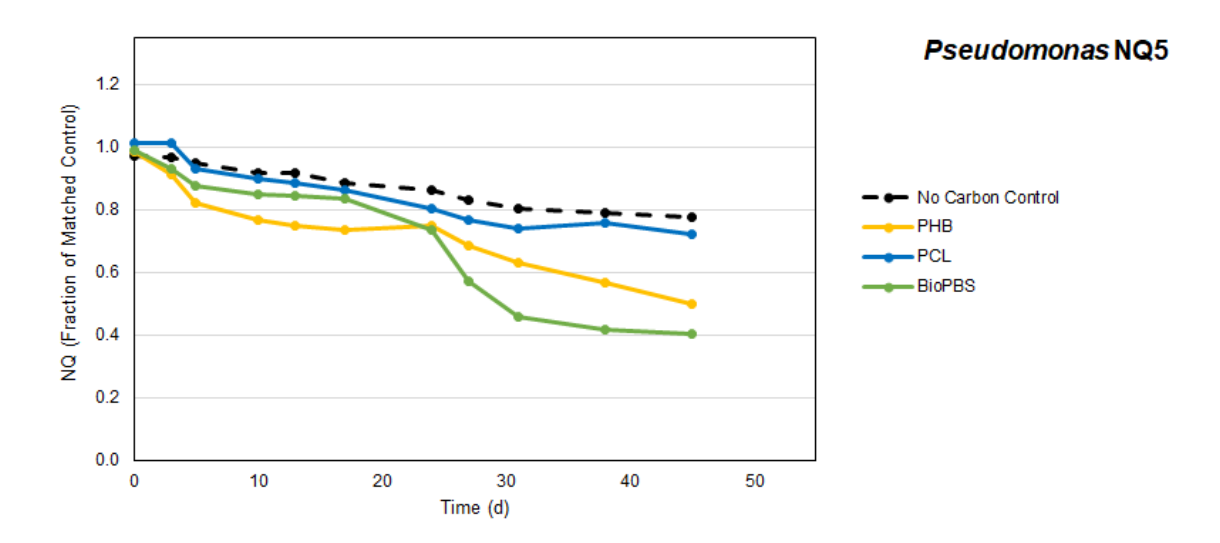
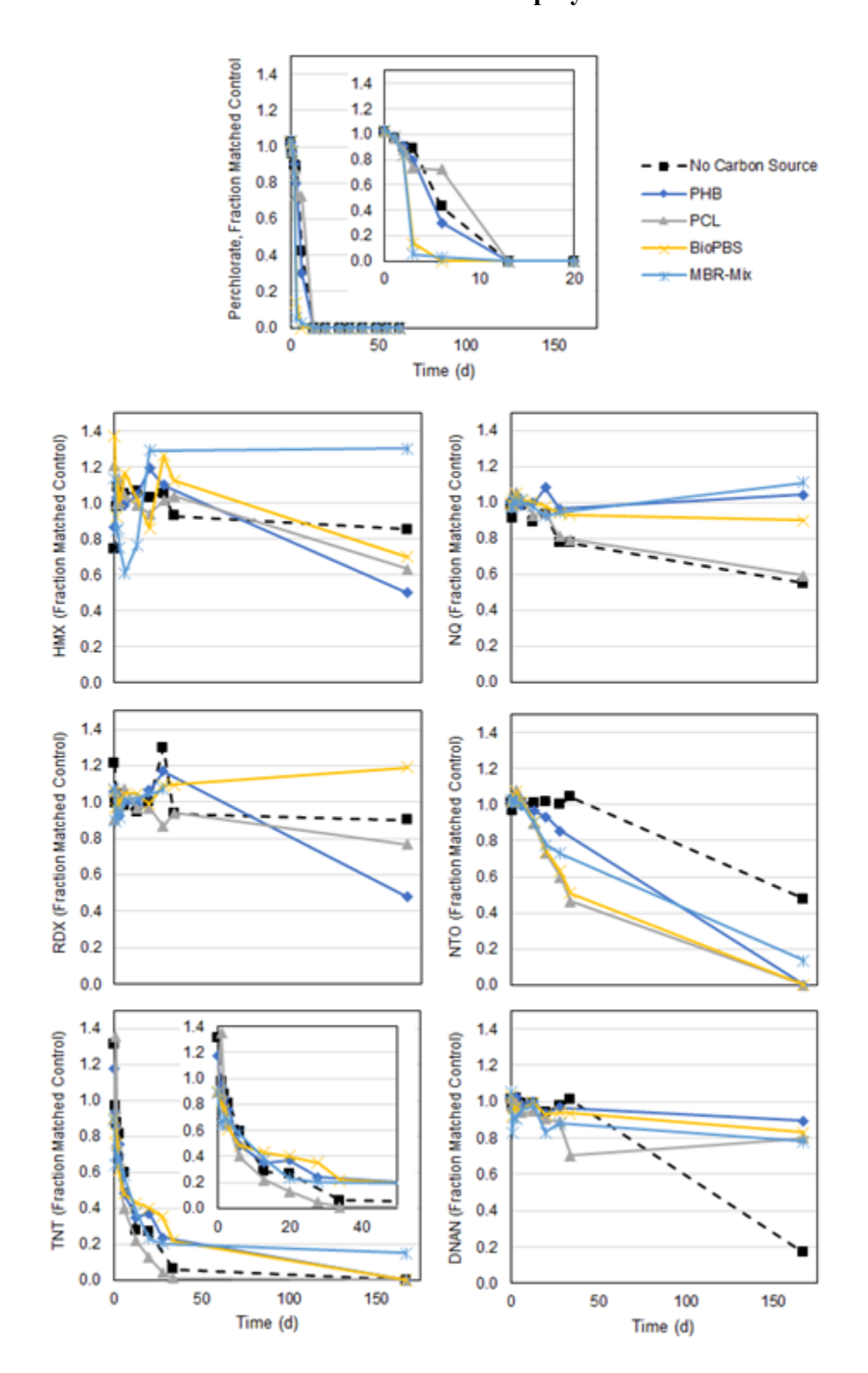


Figure E-6. Anoxic degradation of energetics by MBR mixed culture in presence of slow-release carbon source biopolymers.



Evaluation of Biochar for Abiotic and Biotic Degradation of Legacy and Insensitive Munition Energetics. The sorption parameters of biochar for selected energetics is presented in Table E-4. Of the compounds tested, DNAN sorption was the greatest, followed by RDX, with minimal sorption of NTO and NQ.

Chemically reduced biochar was able to abiotically reduce NTO, DNAN, and RDX (Figure E-7). Additionally, oxidized biochar was shown to serve as a electron acceptor during microbial utilization of acetate, formate, and H₂, and the final reduced biochar was able to serve as an electron donor for microbial perchlorate reduction (Figure E-8).

These results indicated that biochar should be included in the suite of materials to develop an effective technology for the removal of energetics from surface runoff.

Table E-4. MC properties and sorption isotherm parameters with Rogue_{OX} in ASR, pH 6.

MC		NTO	NQ	DNAN	RDX
Structure		O_2N N N N	H ₂ N NO ₂	OCH ₃ NO ₂	O_2 N, $N \longrightarrow N$, NO_2
Formulation		IMX-101 IMX-104	IMX-101	IMX-101 IMX-104	IMX-104
Physical properties ^a	MW (g mol ⁻¹) Solubility (mg L ⁻¹) Log K_{OW}	130.08 16 642 (ref. 5) 0.37–1.03 (ref. 5)	104.07 2600 (ref. 75)–5000 (ref. 69) 0.10 (ref. 75)	198.13 276 (ref. 5) 1.64 (ref. 5)	222.26 60 (ref. 5) 0.81-0.87 (ref. 5)
Isotherm parameters b	$Log K_{ m OC} \ C_{ m s,max} \ (\mu m mol \ g^{-1}) \ C_{ m s.max} \ (\%, \ m w/w)$	3.03 (ref. 5) 154 2.0	— 388 4.0	3.11 (ref. 5) 476 9.4	0.88–2.40 (ref. 5) 213 4.7
	$K_{\rm L} \left(\mu { m M}^{-1} \right)$ R^2	0.07 0.94	0.02 0.96	2.96 0.97	0.44 0.98

 $[^]a$ MW: molecular weight, $K_{\rm OW}$ and $K_{\rm OC}$: octanol-water and organic carbon-water partition coefficients, respectively. Solubility at 25 $^{\circ}$ C. b Parameters of the isotherms are obtained through Langmuir isotherm fitting, as shown in Fig. 5.

Figure E-7. Abiotic reduction of NTO, DNAN, and RDX by biochar in ASR, pH 6.

(a) Aqueous concentration (C_{aq}) of NTO and 3-amino-1,2,4-triazol-5-one (ATO) over time with 0.80 g/L of SRB or Rogue. (b) NTO mass balance. (c) C_{aq} of DNAN and 2-ANAN/4-ANAN over time with 0.44 g/L of Rogue. (d) DNAN mass balance. (e) C_{aq} of RDX, MNX, and NO₂ over time with 0.44 g/L of Rogue. (f) RDX mass balance. "total" is the DNAN or RDX added to blank. Subscripts "aq" and "s" denote mass in the aqueous phase at the end of the experiment (ca. 400 h) and that extracted from the solid, respectively.

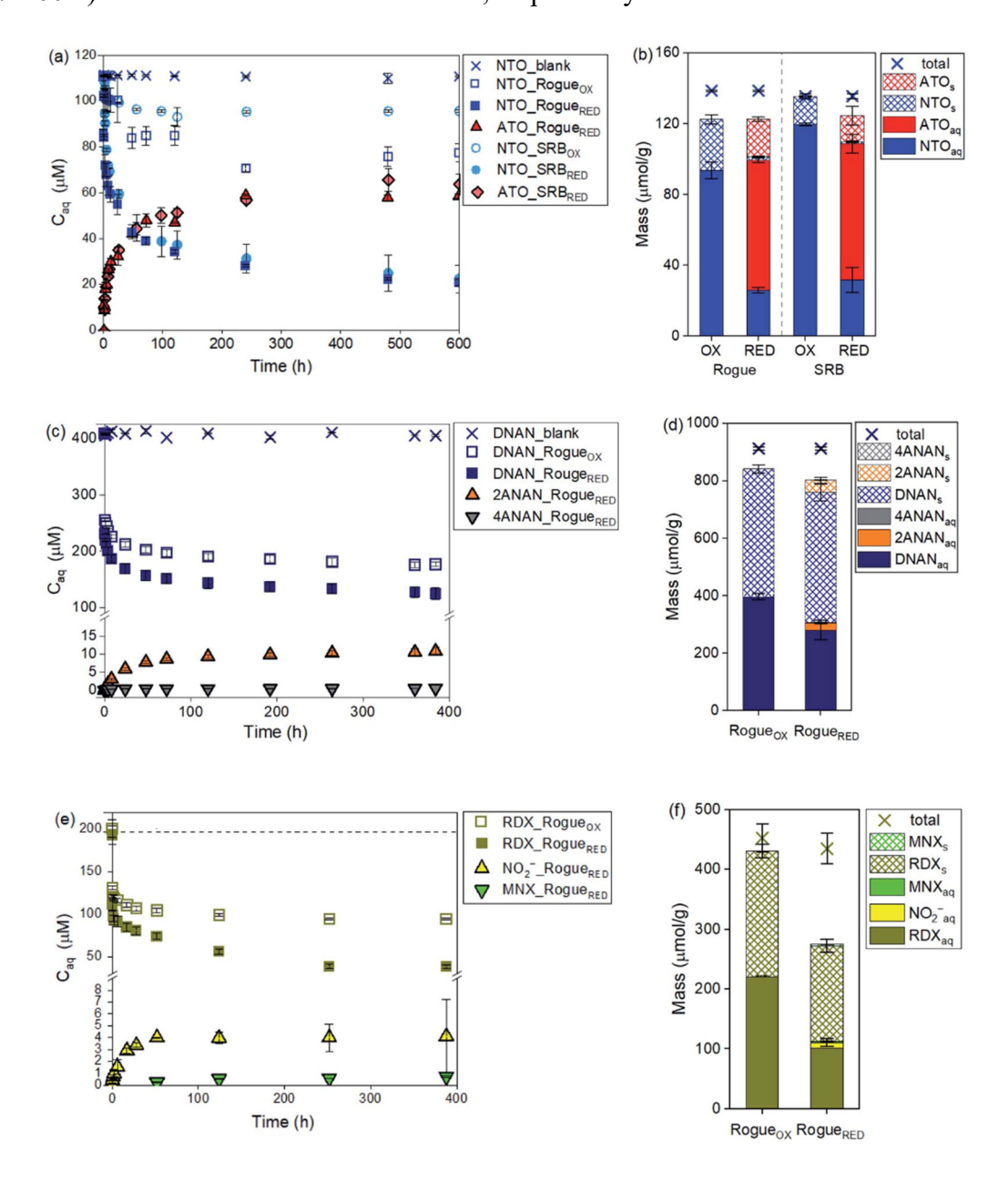
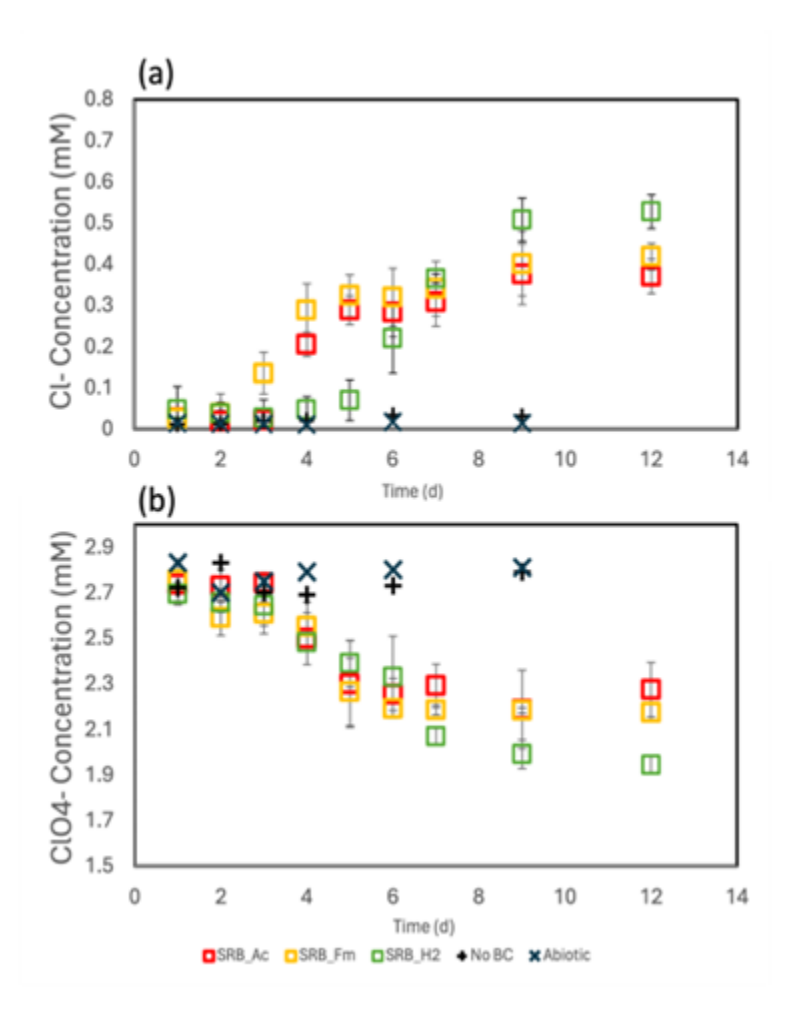


Figure E-8. Microbial perchlorate reduction with microbially reduced biochar as an electron donor.

Error bars represent one standard deviation from triplicate reactors.



Column Study Evaluation of Combined Sorption/Biodegradation of Legacy and Insensitive Munition Energetics. Figure E-9 presents the breakthrough of the energetics (relative to the tracer) in the different columns over time. There was sustained almost complete removal of RDX and ClO₄⁻, and more removal of the other energetics in the bioactive columns compared to the sorption only columns, over the course of the experiments. For reference, 100 PV is approximately equivalent to three months of operation. The higher effectiveness of sorption/biodegradation compared to sorption only is further demonstrated in Figure E-10, where the energetics removal in the bioactive columns was shown to be 2- to 25-fold higher relative to that observed in the sorption only column. There also was an apparent added benefit of biochar for NQ removal during both column experiments, and for HMX also during the second column experiment.

Figure E-9. Representative breakthrough curves of energetics during the column sorption-biodegradation experiments.

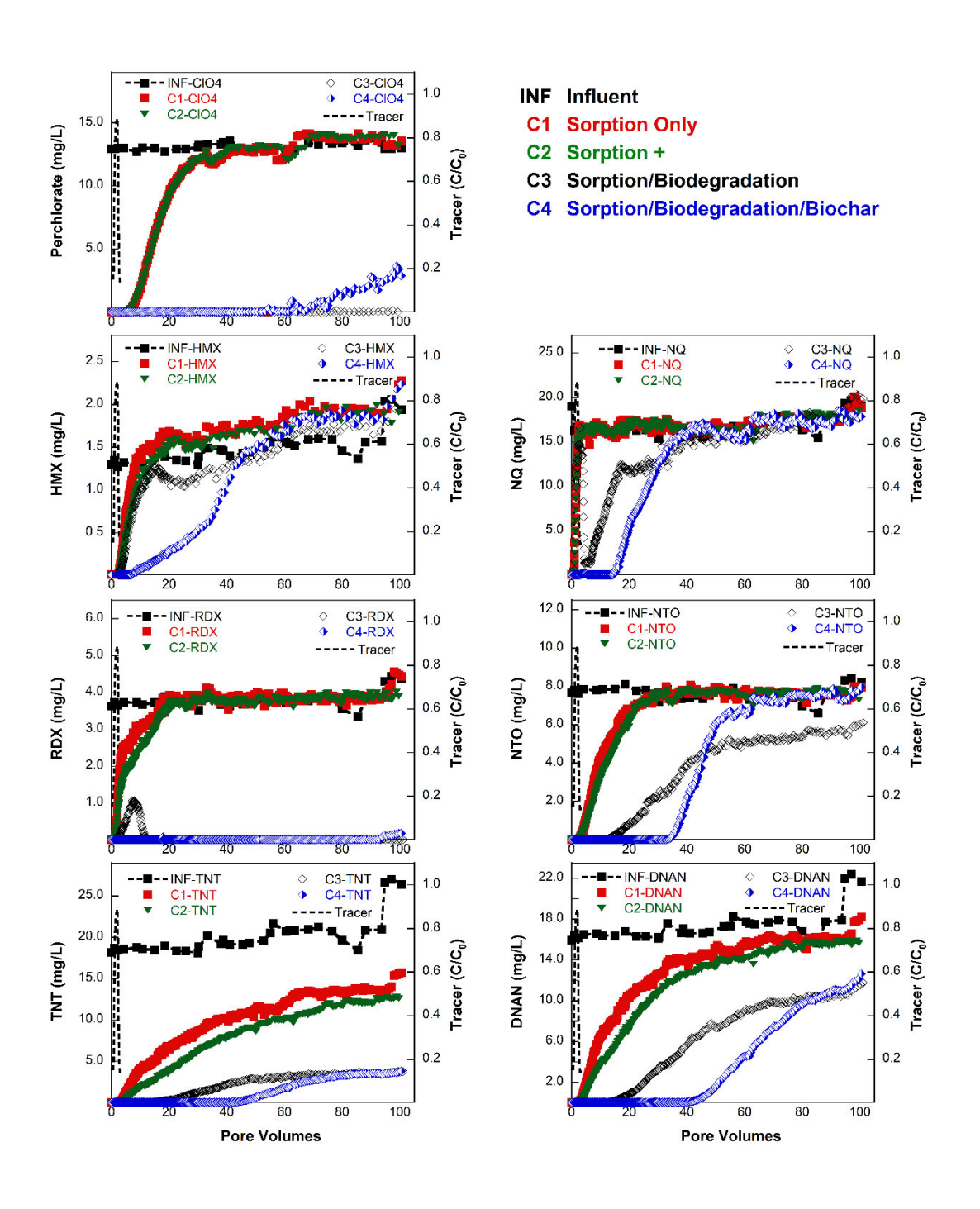
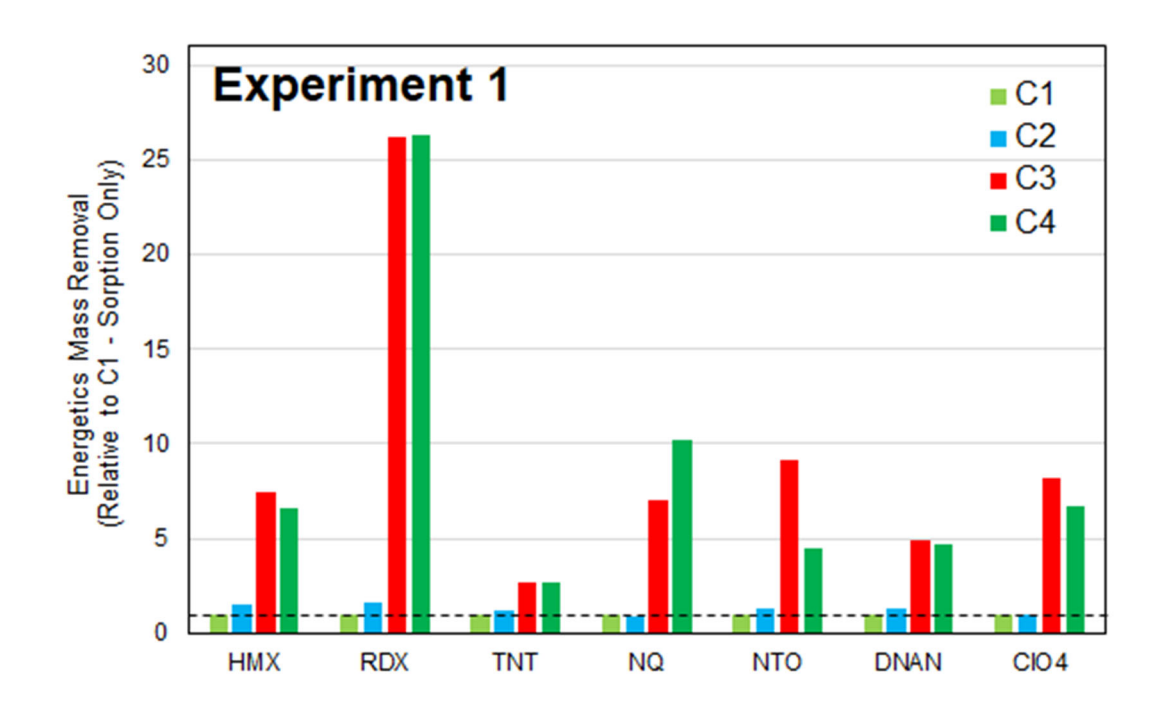
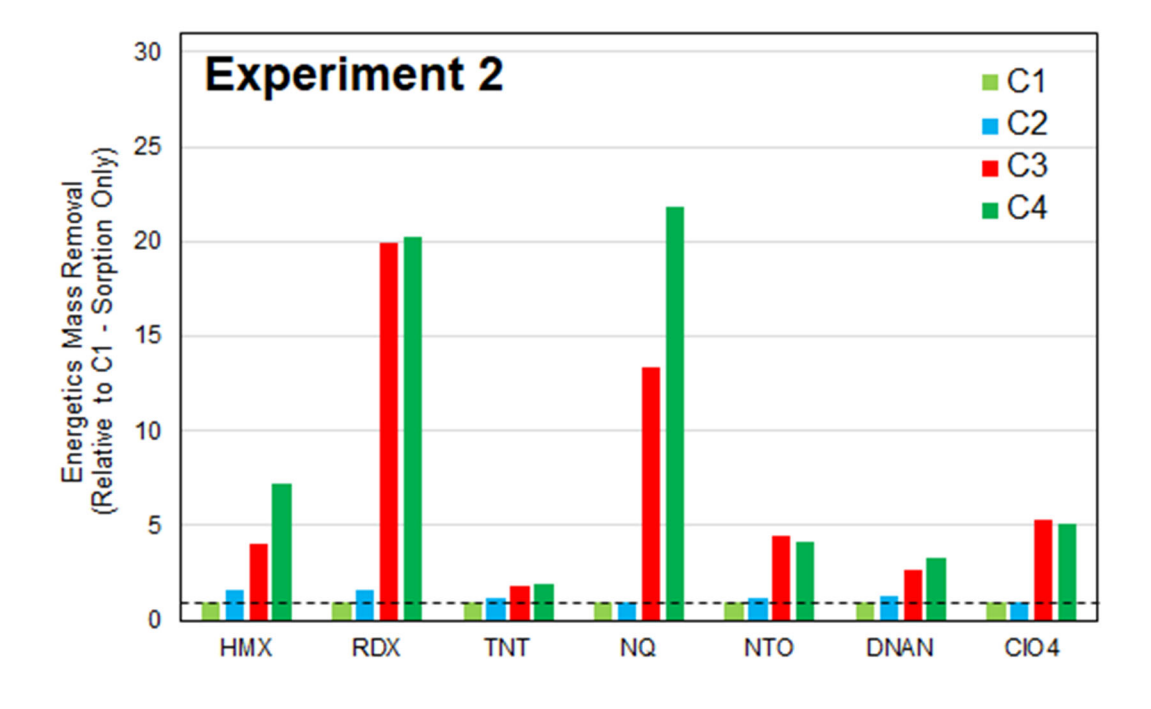


Figure E-10. Energetic mass removal relative to the sorption only removal observed column C1 during the first and second column sorption-biodegradation experiments.

Dashed line given for reference to C1 removal = 1.





ES4. Conclusions and Implications for Future Research/Implementation:

While this project indicated that there was sporadic detections of energetics in the surface runoff at NSWC Dahlgren, it would be recommended that a more thorough evaluation at multiple sites be undertaken. More frequent sample collection would be beneficial, especially if it can be more closely aligned with range activities.

This project also identified novel sorbents and slow-release carbon sources that would be effective to promote the sorption/biodegradation of a range of legacy and insensitive munition constituents from surface runoff, as well as demonstrating the added benefit of biochar for both sorption and biotic/abiotic degradation of these compounds.

The results of this project lay the foundation for a passive, sustainable surface runoff treatment technology, and should be demonstrated at the pilot scale at an appropriate field site, specifically:

- The "trap" component of the technology utilizing peat moss and cationized pine shavings would be relatively robust for all the target energetics except NQ. The relative placement of the sorbent media, as well as the mass of media, may need some additional testing to optimize sorptive removal of the energetics based on characterization of the energetics in the runoff at a given site.
- The "treat" component of the technology using a mixed inoculum, combined with the natural inoculation of the treatment media via exposure to the surface runoff, is expected to be effective for all of the energetics, especially for RDX, TNT, DNAN, and perchlorate. The biological removal of HMX, NTO, and NQ was demonstrated to be affected by the presence of labile carbon at longer timeframes of column operation. This is expected to be mitigated by the addition of more of the biodegradable biopolymer carbon sources in the system.
- The development and production of the custom inoculants would not be a major hindrance to the use of the technology. Companies such as Aptim have the experience and industrial infrastructure to address this issue. We also have archived the anaerobic and aerobic MBR biomass which was used as the main mixed inoculum for the column studies, and the other pure cultures are also archived. These can be used as a starting point for fresh inoculum for further development and optimization of the technology, e.g., at pilot or field scale.
- The mix of energetics in the runoff at a given site may require some fine tuning of the sorbent mix or inocula to achieve the most efficient treatment.

It should be noted that NQ proved to be the most recalcitrant energetic, exhibiting the least removal over the duration of the column experiments compared to the other energetics. More efforts focused on effective sorbents for this compound, or on identifying more robust biodegradative cultures, is warranted. These efforts would not only benefit the technology developed during this project, but also the overall NQ remediation area. In parallel, some effort should be directed at understanding the potential extent of NQ contamination at DoD sites, so that the relative risk and focus on NQ remediation can be correctly assessed.

ES5. Literature Cited:

- Ahmad, M., Rajapaksha, A.U., Lim, J.E., Zhang, M., Bolan, N., Mohan, D., Vithanage, M., Lee, S.S., Ok, Y.S., 2014. Biochar as a sorbent for contaminant management in soil and water: A review. Chemosphere 99, 19-33. https://doi.org/10.1016/j.chemosphere.2013.10.071.
- Brown, P.A., Gill, S.A., Allen, S.J., 2000. Metal removal from wastewater using peat. Water Research 34, 3907-3916.https://doi.org/10.1016/S0043-1354(00)00152-4.
- Burba, P., Willmer, P.G., 1983. Cellulose: a biopolymeric sorbent for heavy-metal traces in waters. Talanta 30, 381-383. https://doi.org/10.1016/0039-9140(83)80087-3.
- Deletic, A., Fletcher, T.D., 2006. Performance of grass filters used for stormwater treatment—A field and modelling study. Journal of Hydrology 317, 261-275.http://dx.doi.org/10.1016/j.jhydrol.2005.05.021.
- Fuller, M.E. 2015. Fate and Transport of Colloidal Energetic Residues. ER-1689. https://www.serdp-estcp.org/content/download/38250/362302/file/ER-1689-FR.pdf.
- Fuller, M.E., Hatzinger, P.B., Rungkamol, D., Schuster, R.L., Steffan, R.J., 2004. Enhancing the attenuation of explosives in surface soils at military facilities: Combined sorption and biodegradation. Environ Toxicol Chem 23, 313-324.
- Fuller, M.E., Lowey, J.M., Schaefer, C.E., Steffan, R.J., 2005. A peat moss-based technology for mitigating residues of the explosives TNT, RDX, and HMX in soil. Soil Sediment Contam 14, 373-385.
- Fuller, M.E., Schaefer, C.E., Steffan, R.J., 2009. Evaluation of a peat moss plus soybean oil (PMSO) technology for reducing explosive residue transport to groundwater at military training ranges under field conditions. Chemosphere 77, 1076-1083.
- Gray, M., Johnson, M.G., Dragila, M.I., Kleber, M., 2014. Water uptake in biochars: The roles of porosity and hydrophobicity. Biomass and Bioenergy 61, 196-205. https://doi.org/10.1016/j.biombioe.2013.12.010.

- Grebel, J.E., Charbonnet, J.A., Sedlak, D.L., 2016. Oxidation of organic contaminants by manganese oxide geomedia for passive urban stormwater treatment systems. Water Research 88, 481-491.http://dx.doi.org/10.1016/j.watres.2015.10.019.
- Hatzinger, P.B., Fuller, M.E., Rungkamol, D., Schuster, R.L., Steffan, R.J., 2004. Enhancing the attenuation of explosives in surface soils at military facilities: Sorption-desorption isotherms. Environ Toxicol Chem 23, 306-312.
- Kappler, A., Wuestner, M.L., Ruecker, A., Harter, J., Halama, M., Behrens, S., 2014. Biochar as an electron shuttle between bacteria and Fe(III) minerals. Environmental Science & Technology Letters 1, 339-344.10.1021/ez5002209.
- Klüpfel, L., Keiluweit, M., Kleber, M., Sander, M., 2014. Redox properties of plant biomass-derived black carbon (Biochar). Environmental Science & Technology 48, 5601-5611.10.1021/es500906d.
- Lapointe, M.-C., Martel, R., Diaz, E., 2017. A conceptual model of fate and transport processes for RDX deposited to surface soils of North American active demolition sites. J Environ Qual 46, 1444-1454.10.2134/jeq2017.02.0069.
- Mohan, D., Sarswat, A., Ok, Y.S., Pittman, C.U., 2014. Organic and inorganic contaminants removal from water with biochar, a renewable, low cost and sustainable adsorbent A critical review. Bioresource Technology 160, 191-202.https://doi.org/10.1016/j.biortech.2014.01.120.
- O'Connell, D.W., Birkinshaw, C., O'Dwyer, T.F., 2008. Heavy metal adsorbents prepared from the modification of cellulose: A review. Bioresource Technology 99, 6709-6724. https://doi.org/10.1016/j.biortech.2008.01.036.
- Oh, S.-Y., Cha, D.K., Chiu, P.C., 2002a. Graphite-mediated reduction of 2,4-dinitrotoluene with elemental iron. Environ Sci Technol 36, 2178-2184.10.1021/es011474g.
- Oh, S.-Y., Cha, D.K., Kim, B.-J., Chiu, P.C., 2002b. Effect of adsorption to elemental iron on the transformation of 2,4,6-trinitrotoluene and hexahydro-1,3,5-trinitro-1,3,5-triazine in solution. Environ Toxicol Chem 21, 1384-1389.

- Oh, S.-Y., Cha, D.K., Kim, B.J., Chiu, P.C., 2004. Reduction of nitroglycerin with elemental iron: Pathway, kinetics, and mechanisms. Environ Sci Technol 38, 3723-3730.10.1021/es0354667.
- Oh, S.-Y., Cha, D.K., Kim, B.J., Chiu, P.C., 2005. Reductive transformation of hexahydro-1,3,5-trinitro-1,3,5-triazine, octahydro-1,3,5,7-tetranitro-1,3,5,7-tetrazocine, and methylenedinitramine with elemental iron. Environ Toxicol Chem 24, 2812-2819.10.1897/04-662R.1.
- Oh, S.-Y., Chiu, P.C., 2009. Graphite- and soot-mediated reduction of 2,4-dinitrotoluene and hexahydro-1,3,5-trinitro-1,3,5-triazine. Environ Sci Technol 43, 6983-6988.
- Oh, S.-Y., Seo, Y.-D., Jeong, T.-Y., Kim, S.-D., 2018. Sorption of nitro explosives to polymer/biomass-derived biochar. Journal of Environmental Quality.10.2134/jeq2017.09.0357.
- Oh, S.-Y., Son, J.-G., Chiu, P.C., 2013. Biochar-mediated reductive transformation of nitro herbicides and explosives. Environ Toxicol Chem 32, 501-508.
- Prévoteau, A., Ronsse, F., Cid, I., Boeckx, P., Rabaey, K., 2016. The electron donating capacity of biochar is dramatically underestimated. Scientific Reports 6, 32870.10.1038/srep32870 https://www.nature.com/articles/srep32870#supplementary-information.
- Roden, E.E., Kappler, A., Bauer, I., Jiang, J., Paul, A., Stoesser, R., Konishi, H., Xu, H., 2010. Extracellular electron transfer through microbial reduction of solid-phase humic substances. Nature Geoscience 3, 417.10.1038/ngeo870 https://www.nature.com/articles/ngeo870#supplementary-information.
- Sander, M., Pignatello, J.J., 2005. Characterization of charcoal adsorption sites for aromatic compounds: insights drawn from single-solute and bi-solute competitive experiments. Environ Sci Technol 39, 1606-1615.10.1021/es0491351.
- Sansalone, J.J., 1999. In-situ performance of a passive treatment system for metal source control. Water Science and Technology 39, 193-200. http://dx.doi.org/10.1016/S0273-1223(99)00023-2.

- Saquing, J.M., Yu, Y.-H., Chiu, P.C., 2016. Wood-derived black carbon (biochar) as a microbial electron donor and acceptor. Environmental Science & Technology Letters 3, 62-66.10.1021/acs.estlett.5b00354.
- Schaefer, C.E., Fuller, M.E., Lowey, J.M., Steffan, R.J., 2005. Use of peat moss amended with soybean oil for mitigation of dissolved explosive compounds leaching into the subsurface: Insight into mass transfer mechanisms. Environ Eng Sci 22, 337-349.
- Seelsaen, N., McLaughlan, R., Moore, S., Ball, J.E., Stuetz, R.M., 2006. Pollutant removal efficiency of alternative filtration media in stormwater treatment. Water Science and Technology 54, 299-305.10.2166/wst.2006.617.
- Sun, T., Levin, B.D.A., Guzman, J.J.L., Enders, A., Muller, D.A., Angenent, L.T., Lehmann, J., 2017. Rapid electron transfer by the carbon matrix in natural pyrogenic carbon. Nature Communications 8, 14873.10.1038/ncomms14873
- https://www.nature.com/articles/ncomms14873#supplementary-information.
- Todde, G., Jha, S.K., Subramanian, G., Shukla, M.K., 2018. Adsorption of TNT, DNAN, NTO, FOX7, and NQ onto cellulose, chitin, and cellulose triacetate. Insights from Density Functional Theory calculations. Surface Sci 668, 54-60.https://doi.org/10.1016/j.susc.2017.10.004.
- Wan Ngah, W.S., Hanafiah, M.A.K.M., 2008. Removal of heavy metal ions from wastewater by chemically modified plant wastes as adsorbents: A review. Bioresource Technology 99, 3935-3948. https://doi.org/10.1016/j.biortech.2007.06.011.
- Xie, T., Reddy, K.R., Wang, C., Yargicoglu, E., Spokas, K., 2015. Characteristics and applications of biochar for environmental remediation: A review. Critical Reviews in Environmental Science and Technology 45, 939-969.10.1080/10643389.2014.924180.
- Xin, D., Xian, M., Chiu, P.C., 2018. Chemical methods for determining the electron storage capacity of black carbon. MethodsX 5, 1515-1520.https://doi.org/10.1016/j.mex.2018.11.007.
- Xu, W., Dana, K.E., Mitch, W.A., 2010. Black carbon-mediated destruction of nitroglycerin and RDX by hydrogen sulfide. Environ Sci Technol 44, 6409-6415.

- Xu, W., Pignatello, J.J., Mitch, W.A., 2013. Role of black carbon electrical conductivity in mediating hexahydro-1,3,5-trinitro-1,3,5-triazine (RDX) transformation on carbon surfaces by sulfides. Environ Sci Technol 47, 7129-7136.10.1021/es4012367.
- Ye, J., Chiu, P.C., 2006. Transport of atomic hydrogen through graphite and its reaction with azoaromatic compounds. Environ Sci Technol 40, 3959-3964.10.1021/es060038x.
- Zhang, J., You, C., 2013. Water holding capacity and absorption properties of wood chars. Energy & Fuels 27, 2643-2648.10.1021/ef4000769.
- Zhu, D., Kwon, S., Pignatello, J.J., 2005. Adsorption of single-ring organic compounds to wood charcoals prepared under different thermochemical conditions. Environ Sci Technol 39, 3990-3998.10.1021/es050129e.
- Zhu, D., Pignatello, J.J., 2005. Characterization of aromatic compound sorptive interactions with black carbon (charcoal) assisted by graphite as a model. Environ Sci Technol 39, 2033-2041.10.1021/es0491376.

Table of Contents

Executive Summary	i
ES1. Background:	i
ES2. Materials and Methods:	iv
ES3. Results and Discussion:	vii
ES4. Conclusions and Implications for Future Research/Implementation:	xix
ES5. Literature Cited:	XX
List of Tables	iv
List of Figures	vi
List of Acronyms	xi
1. Project Background, Objectives, and Approach	1
REFERENCES	8
2. Surface Runoff Characterization.	13
2.1 METHODS	13
2.1.1 Field site.	13
2.1.2 Field instrumentation.	13
2.1.3 Sample collection.	14
2.1.4 Sample processing.	14
2.1.5 Sample analyses.	15
2.2 RESULTS and DISCUSSION	23
2.2.1 Sampling events, weather data, and range activity.	23
2.2.2 Geochemistry.	23
2.2.3 Energetics.	23
2.2.4 Metals	24
2.2.5 Other analytes.	24
2.3 CONCLUSIONS	24
REFERENCES	35
3. Evaluation of Novel Sorbents for Legacy and Insensitive Munition Energetics	36
3.1 METHODS	36
3.1.1 Chemicals and media	36
3.1.2 Cationization of cellulosic materials	36
3.1.3 Batch screening	37
3.1.4 Analytical	38
3.1.5 Data analysis	38

3.2 RESULTS and DISCUSSION	39
3.2.1 NTO removal	39
3.2.2 DNAN removal	48
3.2.3 NQ removal	48
3.2.3 Legacy and insensitive MC isotherms	50
3.3 CONCLUSIONS	51
REFERENCES	51
4. Evaluation of Slow-Release Carbon Sources for Biodegradation of Legacy and Munition Energetics	
4.1 METHODS	54
4.1.1 Chemicals and media	54
4.1.2 Slow-release carbon source screening	54
4.2 RESULTS and DISCUSSION	55
4.2.1 RDX degradation	55
4.2.2 NQ degradation	57
4.2.3 Mixed energetics degradation	58
4.3 CONCLUSIONS	60
REFERENCES	61
5. Evaluation of Biochar for Abiotic and Biotic Degradation of Legacy and Insensitive Energetics	
5.1 Sorption of MC to Biochar	62
5.1.1 METHODS	62
5.1.2 RESULTS and DISCUSSION	63
5.2 Abiotic Reduction of MCs by Reduced Biochar	66
5.2.1 METHODS	67
5.2.2 RESULTS and DISCUSSION	69
5.3 Microbial Reduction of Perchlorate and Nitrate with Reduced Biochar	76
5.3.1 METHODS	76
5.3.2 RESULTS and DISCUSSION	77
5.4 Microbial Regeneration of Reduced Biochar for Perchlorate Reduction	81
5.4.1 METHODS	81
5.4.2 RESULTS and DISCUSSION	82
REFERENCES	87
6. Column Study Evaluation of Combined Sorption/Biodegradation of Legacy and Munition Energetics	Insensitive

6.1 METHODS	92
6.1.1 Chemicals and media	92
6.1.2 Column setup and packing	92
6.1.3 Column operation	93
6.1.4. Analytical	95
6.1.5. Data analysis for the column sorption experiment	95
6.1.6. Data analysis for column sorption-biodegradation experiments	96
6.2 RESULTS and DISCUSSION	99
6.2.1. Column sorption experiment	99
6.2.2. Column sorption-biodegradation experiments	109
6.3 CONCLUSIONS	142
REFERENCES	143
7. Conclusions and Recommendations	145

APPENDIX A: Supporting Data APPENDIX B: List of Scientific/Technical Publications

APPENDIX C: SPE Protocols

List of Tables

Table E-1. Slow-release carbon source information
Table E-2. Summary of energetics concentrations detected in surface runoffviii
Table E-3. Freundlich and Langmuir adsorption parameters for insensitive and legacy explosives.
ix
Table E-4. MC properties and sorption isotherm parameters with Rogueox in ASR, pH 6 xiv
Table 2-1. Analytical methods employed during surface runoff sample characterization 17
Table 2-2. List of potential binders and plasticizers in surface runoff
Table 2-3. Summary of surface runoff geochemical parameters
Table 2-4. Summary of energetics concentrations detected in surface runoff
Table 2-5. Summary of TAL metals concentrations in surface runoff
Table 3-1. Freundlich and Langmuir adsorption parameters for insensitive and legacy explosives.
Table 4-1. Slow-release carbon source information
Table 5-1. Conditions used for the MC sorption experiment
Table 5-2. MC properties and sorption isotherm parameters with Rogueox in ASR, pH 6 64
Table 5-3. Physical-chemical properties of Soil Reef biochar and Rogue biochar
Table 5-4. Summary of MC reduction results with biochar at pH 6.0
Table 6-1. Retardation factors (R) for all energetics in the three columns
Table 6-2. Calculated sorption capacity for all energetics based on batch and column experiments
at 50% breakthrough.
Table 6-3. Calculated sorption capacity for all energetics based on batch and column experiments
and the Thomas column adsorption kinetic model
Table 6-4. Preliminary mass and volume sizing for a passive biofilter to treat NSWC Dahlgren
surface runoff based on maximum sorption capacity from sorption-only column
experiment and runoff characterization
Table 6-5. Comparison of sorption capacities (q_0) for energetics from the sorption-only experiment
versus the sorption-only column (C1) during the sorption-biodegradation
experiments

Table 6-6. Revised mass and volume sizing for a passive biofilter to treat NSWC Dahlgren surface runoff based on sorption-only derived from maximum sorption capacity from sorption-only column (C1) during sorption-biodegradation experiments. 125

List of Figures

Figure E-1. Location of NSWC Dahlgren, VA and sampling area.	V
Figure E-2. Schematic and photograph of columns used in this work	ii
Figure E-3. Removal of dissolved NTO (top) and DNAN (bottom).	X
Figure E-4. Aerobic RDX degradation by Gordonia KTR9 and Rhodococcus DN22 in the presence	e
of slow-release carbon source biopolymers	κi
Figure E-5. Aerobic NQ degradation by Pseudomonas NQ5 in presence of slow-release carbo	n
source biopolymersx	ii
Figure E-6. Anoxic degradation of energetics by MBR mixed culture in presence of slow-releas	se
carbon source biopolymersxi	.11
Figure E-7. Abiotic reduction of NTO, DNAN, and RDX by biochar in ASR, pH 6 x	V
Figure E-8. Microbial perchlorate reduction with microbially reduced biochar as an electron dono	r.
XX	vi
Figure E-9. Representative breakthrough curves of energetics during the column sorption	1-
biodegradation experimentsxv	ii
Figure E-10. Energetic mass removal relative to the sorption only removal observed column C	:1
during the first and second column sorption-biodegradation experiments xvi	ii
Figure 1-1. Predicted relative mass fluxes of TNT, RDX, and HMX into soil over time with an	ıd
without the application of a layer of peat-based treatment material at the soil surface	æ
(adapted from ER-0434 Final Report).	3
Figure 1-2. Examples of MC sorption and reductive transformation by biochar	4
Figure 1-3. Nitrate removal by Geobacter metallireducens using reduced biochar as electro)1)
donor.	5
Figure 1-4. Flowchart illustrating the relationship of the various tasks during this project	7
Figure 2-1. Location of NSWC Dahlgren, VA.	8
Figure 2-2. Illustrations and photographs of the surface runoff samplers utilized during this projec	t.
1	9
Figure 2-3. Location of the surface runoff samplers at NSWC Dahlgren, Churchill Range 2	0
Figure 2-4. Placement of the runoff flow meter sensor and datalogger	1
Figure 2-5. Photograph of the weather station installed at NSWC Dahlgren	2

Figure 2-6. Recorded precipitation and runoff sample collection (red squares) during this project
Figure 2-7. Recorded runoff flow (a) and cumulative runoff volume (b)
Figure 2-8. Mass of legacy and insensitive munition constituents detonated on the range and runof
sampling events (red squares)
Figure 2-9. GC-MS analysis of control ASR passed through the surface runoff sampling device
after 100X preconcentration via C18 SPE
Figure 2-10. GC-MS analysis of pooled dissolved (<0.7 µm) analytes in October 2019 surface
runoff samples after 100X preconcentration via C18 SPE
Figure 2-11. GC-MS analysis of pooled total analytes in October 2019 surface runoff samples after
100X preconcentration via C18 SPE
Figure 2-12. GC/MS total ion chromatograph of composite surface runoff samples collected in
January, June, and November 2020 after processing with C18 SPE to concentrate
potential binder, waxes, and plasticizers
Figure 3-1. Reaction mechanism of CHPTAC with cellulose
Figure 3-2. Reaction of cotton linters with cationization agent CHPTAC and photograph of native
and cationized cotton linters after exposure to dissolved NTO
Figure 3-3. Removal of NTO (top) and DNAN (bottom) from ASR. Data represent average o
duplicates ± standard deviation
Figure 3-4. Effect of CHPTAC concentration on removal of NTO by cationized pine shavings
(top) and amount of CHPTAC incorporation based on change in nitrogen conten
(bottom)44
Figure 3-5. Relationship between calculated degree of CHPTAC incorporation into differen
materials and the percent NTO removed from solution after 24 h
Figure 3-6. Initial and final solution pH and removal of NTO by cationized pine shavings 46
Figure 3-7. Impact of peat moss on removal of NTO from solution by CAT materials (top) and
final solution pH (bottom)
Figure 3-8. Impact of major anions on removal of NTO from solution by CAT materials 48
Figure 3-9. Impact of mercerization and cationization on removal of DNAN from solution by CAT
pine shavings based after 24 h

Figure 3-10. Impact of degree of CHPTAC incorporation on removal of DNAN from solution	on by
CAT pine shavings based after 24 h.	50
Figure 4-1. Aerobic RDX degradation by Gordonia KTR9 and Rhodococcus DN22 in the pre	sence
of slow-release carbon source biopolymers.	56
Figure 4-2. Anoxic RDX degradation by Pseudomonas I-C in presence of slow-release ca	arbor
source biopolymers.	57
Figure 4-2. Aerobic NQ degradation by Pseudomonas NQ5 in presence of slow-release ca	arbor
source biopolymers.	57
Figure 4-3. Anoxic degradation of energetics by MBR mixed culture in presence of slow-re-	elease
carbon source biopolymers.	59
Figure 5-1. Sorption of MCs to Rogueox over time.	65
Figure 5-2. Sorption of MCs a) NTO, b) NQ, c) DNAN, and d) RDX to Rogueox in ASR	at pH
6.0 and the fitted Langmuir isotherms.	66
Figure 5-3. Abiotic reduction of NTO by biochar at several pH values	73
Figure 5-4. Abiotic reduction of NTO by biochar at pH 10.	74
Figure 5-5. Electron balance for NTO reduction by SRB _{RED} .	74
Figure 5-6. Abiotic reduction of NTO, DNAN, and RDX by biochar in ASR, pH 6	75
Figure 5-7. Microbial reduction of perchlorate with chemically-reduced biochar as the ele	ectror
donor.	79
Figure 5-8. Microbial reduction of nitrate with chemically-reduced biochar as the electron d	lonor
	80
Figure 5-9. Microbial methanogenesis and respiration using oxidized biochar as an ele	ectror
acceptor	84
Figure 5-10. Measured electron accepting capacity (EAC) of biochar after microbial reduction	on.85
Figure 5-11. Microbial perchlorate reduction with microbially reduced biochar as an ele	ectror
donor	86
Figure 6-1. Schematic and photograph of columns used in this work	97
Figure 6-2. Column composition for sorption experiment.	98
Figure 6-3. Column composition for sorption-biodegradation experiment	99
Figure 6-4. Column effluent pH values during the column sorption/desorption experiment	104

Figure 6-5. Energetics breakthrough curves during the column sorption/desorption experiment
Figure 6-6. Blowup of the energetics breakthrough curves to focus on the sorption and desorption
behavior106
Figure 6-7. Relative breakthrough of NQ, NTO, ClO ₄ -, and the chloride tracer in the three
sorption/desorption columns
Figure 6-8. Example Thomas column adsorption kinetic modelling of breakthrough curves for the
peat plus CAT pine (layered) column data
Figure 6-9. Column influent and effluent pH and ORP, influent DO, and effluent TOC during the
first column sorption-biodegradation experiment
Figure 6-10. Summary breakthrough curves for energetics during the first column sorption-
biodegradation experiment
Figure 6-11. Perchlorate breakthrough during the first column sorption-biodegradation
experiment114
Figure 6-12. Breakthrough of legacy energetics HMX, RDX, and TNT during the first column
sorption-biodegradation experiment
Figure 6-13. Fraction of RDX detected as NDAB concentrations during the first column sorption-
biodegradation experiment116
Figure 6-14. Effluent concentrations of 4-amino-2,6-dinitrotoluene (4-AM-2,6-DNT) and 2-
amino-4,6-dinitrotoluene (2-AM-4,6-DNT) during the first column sorption-
biodegradation experiment117
Figure 6-15. Effluent concentrations of NQ, NTO, and DNAN during the first column sorption-
biodegradation experiment
Figure 6-16. Blowup of NQ effluent concentrations in C3 and C4 during the first column sorption-
biodegradation experiment119
Figure 6-17. Effluent concentrations of 2-ANAN during the first column sorption-biodegradation
experiment120
Figure 6-18. Column influent and effluent pH and ORP, influent DO, and effluent TOC during the
second column sorption-biodegradation experiment
Figure 6-19. Summary breakthrough curves of energetics during the second column sorption-
biodegradation experiment

Figure 6-20. Perchlorate breakthrough during the first and second column sorption-biodegradation
experiments
Figure 6-21. HMX breakthrough during the first and second column sorption-biodegradation
experiments
Figure 6-22. RDX breakthrough during the first and second column sorption-biodegradation
experiments
Figure 6-23. Effluent NDAB during the first and second column sorption-biodegradation
experiments
Figure 6-24. TNT breakthrough during the first and second column sorption-biodegradation
experiments
Figure 6-25. Effluent 2-ADNT and 4-ADNT during the first and second column sorption
biodegradation experiments
Figure 6-26. NQ breakthrough during the first and second column sorption-biodegradation
experiments
Figure 6-27. NTO breakthrough during the first and second column sorption-biodegradation
experiments
Figure 6-28. DNAN breakthrough during the first and second column sorption-biodegradation
experiments
Figure 6-29. Effluent 2-ANAN during the first and second column sorption-biodegradation
experiments
Figure 6-30. Changes in effluent ORP in response to fructose addition and bioaugmentation of C3
and C4 during the second column sorption-biodegradation experiments 138
Figure 6-31. Effluent energetics concentrations in response to fructose addition and
bioaugmentation during the second column sorption-biodegradation experiment
Figure 6-32. Absolute energetic mass removal during the first and second column sorption-
biodegradation experiments
Figure 6-33. Energetic mass removal relative to the sorption only removal observed column Cl
during the first and second column sorption-biodegradation experiments 141

List of Acronyms

AFC	amine functionalized chitin
2-ANAN	2-amino-4-nitroanisole
4-ANAN	4-amino-2-nitroanisole
2-AM-4,6-DNT	2-amino-4,6-dinitrotoluene
4-AM-2,6-DNT	4-amino-2,6-dinitrotoluene
ASR	artificial surface runoff
ATL	Analytical Testing Laboratory (Aptim)
ATO	3-amino-1,2,4-triazol-5-one
BC	biochar
BioPBS	polybutylene succinate
BSM	basal salts medium
CAT	cationized
CHPTAC	3-chloro-2-hydroxypropyl trimethylammonium chloride
DAD	diode array detector
DE	Delaware
DNAN	2,4-dinitroanisole
DNT	dinitrotoluene
DNX	1,3,5-hexahydro-1,3-dinitroso-5-nitro-triazine
DO	dissolved oxygen
DoD	Department of Defense
EAC	electron accepting capacity
EDC	electron donating capacity
EPA	Environmental Protection Agency
ESC	electron storage capacity
g	gram
GAC	granular activated carbon
h	hour
HBX	high blast explosive
HDPE	high density polyethylene
HMX	1,3,5,7-tetranitro-1,3,5,7-tetrazocane
IHE	insensitive high explosives
IPA	isopropyl alcohol
L	liter
LC	liquid chromatograph
MBR	membrane bioreactor
MC	munitions constituents
mg	milligram
μg	microgram
mM	millimolar
MNX	1,3,5-hexahydro-1-nitroso-3,5-dinitro-1,3,5-triazine
MS	mass spectrometer
NAC	nitroaromatic compounds

NDAB	4-nitro-2,4-diazabutanal
NJ	New Jersey
NQ	nitroguanidine
NSWC	Naval Surface Warfare Center
NTO	3-nitro-1,2,4-triazol-5-one
OD600	optical density at 600 nm
ORP	oxidation-reduction potential
PAD	photodiode array detector
PCL	polycaprolactone
PHB	polyhydroxybutyrate
PLA	polylactic acid
PV	pore volume
RDX	1,3,5-hexahydro-1,3,5-trinitro-1,3,5-triazine
SEFA	sucrose esters of fatty acid
SRB	Soil Reef biochar
TCD	thermal conductivity detector
TG	tetraethylene glycol dimethyl ether
THF	tetrahydrofuran
TNT	2,4,6-trinitrotoluene
TNX	1,3,5-hexahydro-1,3,5-trinitroso-1,3,5-triazine
TOC	total organic carbon
TS	total solids
UD	University of Delaware
V	volt

1. Project Background, Objectives, and Approach

a. Background. Surface runoff characteristics and treatment approaches. During large precipitation events, the rate of water deposition exceeds the rate of water infiltration, resulting in surface runoff (also called stormwater runoff). Land characteristics, including soil texture, presence of impermeable surfaces (natural and artificial), slope, and density and type of vegetation, all influence the amount of surface runoff from a given land area. The same factors, combined with the amount of precipitation, also control the duration of contact between the soil and the water, and the velocity of the runoff, which impacts how contaminants on or near the soil surface are transported by the runoff, either as dissolved or particulate species. Natural and/or engineered flow paths determine the ultimate receptor of the runoff and entrained contaminants.

The use of passive systems such as retention ponds and biofiltration cells for treatment of surface runoff is well established for urban and roadway runoff. Treatment may be achieved by directing runoff into and through a small constructed wetland, often at the outlet to a retention basin, or via filtration, directing runoff through a more highly engineered channel or vault containing the treatment materials. Filtration-based technologies have proven to be effective for the removal of metals, organics, and suspended solids (Sansalone, 1999; Deletic and Fletcher, 2006; Seelsaen et al., 2006; Grebel et al., 2016).

<u>Surface runoff on ranges.</u> Surface runoff represents a major potential mechanism through which energetics residues and related materials are transported off-site from range soils to groundwater and surface water receptors. This process is particularly important for energetics that are watersoluble (e.g., NTO and NQ) or generate soluble daughter products (e.g., DNAN and TNT). While traditional MC such as RDX and HMX have limited aqueous solubility, they also exhibit recalcitrance under most natural conditions. RDX and perchlorate are frequent groundwater contaminants on military training ranges. In a previous small study, MC were detected in surface runoff from an active live-fire range (Fuller, 2015), and more recent sampling has detected MC in marsh surface water adjacent to the same installation (personal communication). Another recent report from Canada also detected RDX in both surface runoff and surface water at low part per billion levels in a survey of several military demolition sites (Lapointe et al., 2017). However, overall, data regarding the contaminant profile of surface runoff from ranges are very limited, and non-energetic constituents (e.g., metals, binders, plasticizers) in runoff have not been examined. Additionally, while contaminated surface runoff is an important concern, mitigation technologies have not yet been developed or widely deployed. To effectively capture and degrade compounds that are present in surface runoff, novel treatment media are needed to sorb a broad range of energetic materials and to transform the retained compounds through abiotic and/or microbial processes.

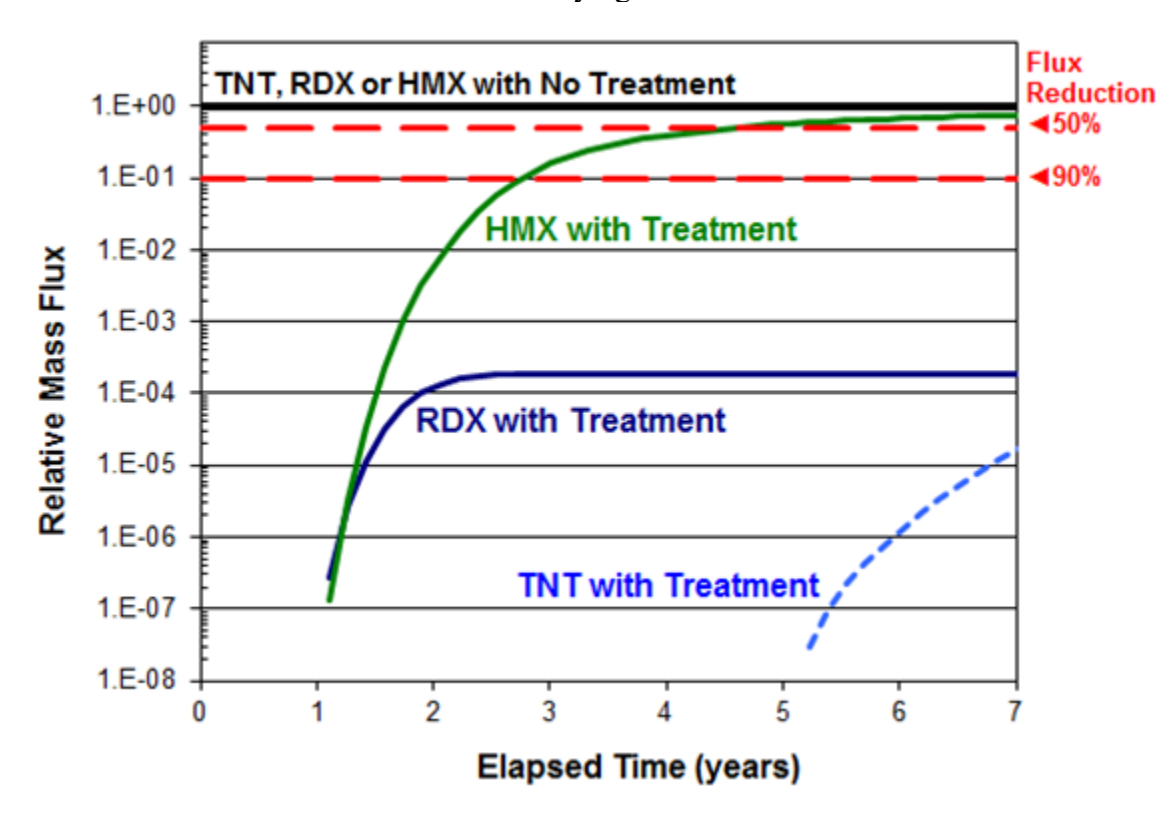
Surface runoff of organic and inorganic contaminants from live fire ranges is a challenging issue for the Department of Defense (DoD). Potentially even more problematic is the fact that inputs to surface waters from large testing and training ranges are from multiple sources, often encompassing hundreds of acres. No technologies are currently effective for controlling non-point energetics-laden surface runoff. While numerous technologies exist to treat collected explosives residues, and contaminated soil and groundwater, the decentralized nature and sheer volume of range runoff precludes their use on site.

Innovative range runoff treatment technology. Previous research demonstrated that a peat-based system provided a natural and sustainable sorptive medium for organic explosives such as HMX, RDX, and TNT (Fuller et al., 2004; Hatzinger et al., 2004; Fuller et al., 2005; Schaefer et al., 2005; Fuller et al., 2009), allowing much longer residence times than predicted from hydraulic loading alone. Peat moss represents a bioactive environment for treatment of the target contaminants. While the bulk microbial reactions are aerobic due to the presence of measurable dissolved oxygen, anaerobic reactions (including methanogenesis) are able to occur in microsites. As noted, the peat-based substrate acts not only as a long term source of reducing equivalents but also as a strong sorbent. This is important in intermittently loaded systems in which a large initial pulse of MC can be temporarily retarded on the peat matrix and then slowly degraded as they desorb (Schaefer et al., 2005; Fuller et al., 2009). This increased residence time enhances the biotransformation of energetics, and promotes the immobilization and further degradation of breakdown products. Abiotic reactions associated with the organic-rich peat are also likely enhanced (e.g., via electron shuttling reactions of humics) (Roden et al., 2010).

During previous work (ESTCP ER-0434), modeling indicated that peat moss amended with crude soybean oil would significantly reduce the flux of dissolved TNT, RDX, and HMX through the vadose zone to groundwater compared to a non-treated soil (Figure 1-1). The technology was validated in field soil plots, showing a greater than 500-fold reduction in the flux of dissolved RDX from macroscale Composition B detonation residues compared to a non-treated control plot (Fuller et al., 2009). Laboratory testing and modeling indicated that the addition of soybean oil increased the biotransformation rates of RDX and HMX at least 10-fold compared to rates observed with peat moss alone (Schaefer et al., 2005). Subsequent experiments also demonstrated the effectiveness of the amended peat moss material for stimulating perchlorate transformation when added to a highly contaminated soil (Fuller et al., unpublished data). These previous data clearly demonstrate the effectiveness of peat-based materials for mitigating transport of both organic and inorganic energetic compounds through soil to groundwater.

Figure 1-1. Predicted relative mass fluxes of TNT, RDX, and HMX into soil over time with and without the application of a layer of peat-based treatment material at the soil surface (adapted from ER-0434 Final Report).

Assumptions: 10 cm of treatment material having a composition of 1:2 peat moss:crude soybean oil (w:w);. Solid explosives applied to top of treatment layer; annual rainfall of 70 cm; mass flux measured at the boundary at the bottom of the treatment layer/top of the underlying soil.



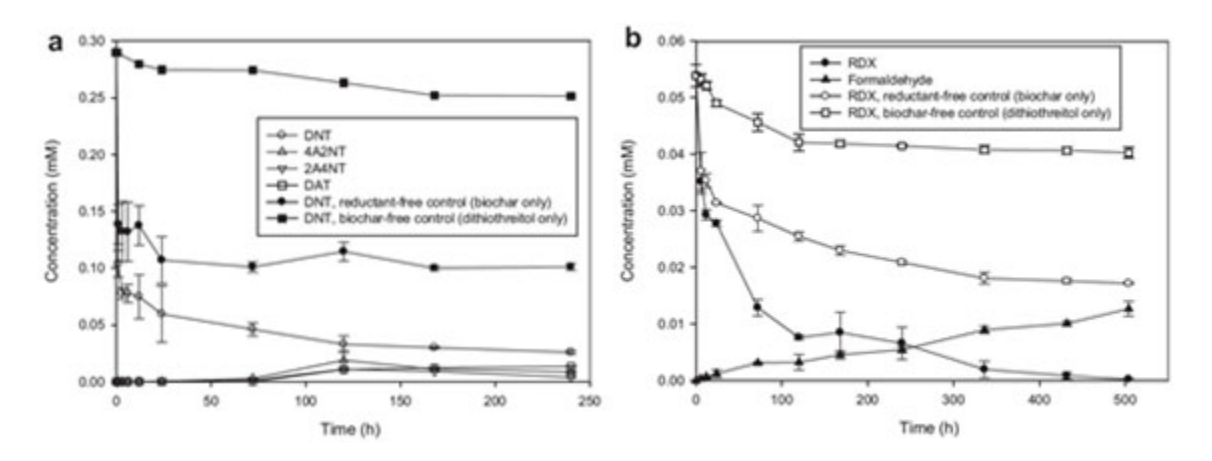
Recent reports have highlighted additional materials that, alone, or in combination with electron donors such as peat moss and soybean oil, may further enhance the sorption and degradation of surface runoff contaminants, including both legacy energetics and IHE. For instance, biochar, a type of black carbon, has been shown to not only sorb a wide range of organic and inorganic contaminants including MCs (Ahmad et al., 2014; Mohan et al., 2014; Xie et al., 2015; Oh et al., 2018), but also facilitate their degradation (Oh et al., 2002b; Ye and Chiu, 2006; Oh and Chiu, 2009; Xu et al., 2010; Oh et al., 2013; Xu et al., 2013). Depending on the source biomass and pyrolysis conditions, biochar can possess a high specific surface area (on the order several hundred m²/g (Zhang and You, 2013; Gray et al., 2014)) and hence a high sorption capacity. Biochar and other black carbon also exhibit especially high affinity for nitroaromatic compounds (NACs) including TNT and 2,4-dinitrotoluene (DNT) (Sander and Pignatello, 2005; Zhu et al., 2005; Zhu and Pignatello, 2005)). This is due to the strong π - π electron donor-acceptor interactions between electron-rich graphitic domains in black carbon and the electron-deficient aromatic ring of the NAC (Zhu et al., 2005; Zhu and Pignatello, 2005). These characteristics make biochar a potentially effective, low-cost, and sustainable sorbent for removing MC and other contaminants from surface runoff and retaining them for subsequent degradation in situ.

Furthermore, black carbon such as biochar can promote abiotic and microbial transformation reactions by facilitating electron transfer. That is, biochar is not merely a passive sorbent for contaminants, but a redox mediator for their degradation. Biochar can promote contaminant degradation through two different mechanisms: electron conduction and electron storage (Sun et al., 2017). First, the microscopic graphitic regions in biochar can sorb contaminants like NACs strongly, as noted above, and also conduct reducing equivalents such as electrons and atomic hydrogen to the sorbed contaminants, thus promoting their reductive degradation. This catalytic process has been demonstrated for TNT, DNT, RDX, HMX, and nitroglycerin (Oh et al., 2002a; Oh et al., 2004, 2005; Oh and Chiu, 2009; Xu et al., 2010), and is expected to occur also for IHE including DNAN and NTO. This is one of the hypotheses we will test during this project.

Second, biochar contains in its structure abundant redox-facile functional groups such as quinones and hydroquinones, which are known to accept and donate electrons reversibly. Depending on the biomass and pyrolysis temperature, certain biochar can possess a rechargeable electron storage capacity (i.e., reversible electron accepting and donating capacity) on the order of several mmol e⁻/g (Klüpfel et al., 2014; Prévoteau et al., 2016; Xin et al., 2018). This means, when "charged", biochar can provide electrons for either abiotic or biotic degradation of reducible compounds such as MC. The abiotic reduction of DNT and RDX mediated by biochar has been demonstrated (Oh et al., 2013), and we expect similar reactions to occur for DNAN and NTO as well. Examples of MC adsorption and degradation by biochar are illustrated in Figure 1-2 for DNT and RDX.

Figure 1-2. Examples of MC sorption and reductive transformation by biochar.

2,4-Dinitrotoluene (DNT) and RDX were removed very slowly even under reducing conditions (in an anaerobic thiol solution). In the presence of biochar, both compounds were adsorbed rapidly, and were subsequently transformed by biochar over 10 days. DNT was reduced to the corresponding aniline products, and RDX underwent a ring cleavage reaction to form formaldehyde. From ref (Oh et al., 2013).

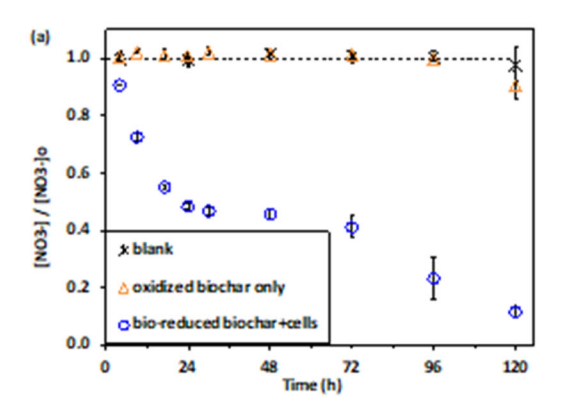


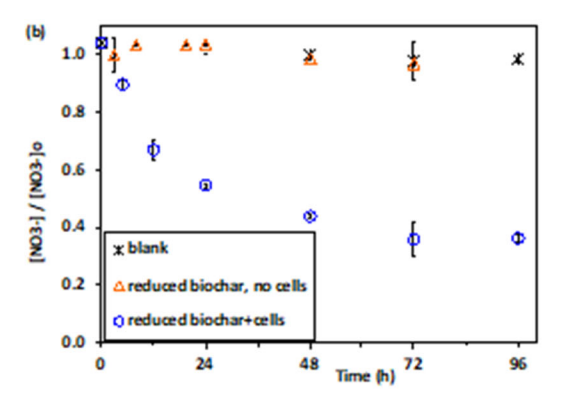
Moreover, recent studies have shown that the electron storage capacity of biochar is also accessible to microbes. For example, soil bacteria such as *Geobacter* and *Shewanella* species can utilize oxidized (or "discharged") biochar as an electron acceptor for the oxidation of organic substrates such as lactate and acetate (Kappler et al., 2014; Saquing et al., 2016), and reduced (or "charged")

biochar as an electron donor for the reduction of nitrate (Saquing et al., 2016). Results of nitrate degradation by *Geobacter* in the presence of reduced biochar as electron donor are shown in Figure 1-3. This is significant because, through microbial access of stored electrons in biochar, contaminants that do not sorb strongly to biochar can still be degraded.

Figure 1-3. Nitrate removal by *Geobacter metallireducens* using reduced biochar as electron donor.

Nitrate did not adsorb to, or react abiotically with, either air-oxidized biochar (a) or dithionite-reduced biochar (b). Nitrate was reduced when cells of *Geobacter metallireducens* were added to either microbially (a) or chemically (b) reduced biochar. Nitrate reduction stopped (b) when the amount of biochar was limiting; i.e., when bio-accessible electrons in biochar were depleted. From ref (Saquing et al., 2016).





Similar to nitrate, perchlorate and other relatively water-soluble energetic compounds (e.g., NTO and NQ) may also be similarly transformed using reduced biochar as an electron donor. Unlike other electron donors, biochar can be recharged through biodegradation of organic substrates (Saquing et al., 2016) and thus can serve as a long-lasting sorbent and electron repository in soil. Similar to peat moss, the high porosity and surface area of biochar not only facilitate contaminant sorption but creates anaerobic/reducing microsites in its inner pores, where reductive degradation of energetic compounds can take place. The ability/efficacy of biochar to promote both abiotic and biotic reduction of IHE and perchlorate will be evaluated in this proposed study.

Another potential sorbent for range contaminants in surface runoff are modified celluloses. Results presented at the 2017 SERDP Symposium showed that cellulose triacetate evidenced enhanced sorption of both legacy TNT and more water soluble IHE like DNAN (L. Gurtowski, Poster 303) compared to other biopolymers including cellulose, chitin, or chitosan. In contrast, chitin and unmodified cellulose were predicted by Density Function Theory methods to be favorable for absorption NTO and NQ, as well as the legacy explosives (Todde et al., 2018). A substantial body of work has shown that modified cellulosic biopolymers can also be effective sorbents for removing metals from solution (Burba and Willmer, 1983; Brown et al., 2000; O'Connell et al., 2008; Wan Ngah and Hanafiah, 2008), and will likely be applicable for some of the metals that may be found in surface runoff at ranges.

Based on the properties of the target compounds, a combination of materials would yield the best results. This project was undertaken to build on the previous findings, as well as to identify other novel materials, resulting in a practical solution for treating contaminated surface runoff.

During the proposed project, additional and/or alternative components to enhance the attenuation of legacy MC as well as newer IHE constituents (and associated nonenergetic compounds, as applicable) in surface runoff. *The key questions that were addressed during this project include:*

- What are the types and concentrations of range contaminants present in range surface runoff?
- What sustainable and economical materials can be used to sorb and/or degrade range contaminants in surface runoff?
- Can biochar enhance the abiotic and biotic degradation of legacy and insensitive munitions constituents, as well as enhance microbial degradation of more soluble energetics (e.g., perchlorate, NTO, NQ)?
- Can biological degradation of range contaminants in surface runoff be enhanced by bioaugmentation with specific degradative organisms?

The treatment technology developed during this project could be translated to the field as part of an integrated surface runoff control plan. This would include some means to direct and collect surface runoff from an MC impacted area in a temporary retention basin. The basin would allow settling of undissolved contaminants and other solids. The outflow of the basin would then pass through the treatment material before being released into the receiving body.

b. Approach.

The technical approach for this project consisted of initial field sampling and laboratory experiments at multiple scales to identify, optimize, and provide proof-of-concept results demonstrating a passive treatment technology for the effective mitigation of a broad range of range runoff contaminants. The objectives of this project were achieved through the following technical tasks, designed to test specific hypotheses:

Task 1. Characterize range surface runoff.

Hypothesis 1: MC and non-energetic compounds are entrained and transported in surface runoff from ranges during storm events.

Task 2. Batch sorption/degradation experiments.

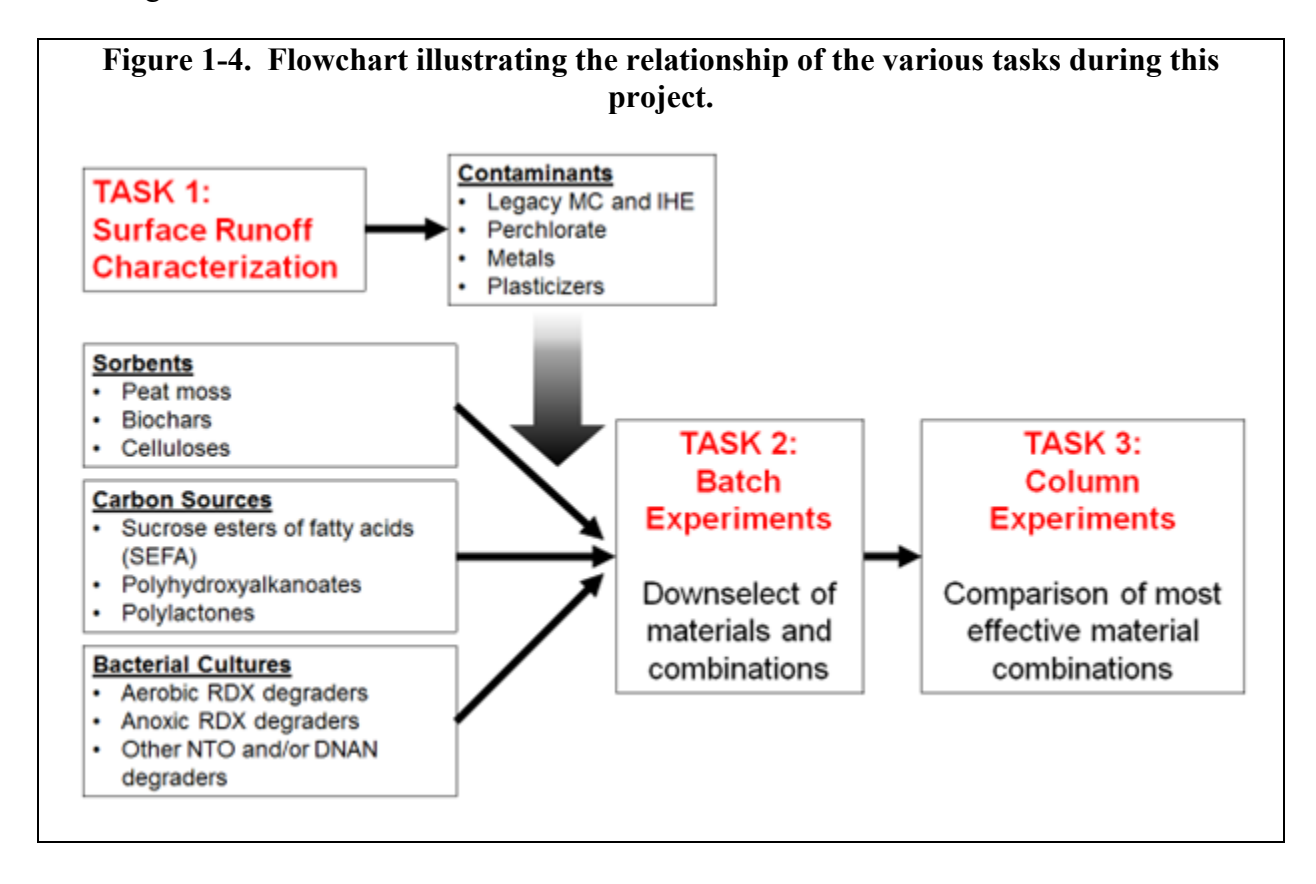
- Hypothesis 2: Biochar is a more effective sorbent than activated carbon for legacy and insensitive munitions constituents.
- Hypothesis 3: Biochar can mediate the abiotic degradation of legacy and insensitive munitions constituents in surface runoff through its capacity to store and transfer electrons.
- Hypothesis 4: Biochar can promote the biotic degradation of legacy and insensitive munitions constituents in surface runoff.

- Hypothesis 5: Slow-release carbon sources can support the biodegradation of legacy and insensitive munitions constituents in surface runoff.
- Hypothesis 6: Bioaugmentation with know explosive degrading bacterial cultures can enhance the degradation of legacy and insensitive munitions constituents in surface runoff.

Task 3. Column sorption/degradation experiments and modeling.

Hypothesis 7: Overall removal of legacy and insensitive munitions constituents from surface water will be greater when slow-release carbon sources and/or bioaugmentation are included than when they are excluded

The flow chart in Figure 1-4 illustrates the relationship of the different tasks, and summarizes the potential runoff contaminants to be tested with the sorbents, carbon sources, and cultures during this project. Methods, Results, and Discussion associated with each task are detailed in the following sections.



REFERENCES

- Ahmad, M., Rajapaksha, A.U., Lim, J.E., Zhang, M., Bolan, N., Mohan, D., Vithanage, M., Lee, S.S., Ok, Y.S., 2014. Biochar as a sorbent for contaminant management in soil and water: A review. Chemosphere 99, 19-33. https://doi.org/10.1016/j.chemosphere.2013.10.071.
- Brown, P.A., Gill, S.A., Allen, S.J., 2000. Metal removal from wastewater using peat. Water Research 34, 3907-3916.https://doi.org/10.1016/S0043-1354(00)00152-4.
- Burba, P., Willmer, P.G., 1983. Cellulose: a biopolymeric sorbent for heavy-metal traces in waters. Talanta 30, 381-383.https://doi.org/10.1016/0039-9140(83)80087-3.
- Deletic, A., Fletcher, T.D., 2006. Performance of grass filters used for stormwater treatment—A field and modelling study. Journal of Hydrology 317, 261-275.http://dx.doi.org/10.1016/j.jhydrol.2005.05.021.
- Fuller, M.E. 2015. Fate and Transport of Colloidal Energetic Residues. ER-1689. https://www.serdp-estcp.org/content/download/38250/362302/file/ER-1689-FR.pdf.
- Fuller, M.E., Hatzinger, P.B., Rungkamol, D., Schuster, R.L., Steffan, R.J., 2004. Enhancing the attenuation of explosives in surface soils at military facilities: Combined sorption and biodegradation. Environ Toxicol Chem 23, 313-324.
- Fuller, M.E., Lowey, J.M., Schaefer, C.E., Steffan, R.J., 2005. A peat moss-based technology for mitigating residues of the explosives TNT, RDX, and HMX in soil. Soil Sediment Contam 14, 373-385.
- Fuller, M.E., Schaefer, C.E., Steffan, R.J., 2009. Evaluation of a peat moss plus soybean oil (PMSO) technology for reducing explosive residue transport to groundwater at military training ranges under field conditions. Chemosphere 77, 1076-1083.
- Gray, M., Johnson, M.G., Dragila, M.I., Kleber, M., 2014. Water uptake in biochars: The roles of porosity and hydrophobicity. Biomass and Bioenergy 61, 196-205. https://doi.org/10.1016/j.biombioe.2013.12.010.

- Grebel, J.E., Charbonnet, J.A., Sedlak, D.L., 2016. Oxidation of organic contaminants by manganese oxide geomedia for passive urban stormwater treatment systems. Water Research 88, 481-491.http://dx.doi.org/10.1016/j.watres.2015.10.019.
- Hatzinger, P.B., Fuller, M.E., Rungkamol, D., Schuster, R.L., Steffan, R.J., 2004. Enhancing the attenuation of explosives in surface soils at military facilities: Sorption-desorption isotherms. Environ Toxicol Chem 23, 306-312.
- Kappler, A., Wuestner, M.L., Ruecker, A., Harter, J., Halama, M., Behrens, S., 2014. Biochar as an electron shuttle between bacteria and Fe(III) minerals. Environmental Science & Technology Letters 1, 339-344.10.1021/ez5002209.
- Klüpfel, L., Keiluweit, M., Kleber, M., Sander, M., 2014. Redox properties of plant biomass-derived black carbon (Biochar). Environmental Science & Technology 48, 5601-5611.10.1021/es500906d.
- Lapointe, M.-C., Martel, R., Diaz, E., 2017. A conceptual model of fate and transport processes for RDX deposited to surface soils of North American active demolition sites. J Environ Qual 46, 1444-1454.10.2134/jeq2017.02.0069.
- Mohan, D., Sarswat, A., Ok, Y.S., Pittman, C.U., 2014. Organic and inorganic contaminants removal from water with biochar, a renewable, low cost and sustainable adsorbent A critical review. Bioresource Technology 160, 191-202. https://doi.org/10.1016/j.biortech.2014.01.120.
- O'Connell, D.W., Birkinshaw, C., O'Dwyer, T.F., 2008. Heavy metal adsorbents prepared from the modification of cellulose: A review. Bioresource Technology 99, 6709-6724. https://doi.org/10.1016/j.biortech.2008.01.036.
- Oh, S.-Y., Cha, D.K., Chiu, P.C., 2002a. Graphite-mediated reduction of 2,4-dinitrotoluene with elemental iron. Environ Sci Technol 36, 2178-2184.10.1021/es011474g.
- Oh, S.-Y., Cha, D.K., Kim, B.-J., Chiu, P.C., 2002b. Effect of adsorption to elemental iron on the transformation of 2,4,6-trinitrotoluene and hexahydro-1,3,5-trinitro-1,3,5-triazine in solution. Environ Toxicol Chem 21, 1384-1389.

- Oh, S.-Y., Cha, D.K., Kim, B.J., Chiu, P.C., 2004. Reduction of nitroglycerin with elemental iron: Pathway, kinetics, and mechanisms. Environ Sci Technol 38, 3723-3730.10.1021/es0354667.
- Oh, S.-Y., Cha, D.K., Kim, B.J., Chiu, P.C., 2005. Reductive transformation of hexahydro-1,3,5-trinitro-1,3,5-triazine, octahydro-1,3,5,7-tetranitro-1,3,5,7-tetrazocine, and methylenedinitramine with elemental iron. Environ Toxicol Chem 24, 2812-2819.10.1897/04-662R.1.
- Oh, S.-Y., Chiu, P.C., 2009. Graphite- and soot-mediated reduction of 2,4-dinitrotoluene and hexahydro-1,3,5-trinitro-1,3,5-triazine. Environ Sci Technol 43, 6983-6988.
- Oh, S.-Y., Seo, Y.-D., Jeong, T.-Y., Kim, S.-D., 2018. Sorption of nitro explosives to polymer/biomass-derived biochar. Journal of Environmental Quality.10.2134/jeq2017.09.0357.
- Oh, S.-Y., Son, J.-G., Chiu, P.C., 2013. Biochar-mediated reductive transformation of nitro herbicides and explosives. Environ Toxicol Chem 32, 501-508.
- Prévoteau, A., Ronsse, F., Cid, I., Boeckx, P., Rabaey, K., 2016. The electron donating capacity of biochar is dramatically underestimated. Scientific Reports 6, 32870.10.1038/srep32870 https://www.nature.com/articles/srep32870#supplementary-information.
- Roden, E.E., Kappler, A., Bauer, I., Jiang, J., Paul, A., Stoesser, R., Konishi, H., Xu, H., 2010. Extracellular electron transfer through microbial reduction of solid-phase humic substances. Nature Geoscience 3, 417.10.1038/ngeo870 https://www.nature.com/articles/ngeo870#supplementary-information.
- Sander, M., Pignatello, J.J., 2005. Characterization of charcoal adsorption sites for aromatic compounds: insights drawn from single-solute and bi-solute competitive experiments. Environ Sci Technol 39, 1606-1615.10.1021/es0491351.
- Sansalone, J.J., 1999. In-situ performance of a passive treatment system for metal source control. Water Science and Technology 39, 193-200. http://dx.doi.org/10.1016/S0273-1223(99)00023-2.

- Saquing, J.M., Yu, Y.-H., Chiu, P.C., 2016. Wood-derived black carbon (biochar) as a microbial electron donor and acceptor. Environmental Science & Technology Letters 3, 62-66.10.1021/acs.estlett.5b00354.
- Schaefer, C.E., Fuller, M.E., Lowey, J.M., Steffan, R.J., 2005. Use of peat moss amended with soybean oil for mitigation of dissolved explosive compounds leaching into the subsurface: Insight into mass transfer mechanisms. Environ Eng Sci 22, 337-349.
- Seelsaen, N., McLaughlan, R., Moore, S., Ball, J.E., Stuetz, R.M., 2006. Pollutant removal efficiency of alternative filtration media in stormwater treatment. Water Science and Technology 54, 299-305.10.2166/wst.2006.617.
- Sun, T., Levin, B.D.A., Guzman, J.J.L., Enders, A., Muller, D.A., Angenent, L.T., Lehmann, J., 2017. Rapid electron transfer by the carbon matrix in natural pyrogenic carbon. Nature Communications 8, 14873.10.1038/ncomms14873
- https://www.nature.com/articles/ncomms14873#supplementary-information.
- Todde, G., Jha, S.K., Subramanian, G., Shukla, M.K., 2018. Adsorption of TNT, DNAN, NTO, FOX7, and NQ onto cellulose, chitin, and cellulose triacetate. Insights from Density Functional Theory calculations. Surface Sci 668, 54-60.https://doi.org/10.1016/j.susc.2017.10.004.
- Wan Ngah, W.S., Hanafiah, M.A.K.M., 2008. Removal of heavy metal ions from wastewater by chemically modified plant wastes as adsorbents: A review. Bioresource Technology 99, 3935-3948. https://doi.org/10.1016/j.biortech.2007.06.011.
- Xie, T., Reddy, K.R., Wang, C., Yargicoglu, E., Spokas, K., 2015. Characteristics and applications of biochar for environmental remediation: A review. Critical Reviews in Environmental Science and Technology 45, 939-969.10.1080/10643389.2014.924180.
- Xin, D., Xian, M., Chiu, P.C., 2018. Chemical methods for determining the electron storage capacity of black carbon. MethodsX 5, 1515-1520.https://doi.org/10.1016/j.mex.2018.11.007.
- Xu, W., Dana, K.E., Mitch, W.A., 2010. Black carbon-mediated destruction of nitroglycerin and RDX by hydrogen sulfide. Environ Sci Technol 44, 6409-6415.

- Xu, W., Pignatello, J.J., Mitch, W.A., 2013. Role of black carbon electrical conductivity in mediating hexahydro-1,3,5-trinitro-1,3,5-triazine (RDX) transformation on carbon surfaces by sulfides. Environ Sci Technol 47, 7129-7136.10.1021/es4012367.
- Ye, J., Chiu, P.C., 2006. Transport of atomic hydrogen through graphite and its reaction with azoaromatic compounds. Environ Sci Technol 40, 3959-3964.10.1021/es060038x.
- Zhang, J., You, C., 2013. Water holding capacity and absorption properties of wood chars. Energy & Fuels 27, 2643-2648.10.1021/ef4000769.
- Zhu, D., Kwon, S., Pignatello, J.J., 2005. Adsorption of single-ring organic compounds to wood charcoals prepared under different thermochemical conditions. Environ Sci Technol 39, 3990-3998.10.1021/es050129e.
- Zhu, D., Pignatello, J.J., 2005. Characterization of aromatic compound sorptive interactions with black carbon (charcoal) assisted by graphite as a model. Environ Sci Technol 39, 2033-2041.10.1021/es0491376.

2. Surface Runoff Characterization

Hypothesis 1: MC and non-energetic compounds are entrained and transported in surface runoff from ranges during storm events.

2.1 METHODS

2.1.1 Field site.

The surface runoff sampling for this project was performed at the Churchill Range Explosives Experimental Area (EEA) at Navy Surface Warfare Center (NSWC) Dahlgren, VA (NSWC Dahlgren) (Figure 2-1). Previous runoff characterization work done under SERDP project ER-1689 detected low concentrations (µg/L levels) of RDX, HMX, and perchlorate, as well as some RDX breakdown products, in surface runoff near a munition testing area at NSWC Dahlgren (Fuller et al., unpublished data). At least some detonations of IHE have also occurred at this site, although no data on the presence of DNAN and NTO have been collected.

2.1.2 Field instrumentation.

The runoff samplers (Nalgene 1100-1000, Waltham, MA) were deployed in the swale that leads to the shallow retention basin located adjacent to the main explosives testing area (Arena 1) on the Churchill Range of NSWC Dahlgren. Samplers were single use. The HDPE bottle supplied by the manufacturer was replaced with a polypropylene bottle (Nalgene 2105-0032) to minimize any sorption of energetic compounds. An illustration of the samplers and a photograph of one of the emplaced samplers is shown in Figure 2-2. These were "first flush" samplers which collect about 1 L of the initial water that passes by the sampler, with a plastic float sealing off the samplers inlet once the sample is collected. New samplers were deployed for each sampling event. Sampler were placed into in-ground mounting tubes secured in the runoff channel using steel posts. The inlet to mounting tubes was positioned approximately 1" above the soil surface.

A total of 10 sampling points were installed using a bobcat auger, into which the surface runoff sampling bottle holders were emplaced. The samplers are in two groups of 3 and a group of 4 along the runoff flow path. The plan was that the water collected in the 3 (or 4) samplers at each location will be pooled after collection in order to provide sufficient volume of runoff for all the planned analyses. Photographs of the sampling locations are shown in Figure 2-3.

A water flow sensor was installed inside the surface runoff drainage pipe (24" diameter) so that the total volume of runoff at the site could be determined, and related to the amount of precipitation. The sensor was installed about 10 feet from the inlet end of the drainage pipe. The sensor cable was routed out the inlet end of the pipe and to the datalogger. The datalogger was placed inside a plastic tote, which was put behind a large steel shield to protect it from the shock and potential debris generated during explosives testing in Arena 1. Photographs of the sensor and datalogger are shown in Figure 2-4.

A solar-powered weather station was setup on the outer edge of the Churchill Range near the Potomac River (noted in Figure 2-1). The weather station will measure and log temperature, solar irradiation, and precipitation. Data will be automatically uploaded to the cloud using a cellular connection for later retrieval and analysis. A photograph of the weather station is shown in Figure 2-5.

2.1.3 Sample collection.

Surface runoff samples were collected several times over the course of the project. Sampling events were coordinated with personnel based on the timing of precipitation events. An attempt was also made to collect samples after heightened range activities in order to determine if energetics in runoff was correlated with recent detonations.

Samplers were deployed into the mounting tubes before the precipitation event, and were collected from the tubes as soon as the water in the swale had receded sufficiently. Samplers were shipped from Dahlgren to Aptim as soon as reasonably feasible.

2.1.4 Sample processing.

Once the samples arrived at Aptim, they were placed at 4°C. The ball float top of each bottle was removed and replaced with a new large mouth bottle cap. The outside of the bottle was rinsed with tap water to remove dirt and mud, dried, and then the weight of the bottle was recorded. The tare weight of an empty bottle and cap was used to calculate the sample volume in each bottle.

The contents of the bottles from each of the three sampling locations were pooled in a precleaned 4 L glass bottle and mixed with a stir bar for at least 30 minutes. The glass bottles had been cleaned and then baked at 550°C for at least 18 h. The stir bars had been soaked/rinsed with methanol, followed by acetonitrile.

```
Location 1 was comprised of bottles 1, 2, and 3.
Location 2 was comprised of bottles 4, 5, and 6.
Location 3 was comprised of bottles, 7, 8, 9, and 10.
```

Aliquots of the well mixed sample (water plus suspended solids) were transferred to bottles for:

- a. Total solids (ATL020 (EPA 160.3))
- b. Total carbon (loss on combustion)
- c. Total TAL metals (EPA 6020) + Hg for the last two samples
- d. Total plasticizers (EPA 525.2 or similar; selected early samples)

The remainder of the sample was then processed by vacuum filtration into a precleaned glass flask (rinsed and baked at 550°C for at least 18 h). A new single use analytical filter funnel (Nalgene 1452045) and filter stack was used for each sample. The filter stack comprised of glass microfiber filters with cutoffs of 5 μ m (top; ValuSep 26547, 47 mm), 2.7 μ m (middle; Whatman GF/D 1823-047, 47 mm), and 0.7 μ m (bottom; Whatman GF/F 1825-047, 47 mm). The filter stack was replaced if it became clogged. The dissolved phase concentration was defined as the concentration measured in a representative surface runoff sample after it had passed through a preweighed filter stack (e.g., <0.7 μ m).

Sufficient filtrate was generated from each sample for the analysis of:

```
a. pH (ATL008 (EPA 150.1))b. Specific conductivity (ATL005 (EPA 120.1))
```

- c. Dissolved anions (ATL017 (EPA 300.0))
- d. Dissolved total organic carbon and total carbon (ATL010 (SM5310B,C,D))
- e. Dissolved TAL metals (EPA 6020) + Hg for the last two samples
- f. Dissolved plasticizers (EPA 525.2 or similar; selected earlier samples)
- g. Legacy explosives (SPE followed by ATL043 (EPA 8330))
- h. NDAB (ATL071)
- i. DNAN (SPE followed by ATL043)
- j. NTO (SPE followed by ATL072)
- k. NQ (ATL072)
- 1. Perchlorate (EPA 6850)

The filtrate portions designated for energetics analyses underwent additional processing. Filtrate for analysis of NDAB was passed though a sterile 0.45 μ m glass microfiber syringe filter into a sterile polypropylene tube. Similarly, filtrate for perchlorate was passed through a sterile 0.45 μ m surfactant free cellulose acetate syringe filter into duplicate sterile polypropylene tubes.

The filtrate for EPA 8330 and DNAN analyses was analyzed unconcentrated and after solid phase extraction (SPE). The SPE protocols are included in Appendix C.

The filters and retained solids were dried overnight at 105°C and weighed again to allow the mass of solids to be calculated. The filter and solids were then extracted with acetonitrile in a water-cooled ultrasonic batch for 18 h. All the filters for a given sample were extracted together.

2.1.5 Sample analyses.

The analytical sampling plan and methods are listed in Table 2-1. Major water quality parameters including pH, major anions, total organic carbon (TOC), total solids (TS), loss on combustion, and conductivity were also be measured.

Dissolved energetic analytes included legacy explosives and their respective breakdown products, insensitive munition constituents (e.g., DNAN, NTO, NQ) and their breakdown products, and perchlorate.

The filter and retained solids extract was analyzed initially, and after a portion had been concentrated approximately 10-fold, for legacy and IM energetics. This allowed the particulate-associated concentration to be calculated.

Additional methods to screen for nonenergetic semivolatile compounds like plasticizer components (e.g., di-(2-ethylhexyl)sebacate (also called dioctyl sebacate), dioctyl adipate), polyisobutylene, stearic acid and related stearates, and paraffin-based materials were also used. The compounds of interest are shown in Table 2-2. These analyses were performed by an outside analytical contract laboratory, the Materials Science and Engineering Division of Smithers, Inc., as follows:

Samples of an artificial surface runoff (ASR) based on the general water chemistry of the actual runoff (Fuller et al., 2022), as well as ASR that had been passed through the surface runoff collection apparatus, were also sent to Smither to serve as blanks/controls.

Smithers performed multiple approaches to examine the runoff for the target compounds, as follows:

Test Protocol 1 – Direct Injection. Direct injection of aqueous samples was carried out using a sample size of 16 mL that had been evaporated to 1 mL using a TurboVap- LV nitrogen evaporator. The sample was filtered through a $0.45~\mu m$ syringe filter and injected into the GC-MS for analysis. The clients samples were compared against a sample of ultrapure HPLC grade water was also analyzed for comparison.

Test Protocol 2 – Liquid-Liquid Extraction. Liquid-liquid extraction was carried out using 50 mL of sample and three, 100 mL aliquots of chloroform in a 1 L separatory funnel. The extracts were evaporated to 10 mL using a TurboVap- LV nitrogen evaporator. GC-MS analysis was carried out using 1 mL of sample extract.

Test Protocol 3 – Analysis of Boundary Layer Film. During liquid-liquid extraction, a film was observed between the aqueous and organic layer. The film was removed and dissolved in 2 mL of methanol and analyzed via GC-MS.

Test Protocol 4 – Solid Phase Extraction, Florisil. In an effort to selectively separate the analytes of interest, each aqueous sample was worked up by passing 4 mL through a Resprep SPE Florisil column. The column was washed with two 1 mL aliquots of HPLC grade methanol. The methanol wash was then transferred to a 2 mL vial and analyzed via GC-MS. Client samples were compared against a sample of ultrapure water also passed through the Florisil column.

Test Protocol 5 – Solid Phase Extraction, C18. In order to obtain a higher concentration of analyte (if present), 100 mL of the aqueous sample were drawn through a Resprep SPE C18 column. The triplicate runoff total and dissolved (<0.7 µm filtered) samples from the 17 October 2019 collection event were pooled prior to processing to obtain sufficient volume. The column was washed with 15 mL of dichloromethane and evaporated to a volume of 1 mL prior to analysis via GC-MS. A control sample of 15 mL dichloromethane was passed through a C18 column and evaporated down to 1 mL to be analyzed for comparison.

Table 2-1. Analytical methods employed during surface runoff sample characterization.

Analyte	Laboratory	Method	TOTAL	DISSOLVED (<0.7 μm)
Legacy Explosives	Aptim	ATL043 ¹ (EPA 8330) with solid phase extraction (SPE)	Y ²	Y
NDAB	Aptim	ATL071 ³	Y2	Y
DNAN	Aptim	ATL043 with SPE ⁴	Y ²	Y
NTO	Aptim	ATL072 with SPE ⁵	Y ²	Y
NQ	Aptim	ATL072 ⁵	Y ²	Y
Perchlorate	External	EPA 6850		Y
Plasticizers, Binders, Waxes	External	Customized GC/MS with SPE	Υ	Y
TAL Metals	External	EPA 200.7	Υ	Y
Anions	Aptim	ATL017 (EPA 300.0)		Y
Ammonia	Aptim	HACH 8155 (Colorimetric)		Y
Total Carbon (TOC/TC)	Aptim	ATL010 (SM5310B,C,D)		Y
Total Solids (TS)	Aptim	ATL020 (EPA 160.3)		
Loss on Combustion	Aptim	ATL024 (SM2540)		
рН	Aptim	ATL008 (EPA 150.1)		Y
Conductivity	Aptim	ATL005 (EPA 120.1)		Y

¹ Note: In-house ATL methods are based on existing EPA Methods or methods published in the peer-reviewed literature, and include appropriate protocols for calibration and quality control.

Table 2-2. List of potential binders and plasticizers in surface runoff.

Dioctyl adipate	CAS: 123-79-5
Di-(2-ethylhexyl)sebacate (DEHS), or dioctyl sebacate	CAS: 122-62-3
Polyisobutylene	CAS: 9003-27-4
Paraffin oil	CAS: 8012-95-1
Paraffin wax	CAS: 8002-74-2
Strearic acid	CAS: 57-11-4
Stearates	(various CAS)

² Sum of explosives detected in filtered solids (converted to mass per vol) plus mass of detected dissolved explosives.

³ ref (Fournier et al., 2002); ⁴ ref (Perreault et al., 2012); ⁵ ref (Krzmarzick et al., 2015)



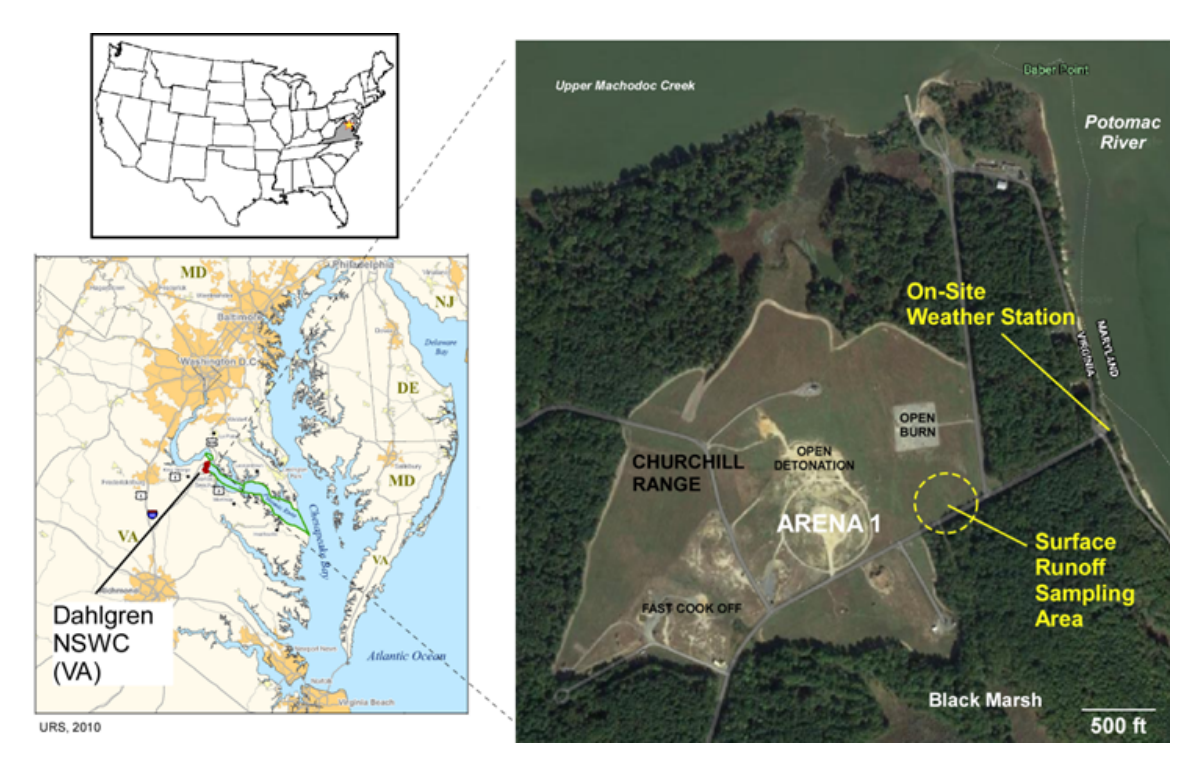


Figure 2-2. Illustrations and photographs of the surface runoff samplers utilized during this project.

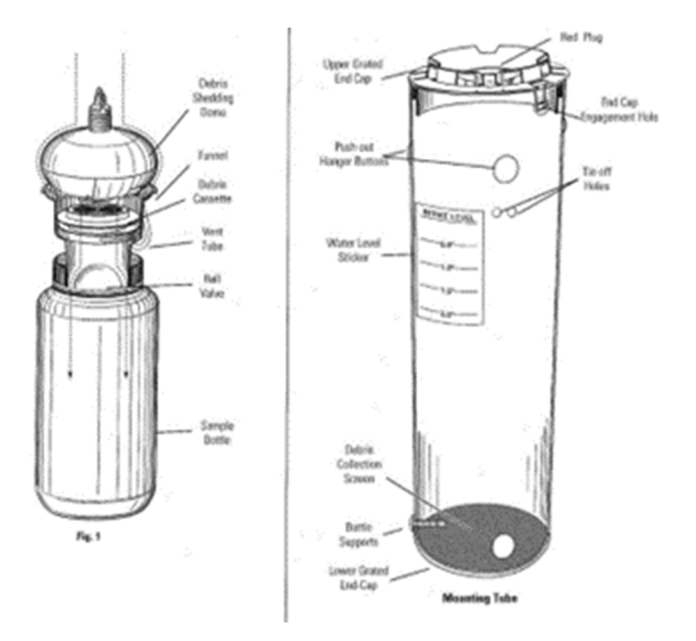








Figure 2-3. Location of the surface runoff samplers at NSWC Dahlgren, Churchill Range.

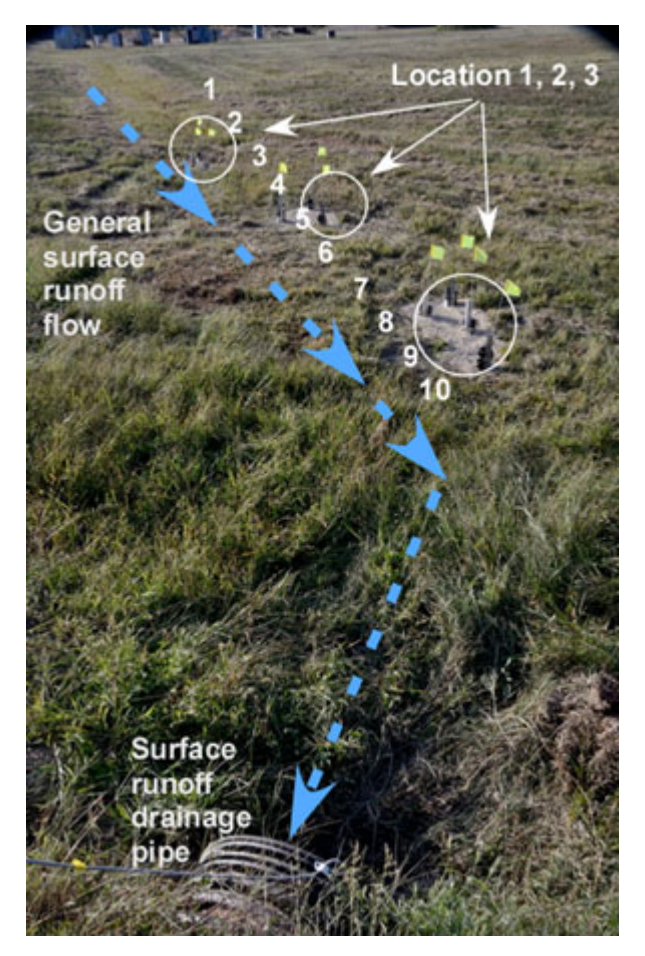
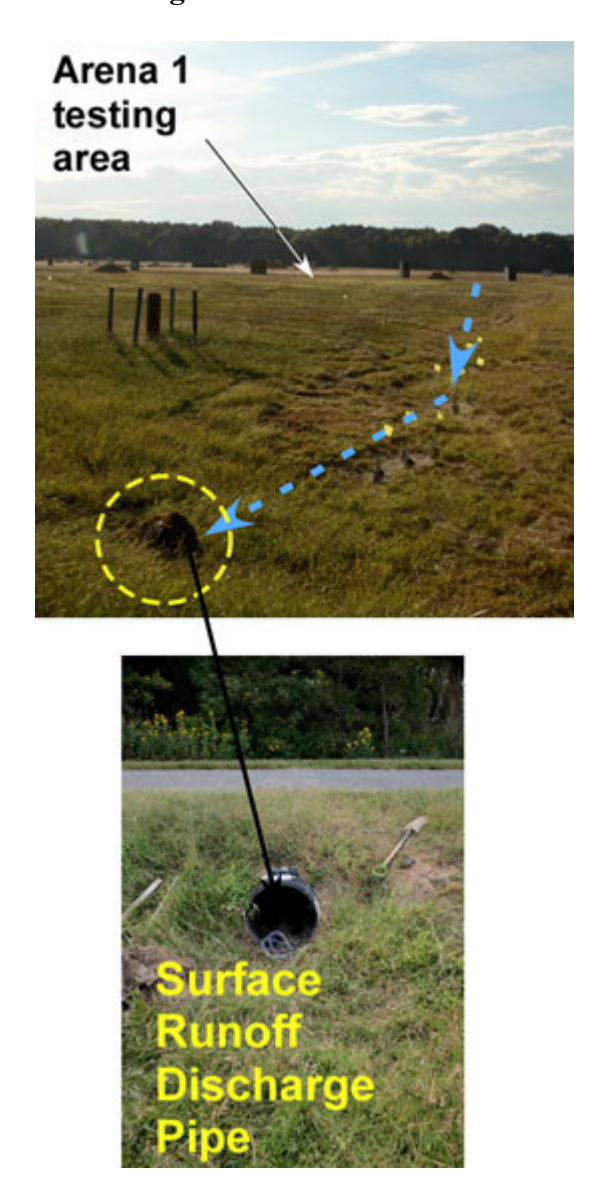
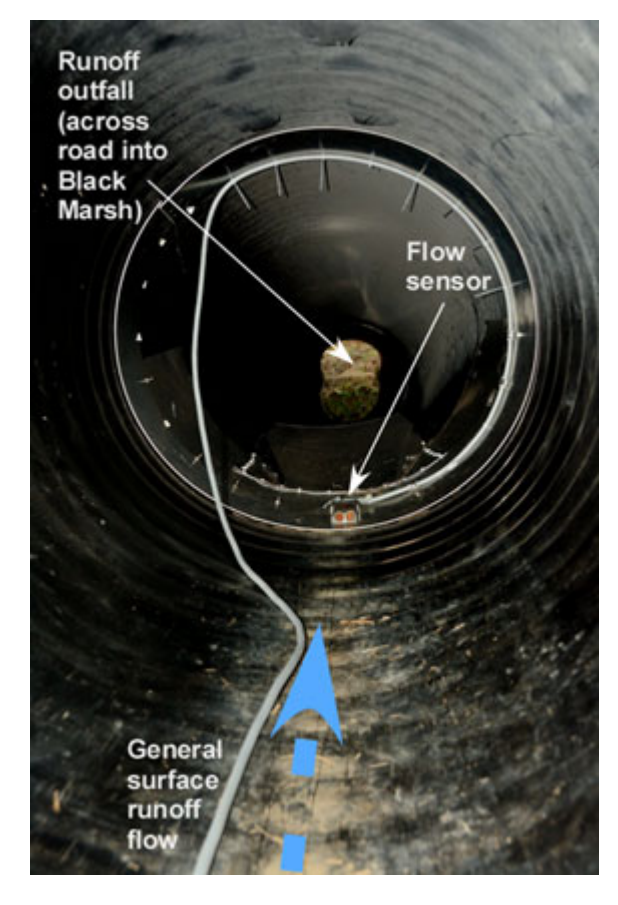




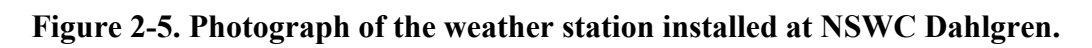
Figure 2-4. Placement of the runoff flow meter sensor and datalogger.













2.2 RESULTS and DISCUSSION

2.2.1 Sampling events, weather data, and range activity.

A total of six sampling events occurred over the course of the project. The dates of these events were: October 2019, January 2020, June 2020, November 2020, July 2021, and November 2022. Graphs of precipitation events and the volumes of runoff passing through the swale where the samplers were located are presented in Figure 2-6 and Figure 2-7, respectively.

Based on information provided by NSWC Dahlgren, the mass of legacy and insensitive munition constituents detonated on the range was calculated for the end of 2019 and most of 2020. These data a shown in Figure 2-8, with the collection of runoff samples also indicated.

2.2.2 Geochemistry.

Table 2-3 summarizes the geochemical characterization of the surface runoff samples. The pH was slightly subneutral on average, and generally contained 10's of mg/L of TOC and low concentrations (1-2 mg/L) of nitrate and ammonia.

2.2.3 Energetics.

The detections of dissolved energetics in surface runoff are shown in Table 2-4. No energetics were detected when filtered solids were extracted. Using the detected concentrations of HMX, RDX, and ClO₄⁻ from the January 2020 sampling event multiplied by the corresponding volume of runoff, the mass loadings into Black Marsh from surface runoff were ~0.1 g for perchlorate, 0.429 g for RDX, and to almost 0.837 g for HMX.

Although there was a reasonable overlap between the range activity data and the collection of runoff samples for 2019/2020, a clear correlation between range activities and presence of energetics in runoff samples was not established. For instance, the October 2019 sample contained only ClO₄⁻, while there had been a modest amount of RDX and TNT detonated within a month or two of runoff collection. Not detecting TNT is reasonable, since it is retained more strongly by sorption to soil, but RDX residue should have been more mobile.

Looking to the end of 2020, there were larger detonations of RDX (1.39 kg), NTO (4.81 kg), and DNAN (2.88) in August. It could reasonably be assumed that the detonations were not 100% complete, and perhaps that ~2% of the energetic mass remained (Taylor et al., 2004). This would amount to energetic residues of approximately 28, 96, and 58 g for RDX, NTO, and DNAN. Between the time of the detonations and the time of runoff sampling, a total of 1.6 x 10^7 L of runoff had passed through the sampling zone, which would result in concentrations of 1.8, 6.1, and 3.7 μ g/L (assuming instantaneous dissolution and all the mass dissolved into all the water at one time). These estimated concentrations are 30- to 60-fold higher than the analytical detection limits using our SPE protocol, so if these energetics were present in the runoff, it would have been expected that they would have been detected, but they were not.

It is likely that other variable may have impacted their detection, including (but not limited to): photolysis, sorption (especially for DNAN), generation of larger residues that dissolved much slower (especially for RDX), or rapid dissolution and transport into the soil rather than overland in surface runoff (especially for NTO). It is also possible that surface runoff coming from the Arena 1 testing area was not effectively sampled by the placement of the runoff samplers.

2.2.4 *Metals*.

TAL metal concentrations in the surface runoff samples are summarized in Table 2-5. Two detections of aluminum and one detection of iron were above the 2018 Secondary Drinking Water Regulations. One detection of vanadium was above the level set in the Unregulated Contaminant Monitoring Rule 3. However, the Blank QC for these compounds for these metals was also elevated, so it is unclear if these were actual in exceedance of any current regulations. No mercury was detected in the samples analyzed.

2.2.5 Other analytes.

The testing performed by Smithers on the October 2019 runoff samples looking for binders and plasticizers are shown in Figures 2-9, 2-10, and 2-11. None of the target analytes listed in Table 1-1 were detected in either the ASR blank or the runoff samples. Tridecane was detected in the ASR control as well as both the dissolved and total runoff sample, indicating it was likely coming from the surface runoff sampling device, which is composed of plastic and rubber components. The dissolved sample (passed through a <0.7 µm filter) did not contain any compounds other than tridecane (Figure 2-10), while the total sample (aqueous runoff plus associated solids) contained multiple other compounds (Figure 2-11). These included several saturated and unsaturated hydrocarbons, and also one unidentified peak. It is suspected that most of these compounds are derived from fresh or aged plant matter entrained in the runoff, and are not directly related to range activities.

Analysis of composite runoff samples (including suspended solids) from January, June, and November of 2020 did not detect any binders or plasticizers (Figure 2-12). The July 2021 sample also contained none of these compounds (data not shown).

Overall, these results would indicate that, at least within the limitations of the methods employed, waxes, plasticizers, and binders are not likely a major contaminant in surface runoff at NSWC Dahlgren.

2.3 CONCLUSIONS

These results indicate that there was sporadic detections of energetics in the surface runoff at NSWC Dahlgren, although total loadings could be close to 1 g during a single event. Metals and other non-energetic compounds (waxes, binders, plasticizers) in runoff from the range appeared to no be not an issue. No clear correlation between the timing of detonation events and detection of energetics in runoff were established.

As more assessment of surface runoff from ranges is conducted, it would be recommended that the flow paths for the runoff be definitively established, and that the capture efficiency be estimated, perhaps through the use of tracer compounds. Additionally, more frequent sample collection would be beneficial, especially if it can be more closely aligned with range activities.

Table 2-3. Summary of surface runoff geochemical parameters.

		BASIC GEOCI	HEMISTRY						
		FILTERED				UNFILTE	RED		
	PQL>>			1	1		20	20	
								Total Carbon	
						Total S	olids	(TC) [Loss on	Percent C
Sample ID		pН	Conductivity	TOC	TC		(TS)	Combustion]	in TS
		S.U.	µmhos/cm	mg/L	mg/L	r	ng/L	mg/L	%
October 2019		6.0 ± 0.2	154 ± 36	44.4 ± 10.6	50.3 ± 27.5	210.0 ±	31.0	166.2 ± 35.3	79 ± 12
January 2020		6.0 ± 0.2	62 ± 11	9.2 ± 2.1	12.9 ± 2.6	145.7 ±	25.7	95.3 ± 12.7	67 ± 9
June 2020		6.6 ± 0.1	91 ± 27	29.3 ± 6.8	48.3 ± 12.1	80.7 ±	41.1	68.1 ± 22.1	90 ± 18
November 2020		6.6 ± 0.2	58 ± 10	31.8 ± 8.5	56.5 ± 6.5	326.8 ± 2	200.6	176.2 ± 62.4	62 ± 26
July 2021		7.0 ± 0.1	77 ± 35	30.0 ± 16.5	42.1 ± 23.8	94.4 ±	63.0	85.1 ± 60.1	92 ± 14
July 2021									

		DISSOLVED	Analytes						
		Anions							
	PQL>>	0.1	0.1	0.1	0.1	0.1	0.1	0.1	0.02
Sample ID		F	CI	SO4	Br	PO4	NO2	NO3	NH4
		mg/L							
October 2019		0.2 ± 0.1	12.6 ± 4.0	16.5 ± 2.5	0.2 ± 0.1	1.0 ± 0.6	0.0 ± 0.0	1.6 ± 0.5	1.4 ± 0.7
January 2020		0.1 ± 0.0	2.2 ± 0.3	9.2 ± 2.8	0.0 ± 0.0	0.1 ± 0.0	0.0 ± 0.0	0.4 ± 0.3	0.2 ± 0.1
June 2020		0.0 ± 0.0	5.6 ± 2.1	4.5 ± 1.4	0.1 ± 0.0	0.5 ± 0.2	0.0 ± 0.0	0.9 ± 0.6	2.1 ± 0.4
November 2020		0.0 ± 0.0	2.6 ± 0.0	3.6 ± 0.8	0.1 ± 0.0	0.0 ± 0.0	0.0 ± 0.0	0.0 ± 0.0	0.4 ± 0.2
July 2021		0.0 ± 0.0	4.8 ± 4.2	11.8 ± 4.1	0.3 ± 0.2	0.4 ± 0.1	0.0 ± 0.0	0.1 ± 0.1	0.8 ± 0.2
November 2022		0.0	10.8	16.8	0.0	1.1	0.0	1.2	0.8

Table 2-4. Summary of energetics concentrations detected in surface runoff.

1	TOTAL (m	g/kg)			
PQL >>	0.04	0.04	0.05	0.5 -	6.5*
Sample Date	HMX	RDX	CIO ₄	НМХ	RDX
October 2019	-	-	0.4 ± 0.0	-	-
January 2020	5.9	1.7 ± 1.3	0.8 ± 0.6	-	-
June 2020	-	-	-	-	-
November 2020	-	-	-	-	-
July 2021	-	-	0.4 ± 0.6	-	-
November 2022	-	-	-	-	-

⁻ below PQL

^{*} PQL varied based on mass of solids > 0.7 μm recovered for extraction

Table 2-5. Summary of TAL metals concentrations in surface runoff.

EPA
Primary Drinking Water Regulations
Lifetime Health Advisory Levels (2018)
Secondary Drinking Water Regulations (2018)
Unregulated Contaminant Monitoring Rule 3

				DISSOLVE	D										
PQL ^a			MCL	Oct 2019		Jan 2020		June 2020		Nov 2020		July 2021		Nov 2022	
μg/L			μg/L	AVG	STDEV	AVG	STDEV	AVG	STDEV	AVG	STDEV	AVG	STDEV	AVG	STDEV
20.0	Aluminum	Al	50	354	124	2,475	3,122	103	1	94	35	320	221	350	_b
6.0	Antimony	Sb	6	0.57	0.09	0.90	0.29	0.63	0.13	1.02	0.07	0.37	0.00	0.98	-
5.0	Arsenic	As	10	0.93	0.15	0.68	0.21	0.50	0.13	1.04	0.10	0.77	0.25	1.00	-
3.0	Barium	Ba	2000	113	27	73	9	64	19	93	9	68	15	83	-
1.0	Beryllium	Be	4	0.12	0.00	0.06	0.10	0.00	0	0.00	0	0.14	0	0.00	-
1.0	Cadmium	Cd	5	0.49	0.21	0.28	0.18	0.12	0.06	0.05	0.00	0.19	0.15	0.34	-
200.0	Calcium	Ca		7,057	731	3,820	1,191	3,553	1,490	4,523	1,177	4,793	1,833	9,200	-
10.0	Chromium	Cr	100	0.75	0.23	2.67	2.72	0.00	0.00.	1.45	0.00.	0.78	0.00.	0.86	-
1.0	Cobalt	Co		0.43	0.39	0.49	0.40	0.27	0	0.71	0	0.68	0	0.25	-
2.0	Copper	Cu	1300	10.3	0.5	3.8	1.1	3.6	0.5		1.2	4.1	1.1	6.8	-
40.0	Iron	Fe	300	209	168	768	539	84	28	1,374	944	164	70	280	-
3.0	Lead	Pb	15	0.45	0.26	1.32	0.68	0.20	0		0	0.32	0	0.46	-
40.0	Magnesium	Mg		2,153	224	1,325	694	940	325	1,127	103	2,110	877	2,600	-
3.5	Manganese	Mn	300	79	121	58	59	35	34	173	257	177	53	26	-
3.0	Nickel	Ni	100	5.7	1.0	2.4	1.6	1.8	0.6	1.9	0.4	0.0	0.0	2.9	-
50.0	Potassium	K		17,300	9,456	2,103	333	7,830	2,606		1,019	7,460	4,183	12,000	-
5.0	Selenium	Se	50	0.00	0.00	0.00	0.00	0.91	0.10		0.00	0.00	0.00	0.00	-
1.0	Silver	Ag	100	0.05	0.00	0.01	0.02	0.05	0.00	0.00	0.00	0.00	0.00	0.03	-
100.0	Sodium	Na		4,403	323	3,247	627	1,823	225	2,447	582	2,780	943	2,900	-
1.0	Thallium	TI	2	0.41	0.36	0.29	0.23	0.35	0		0	0.00	0	0.31	-
6.0	Vanadium	V	21	3.8	0.9	6.4	3.2	4.3	1.0		1.9	1.6	0.4	25.0	-
20.0	Zinc	Zn	2000	163	28	250	167	238	47	82	12	257	58	110	-
0.2	Mercury	Hg	2	NA°	NA	NA	NA	NA	NA	NA		0.0	0.0	0.0	-

				TOTAL											
PQL			MCL	Oct 2019		Jan 2020		June 2020		Nov 2020		July 2021		Nov 2022	
µg/L			μg/L	AVG	STDEV	AVG	STDEV	AVG	STDEV	AVG	STDEV	AVG	STDEV	AVG	STDEV
20.0	Aluminum	Al	50	1,690	805	4,733	1,886	1,120	139	6,907	5,742	718	256	2,500	-
6.0	Antimony	Sb	6	0.46	0.09	0.66	0.30	0.69	0.13	1.10	0.11	0.41	0.02	1.10	
5.0	Arsenic	As	10	1.17	0.21	1.33	0.32	0.82	0.18	5.67	3.32	0.84	0.21	1.70	
3.0	Barium	Ba	2000	70	17	36	3	25	10	69	43	32	14	39	
1.0	Beryllium	Be	4	0.16	0.07	0.21	0.06			0.31	0	0.15	0	0.14	
1.0	Cadmium	Cd	5	0.81	0.05	0.31	0.12	0.24	0.13	0.40	0.32	0.46	0.11	0.47	-
200.0	Calcium	Ca	-	7,343	1,018	4,110	918	3,820	1,499	5,963	1,367	4,937	2,040	9,500	
10.0	Chromium	Cr	100	2.40	0.95	6.10	2.34	1.40	0.17	9.27	0.00.	1.16	0.00.	3.90	
1.0	Cobalt	Co		1.27	0.12	1.63	0.67	0.38	0.18	10.67	0	0.98	0	0.69	
2.0	Copper	Cu	1300	12.3	1.2	8.5	2.3	6.8	1.7	13.5	7.2	8.2	4.0	14.0	
40.0	Iron	Fe	300	998	560	3,420	1,654	717	47	22,380	14,912	541	179	1,900	
3.0	Lead	Pb	15	2.17	0.47	4.80	1.23	1.33	0.35	9.67	0	0.95	0	2.70	
40.0	Magnesium	Mg		2,143	234	1,397	117	1,089	313	2,223	1,069	1,361	640	5,400	
3.5	Manganese	Mn	300	249	52	118	38	69	24	2,437	1,190	216	54	54	
3.0	Nickel	Ni	100	6.8	0.4	4.3	1.0	2.7	1.1	6.8	4.7	0.0	0.0	4.1	
50.0	Potassium	K		17,933	9,437	2,443	235	8,273	2,520	6,330	1,247	7,947	4,402	12,000	
5.0	Selenium	Se	50	0.00	0.00	0.00	0.00	0.00	0.00	0.61	0.00	0.00	0.00	0.00	
1.0	Silver	Ag	100	0.07	0.02	0.08	0.02	0.10		0.13	0.07	0.04	0.01	0.07	
100.0	Sodium	Na		3,890	342	2,723	671	1,473	243	2,063	595	2,373	1,055	2,900	
1.0	Thallium	TI	2	1.25	1.60	0.68	0.72	0.70	0.71	0.78	0	0.13	0	0.51	
6.0	Vanadium	V	21	5.5	1.1	10.9	4.2	5.9	0.5	16.0	10.6	2.4	0.4	23.0	
20.0	Zinc	Zn	2000	108	4	251	175	290	106	125	53	308	58	110	
0.2	Mercury	Hg	2	NA	NA	NA	NA	NA	NA	NA		0.0	0.0	0.0	

U.2 Mercury Hg 2 NA NA NA NA NA NA NA NA Highlighted values indicate high values in QC blanks also detected.

**A Values below the PQL reflect inclusion of J (estimated) values in the calculation of the average and standard deviation.

Not applicable.

Not analyzed.

Figure 2-6. Recorded precipitation and runoff sample collection (red squares) during this project.

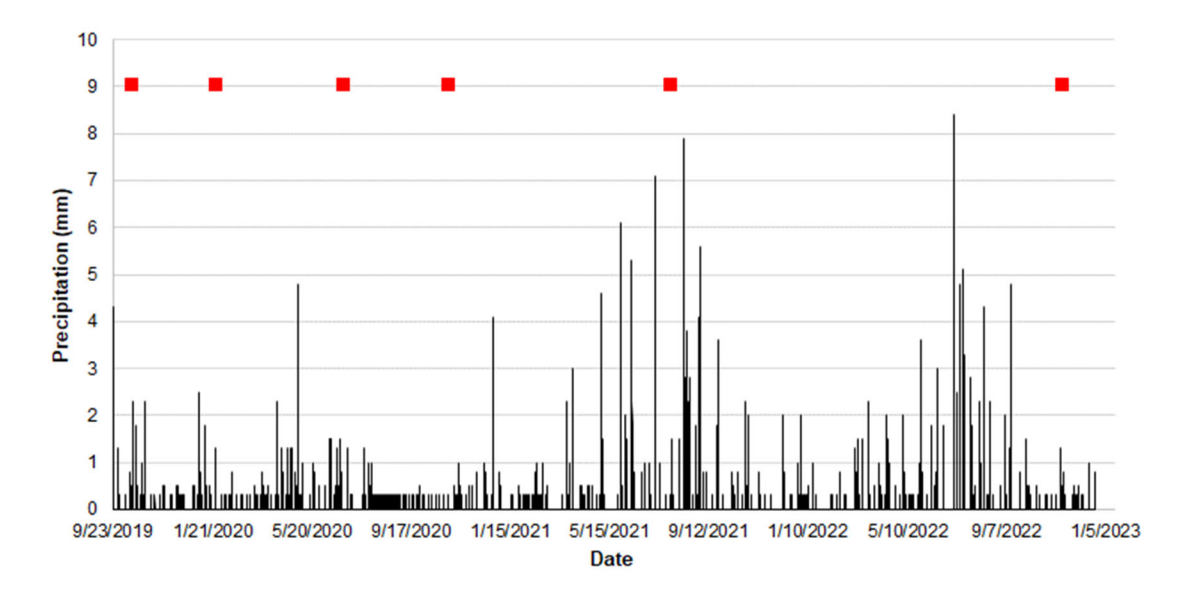
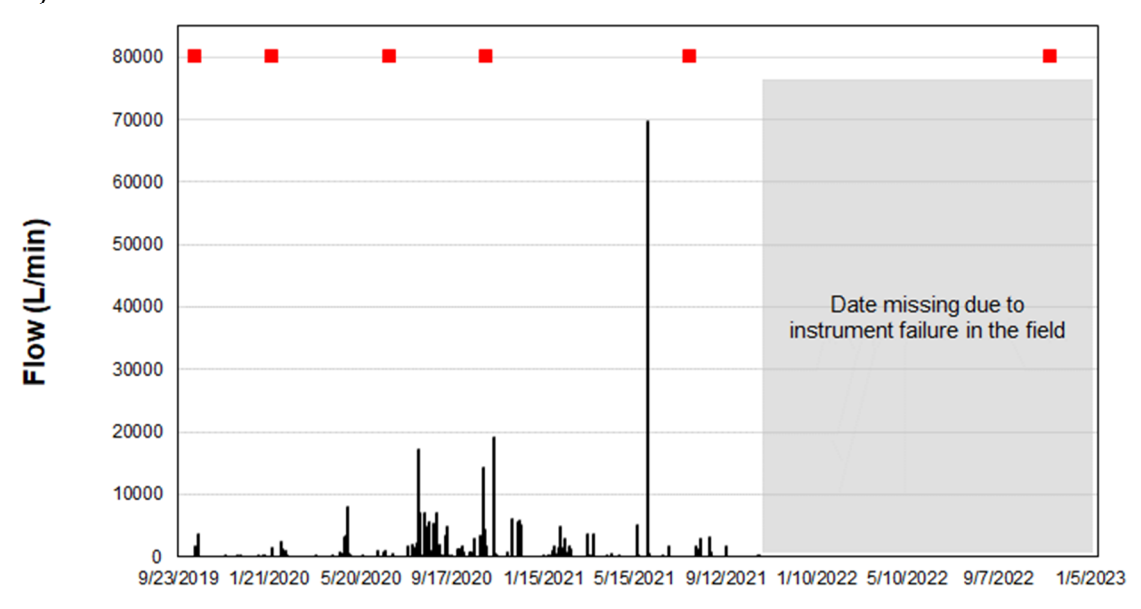


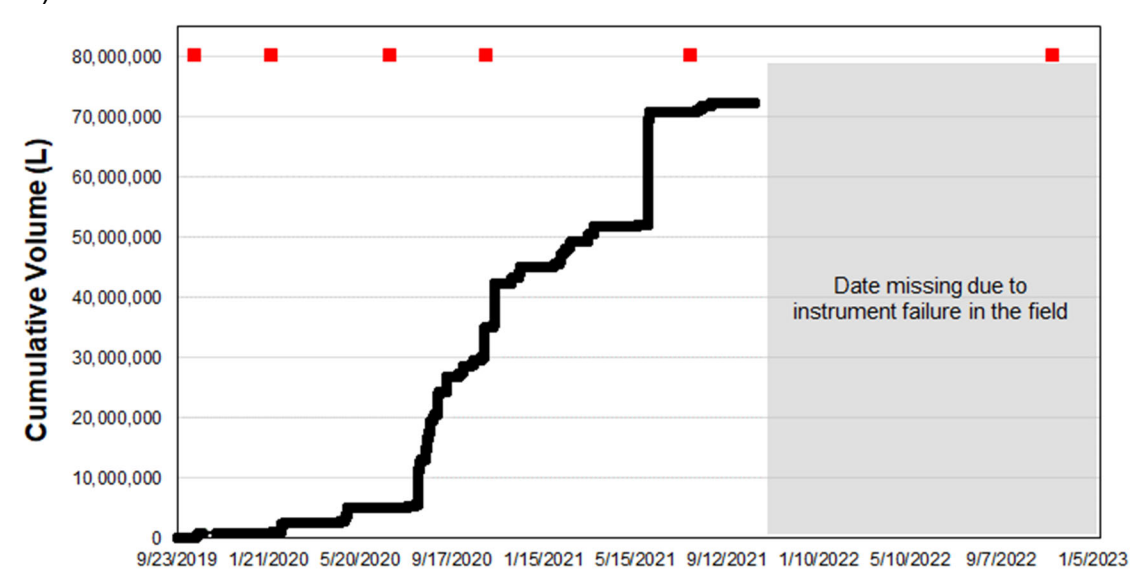
Figure 2-7. Recorded runoff flow (a) and cumulative runoff volume (b).

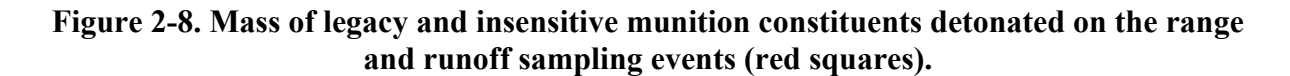
Runoff collection events are designated by the red squares. The flow sensor had a non-recoverable failure at the end of 2021, with data loss thereafter.

a) Runoff flow



b) Cumulative runoff volume





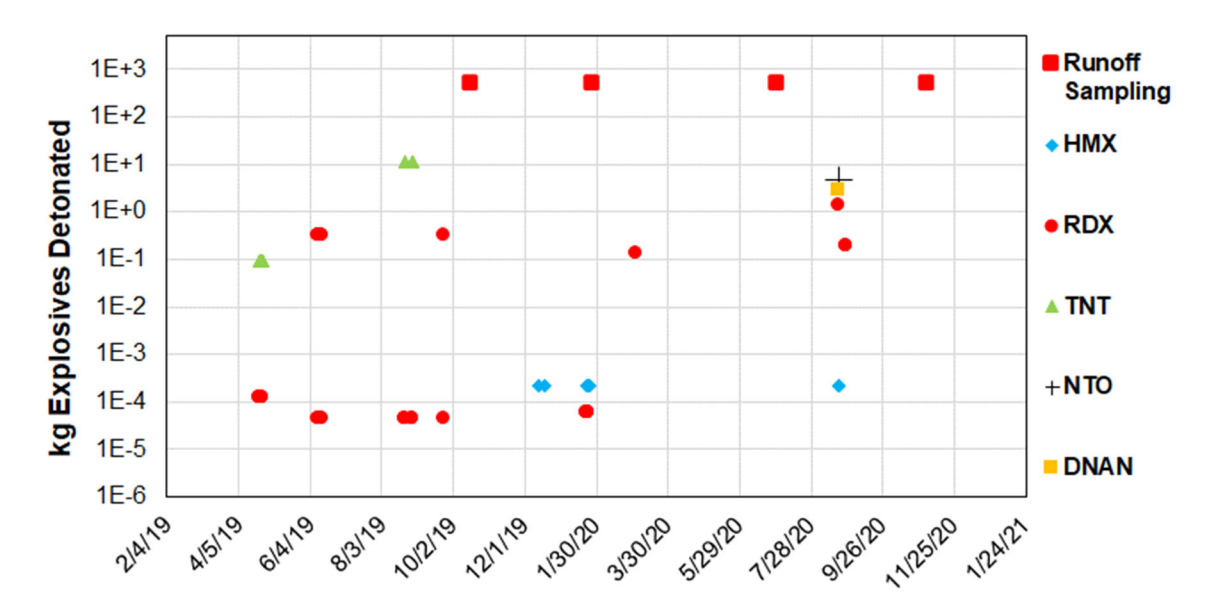
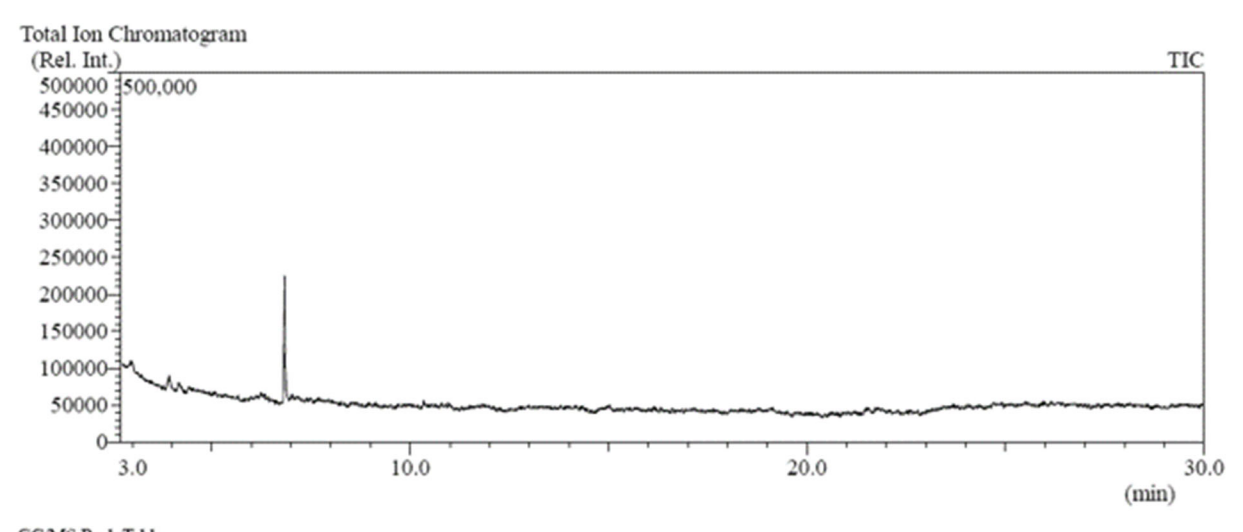
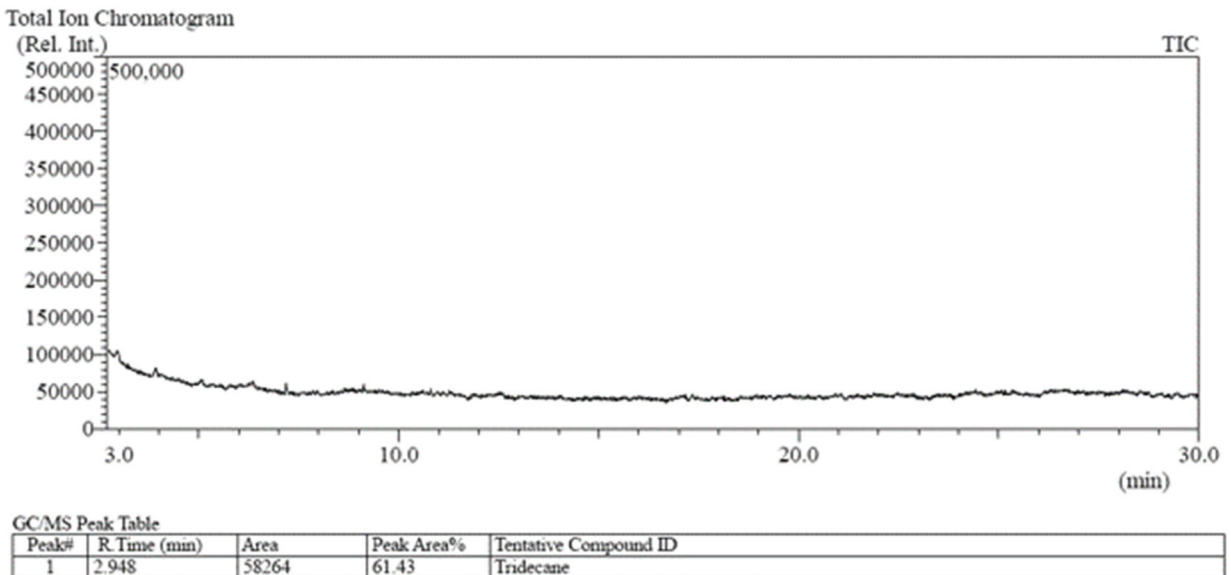


Figure 2-9. GC-MS analysis of control ASR passed through the surface runoff sampling device after 100X preconcentration via C18 SPE.



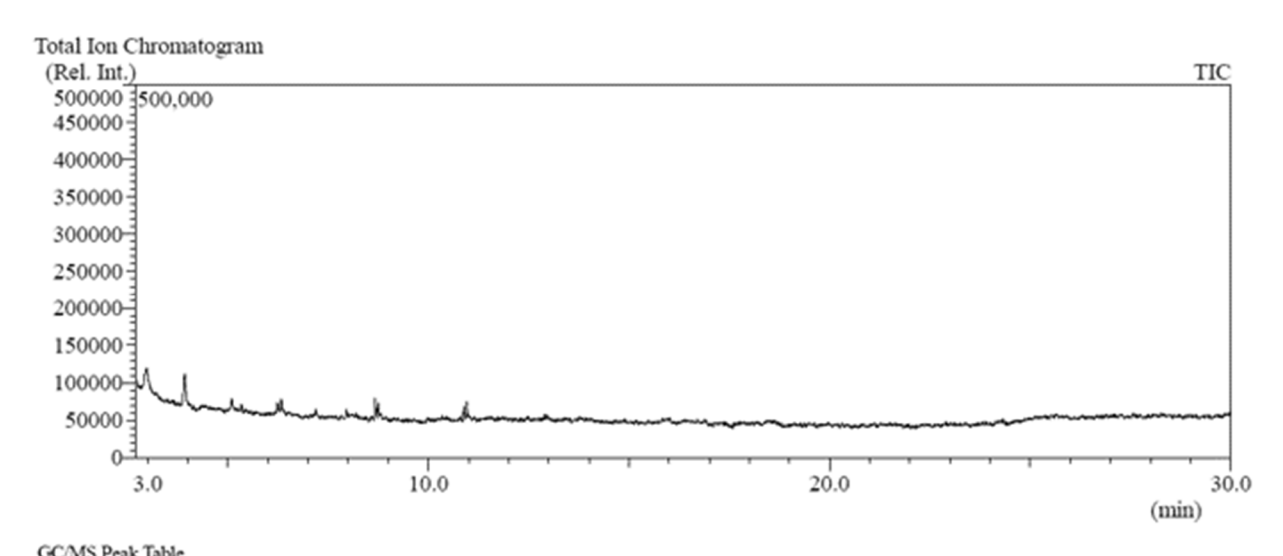
GC/MS Peak Table								
Peak#	R.Time (min)	Area	Peak Area%	Tentative Compound ID				
1	2.961	34817	6.00	No Library Match (m/z: 86, 71, 57, 43)				
2	3.929	85942	14.80	Tridecane				
3	4.160	50460	8.69	Thiourea, tetramethyl-				
4	6.832	409280	70.50	Quinoline, 1,2-dihydro-2,2,4-trimethyl-				
		580499	100.00					

Figure 2-10. GC-MS analysis of pooled dissolved (<0.7 μm) analytes in October 2019 surface runoff samples after 100X preconcentration via C18 SPE.



GC/MS Peak Table									
Peak#	R.Time (min)	Area	Peak Area%	Tentative Compound ID					
1	2.948	58264	61.43	Tridecane					
2	3.920	36586	38.57	Tridecane					
		94850	100.00						

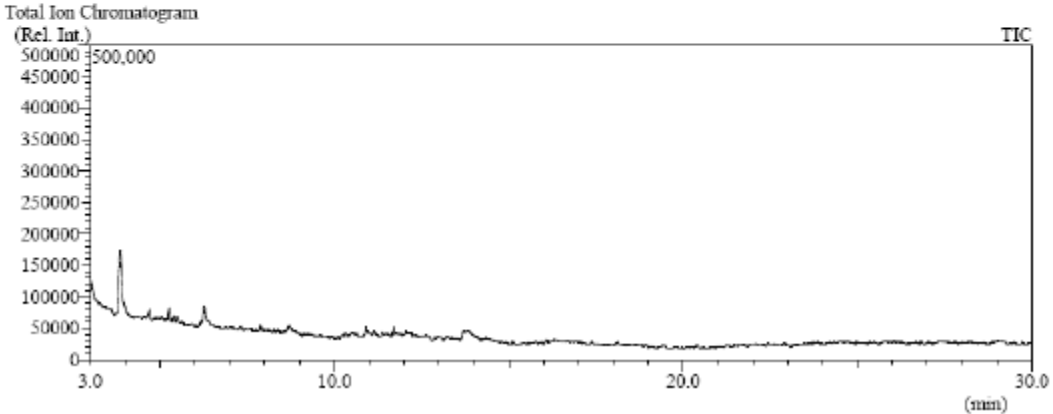
Figure 2-11. GC-MS analysis of pooled total analytes in October 2019 surface runoff samples after 100X preconcentration via C18 SPE.



GC/MS F	Peak Table			
Peak#	R.Time (min)	Area	Peak Area%	Tentative Compound ID
1	2.978	165940	23.17	Undecane
2	3.927	203405	28.41	Tridecane
3	5.341	19726	2.75	Hexadecane
4	6.230	52961	7.40	1-Tridecene
5	6.330	61847	8.64	Tetradecane
6	7.193	18581	2.59	No Library Match (m/z: 327, 281, 147, 73)
7	8.664	67850	9.48	3-Octadecene, (E)-
8	8.751	48952	6.84	Tetradecane
9	10.887	33968	4.74	9-Eicosene, (E)-
10	10.957	42856	5.98	Hexadecane
		716086	100.00	

Figure 2-12. GC/MS total ion chromatograph of composite surface runoff samples collected in January, June, and November 2020 after processing with C18 SPE to concentrate potential binder, waxes, and plasticizers.

(a) January 2020 GCMS Peak Table Feak R. Time (min) | Area | Peak Area% | Tentative Compound ID | 1 2.926 | 517514 | 31.09 | Decane, 3.7-dimethyl- | 2 3.864 | 610252 | 36.66 | Dodecane | 3 4.699 | 44669 | 2.68 | Heptadecane | 4 5.264 | 69872 | 4.20 | Dodecane, 4.6-dimethyl- | 5 5.387 | 30869 | 1.85 | Nomae, 5-(2-methylpropyl)- | 6 3.495 | 335183 | 2.11 | Undecane, 3.8-dimethyl- | 7 6.187 | 29033 | 1.74 | 1-Tentadecane | 8 6.265 | 163830 | 9.84 | Pentadecane | 9 7.880 | 26002 | 1.56 | Hexadecane | | 10 8.702 | 40059 | 2.41 | Heptadecane | | 11 10.903 | 35057 | 2.11 | No Library Match | | 12 11.144 | 32813 | 1.97 | No Library Match | | 13 11.703 | 29332 | 1.76 | (E)-1-(6.10-Dimethylandec-5-en-2-yll)-4-methylbenzene | | Total Ion Chromatogram (Rel. Int.) | Tile



(b) June 2020

	GC/MS Peak Table									
Peak#	R.Time (min)	Area	Peak Area%	Tentative Compound ID						
1	2.926	346140	37.23	Decane, 3,7-dimethyl-						
2	3.865	352740	37.94	Tridecane						
3	4.698	46447	5.00	Undecane, 3,8-dimethyl-						
4	5.258	72183	7.76	Dodecane, 4,6-dimethyl-						
5	5.383	33139	3.56	Undecane, 3,8-dimethyl-						
6	6.291	79170	8.51	Tetradecane						
		929819	100.00							

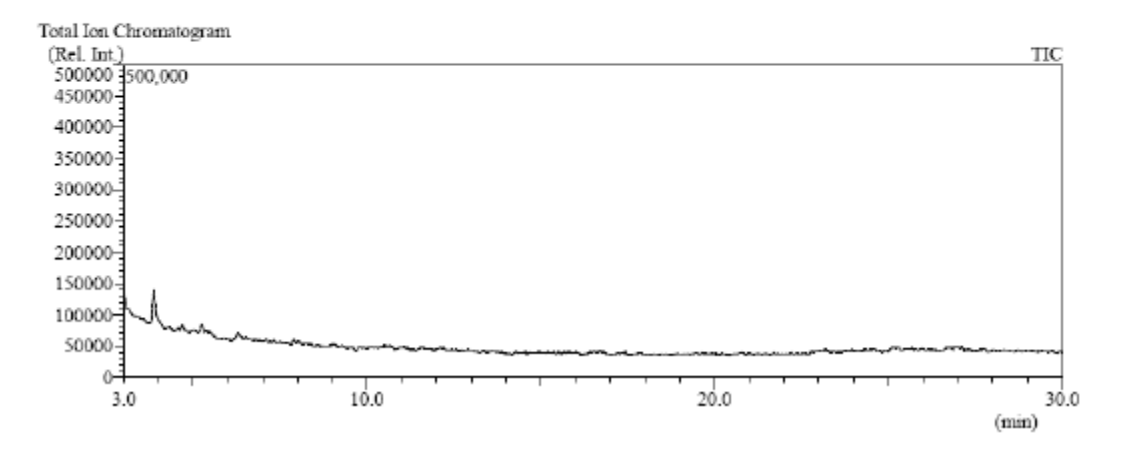
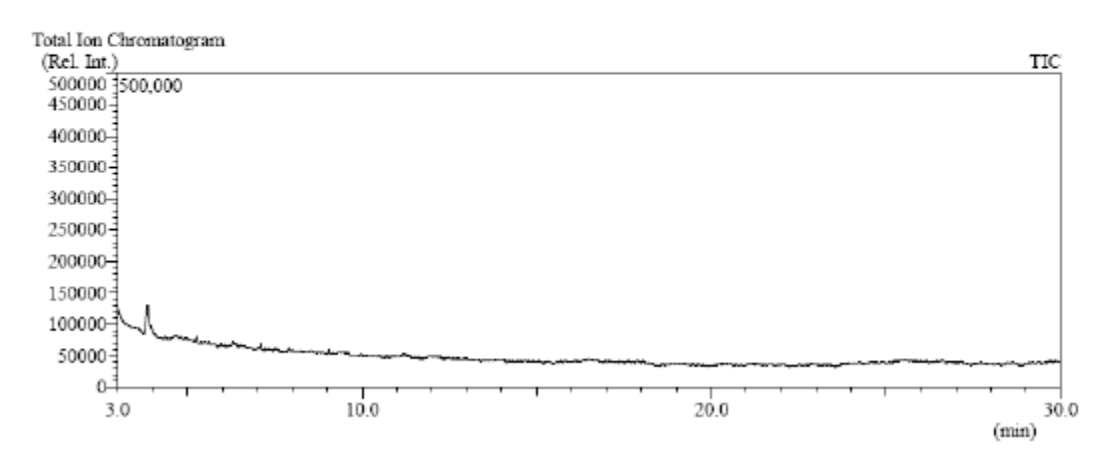


Figure 2-12. (cont.)

(c) November 2020

G(GC/MS Peak Table								
	'eak#	R.Time (min)	Area	Peak Area%	Tentative Compound ID				
	1	2.918	266409	46.40	Decane, 3,7-dimethyl-				
	2	3.867	279921	48.76	Dodecane				
	3	5.265	27767	4.84	Undecane, 3,8-dimethyl-				
			574097	100.00	·				



REFERENCES

- Fournier, D., Halasz, A., Spain, J., Fiurasek, P., Hawari, J., 2002. Determination of key metabolites during biodegradation of hexahydro-1,3,5-trinitro-1,3,5-triazine with *Rhodococcus* sp. strain DN22. Appl Environ Microbiol 68, 166-172.
- Fuller, M.E., Farquharson, E.M., Hedman, P.C., Chiu, P., 2022. Removal of munition constituents in stormwater runoff: Screening of native and cationized cellulosic sorbents for removal of insensitive munition constituents NTO, DNAN, and NQ, and legacy munition constituents HMX, RDX, TNT, and perchlorate. J Hazard Mater 424, 127335.https://doi.org/10.1016/j.jhazmat.2021.127335.
- Krzmarzick, M.J., Khatiwada, R., Olivares, C.I., Abrell, L., Sierra-Alvarez, R., Chorover, J., Field, J.A., 2015. Biotransformation and degradation of the insensitive munitions compound, 3-nitro-1,2,4-triazol-5-one (NTO), by soil bacterial communities. Environ Sci Technol 49, 5681–5688.10.1021/acs.est.5b00511.
- Perreault, N.N., Halasz, A., Manno, D., Thiboutot, S., Ampleman, G., Hawari, J., 2012. Aerobic mineralization of nitroguanidine by *Variovorax* strain VC1 isolated from soil. Environ Sci Technol 46, 6035-6040.
- Taylor, S., Hewitt, A., Lever, J., Hayes, C., Perovich, L., Thorne, P., Daghlian, C., 2004. TNT particle size distributions from detonated 155-mm howitzer rounds. Chemosphere 55, 357-367.

3. Evaluation of Novel Sorbents for Legacy and Insensitive Munition Energetics

3.1 METHODS

3.1.1 Chemicals and media

TNT, RDX, HMX, and NTO were purchased from Accurate Energetic Systems LLC (McEwen, TN). DNAN, NQ, and the cationizing agent 3-chloro-2-hydroxypropyl trimethylammonium chloride (CHPTAC) were purchased from Sigma-Aldrich (St. Louis, MO, USA). All other chemicals were reagent grade or higher.

An artificial surface runoff (ASR) used for this work was based on the analysis of the major anions and cations in stormwater collected from an east coast U.S. Navy facility, and consisted of (mg/L): Na₂SO₄, 16; MgCl₂•6H₂O, 10; CaCl₂•2H₂O, 10; KCl, 18; NaCl, 10; (NH₄)₂SO₄, 2; Ca(NO₃)₂•4H₂O, 1.5. The pH of ASR was adjusted to 6 standard units (S.U.) with 0.5 N HCl and NaOH, as needed.

The materials screened included *Sphagnum* peat moss, as well as native and cationized versions of: pine sawdust, pine shavings, aspen shavings, cotton linters, chitin, chitosan, burlap (landscaping grade), coconut coir, raw cotton, raw organic cotton, cleaned raw cotton, and cotton fabric. Commercially cationized fabrics were also examined: Inman Mills 207433-145 (Inman, SC); Tintoria Piana 25% and 55% cationized cotton (Cartersville GA).

3.1.2 Cationization of cellulosic materials

The cationization process for the various materials was based on the method of Fu et al. (2013) (Fu et al., 2013). The chemical reaction between CHPTAC and cellulosic materials is illustrated in Figure 3-1. For small batches (3-6 g), the material to be cationized was packed into a 60 ml polypropylene syringe barrel. For each gram of material, a solution was prepared comprised of 1.7 mL CHPTAC solution (60 wt% CHPTAC), 1.4 mL 10 N NaOH, and 3.6 mL laboratory grade purified H₂O. This equates to a CHPTAC concentration of 150 g/L (0.8 M) in 2.13 N NaOH. The material was thoroughly wetted, then the syringe plunger was inserted into the barrel, the syringe was inverted, and the wetted material was compressed to remove air bubbles. The luer outlet of the syringe was then capped and the mixture reacted at room temperature for 18-24 h. The cationized material was then removed from the syringe and rinsed with tap water, collecting the solids via vacuum filtration onto a 100 mesh stainless steel screen. The material was then transferred to a large glass beaker on a stir plate. Once the material was dispersed in the water, the pH was adjusted to approximately 6 with HCl. After vacuum filtration, the material was given a final rinse in laboratory grade purified water. The washed cationized material was then air dried and stored in a plastic bag until use. Larger batches (20+ g) were prepared similarly, except that nested polypropylene beakers, which allowed the upper beaker to act as a plunger to compress the material to remove air bubbles from the reaction prior to incubation.

The effect of different CHPTAC concentrations and replacing the water in the cationization solution with a solvent (isopropyl alcohol (IPA), tetrahydrofuran (THF), or tetraethylene glycol dimethyl ether (TG)) (Odabas et al., 2016) on the effectiveness of the cationized material for NTO removal was also examined.

3.1.3 Batch screening

The initial focus of the screening was identification of potential sorbents for DNAN, NTO, and NQ. Testing was done with ASR with all three compounds at an approximate concentration of 20 mg/L. Concentrations of the explosives were selected to ensure collection of accurate and reproducible analytical data even in the event of a high percentage of removal of the analyte by the sorbents. The basic screening was performed by mixing 0.2 g (air dry) of each sorbent material with 20 ml of ASR spiked with the target compounds in 40 ml clear glass vials sealed with teflon lined septa. A minimum of duplicate vials were shaken horizontally at 200 rpm at room temperature (20-22°C). Preliminary screening indicated that NTO (and the other target compounds) were essentially at equilibrium after 4 hours (data not shown), but experiments were standardized at an incubation period of 18-24 h. Aliquots (1 ml) were transferred to 1.5 ml polypropylene tubes, centrifuged for 3 minutes at 14,000 rpm, and 0.5 ml of the cleared supernatant was then mixed with 0.5 ml of methanol prior to HPLC analysis as described below. The final pH of the controls and the treatments were routinely measured.

Additionally, the competitive effects of higher and lower concentrations of the major anions, and the effects of the initial solution pH on the sorption of NTO were examined. For competing anion effects, several CAT materials were placed in solutions containing DNAN, NTO, and NQ, and 0.1X, 1X, and 10X of the normal ASR concentrations of Cl^- , NO_3^- , $SO_4^{2^-}$, and sampled and analyzed as described above. To examine pH effects, CAT pine was combined with ASR containing NTO at initial pH values of ~3.8 (e.g., the pH of ASR with NTO without any pH adjustment), 4.5, 5.5, 6.5, 7.5, and 8.5 S.U. (adjusted with 0.5 N NaOH).

The removal of the insensitive MC by CAT pine, CAT burlap, and CAT cotton was also examined in actual runoff from the east coast U.S. Navy facility that the ASR was based on. The runoff was allowed to settle for approximately 30 minutes, then the overburden water was combined with NTO, DNAN, and NQ, and the pH was adjusted to ~6.1 S.U. using 0.5 N NaOH. Sample and analysis was performed as described above.

As peat moss was previously demonstrated to be an effective sorbent for the legacy explosives (Hatzinger et al., 2004), and that it a useful bulk material for biofilter applications, peat moss was mixed with some of the CAT materials to examine the effects on the extent of NTO sorption. Peat moss was combined with the CAT materials at ratios (w:w) of 1:1, 2:1 and 3:1 (peat mosss:CAT material). Additionally, the effects of water extractable compounds in peat moss equivalent to the 3:1 peat moss:CAT material ratio was examined. Briefly, a peat moss extract was prepared by mixing peat moss with water for several hours, then passing the solution first through coffee filters to remove larger particles. The resulting solution was then passed through glass microfiber filters with pore sizes of 5, 2.7, 0.7 and finally 0.45 μm. For one treatment, the extract was combined with NTO, ASR components, and water, and the pH was brought to ~6 S.U. For a second treatment, NTO, ASR components, and water were combined and brought to pH 6, then the peat extract was added, resulting in a solution with an initial pH of ~4.3 S.U.

Follow-on multipoint isotherms were performed with peat moss, CAT pine, CAT burlap and CAT raw cotton done with ASR containing RDX, TNT, DNAN, NTO, and NQ at ~10 mg/L, HMX at ~3 mg/L, and perchlorate at ~6 mg/L (molar equivalent of NTO).

3.1.4 Analytical

The HPLC analytical methods for NTO and DNAN have been previously published (Fuller et al., 2021). NQ was analyzed using the same HPLC method as NTO, with detection at 217 nm. HMX, RDX, and TNT were analyzed by using HPLC according to a modified EPA Method 8330 using an Agilent 1100 HPLC (Santa Clara, CA) equipped with a Dionex 3000 (Sunnyvale, CA) PAD (photodiode array) UV-Vis detector to collect peak spectral data. The variable wavelength detector collected data at both 254 and 230 nm. The chromatography column used to separate the nitroaromatics was an Acclaim Explosive E1 C-18 reverse phase HPLC column (Thermo Scientific, Waltham, MA; 25 cm x 4.6 mm, 5 µm particle diameter). A methanol:water gradient was used as the mobile phase as follows: 0-3 mins (20:80); gradient ramp from 3.0-9.0 min (20:80 up to 38:62); 9.0-15.0 min (38:62); gradient ramp from 15.-20.5 min (38:62 to 43:57); 20.5-44.0 min (43:57); 44.0-51 min (80:20, to wash column); 51-64 min (20:80) to re-equilibrate column at the end of each sample run. Perchlorate was analyzed by ion chromatography using a modified EPA Method 300.0.

Nitrogen content of native and cationized materials was determined using a CHNS elemental analyzer (vario EL Cube, Elementar, Langenselbold, Germany) in the Advanced Materials Characterization Lab at the University of Delaware. Briefly, each test material was pretreated at 105°C for 20 min and 10-mg moisture-free samples were prepared in replicates for CNHS measurement. Following catalytic oxidation, organic nitrogen was converted into N₂ and quantified by a thermal conductivity detector (TCD). Prior to analysis, the instrument was calibrated using a sulfanilamide standard run in triplicate.

3.1.5 Data analysis

The adsorption data was fitted into the most widely used Freundlich and Langmuir and isotherm models. The Freundlich model can be expressed as

$$q_e = K_f C_e^{\frac{1}{n}} \tag{1}$$

where q_e is the equilibrium sorbed concentration (mg/g); C_e is the equilibrium sorbate concentration in solution (mg/L); K_f and n are the fitted Freundlich parameters of adsorption capacity ((mg/g)(mg/L)^{-1/n}) and adsorption intensity (unitless), respectively. The Langmuir model can be expressed as

$$q_e = \frac{q_m b C_e}{1 + b C_e} \tag{2}$$

where q_e and C_e are the same a in the Freundlich equation; q_m and b are the fitted Langmuir parameters of maximum adsorption amount (mg/g) and the energy of adsorption constant (L/mg), respectively. Experimental data was fitted using the custom nonlinear curve fitting functionality of KaleidaGraph (v4.5.2, Synergy Software, Reading, PA).

The amount of CHPTAC incorporated into the various materials was estimated based on the difference in the nitrogen content between the raw and cationized materials.

3.2 RESULTS and DISCUSSION

3.2.1 NTO removal

The reaction of cotton linters with the cationization agent CHPTAC, and a photograph of native and cationized cotton linters in the presence of dissolved NTO is shown in Figure 3-2. The cationized cotton demonstrated a visual color change to yellow in the presence of NTO.

None of the native materials sorbed NTO, but cationization (designated as CAT henceforth) of all the materials demonstrated increased removal of NTO (Figure 3-3), albeit only slightly in the case chitin. CAT cotton linters and CAT pine shavings performed quite well, resulting in sorption of more than 70% of the initial NTO. The NTO removal reported herein by cationized cellulosic materials was significantly more than that reported for amine functionalized chitin (AFC) based on the information provided in the patent, e.g., 1800-fold more removal of NTO per gram of CAT pine compared to AFC (Gurtowski, 2022). The observed extent of NTO removal by CAT pine in these single point evaluations was similar to the extent of orthophosphate anion removal by cationized pine bark previously reported (e.g., ~90% removal at initial concentrations of <10's of mg/L) (Tshabalala et al., 2004).

The commercially available cationized fabrics removed less than 20% of the NTO from solution (data not shown). The fabrics were designated as containing 25% and 50% of cationized cotton. These percentages would need to be multiplied by the degree of CHPTAC incorporation in the cationized cotton used, which was not provided by the manufacturer. Therefore, these fabrics likely had a much lower number of positively charged NTO binding sites than the CAT materials prepared in our laboratory.

The CHPTAC concentration used during the cationization process directly impacted the ability of CAT pine to remove NTO from solution (Figure 3-4). NTO removal increased as CHPTAC increased from 38 to 225 g/L, but then decreased at 300 g/L. CHPTAC concentration showed a positive relationship with CHPTAC incorporation based on the change in nitrogen content before and after cationization (Figure 3-5), and followed the same pattern as observed for NTO uptake, e.g., the CHPTAC incorporation decreased in the CAT pine produced with the 300 g/L compared to 225 g/L CHPTAC. Therefore, part of the lower NTO removal by the pine cationized using 300 g/L CHPTAC is a result of less CHPTAC incorporation (e.g., fewer cationic sites). The leveling off the NTO removal at higher CHPTAC concentrations is similar to previous work showing leveling off of dye uptake into cotton fabrics cationized with higher CHPTAC concentrations (Hashem and El-Shishtawy, 2001; Fu et al., 2013). The previous research did not use CHPTAC concentrations greater than 200 g/L, so the current result showing decreasing cationization above this concentration is a new finding. The reasons for the decreased cationization at the highest concentration was not further investigated, but may be due to increased self-reaction of the epoxide formed during the process (hence, less overall reaction of the epoxide with the cellulose). The authors of the previously published information did not go to as high a CHPTAC concentration as in this current work, so it is possible that they would also have seen a decrease in cationization, reflected in a a decrease in dye uptake.

It was observed that the CAT materials tended to buffer the pH of the ASR test solution towards circumneutral values. With CAT pine, initial acidic pH values of 3.5 to 4 S.U. were brought to around 7, and an initial basic pH value of 8.5 was brought down to slightly above 7. (Figure 3-6).

Due to this buffering effect, NTO removal was not affected by the initial pH of the solution. Even at an initial acidic pH near the NTO pK_a of 3.7, where there would be a ~50:50 mix of neutral (protonated) and charged (deprotonated) NTO, the uptake of the charged NTO would lead to further deprotonation of the remaining neutral NTO, thus resulting in additional sorption to the CAT materials. The exact mechanism behind the buffering ability of the CAT materials was not determined, but was assumed to be due to exchange between hydroxide anion associated with the positively charged sites on the CAT materials and anions in the solution (e.g., chloride), thus leading to acid neutralization. This is actually a secondary benefit of the CAT materials, in that circumneutral pH values are favorable for the biological processes required to transform and degrade both insensitive and legacy MC.

The combination of peat moss with CAT materials had mixed effects on NTO removal. A 1:1 ratio of CAT pine, CAT burlap, or CAT cotton did not significantly change NTO removal (Figure 4). With a 2:1 peat moss:CAT material ratio, little impact was observed for CAT pine or CAT burlap, but NTO removal by CAT cotton was reduced by over 50%. At 3:1 ratio, NTO removal was reduced by 20%, 46% and 61% with CAT pine, CAT burlap, and CAT cotton, respectively. When water extractable peat moss compounds equivalent to a 3:1 peat moss:CAT material ratio were included, NTO removal decreased by compared to no peat addition. The final solution pH decreased as the amount of solid peat moss increased (Figure 3-7). However, even with a 3:1 peat moss:CAT ratio, the final pH was still at least 0.5 S.U. above the pK_a of NTO, and the pH in the presence of peat extractables was similar to that with no peat present (e.g., >6.5 S.U.). Therefore, the observed changes in NTO removal were not due to NTO becoming a neutral species in acidic solution. Rather, we postulate that the effects of peat moss on NTO removal were attributable to competition between anionic compounds (e.g., organic acids) and NTO for the positively charges sites on the CAT materials. These results are quite encouraging, given that the final application is expected to be a combination of peat moss plus one or more of the CAT materials. The competition between peat-derived anionic compounds and NTO would be expected to decrease over time as those compounds are leached and/or degraded.

Competition was also observed between the concentration of major anions (chloride, nitrate, sulfate) and the removal of NTO by CAT materials (Figure 3-8). A 10-fold decrease in the major anions resulted in approximately 2-fold more NTO removal, while a 10-fold increase resulted in 3- to 5-fold less NTO removal, relative to the control concentrations in 1X ASR. The range of anion concentrations measured in the Navy site runoff collected periodically over a year has indicated that major anion concentrations in natural runoff are never extremely high, and are more likely to be below the anion concentrations in the ASR used for this testing. Therefore, the performance of these CAT materials with respect to NTO removal is not expected to be affected by competing anions.

Taken in total, the removal of NTO is theorized to be predominantly by ionic interactions between the positively charged cationized materials and the negatively charged NTO molecule. As such, the application of simple ion exchange models would be expected to explain the interactions/removal of NTO by these materials.

The main application of cationization has been in the textile industry as a means to increase anionic dye uptake into cotton, improving both color depth and color retention upon washing (Fu et al.,

2013; Arivithamani and Dev, 2017), and as strength-enhancing process in the pulp and paper industry (Jouybari et al., 2017). Cationization of cellulosic materials has also been evaluated to remove anionic dyes in wastewater (Baouab et al., 2001; Hashem and El-Shishtawy, 2001; Hu et al., 2016), and anions like orthophosphate from surface runoff (Tshabalala et al., 2004). A recent patent described the use of amine functionalized chitin for the removal of MC from aqueous solutions, including NTO (Gurtowski, 2022), but the current work is the first known report of cationized cellulosic materials for NTO removal.

Figure 3-1. Reaction mechanism of CHPTAC with cellulose.

Figure 3-2. Reaction of cotton linters with cationization agent CHPTAC and photograph of native and cationized cotton linters after exposure to dissolved NTO.

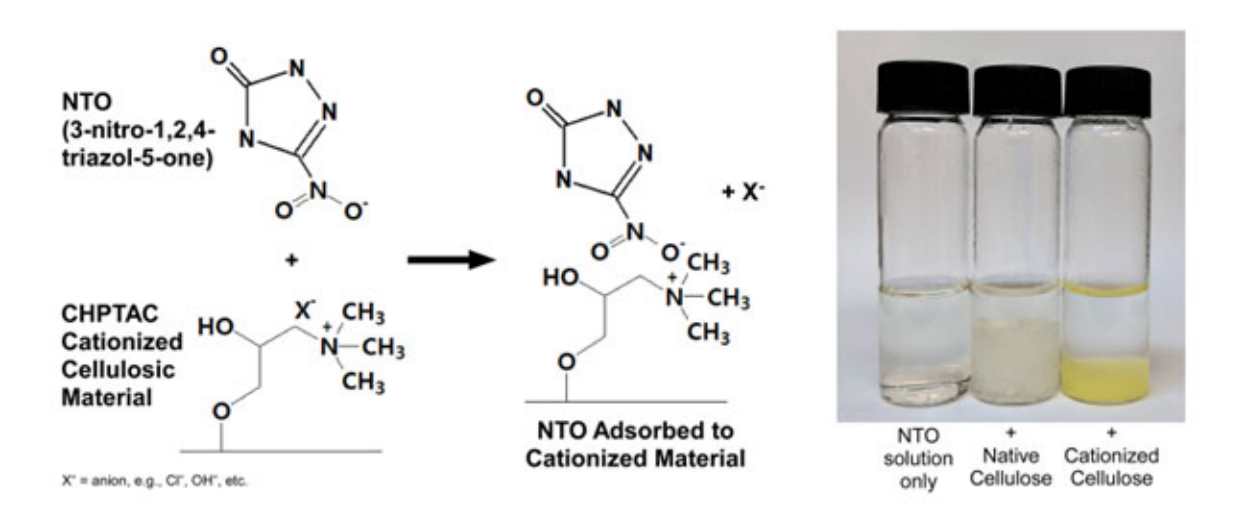


Figure 3-3. Removal of NTO (top) and DNAN (bottom) from ASR. Data represent average of duplicates ± standard deviation.

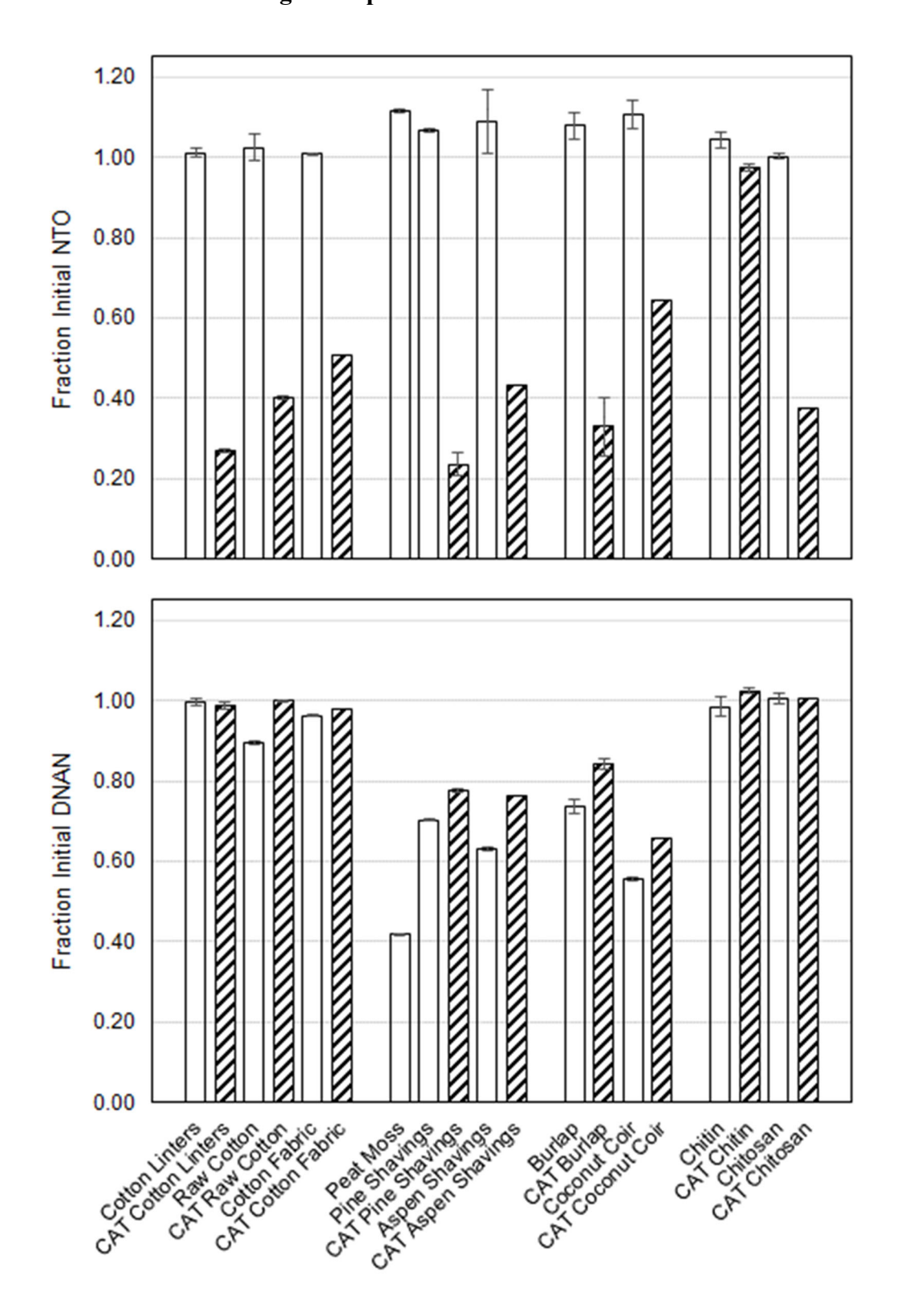


Figure 3-4. Effect of CHPTAC concentration on removal of NTO by cationized pine shavings (top) and amount of CHPTAC incorporation based on change in nitrogen content (bottom).

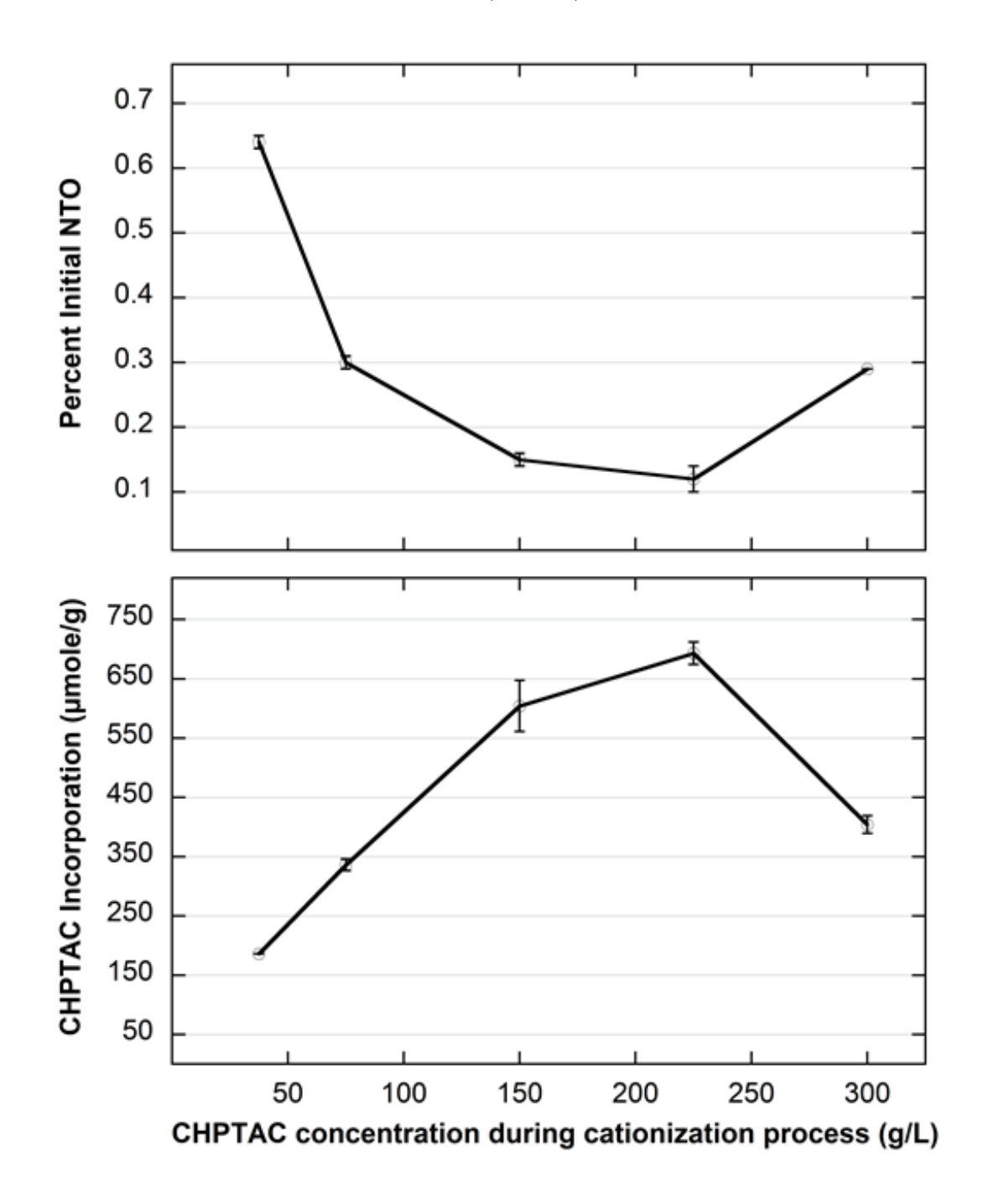
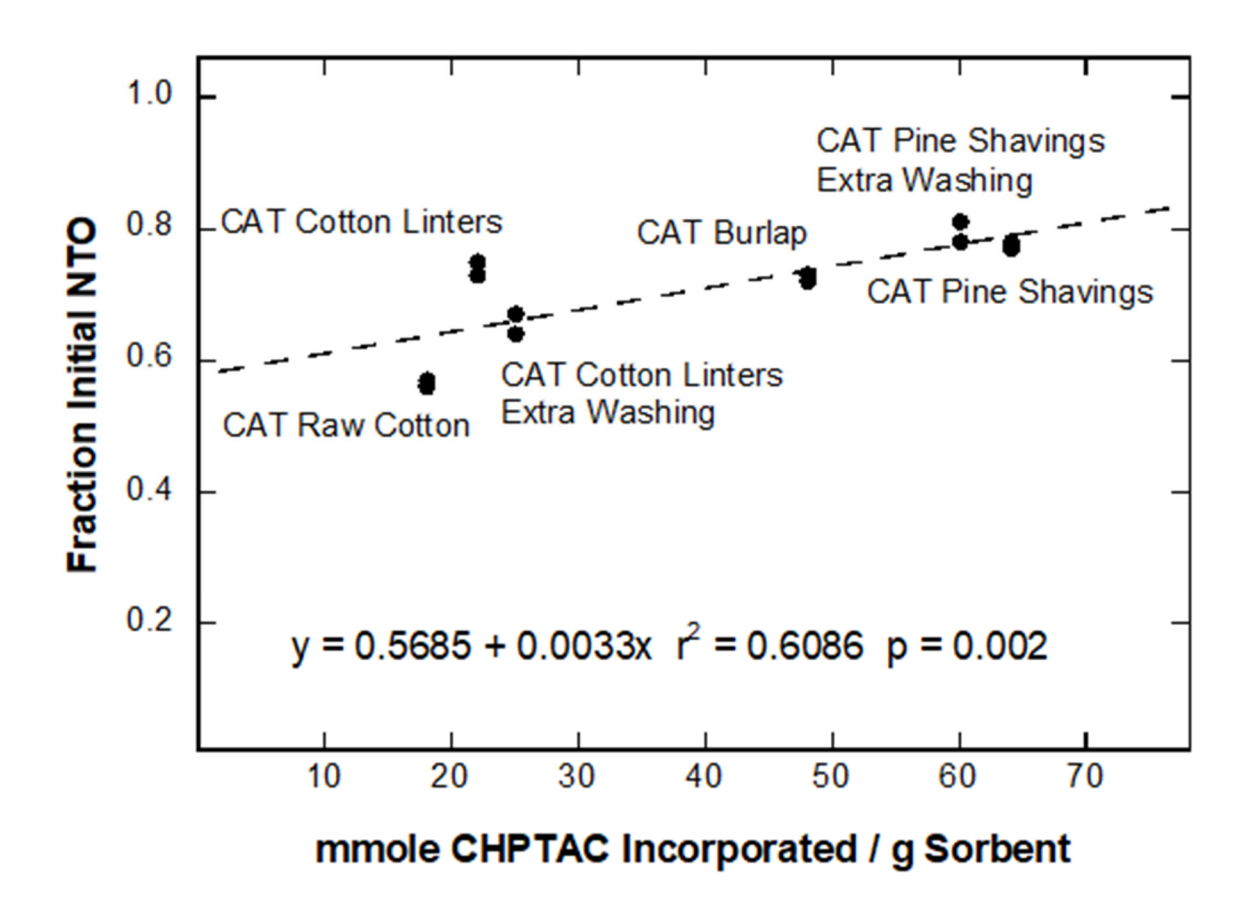
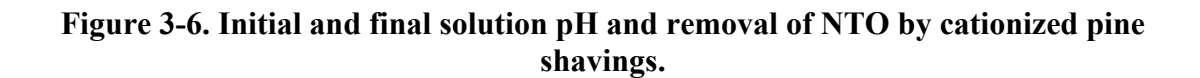


Figure 3-5. Relationship between calculated degree of CHPTAC incorporation into different materials and the percent NTO removed from solution after 24 h.





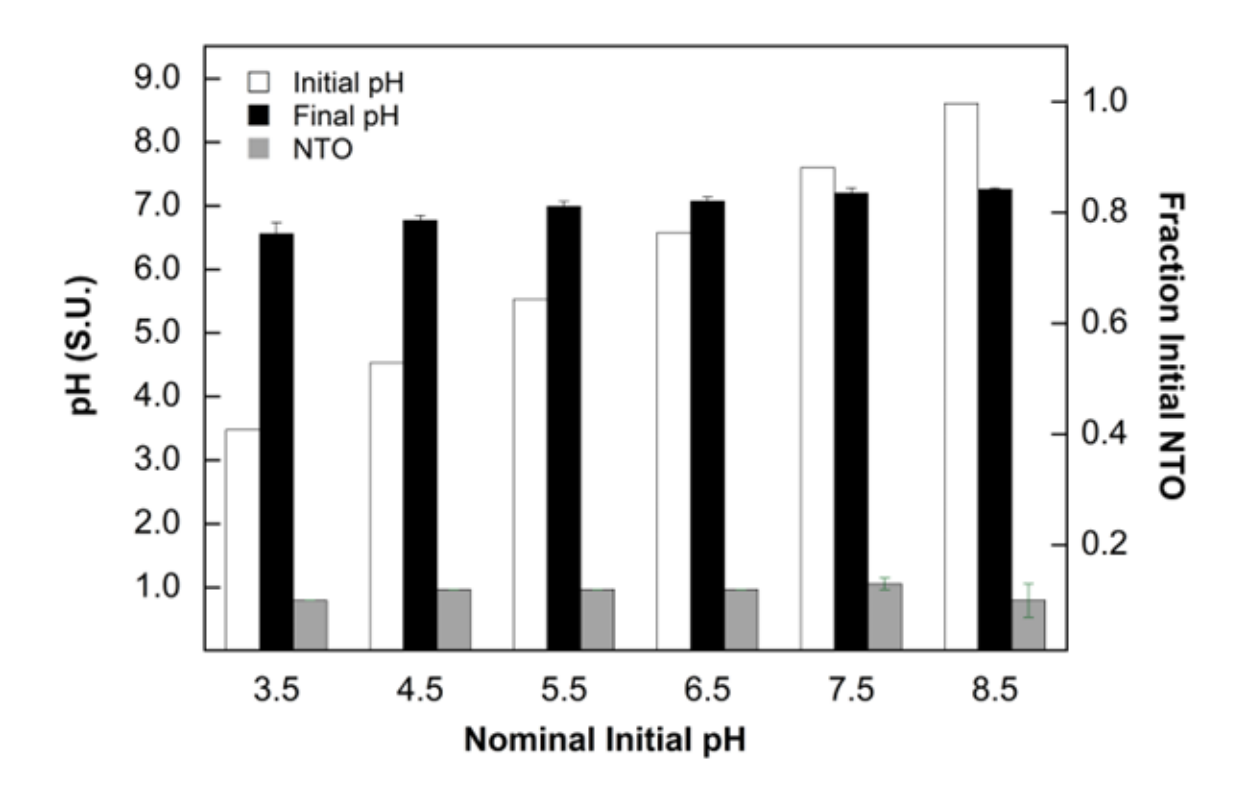
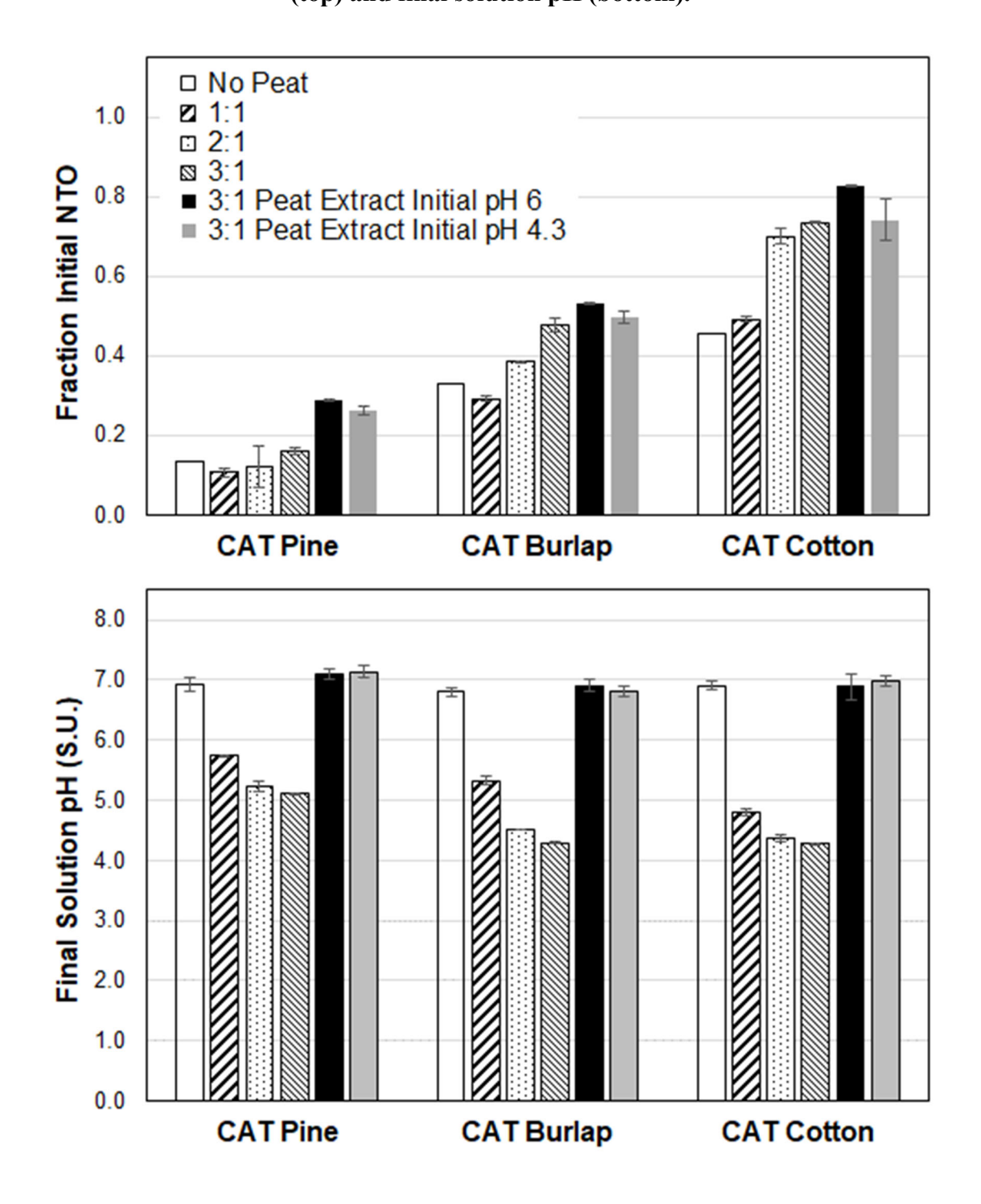


Figure 3-7. Impact of peat moss on removal of NTO from solution by CAT materials (top) and final solution pH (bottom).



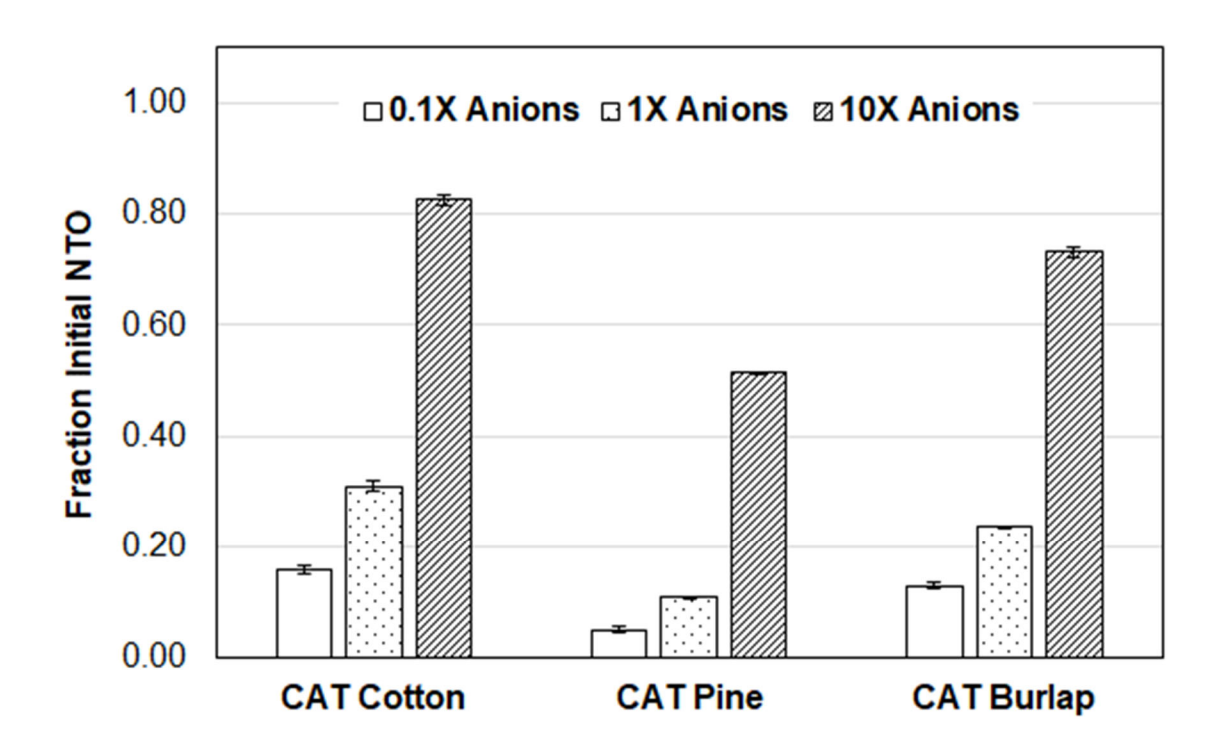


Figure 3-8. Impact of major anions on removal of NTO from solution by CAT materials.

3.2.2 DNAN removal

The greatest DNAN removal was observed with peat moss, with pine and aspen shavings, burlap, and coconut coir exhibiting slightly lower DNAN sorption (Figure 3-3). In most cases, cationization of these materials resulted in somewhat lower DNAN removal. This is likely due to a combination of delignification of the materials by exposure to the NaOH (Xu et al., 2020), leading to loss of more hydrophobic zones. During the cationization process, the initial rinse from most of the materials had a brown/orange hue, indicative of aromatic lignin-like compounds. When pine shavings and burlap were treated with the same concentration of NaOH as used during the cationization process (e.g., mercerization), but in the absence of CHPTAC, DNAN removal was also reduced compared to the corresponding raw materials, and was only slightly higher than their cationized versions (Figure 3-9). Additionally, cationization leads to an increase in positively charged sites due to incorporation of CHPTAC, and a decrease in overall hydrophobicity, which could be less likely to bind DNAN. However, DNAN removal was not observed to significantly vary with CAT pine possessing varying levels of CHPTAC incorporation (Figure 3-10).

3.2.3 NQ removal

None of the materials tested sorbed NQ to any significant extent (<10% removal). This is not entirely unexpected, given that previous research has indicated that NQ is poorly retained in soil due to low sorption to natural minerals and organic matter (Haag et al., 1990; Temple et al., 2018). These findings are also in line with another report of low NQ removal by unmodified cellulose, chitin, and chitosan (Gurtowski et al., 2018). This indicates an area for additional research, as

insensitive munition compositions, as well as several propellant formulations, have the potential to lead to NQ contamination of surface runoff on military ranges.

Figure 3-9. Impact of mercerization and cationization on removal of DNAN from solution by CAT pine shavings based after 24 h.

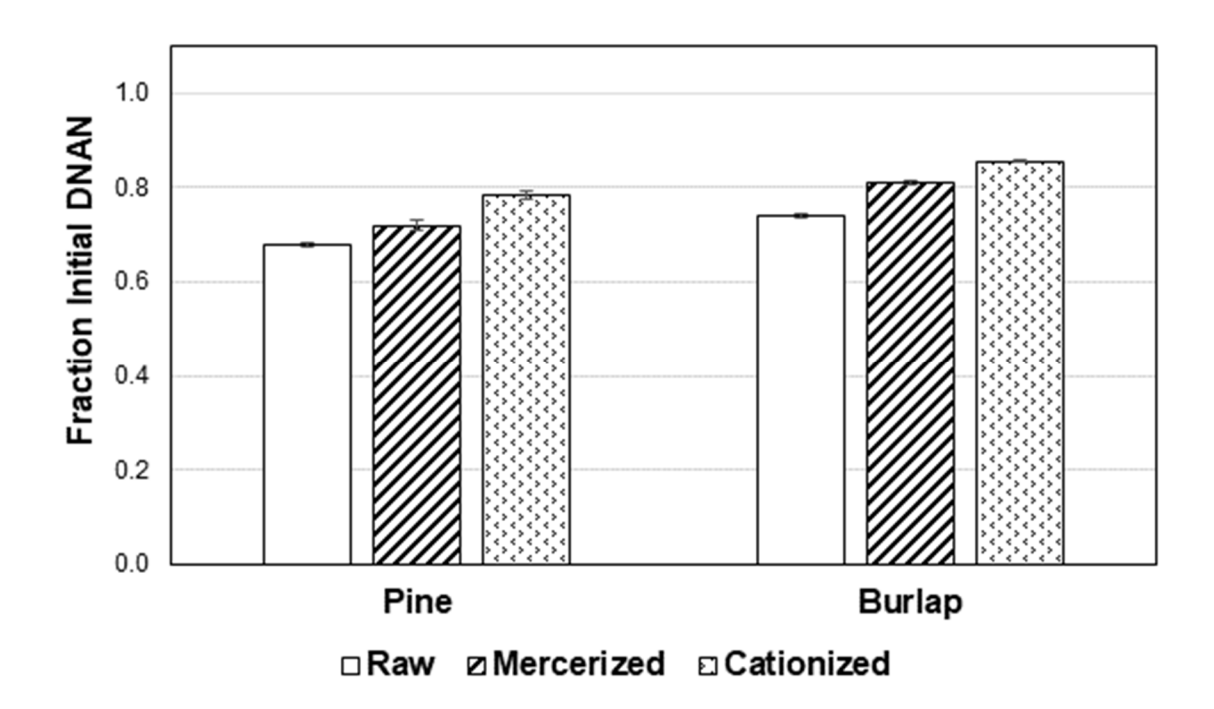
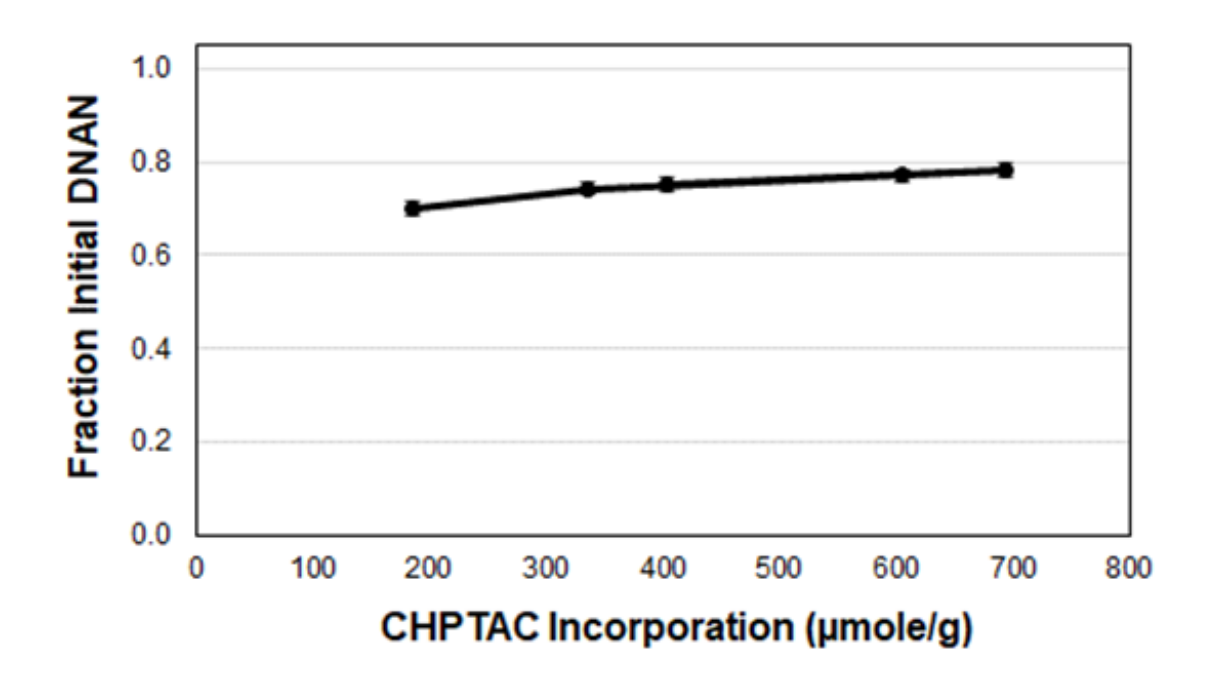


Figure 3-10. Impact of degree of CHPTAC incorporation on removal of DNAN from solution by CAT pine shavings based after 24 h.



3.2.3 Legacy and insensitive MC isotherms

Freundlich and Langmuir adsorption parameters are shown in Table 3-1. Initial single point sorption testing with legacy explosives indicated that CAT pine and CAT burlap removed approximately 20% of HMX, 10% of RDX, and 50-60% of TNT from solution. However, no sorption parameters for HMX or RDX with any of the CAT materials were obtained from the isotherm data. Additionally, no parameters for NTO were obtained with peat moss, or for perchlorate with peat moss or CAT cotton. Model fit r^2 values were generally greater than 0.9, although the fits for CAT cotton were significantly lower (~0.6).

The trend in the Langmuir maximum sorption amount (q_m) for NTO was CAT pine > CAT burlap > CAT cotton, with the CAT pine q_m approximately five times greater than CAT cotton (4.1 vs. 0.8 mg NTO/g sorbent). For TNT, the peat q_m was approximately three times greater than that for CAT pine (3.6 vs. 1.3 mg TNT/g sorbent). This follows what was observed during the single point evaluation.

Table 3-1. Freundlich and Langmuir adsorption parameters for insensitive and legacy explosives.

		NTO			DNAN			CIO4		
		K _f	n	r²	Kr	n	r ²	K _f	n	r²
Freundlich	Peat	.*			0.38 ± 0.05	1.71 ± 0.20	0.89			-
	CAT Pine	0.94 ± 0.05	1.61 ± 0.11	0.97	0.01 ± 0.01	0.70 ± 0.13	0.76	1.54 ± 0.06	2.42 ± 0.16	0.97
	CAT Burlap	0.41 ± 0.05	2.43 ± 0.41	0.82				0.53 ± 0.03	2.42 ± 0.26	0.92
	CAT Cotton	0.26 ± 0.06	2.53 ± 0.76	0.57		-			-	-
		q _m (mg/g)	b (L/mg)	r²	q _m (mg/g)	b (L/mg)	r ²	q _m (mg/g)	b (L/mg)	r²
Langmuir	Peat		-		2.57 ± 0.33	0.13 ± 0.03	0.92		-	-
	CAT Pine	4.07 ± 0.26	0.30 ± 0.04	0.99				3.63 ± 0.18	0.89 ± 0.13	0.97
	CAT Burlap	1.29 ± 0.12	0.36 ± 0.08	0.89		-		1.26 ± 0.06	0.76 ± 0.10	0.97
	CAT Cotton	0.83 ± 0.15	0.30 ± 0.15	0.58						
		нмх			RDX			TNT		
		K,	n	r ²	K,	n	r ²	K,	n	r ²

-		K _f	n	r ²	K_f	n	r²	K _f	n	r²
Freundlich	Peat	0.08 ± 0.00	1.70 ± 0.18	0.91	0.11 ± 0.02	2.75 ± 0.63	0.69	1.21 ± 0.15	2.78 ± 0.67	0.81
	CAT Pine		-	-	-	-	-	1.02 ± 0.04	4.01 ± 0.44	0.93
	CAT Burlap	-	-	-	-	-	-	0.36 ± 0.02	1.59 ± 0.09	0.98
	CAT Cotton	-	-	-	-	-	-	-	-	-
		q _m (mg/g)	b (L/mg)	r²	q _m (mg/g)	b (L/mg)	r ²	q _m (mg/g)	b (L/mg)	r²
Langmuir	Peat	0.29 ± 0.04	0.39 ± 0.09	0.93	0.38 ± 0.05	0.23 ± 0.08	0.69	3.63 ± 0.18	0.89 ± 0.13	0.97
	CAT Pine	-	-	-	-	-	-	1.26 ± 0.06	0.76 ± 0.10	0.97
	CAT Burlap	-	-	-	-	-	-	-	-	-
	CAT Cotton	-	-	-	-	-	-	-	-	-

a No successful model fit

3.3 CONCLUSIONS

The identification of cationized materials for the removal of the insensitive MC compound NTO from aqueous solution, combined with the previous findings regarding the effectiveness of peat moss for removal of the legacy MC compounds HMX, RDX, and TNT, provide a foundation for further development of a passive treatment technology for MC in surface runoff. These data indicated that a combination of peat moss and CAT pine would be required to effectively remove both insensitive and legacy MC from aqueous solution (excluding NQ). Follow-on work will include flow-through column and bench-scale biofilter testing, to assess not only sorption effectiveness and sorbent longevity under the dynamic conditions expected to occur in the field, but also combining sorption with abiotic and biotic degradation processes to work toward a wholistic approach for removal and destruction of the legacy and insensitive MC in stormwater runoff.

REFERENCES

Arivithamani, N., Dev, V.R.G., 2017. Industrial scale salt-free reactive dyeing of cationized cotton fabric with different reactive dye chemistry. Carbohydrate Polymers 174, 137-145.https://doi.org/10.1016/j.carbpol.2017.06.045.

- Baouab, M.H.V., Gauthier, R., Gauthier, H., El Baker Rammah, M., 2001. Cationized sawdust as ion exchanger for anionic residual dyes. Journal of Applied Polymer Science 82, 31-37.10.1002/app.1820.
- Fu, S., Hinks, D., Hauser, P., Ankeny, M., 2013. High efficiency ultra-deep dyeing of cotton via mercerization and cationization. Cellulose 20, 3101-3110.10.1007/s10570-013-0081-6.
- Fuller, M.E., Rezes, R.T., Hedman, P.C., Jones, J.C., Sturchio, N.C., Hatzinger, P.B., 2021. Biotransformation of the insensitive munition constituents 3-nitro-1,2,4-triazol-5-one (NTO) and 2,4-dinitroanisole (DNAN) by aerobic methane-oxidizing consortia and pure cultures. J Hazard Mater 407, 124341.https://doi.org/10.1016/j.jhazmat.2020.124341.
- Gurtowski, L.A., Griggs, C.S., Gude, V.G., Shukla, M.K., 2018. An integrated theoretical and experimental investigation of insensitive munition compounds adsorption on cellulose, cellulose triacetate, chitin and chitosan surfaces. Journal of Environmental Sciences 64, 174-180. https://doi.org/10.1016/j.jes.2017.06.012.
- Gurtowski, L.A., inventor; United States of America as Represented by The Secretary of The Army, assignee, filed April 2, 2020., 2022. Amine functionalized chitin for removing munitions compounds from solutions. US Patent Application 20200102406. United States of America as Represented by The Secretary of The Army (Alexandria, VA, US), United States.
- Haag, W.R., Spanggord, R., Mill, T., Podoll, R.T., Chou, T.-W., Tse, D.S., Harper, J.C., 1990. Aquatic environmental fate of nitroguanidine. Environ Toxicol Chem 9, 1359-1367. https://doi.org/10.1002/etc.5620091105.
- Hashem, A., El-Shishtawy, R.M., 2001. Preparation and characterization of cationized cellulose for the removal of anionic dyes. Adsorption Science & Technology 19, 197-210.10.1260/0263617011494088.
- Hatzinger, P.B., Fuller, M.E., Rungkamol, D., Schuster, R.L., Steffan, R.J., 2004. Enhancing the attenuation of explosives in surface soils at military facilities: Sorption-desorption isotherms. Environ Toxicol Chem 23, 306-312.
- Hu, Y., Li, S., Jackson, T., Moussa, H., Abidi, N., 2016. Preparation, characterization, and cationic functionalization of cellulose-based aerogels for wastewater clarification. Journal of Materials 2016, 3186589.10.1155/2016/3186589.

- Jouybari, I.R., Yoosefi, M., Azadfallah, M., 2017. Preparation of cationic CMP and softwood long fibers as strength-enhancing additive to CMP pulp. BioResources 12, 3890-3904.
- Odabas, N., Amer, H., Bacher, M., Henniges, U., Potthast, A., Rosenau, T., 2016. Properties of cellulosic material after cationization in different solvents. ACS Sustainable Chemistry & Engineering 4, 2295-2301.10.1021/acssuschemeng.5b01752.
- Temple, T., Ladyman, M., Mai, N., Galante, E., Ricamora, M., Shirazi, R., Coulon, F., 2018. Investigation into the environmental fate of the combined Insensitive high explosive constituents 2,4-dinitroanisole (DNAN), 1-nitroguanidine (NQ) and nitrotriazolone (NTO) in soil. Sci Total Envir 625, 1264-1271. https://doi.org/10.1016/j.scitotenv.2017.12.264.
- Tshabalala, M.A., Karthikeyan, K.G., Wang, D., 2004. Cationized milled pine bark as an adsorbent for orthophosphate anions. Journal of Applied Polymer Science 93, 1577-1583.10.1002/app.20637.
- Xu, E., Wang, D., Lin, L., 2020. Chemical structure and mechanical properties of wood cell walls treated with acid and alkali solution. Forests 11, 87.

4. Evaluation of Slow-Release Carbon Sources for Biodegradation of Legacy and Insensitive Munition Energetics

Hypothesis 5: Slow-release carbon sources can support the biodegradation of legacy and insensitive munitions constituents in surface runoff.

4.1 METHODS

4.1.1 Chemicals and media

Sources of energetic compounds, peat moss, pine shavings, and the synthesis of cationized pine shavings were described previously (Fuller et al., 2022). Slow-release carbon source biopolymer information is shown in Table 4-1. All other chemicals were reagent grade or higher. The artificial surface runoff (ASR) solution and Hareland's basal salts medium (BSM) were described previously (Hareland et al., 1975; Fuller et al., 2022).

4.1.2 Slow-release carbon source screening

Multiple pure bacterial strains and mixed cultures were screened for their ability to utilize the solid biopolymers as a carbon source to support energetic compound transformation and degradation. Pure strains included the aerobic RDX degrader *Rhodococcus* sp. DN22 (DN22 henceforth) (Coleman et al., 1998) and *Gordonia* sp. KTR9 (Coleman et al., 1998) (KTR9 henceforth), the anoxic RDX degrader *Pseudomonas fluorecens* I-C (Pak et al., 2000; Fuller et al., 2009) (I-C henceforth), and the aerobic NQ degrader *Pseudomonas extremaustralis* NQ5 (Kim et al., 2024) (NQ5 henceforth). Anaerobic mixed cultures were obtained from a membrane bioreactor (MBR) degrading a mixtures of six explosives (HMX, RDX, TNT, NTO, NQ, DNAN), perchlorate, and nitrate (Fuller et al., 2023). Pure cultures were grown in their respective media, concentrated by centrifugation, and washed twice to prepare inocula for the biopolymer screening.

Solid carbon sources were used as received without any effort to sterilize the materials. Screening was performed in either 40 ml screw cap glass vials or 60 ml glass serum bottles, both with Teflon®-lined septa. Pure culture screening was performed with 20 ml of BSM amended with the respective explosive plus 0.2 g of the biopolymer. For strains KTR9, DN22, and NQ5, BSM without any added ammonium was used, as these strains use RDX or NQ as the sole nitrogen source. Sterile controls without biopolymers (to account for sorption), as well as sterile controls without biopolymers (to account for all other losses), were included. All treatments were prepared in duplicate. The anaerobic MBR mixed culture was screened similarly, except that ASR was used as the base medium. Samples were removed over time for analysis of energetics concentrations. Due to measurable sorption, degradation by the cultures was assessed relative to the biopolymer-matched sterile controls.

Analysis for organic energetics and perchlorate were the same as those described in section 3.1.4 above.

Table 4-1. Slow-release carbon source information.

Material	Description	Source	Notes
PLA6	polylactic acid	Goodfellow	high MW thermoplastic polyester
PLA80	polylactic acid	Goodfellow	low MW thermoplastic polyester
PHB	polyhydroxybutyrate	Goodfellow	bacterial biopolyester
PCL	polycaprolactone	Sarchem Labs	biodegradable polyester
BioPBS	polybutylene succinate	Mitsubishi Chemical Performance Polymers	bio-based product; compostable
SEFA SP10	sucrose ester of fatty acids	Sisterna	food and cosmetic additive
SEFA SP70	sucrose ester of fatty acids	Sisterna	food and cosmetic additive

4.2 RESULTS and DISCUSSION

4.2.1 RDX degradation

Several of the biopolymers supported degradation of energetics by pure and mixed cultures. Results are presented as the percent of the matched carbon source only control over time. RDX biodegradation by KTR9 and DN22 varied based on the carbon source provided (Figures 4-1). Both strains degraded RDX with SEFA10 and SEFA70, PHB, and PCL. DN22 also exhibited degradation with BioPBS. DN22 generally degraded RDX faster than KTR9. Neither strain evidenced RDX degradation with the polylactides PLA6 or PLA80. Additionally, degradation of a second spike of RDX was also observed, indicating sustained support of biodegradation as the carbon sources were slowly utilized.

Anoxic RDX degradation by strain I-C was supported by SEFA 10 and SEFA70, and partial degradation (~50%) was observed with all the other biopolymers except PHB (Figure 4-2).

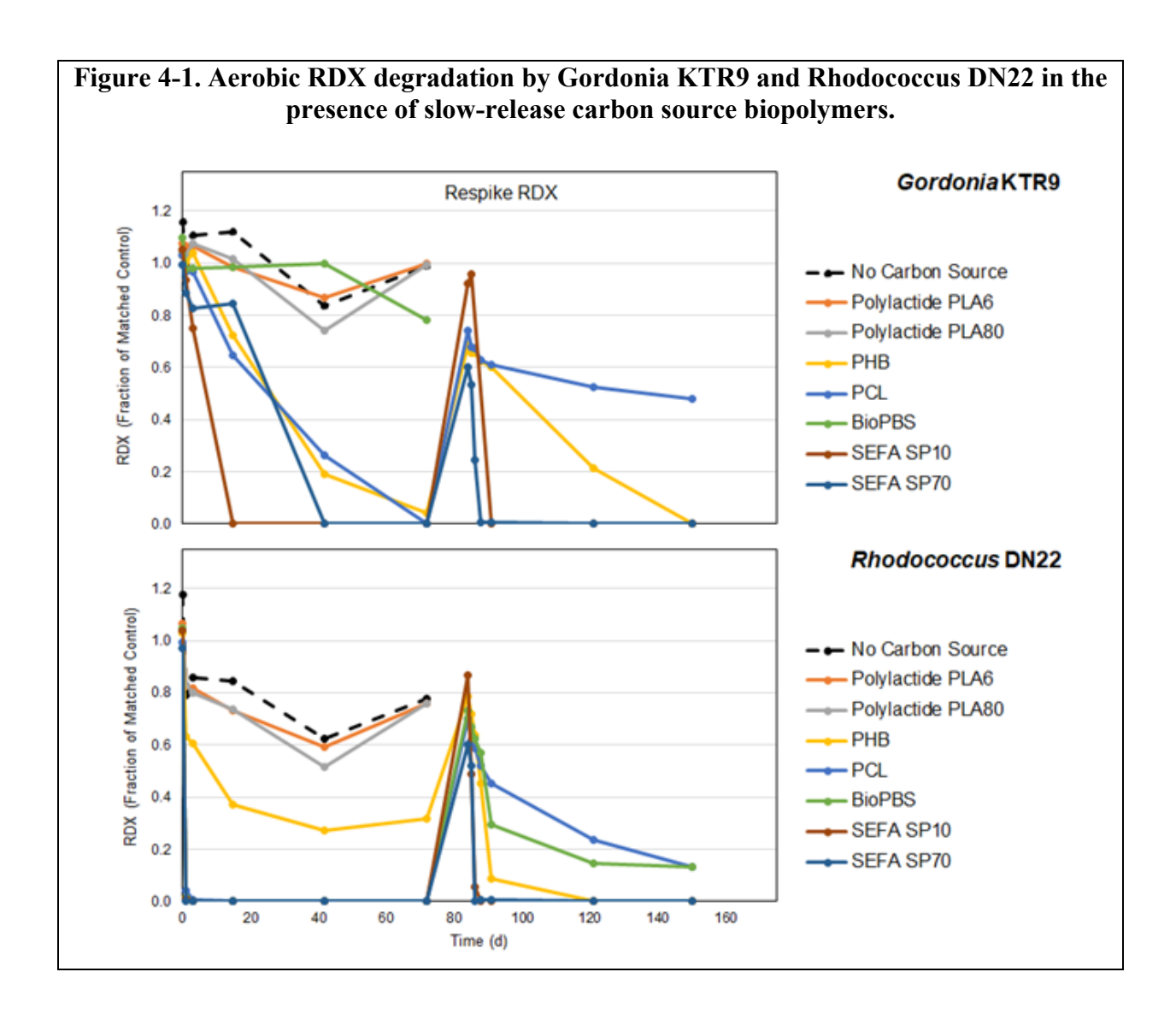
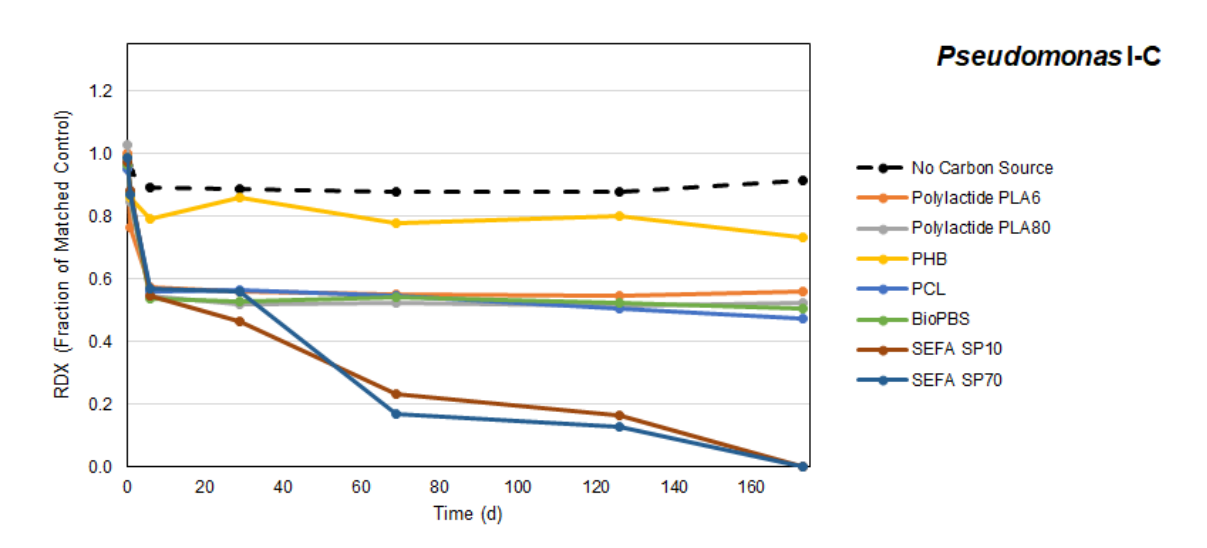


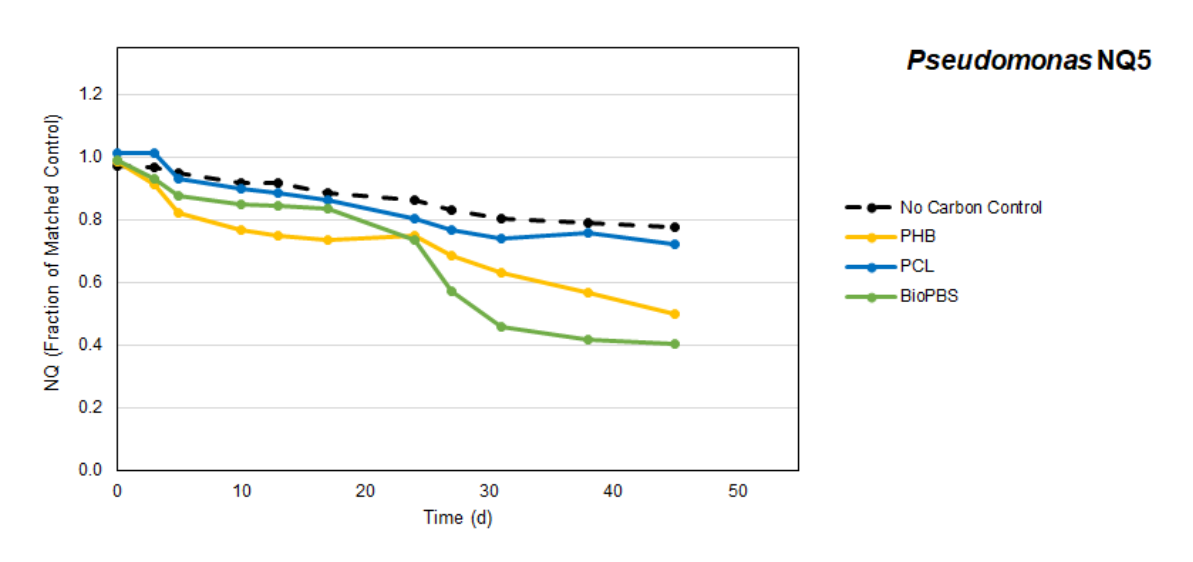
Figure 4-2. Anoxic RDX degradation by *Pseudomonas* I-C in presence of slow-release carbon source biopolymers.



4.2.2 NQ degradation

NQ degradation was not significantly enhanced by PCL compared to the treatment with no added carbon, but both PHB and BioPBS supported approximately 50 to 60% of the NQ to be degraded (Figure 4-2).

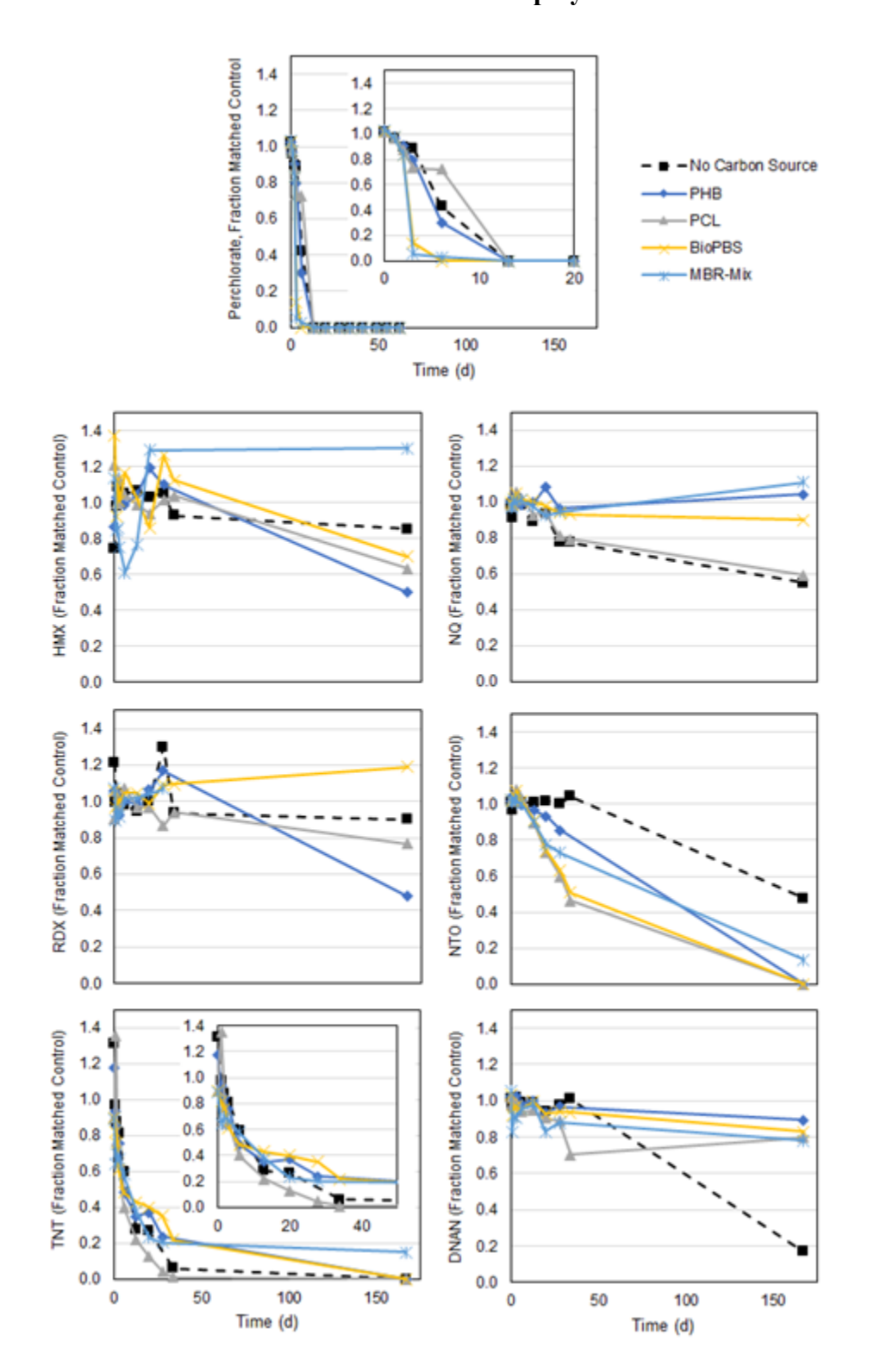
Figure 4-2. Aerobic NQ degradation by *Pseudomonas* NQ5 in presence of slow-release carbon source biopolymers.



4.2.3 Mixed energetics degradation

The degradation of mixed energetics by the MBR enrichment culture under anoxic conditions with PHB, PCL, and BioPBS is shown in Figure 4-3. Without any added carbon source, the MBR culture demonstrated complete degradation of ClO₄⁻ and TNT, and partial degradation of NQ, NTO, and DNAN. This is likely due to either endogenous intracellular carbon storage possessed by the cells, or due to exogenous carbonaceous matter that was added with the MBR inoculum, even though the culture was washed before use. The presence of BioPBS resulted in slightly faster degradation of ClO₄⁻. Degradation of NTO and HMX was was greater in the presence of all three polymers, and PHB supported more RDX degradation. Degradation of NQ and DNAN was not enhanced by any of the polymers.

Figure 4-3. Anoxic degradation of energetics by MBR mixed culture in presence of slow-release carbon source biopolymers.



4.3 CONCLUSIONS

These results indicated that combining bioaugmentation with these bacterial cultures with addition of the slow-release carbon sources PHB, PCL, and BioPBS would be effective for biodegrading the mixture of energetics that were going to be tested in the column experiments.

While the SEFA compounds were also demonstrated to support RDX degradation, the fact that these compounds were fine powders precluded their use in the column experiments, as it was assumed they would not be well retained in the porous matrix.

REFERENCES

- Coleman, N.V., Nelson, D.R., Duxbury, T., 1998. Aerobic biodegradation of hexahydro-1,3,5-trinitro-1,3,5-triazine (RDX) as a nitrogen source by a *Rhodococcus* sp., strain DN22. Soil Biol Biochem 30, 1159-1167.
- Fuller, M.E., Farquharson, E.M., Hedman, P.C., Chiu, P., 2022. Removal of munition constituents in stormwater runoff: Screening of native and cationized cellulosic sorbents for removal of insensitive munition constituents NTO, DNAN, and NQ, and legacy munition constituents HMX, RDX, TNT, and perchlorate. J Hazard Mater 424, 127335.https://doi.org/10.1016/j.jhazmat.2021.127335.
- Fuller, M.E., Hedman, P.C., Chu, K.-H., Webster, T.S., Hatzinger, P.B., 2023. Evaluation of a sequential anaerobic-aerobic membrane bioreactor system for treatment of traditional and insensitive munitions constituents. Chemosphere 340, 139887.https://doi.org/10.1016/j.chemosphere.2023.139887.
- Fuller, M.E., McClay, K., Hawari, J., Paquet, L., Malone, T.E., Fox, B.G., Steffan, R.J., 2009. Transformation of RDX and other energetic compounds by xenobiotic reductases XenA and XenB. Appl Microbiol Biotechnol 84, 535-544.
- Hareland, W.A., Crawford, R.L., Chapman, P.J., Dagley, S., 1975. Metabolic function and properties of 4-hydroxyphenylacetic acid 1-hydroxylase from *Pseudomonas acidovorans*. J Bacteriol 121, 272-285.
- Kim, J., Fuller, M.E., Hatzinger, P.B., Chu, K.-H., 2024. Isolation and characterization of nitroguanidine-degrading microorganisms. Sci Total Envir 912, 169184. https://doi.org/10.1016/j.scitotenv.2023.169184.
- Pak, J.W., Knoke, K.L., Noguera, D.R., Fox, B.G., Chambliss, G.H., 2000. Transformation of 2,4,6-trinitrotoluene by purified xenobiotic reductase B from *Pseudomonas fluorescens* I-C. Appl Environ Microbiol 66, 4742-4750.

5. Evaluation of Biochar for Abiotic and Biotic Degradation of Legacy and Insensitive Munition Energetics

- Hypothesis 2: Biochar is a more effective sorbent than activated carbon for legacy and insensitive munitions constituents.
- Hypothesis 3: Biochar can mediate the abiotic degradation of legacy and insensitive munitions constituents in surface runoff through its capacity to store and transfer electrons.
- Hypothesis 4: Biochar can promote the biotic degradation of legacy and insensitive munitions constituents in surface runoff.

5.1 Sorption of MC to Biochar

Black carbon is known to possess high sorption affinity and capacity for NACs due to the electron doner-acceptor interactions (π - π orbital overlap) between the electron-rich graphene moieties in black carbon and the electron-withdrawing nitro groups in NACs (such as TNT and DNAN) (Cornelissen et al., 2005; Zhu et al., 2005; Xiao and Pignatello, 2015). Biochar is a class of pyrogenic black carbon that can be prepared inexpensively from waste biomass, such as wood chips, and has been used as sorbent because of its significant BET surface area (on the order of a few hundred m^2/g) (Xin et al., 2020; Xin et al., 2022). The goal of this portion of the project was to evaluate the effectiveness and capacity of biochar as a sorbent for MC removal from stormwater. We tested the equilibrium sorption of four MCs – NQ, NTO, DNAN, and RDX – to a commercial wood-derived biochar in an artificial stormwater runoff (ASR).

5.1.1 METHODS

<u>Biochar</u>. Rogue biochar (Oregon Biochar Solutions, OR) was made from Douglas Fir and Ponderosa pine through fast pyrolysis at 900 °C. It was chosen for the sorption study because its BET surface area $(407\pm9~\text{m}^2/\text{g})$ was the highest among the five commercial biochars we had tested. Biochar particles in the size range of 250-500 mm were ground at 4,000 rpm for 3 min using a Beadbug 3 bead homogenizer (Benchmark Scientific, Sayreville, NJ) to obtain <53 mm particles. Ground biochar was then washed in continuously aerated deionized water to deplete all stored electrons and ensure the electron donating capacity (EDC) of the biochar was zero with respect to the O₂/H₂O redox couple (E_H = +0.81 V vs. standard hydrogen electrode, or SHE, at pH 7.0 and 0.21 atm P_{O2}). The pre-aeration was performed to ensure that no abiotic reduction of MCs would occur during the sorption experiments. Detailed characterization results of the biochar have been reported in Xin et al. (2022).

<u>Sorption Experiments</u>. Sorption of MCs to air-oxidized Rogue biochar (Rogueox) was investigated through batch experiments carried out in ASR which contained 0.38 mM Na⁺, 0.24 mM K⁺, 0.09 mM NH⁴⁺, 0.08 mM Ca²⁺, 0.05 mM Mg²⁺, 0.65 mM Cl⁻, 0.15 mM SO₄²⁻ and 0.02 mM NO₃⁻. ASR was prepared based on the composition of stormwater samples collected from an east coast U.S. Navy facility. Aqueous samples were collected at different incubation times, syringe-filtered, and analyzed by HPLC to assess the contact time required to reach sorption equilibrium.

Equilibrium experiments were conducted to obtain sorption isotherms for NTO, NQ, DNAN, and RDX on Rogueox in ASR at pH 6.0. A series of duplicate amber borosilicate batch reactors were set up that contained ASR and an MC at different initial concentrations. For each MC the solid-to-solution ratio was chosen (Table 5-1) based on the preliminary test results. Samples (0.8 mL) were

collected at different incubation times and passed through 0.2- μ m PTFE syringe filters for HPLC analysis. Experiments were run for up to 400 h until an apparent sorption equilibrium was reached (i.e., when variations in aqueous concentrations were less than 1% per hour). pH was maintained at 6.0±0.2 using 0.05 N HCl. For each MC, the mass sorbed per gram of biochar (C_s) was plotted against the equilibrium aqueous concentration (C_{eq}) and the data were fitted to a Langmuir isotherm (eq 1) using the least-square method.

$$C_s = \frac{K_L C_{eq} C_{s,max}}{1 + K_L C_{eq}}$$
 [Eq. 1]

To establish mass balance, NTO and NQ (and potential daughter product) were extracted with a $3.7 \, (v/v)$ mixture of acetonitrile and 0.1% trifluoroacetic acid, and DNAN and RDX (and potential daughter products) were extracted with an 8.2 mixture of acetonitrile and 0.1% trifluoroacetic acid. Each biochar sample was extracted three times.

Analyses. MCs were analyzed using an Agilent 1200 Series HPLC (Santa Clara, CA) equipped with an Agilent 1260 diode array detector. The hydrophilic analytes NTO and NQ were separated using a Thermo Scientific (Waltham, MA) Hypercarb porous graphitic carbon column (4.6 mm × 100 mm, 5 μm particle size). A mixture of acetonitrile and 0.1% trifluoroacetic acid was used as eluent at a flow rate of 2.0 mL/min. The run time was 10 min and the temperature was 34°C. NTO and NQ were detected at 7.9 and 5.8 min and quantified based on absorbance at 318 and 260 nm, respectively. The hydrophobic analytes DNAN and RDX were separated using an Agilent Zorbax SB-C18 column (4.6 mm × 50 mm, 3.5 μm particle size). A mixture of phosphate buffer and methanol was used as eluent at a flow rate of 1.7 mL/min. The run time was 7 min and the temperature was ambient. DNAN and RDX were detected at 4.8 and 3.4 min, respectively, and quantified based on absorbance at 214 nm.

Table 5-1. Conditions used for the MC sorption experiment.

MC	C_{aq0}	Biochar	Dose	pН	Background solution	Replicates
NTO	5-125 μM	$Rogue_{OX}$	0.20 g/L	6	ASR	2
NQ	20-250 μM	$Rogue_{OX}$	0.44 g/L	6	ASR	2
DNAN	30-300 μ <u>M</u>	$Rogue_{OX}$	0.33 g/L	6	ASR	2
RDX	10-125 <u>μΜ</u>	$Rogue_{OX}$	0.88~g/L	6	ASR	2

5.1.2 RESULTS and DISCUSSION

Unlike NTO, which is negatively charged at circumneutral pH (pKa 3.76) (Lee et al., 1987; Cárdenas-Hernández et al., 2020), NQ, DNAN, and RDX are neutral and less water-soluble, and hence sorption may play a greater role in their removal by biochar. As shown in Figure 5-1, all MCs were removed rapidly from solution as soon as Rogueox was added. Removal subsequently slowed but continued for up to 340 h until apparent equilibrium was reached. The equilibrium concentrations of sorbed and aqueous MCs from Figure 5-1 were then used to construct sorption isotherms.

The sorbed and aqueous concentrations of each MC were fitted separately to a Langmuir isotherm as shown in Figure 5-2 and Table 5-2. The maximum sorption capacities (C_{s,max}) of Rogueox for NTO, NQ, DNAN, and RDX were determined to be 154, 388, 476, and 213 µmol/g in ASR at pH 6.0, corresponding to approximately 2.0, 4.0, 9.4, and 4.7% of the biochar mass, respectively. As expected, the negatively charged NTO exhibited the lowest sorption capacity, whereas DNAN (an NAC) exhibited the highest. Approximately 83–88% of the sorbed MC mass was removed by solvent extraction, but no known reduction intermediates or products throughout the incubations were detected, suggesting all MCs were removed from solution by Rogueox predominantly or exclusively through sorption.

The $C_{s,max}$ and K_L values, which represent the sorption capacity of Rogueox and its affinity for MCs, respectively, are highest for DNAN. This was expected based on the nitroaromatic structure and high Kow and Koc of DNAN (Table 5-2). In contrast, despite its low solubility, RDX exhibited significantly lower $C_{s,max}$ and K_L than DNAN because of its non-aromatic structure and hence incapability of π - π interactions. Finally, although NQ has a high water solubility and the lowest molecular weight of the MCs, its $C_{s,max}$ is twice that for NTO on a mass basis, suggesting the marked effect of charge on preventing sorption. Overall, Rogue biochar showed moderate to high sorption capacities for MCs (2.0–9.4% by weight), particularly for DNAN and presumably other NACs.

Table 5-2. MC properties and sorption isotherm parameters with Rogueox in ASR, pH 6.

MC		NTO	NQ	DNAN	RDX
Structure		O_2N N N N	H ₂ N NO ₂	OCH ₃ NO ₂	NO_2 NO_2 NO_2 NO_2 NO_2
Formulation		IMX-101 IMX-104	IMX-101	IMX-101 IMX-104	IMX-104
Physical properties ^a	MW (g mol ⁻¹) Solubility (mg L ⁻¹) Log K_{OW}	130.08 16 642 (ref. 5) 0.37–1.03 (ref. 5)	104.07 2600 (ref. 75)–5000 (ref. 69) 0.10 (ref. 75)	198.13 276 (ref. 5) 1.64 (ref. 5)	222.26 60 (ref. 5) 0.81–0.87 (ref. 5)
Isotherm parameters b	$egin{aligned} &\operatorname{Log} K_{\operatorname{OC}} \ &C_{\operatorname{s,max}} \left(\operatorname{\mu mol} \ \operatorname{g}^{-1} ight) \ &C_{\operatorname{s,max}} \left(\operatorname{\%, w/w} ight) \ &K_{\operatorname{L}} \left(\operatorname{\mu M}^{-1} ight) \ &R^2 \end{aligned}$	3.03 (ref. 5) 154 2.0 0.07 0.94	388 4.0 0.02 0.96	3.11 (ref. 5) 476 9.4 2.96 0.97	0.88-2.40 (ref. 5) 213 4.7 0.44 0.98

 $[^]a$ MW: molecular weight, $K_{\rm OW}$ and $K_{\rm OC}$: octanol-water and organic carbon-water partition coefficients, respectively. Solubility at 25 $^{\circ}$ C. b Parameters of the isotherms are obtained through Langmuir isotherm fitting, as shown in Fig. 5.

Figure 5-1. Sorption of MCs to Rogue_{OX} over time.

Experiments were performed in ASR at pH 6.0 with different initial MC concentrations. (a) NTO to 0.20 g/L Rogueox (b) NQ to 0.44 g/L Rogueox (c) DNAN to 0.33 g/L Rogueox (d) RDX to 0.88 g/L Rogueox.

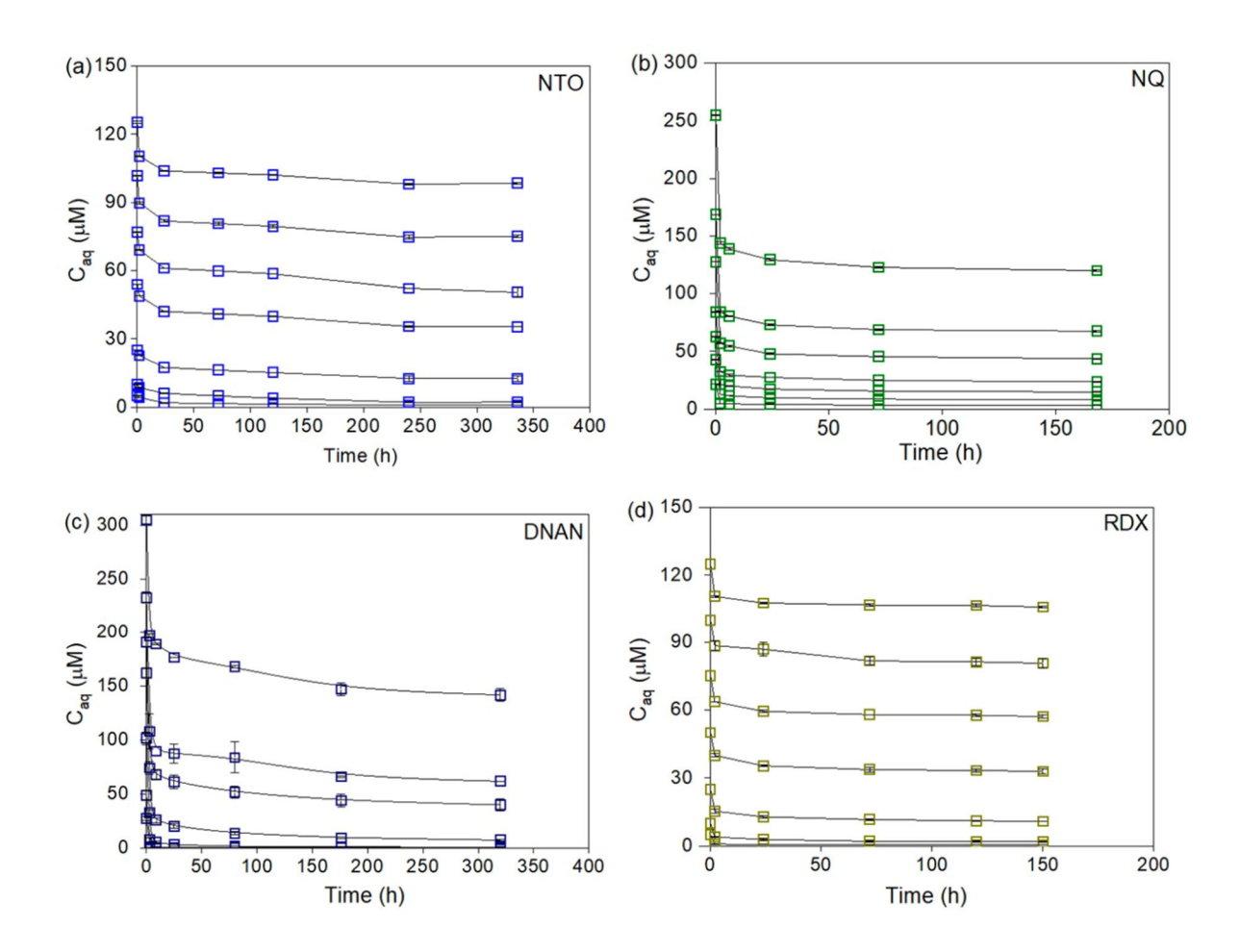
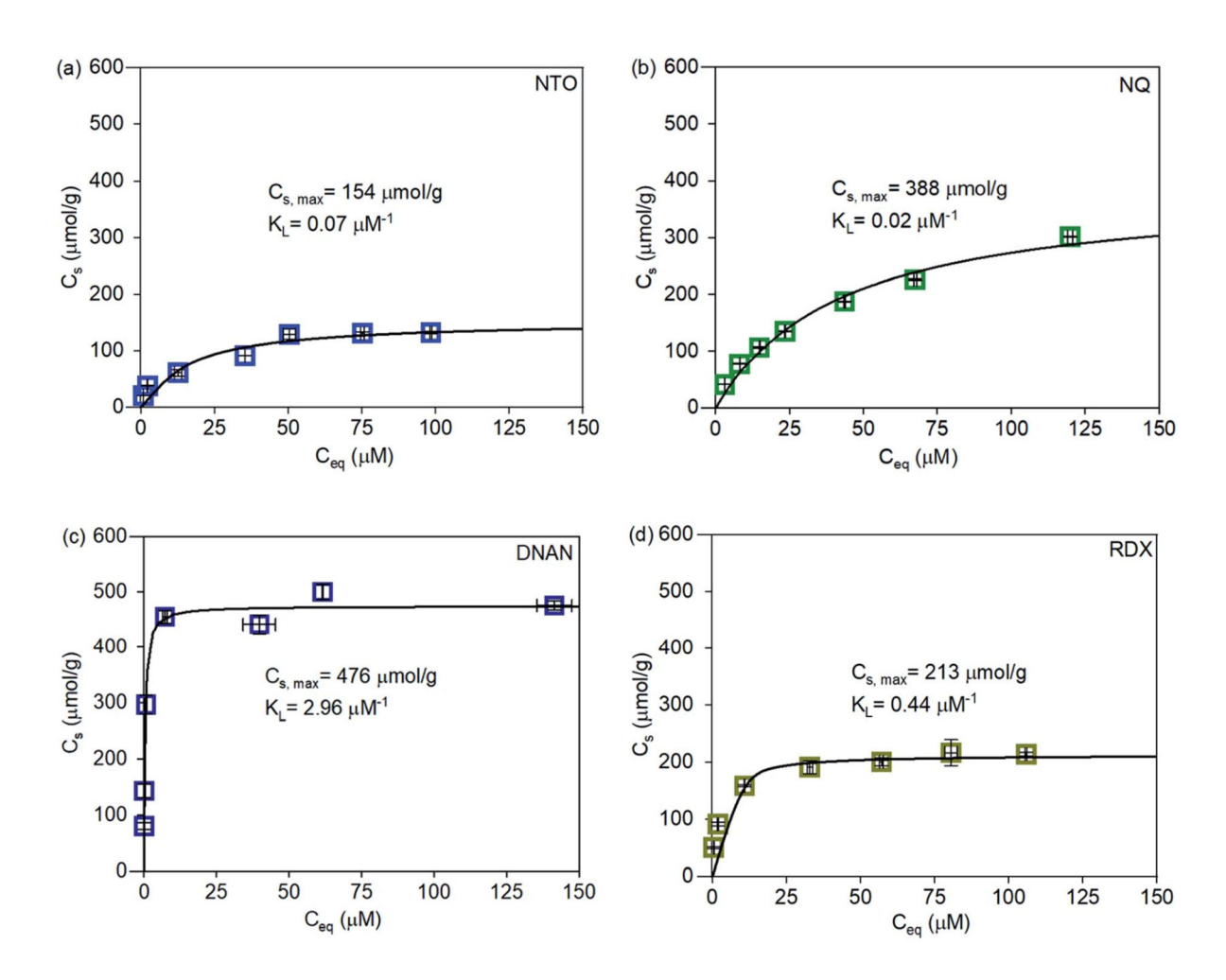


Figure 5-2. Sorption of MCs a) NTO, b) NQ, c) DNAN, and d) RDX to Rogue_{OX} in ASR at pH 6.0 and the fitted Langmuir isotherms.



5.2 Abiotic Reduction of MCs by Reduced Biochar

In addition to being a sorbent, black carbon is reactive and can mediate oxidation-reduction (redox) reactions through two different mechanisms: electron conduction (Oh et al., 2002; Oh and Chiu, 2009; Xu et al., 2010; Oh et al., 2013a; Oh et al., 2013b) and electron storage (Klüpfel et al., 2014; Saquing et al., 2016). The first mechanism requires an external electron donor and MC to be in simultaneous contact with a conductive (i.e., graphitic) moiety in biochar (Cao et al., 2012; Xiao and Chen, 2017). This mechanism has been demonstrate for the reductive degradation of 2,4-dinitrotoluene, RDX, and nitroglycerin (Oh and Chiu, 2009; Xu et al., 2010; Oh et al., 2013a; Oh et al., 2013b).

The second mechanism, which is the predominant redox mechanism for non-conductive, low-temperature black carbon like plant-derived biochar, involves electron storage through reversible reactions of redox-facile functional groups such as quinones and hydroquinones in biochar structure. Electrons can be stored through reduction of biochar's quinone groups and removed via

oxidation of its hydroquinones (Klüpfel et al., 2014). The capacity of biochar to store and reversibly exchange electrons with its surroundings is termed electron storage capacity (ESC). ESC is operationally defined as the sum of electron donating capacity (EDC = sum of all electrons stored in the hydroquinones) and electron accepting capacity (EAC = combined capacity of the quinones to accept electrons) (Klüpfel et al., 2014; Saquing et al., 2016; Xin et al., 2019). Biochar ESC can vary from 0.2 to 7 mmol e⁻/g, is distributed over a broad range of reduction potential (E_H), and is highly reversible over repeated redox cycles (Klüpfel et al., 2014; Prévoteau et al., 2016; Zhang et al., 2018; Xin et al., 2019; Zhang et al., 2019; Xin et al., 2021).

We hypothesized that, through its ESC, biochar can be an electron donor and reductively transform MCs when its ESC is filled (i.e., when its quinones are reduced to hydroquinones). We performed batch reduction experiments to assess whether electrons stored in biochar would be available for the abiotic reduction of MCs (chemically, without microbes or redox mediators). We tested the reactivity of all four MCs (NTO, NQ, DNAN, RDX), with particular emphasis on NTO. This is because NTO has the highest reactivity among all the MCs (Cárdenas-Hernández et al., 2023; Murillo-Gelvez et al., 2023) and because NTO sorbs to biochar minimally which would enable high mass recovery.

5.2.1 METHODS

Biochar. Two commercial wood biochars, Soil Reef biochar (SRB) and Rogue biochar (Rogue) were used. The physical-chemical properties of SRB and Rogue were measured and summarized in Table 5-3. For each biochar, two types of samples were prepared: air-oxidized biochar (SRBox and Rogueox) and dithionite-reduced biochar (SRBRED and Roguered). SRBox or Rogueox were depleted of electrons (i.e., EDC = 0) and served as sorption controls, whereas SRBred or Roguered were fully charged (i.e., EDC = ESC) and were used to study MC reduction. To prepare dithionite-reduced biochars, SRBox and Rogueox were placed in an anaerobic glove box (Coy Laboratory, Grass Lake, MI) under $98 \pm 0.5\%$ N₂ and $2.0 \pm 0.5\%$ H₂ (Po₂ < 5 ppm) to deoxygenate. SRBox and Rogueox were then reduced with freshly prepared 25 mM sodium dithionite in 100 mM citrate buffer at pH 6.4 for 3 days (measured $E_H = -0.43$ V vs. SHE). Dithionite was added in excess and was replenished as needed. After reduction, SRBred and Roguered were collected on a glass microfiber filter, rinsed with copious deoxygenated deionized water, vacuum-dried, and stored in a desiccator in the glove box until use.

<u>NTO Reduction</u>. Batch experiments were performed with SRB for NTO reduction in pH 6, 8, and 10 buffer solutions. To initiate an experiment, a predetermined amount of SRB_{OX} or SRB_{RED} (0.40 or 0.80 g L⁻¹) was added to an amber borosilicate reactor containing 125 mL of 110 μM NTO in 50 mM pH buffer. MES, Tris, and CAPSO were used to maintain the pH at 6.0 ± 0.1 , 8.0 ± 0.1 , and 10.0 ± 0.1 , respectively. Blanks without biochar were prepared identically. All reactors were placed on an orbital shaker at 100 rpm. Samples (0.625 mL) were withdrawn at different reaction times and immediately passed through a 0.22-μm PTFE syringe filter for HPLC analysis. Experiments were performed for up to 600 h until the concentration of 3-amino-1,2,4-triazol-5-one (ATO), the sole NTO reduction product, plateaued.

<u>Biochar EDC Measurement</u>. The electron content (i.e., EDC) of fresh SRB_{RED} and spent SRB_{RED} (recovered from the NTO reduction experiment) was measured using ferricyanide as an oxidant ($E_H = +0.43 \text{ V}$ vs. SHE) (Aeschbacher et al., 2010). Reactors containing fresh SRB_{OX} and SRB_{OX}

exposed to the same NTO solution for the same duration were included as controls. SRB samples were placed in 0.23 L of 1 mM ferricyanide solution in 50 mM MES, Tris, or CAPSO buffer. Electrons transferred from SRB to ferricyanide were determined based on the amount of ferricyanide consumed. The concentration of ferricyanide was measured by absorbance at 420 nm using a Vernier LabQuest 2 UV-vis spectrophotometer (Beaverton, OR). The extinction coefficients of ferricyanide at pH 6, 8, and 10 were 1135 ± 40 , 1152 ± 40 , and 1058 ± 40 M⁻¹cm⁻¹, respectively. Each SRB sample was oxidized with ferricyanide for up to 72 h. After EDC measurement, SRB was collected by filtration and vacuum-dried at 65 °C for weight measurement.

<u>DNAN and RDX Reduction</u>. Batch experiments for MCs reduction in ASR were conducted using similar procedures as for the sorption experiments described in section 5.1.1. Batch experiments were performed with Rogueox or Roguered for NTO, NQ, DNAN, and RDX in ASR at pH 6.0. To compare SRB and Rogue, an additional experiment with SRB (SRBox or SRBred) was run for NTO in ASR at pH 6.0 under identical conditions.

Analyses. MCs were analyzed using an Agilent 1200 Series HPLC (Santa Clara, CA) equipped with an Agilent 1260 diode array detector. The hydrophilic analytes NTO, ATO, and NQ were separated using a Thermo Scientific (Waltham, MA) Hypercarb porous graphitic carbon column (4.6 mm × 100 mm, 5 µm particle size). A mixture of acetonitrile and 0.1% trifluoroacetic acid was used as eluent at a flow rate of 2.0 mL/min. The run time was 10 min and the temperature was 34.0 °C. NTO, ATO, and NQ were detected at 7.9, 4.3, and 5.8 min and quantified based on absorbance at 318, 210, and 260 nm, respectively. The hydrophobic analytes, including DNAN, RDX, HMX, and their daughter products, were separated using an Agilent Zorbax SB-C18 column (4.6 mm × 50 mm, 3.5 μm particle size). A mixture of phosphate buffer and methanol was used as eluent at a flow rate of 1.7 mL/min. The run time was 7 min and the temperature was ambient. DNAN and RDX were detected at 4.8 and 3.4 min, respectively, and quantified based on absorbance at 214 nm. The same method was used to quantify daughter products of DNAN (Liang et al., 2013) and RDX (Bernstein et al., 2013). 2-ANAN, 4-ANAN, and DAAN were measured at 4.2 min (254 nm), 3.2 min (234 nm) and 2.3 min (210 nm), respectively, and MNX, DNX, and TNX were detected at 2.9, 2.4, and 1.9 min, respectively, based on absorbance at 234 nm. Nitrite, a potential RDX reduction product (Tong et al., 2021) as measured using Hach NitriVer® 3 reagent (Loveland, CO) and a Vernier LabQuest 2 UV-vis spectrophotometer (Beaverton, OR).

Table 5-3. Physical-chemical properties of Soil Reef biochar and Rogue biochar.

		Soil Reef biochar (SRB)	Rogue biochar (Rogue)		
Vendor		The Biochar Company a	Oregon Biochar Solutions		
Source material		Southern Yellow Pine	Douglas Fir + Ponderosa Pir		
Pyrolysis temperatu	ire (°C)	550 (slow pyrolysis)	900 (fast pyrolysis)		
Elemental C		72.01±5.00	68.47±10.00		
composition (%)	Н	1.96 ± 0.02	1.50±0.20		
	N	0.36 ± 0.08	0.28 ± 0.07		
	S	0.26 ± 0.03	0.24±0.15		
	O	20.82±5.00	16.99±10.00		
Ash (%)		4.59±1.30	12.52±0.50		
pH		7.53±0.05	8.88±0.08		
BET (m^2/g)		158±3	407±9		
CEC a (mmol/g)		0.42±0.02	0.12±0.03		
ESC (mmol/g) mea	sured with	3.54±0.13	7.07±0.15		
Ti(III) citrate and D	Ю	(2.43±0.00) ^b	(6.78±0.20) ^b		

Errors represent the range of results from duplicates.

5.2.2 RESULTS and DISCUSSION

Figure 5-3 shows NTO removal by SRBox and SRB_{RED} at pH 6, 8 and 10, and the mass balance at the end of each experiment. SRBox sorbed NTO in small quantities most of which were recovered by extraction. NTO sorption decreased with increasing pH, with 80%, 93% and 99% of the initial mass remaining in solution at equilibrium at pH 6, 8, and 10, respectively (solid blue bars in Figure 5-3(d)). As NTO is anionic (pKa 3.76) (Lee et al., 1987) at all three pH values, the decreasing sorption (24, 10, and 2 μ mol/g, respectively) was most likely due to increasingly negative surface charge of SRB with pH (Mukherjee et al., 2011). Extraction of SRBox from pH 6 and pH 8 reactors with CAPSO buffer yielded mass balances of 94% and 101%, respectively.

In contrast, significantly more NTO was removed from solution by SRB_{RED} and ATO was formed concomitantly, indicating NTO was chemically transformed to ATO by SRB_{RED}, as shown in Eq. 2.

^a CEC measured using EPA Method 9080.

^b Regenerable ESC, measured over two additional redox cycles.

Reduction of NTO to ATO was rapid in the first 24 h and continued at decreasing rates for up to 600 h. Note that panel (a)–(c) of Figure 5-3 are semi-log plots and therefore the changing slopes represent decreasing pseudo-first-order rate constants. The decreasing NTO reduction rate constants could be due to one of two reasons (or both). First, it has been shown that a large portion of ESC resides in the interior of biochar particles (Xin et al., 2019), and the rate of access ESC is limited by pore diffusion (of NTO into biochar interior), which is approximately two orders of magnitude slower than diffusion in the bulk solution. Second, the ESCs of biochar are distributed over a range of reduction potentials (Aeschbacher et al., 2011; Xin et al., 2019), and hence would react with NTO at a wide spectrum of rate constants. The decreasing NTO reduction rate over time likely reflects a combination of slow diffusion through tortuous channels to access ESC residing in deep pores in biochar interior, and slow reaction with functional groups of increasing reduction potentials (i.e., decreasing reactivity).

The combined aqueous NTO and ATO masses were about 80% at pH 6 and 8 and virtually 100% at pH 10. This suggests that ATO was sorbed to a similar extent at pH 6 and 8 but negligibly at pH 10. As the pK_a of ATO had not been reported, we performed a titration and determined the pK_a of ATO to be 8.71 (Dontsova et al., 2018). This is in agreement with the pH effect on ATO sorption, as ATO would be predominantly neutral at pH 6 and 8 and negatively charged at pH 10, where sorption would be hindered by electrostatic repulsion between the negatively charged ATO and negatively charged biochar surface (pH_{zpc} 2–3) (Mukherjee et al., 2011).

Figure 5-4 shows aqueous NTO removal and ATO formation with 0, 0.40, and 0.80 g/L of SRBox or SRB_{RED} at pH 10. NTO removal and ATO formation were observed with SRB_{RED}, but not SRBox. When the SRB_{RED} mass increased from 0.40 to 0.80 g/L, the amounts of NTO removed and ATO produced both doubled (Figure 5-4(c)), indicating the quantity of electrons per gram of SRB_{RED} available for NTO reduction within 600 h (i.e., the fraction of the ESC that was accessible to and of sufficiently low reduction potential to reduce NTO) was constant. Given the fact that 6 electrons per molecule are required to convert NTO to ATO (Eq. 2), the portion of ESC that was available for NTO reduction at pH 10 was 499 and 503 μ mol e $^-$ /g SRB, respectively, based on the amounts of NTO reduced (83.2 \pm 0.8 μ mol/g) and ATO produced (83.9 \pm 1.6 μ mol/g). At pH 6 and 8, the total ATO formed with 0.80 g/L of SRB_{RED} were 100 \pm 7 and 82 \pm 8 μ mol/g, corresponding to 600 and 492 μ mol e $^-$ /g, respectively, as shown in Figure 5-5 (red bars).

Although the reduction potential distribution of biochar's ESC has not been delineated, it appears to cover a broad range of potential. Because one gram of SRBox can store up to 4.0 mmol of e^- with dithionite as a reductant ($E_H = -0.43 \text{ V}$ vs. SHE at pH 6.4) (Selwyn and Tse, 2008; Xin et al., 2019), the result above suggests that only 500–600 μ mol/g of the stored electrons in SRB_{RED}, or 12–15% of SRB's ESC, had sufficiently low reduction potential to reduce NTO. An effort to

establish an electron balance for NTO reduction by SRB_{RED} using dissolved oxygen as an oxidant ($E_H = +0.80 \text{ V}$ vs. SHE at pH 7) was hindered by the volatile nature of O₂. Therefore, ferricyanide ($E_H = +0.43 \text{ V}$ vs. SHE at pH 7) was used instead to retrieve electrons from SRB_{RED} before and after reaction with NTO (Xin et al., 2018). If all the electrons accessible to and reactive toward NTO can also reduce ferricyanide, then the amount of electrons remaining in used SRB_{RED} at the end of the NTO reduction experiment would be the difference between all retrievable electrons from unused fresh SRB_{RED} and the electrons consumed by NTO. The data in Figure 5-5 confirm this relationship and show the ESC of SRB that is reactive towards NTO was only 26–38% of that reactive towards ferricyanide, suggesting that NTO is significantly more difficult to reduce than ferricyanide.

The reactivity of biochar toward DNAN, RDX, and NQ was assessed by comparing MC removal by Rogueox (sorption only) and by Roguered (sorption plus reduction). NQ was removed from solution at similar rates and to the same extent with both SRB_{OX} and SRB_{RED} (Xin et al., 2022), suggesting NQ was removed by sorption only and was *not* reduced by SRB_{RED}. Consistent with this result, a recent study showed that NQ was nonreactive toward carbonaceous reductants such as dithionite-reduced hydroquinones and humic acids (Murillo-Gelvez et al., 2023). Therefore, abiotic reduction by carbonaceous materials may not be an important fate mechanism for NQ, even under highly reducing conditions.

In contrast, NTO, DNAN, and RDX were all reducible by reduced biochar. As shown in Figure 5-6(a), reduction of NTO by SRB_{RED} in ASR at pH 6 was in good agreement with that in MES buffer (Figure 5-3(a)), suggesting that the solution matrix did not influence the reactivity of either NTO or biochar. Under the same conditions, NTO was similarly reduced to ATO by Rogue_{RED}, indicating that the reactivity of reduced biochar toward NTO is likely general, not specific to SRB. Interestingly, Rogue_{RED} and SRB_{RED} converted similar amounts of NTO to ATO (91 and 94 µmol/g, respectively, Table 5-4). This suggests that the fraction of Rogue ESC reactive toward NTO was about 564 µmol/g, approximately the same as that for SRB (546 µmol/g), despite the higher ESC of Rogue. Note that the amount of NTO reduced per gram of SRB or Rogue depends on not the total ESC, but the fraction of ESC that has sufficiently low E_H (i.e., contains sufficiently reducing electrons) to degrade NTO.

Rogue_{OX} removed 518 μmol/g of DNAN and 232 μmol/g of RDX at the end of the experiment (Table 5-4), consistent with the fitted C_{s,max} values of 476 and 213 μmol/g, respectively (Table 5-3). In comparison, Rogue_{RED} removed additional 112 μmol/g of DNAN and 100 μmol/g of RDX, suggesting that these MCs were not only sorbed but chemically reduced by Rogue_{RED}. This was confirmed through identification of reduced products of DNAN and RDX. Unlike NTO, however, DNAN and RDX sorbed more strongly to Rogue and the sorbed molecules were not readily available for reduction. Therefore, only relatively small fractions of the DNAN and RDX removed from water was recovered as reduction products.

Abiotic reduction of DNAN by Rogue_{RED} was confirmed by the detection of 66 μ mol/g of 2-ANAN and a trace amount (<2 μ mol/g) of 4-ANAN in the aqueous and solid phases combined. DAAN was not observed in either the aqueous phase or the solid phase (through extraction) throughout the experiment. Additional experiments carried out under the same conditions using 2-ANAN as the starting reactant confirmed that no DAAN was produced from 2-ANAN (Xin et al.,

2022). Based on the yields of 2-ANAN and 4-ANAN and that six electrons are required to reduce DNAN to 2-ANAN or 4-ANAN, the fraction of Rogue's ESC that was reactive toward DNAN was $402 \mu \text{mol/g}$, approximately 30% lower than that toward NTO. This result is consistent with the recent reports that NTO is more reactive than DNAN toward abiotic reductants (Pennington and Brannon, 2002; Arthur et al., 2018; Menezes et al., 2021).

In RDX reactors, small quantities of NO₂⁻ (ca. 5 μM) and MNX (<1 μM) were measured with Rogue_{RED}, but not Rogue_{OX}. MNX and NO₂⁻ are known RDX degradation products, and thus their detection supports the conclusion that RDX was transformed by Rogue_{RED}. Specifically, MNX and NO₂⁻ were formed through reduction, since an addition of two electrons is required for MNX formation and reductive denitration of RDX to form NO₂⁻ has been well-documented (Oh et al., 2005; Tong et al., 2021). RDX degradation was further confirmed by the accumulation of NO₂⁻ following repeated additions of RDX in reactors containing Rogue_{RED} (Xin et al., 2022). The mass recovery of RDX with Rogue_{RED} was only 64%, considerably lower than the 96% RDX mass recovery obtained with Rogue_{OX} following the same extraction procedures. This suggests that approximately 36% of the initial RDX was transformed by Rogue_{RED}, possibly to ring cleavage or other fragmentation products.

In summary, the results of the abiotic reduction experiments show that (1) NTO, DNAN, and RDX (but not NQ) can be chemically transformed by reduced biochar, and (2) only a fraction of the total ESC was sufficiently reducing to effect MC reduction, and the extent of reduction was influenced by the extent of sorption. Taken together, wood-based biochar can remove multiple classes of MCs – nitroaromatics, nitramines, and azoles – from synthetic stormwater through a combination of sorption and abiotic reduction.

Table 5-4. Summary of MC reduction results with biochar at pH 6.0.

MC		NTO	NTO	NTO	DNAN	RDX
-1-1-						_
Biochar		SRB	SRB	Rogue	Rogue	Rogue
Background solution		50 mM MES	ASR	ASR	ASR	ASR
Removal by RED ^a	$(\mu \text{mol g}^{-1})$	112 ± 8	103 ± 8	112 ± 2	630 ± 20	332 ± 19
Removal by OX ^b		24 ± 0	15 ± 2	44 ± 6	518 ± 5	232 ± 20
Δ removal ^c		88 ± 8	88 ± 6	68 ± 6	112 ± 16	100 ± 6
Product(s) formed		100 ± 7^d	91 ± 6^d	94 ± 2^d	67 ± 7^e	14 ± 6^f
e ⁻ transferred ^g		600 ± 40	546 ± 40	564 ± 14	402 ± 40	_

^a RED: reduced biochar (SRB_{RED} or Rogue_{RED}). ^b OX: oxidized biochar (SRB_{OX} or Rogue_{OX}). ^c Δ Removal: additional MC removal by reduced biochar than oxidized biochar (removal by RED – removal by OX). ^d ATO formed. ^e 2ANAN and 4ANAN formed. ^f MNX and NO₂⁻ formed. ^g e⁻ transferred (μmol e⁻ g⁻¹) = product(s) formed (μmol g⁻¹) × 6 (mol e⁻ mol⁻¹ product).

Figure 5-3. Abiotic reduction of NTO by biochar at several pH values.

Aqueous concentration (C_{aq}) of NTO and ATO over time with 0.80 g/L of SRB_{OX} or SRB_{RED} at (a) pH 6 (50 mM MES) (b) pH 8 (50 mM Tris), and (c) pH 10 (50 mM CAPSO). (d) Mass balance at the end of reduction experiment. The y-axis in panels (a) to (c) shows the natural logarithm of C_{aq} of NTO and ATO relative to the initial NTO concentration ($C_{aq0} = 110 \mu M$). The total mass is based on blank without SRB. NTO_{aq} and ATO_{aq} are the final masses in the aqueous phase, and NTO_s and ATO_s the sorbed masses extracted from the solid.

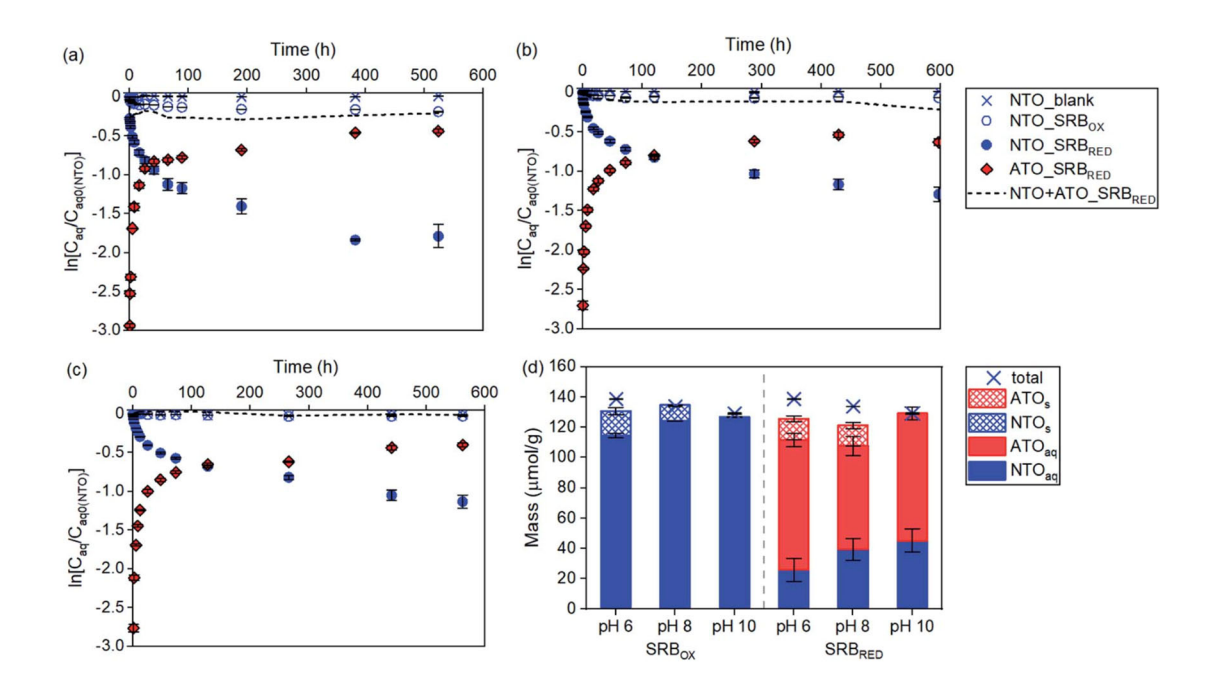


Figure 5-4. Abiotic reduction of NTO by biochar at pH 10.

(a) Aqueous concentrations (C_{aq}) of NTO and ATO over time with 0.80 g/L of SRB_{OX} or SRB_{RED} at pH 10. (b) C_{aq} of NTO and ATO over time with 0.40 g/L of SRB_{OX} or SRB_{RED} at pH 10. (c) Concentrations of ATO produced and NTO removed by SRB_{RED} .

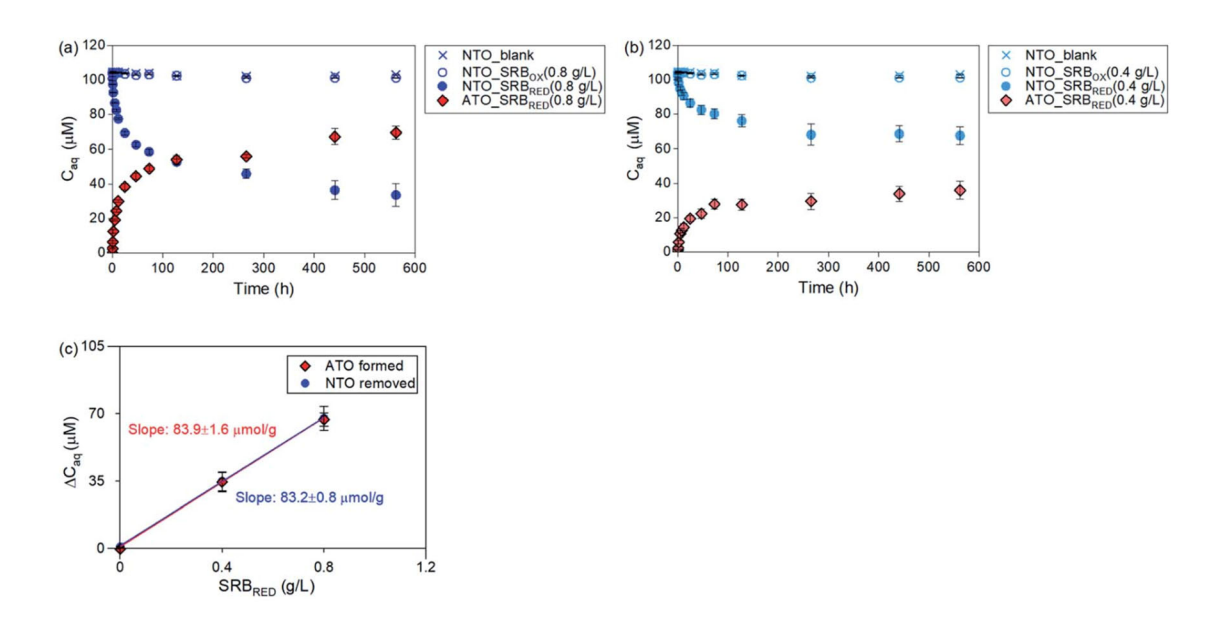


Figure 5-5. Electron balance for NTO reduction by SRB_{RED} .

Electrons of fresh SRB_{RED} consumed by NTO were calculated based on ATO production.

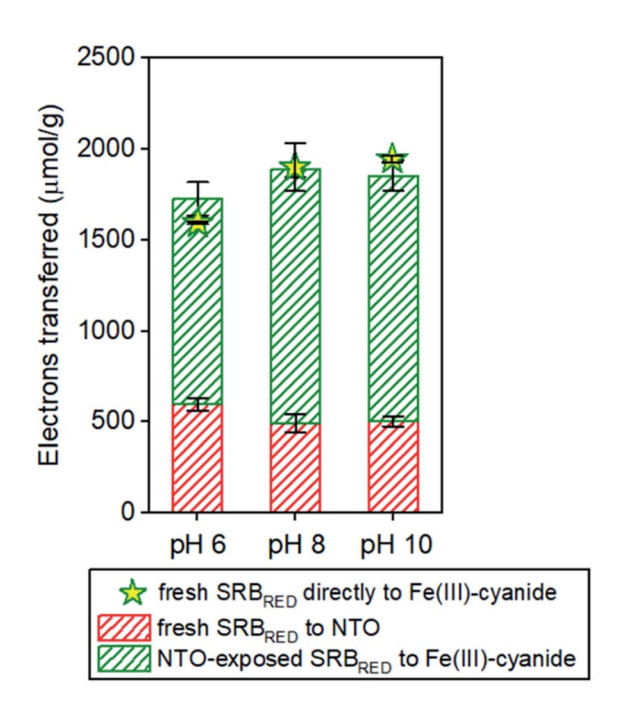
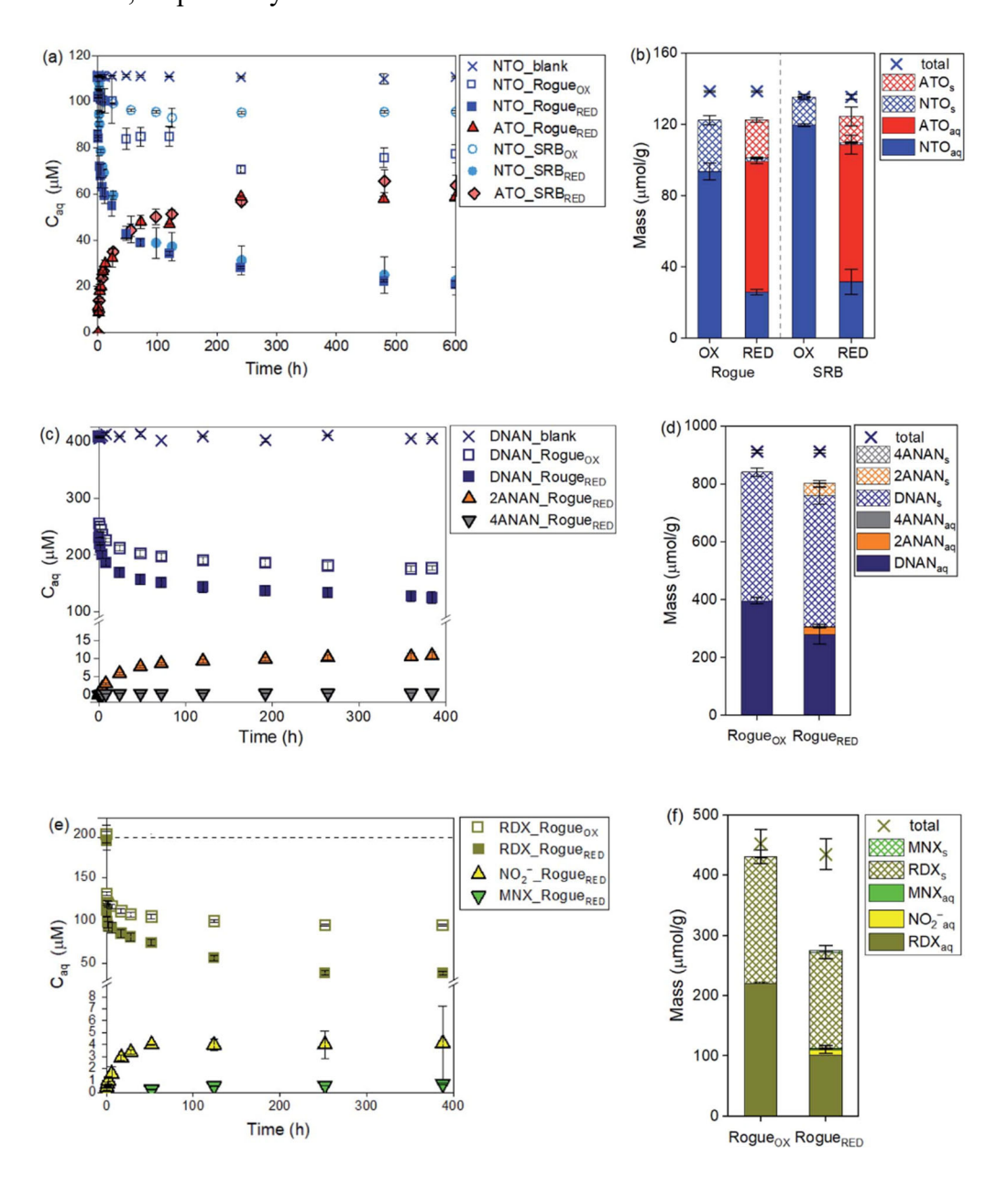


Figure 5-6. Abiotic reduction of NTO, DNAN, and RDX by biochar in ASR, pH 6.

(a) Aqueous concentration (C_{aq}) of NTO and ATO over time with 0.80 g/L of SRB or Rogue. (b) NTO mass balance. (c) C_{aq} of DNAN and 2-ANAN/4-ANAN over time with 0.44 g/L of Rogue. (d) DNAN mass balance. (e) C_{aq} of RDX, MNX, and NO₂ over time with 0.44 g/L of Rogue. (f) RDX mass balance. "total" is the DNAN or RDX added to blank. Subscripts "aq" and "s" denote mass in the aqueous phase at the end of the experiment (ca. 400 h) and that extracted from the solid, respectively.



5.3 Microbial Reduction of Perchlorate and Nitrate with Reduced Biochar

While most MCs are susceptible to abiotic reduction (with NQ being an exception) and can react directly with biochar, oxyanions like perchlorate are *chemically* inert, even though their reduction by reduced biochar is thermodynamically favorable. It was hypothesized that microbes could utilize reduced biochar as an electron donor and perchlorate (or other oxyanions like nitrate) as an electron acceptor, e.g., that reduced biochar can transform perchlorate *microbiologically*. Such transformation would convert the problematic oxyanions into innocuous end products such as chloride (Cl⁻) and nitrogen gas (N₂). Batch experiments were performed to test this hypothesis.

5.3.1 METHODS

<u>Biochar</u>. Rogue biochar obtained from Oregon Biochar Solutions was dried at 65°C and ground to below 100 μ m. The ground biochar was suspended in continuously aerated phosphate buffer at pH 7.0 \pm 0.2 and shaken at 100 rpm for four weeks. The long aeration time allowed for complete depletion of any residual electrons stored in the deep pores of biochar interior. After oxidation, the biochar was collected on a Whatman glass microfiber filter (pore size 0.4 μ m) using a Buchner funnel vacuum. The biochar was then dried at 65°C and stored in a desiccator before use.

Chemically reduced biochar was prepared by placing oxidized biochar in a Coy anaerobic glove box with an N_2/H_2 atmosphere (98:2, v/v). Biochar was added to 500 mL of basal salt medium (pH 7.0 ± 0.2) containing 25 mM dithionite as a reductant. The content was mixed at 100 rpm for 24 h. The process was repeated two times to ensure complete reduction. The reduced biochar was rinsed with deoxygenated deionized water, vacuum-dried in a glovebox, and stored in a desiccator under N_2/H_2 .

Culture. Topsoil (~30 cm) was collected from a garden outside of the Harker ISE Building at the University of Delaware in Newark, DE, in March 2022 (39.6788666, –75.7489206) and was used as a seed culture. A soil suspension was prepared inside the glovebox using 3.0 g of soil and 1.125 L of basal salt medium prepared with deoxygenated deionized water. The salt medium contained 0.42 g/L of NaHCO₃, 0.78 g/L of NaH₂PO₄, 0.012 g/L of NH₄Br, 0.1 g/L of KH₂PO₄, 10 mL of trace mineral solution, and 10 mL of vitamin supplement. Culture bottles were filled completely with no headspace, to eliminate H₂ from the glovebox atmosphere as a possible electron donor, and wrapped with aluminum foil, to prevent photosynthesis. Perchlorate (or nitrate) and reduced biochar were added at predetermined times as the sole electron acceptor and donor, respectively. Aqueous samples were taken over time, syringe-filtered (0.22 μm), and analyzed for perchlorate or nitrate and their reduction products (e.g., chlorate, chloride, nitrite).

Perchlorate Reduction. Batch bioreactors were prepared using 160-mL serum bottles in triplicates in an anaerobic glovebox: a) 1 g of reduced Rogue biochar (1 g RedBc) with 100 mL of liquid culture, b) 2 g of reduced biochar (2 g RedBc) with 100 mL of liquid culture, c) 1 g of oxidized biochar (OxBc) with 100 mL of liquid culture as biotic control, and d) 1 g of reduced biochar with 100 mL of fresh sterile basal salt medium as abiotic control. Each reactor was sealed with a rubber stopper and aluminum crimp to ensure anaerobic conditions and was wrapped with aluminum foil to avoid photosynthesis. The initial perchlorate concentration in all reactors was 3.3 mM. Reactors were removed from the glovebox and purged with grade-5 N₂ for 20 min to eliminate H₂. Liquid samples were taken at predetermined times using a sterile syringe with a side port needle and passed through a 0.22-μm PTFE syringe filter (Thermo-Fisher Scientific, MA) for analysis.

Nitrate Reduction. Nitrate reduction was investigated using ¹⁵N-labeled nitrate (¹⁵NO₃⁻, 98% ¹⁵N). Bioreactors were set up in duplicates in an anaerobic glovebox (N₂/H₂, 98:2) using 160-mL sterile glass serum bottles: a) RedBc+Microbes: 120 mL of medium containing 3.5 mM ¹⁵NO₃-inoculated with 1% (v/v) microbial culture and 0.5 g of chemically reduced Rogue biochar; b) OxBc control: 120 mL of medium containing 3.5 mM of ¹⁵NO₃-inoculated with 1% (v/v) culture and 0.5 g of airoxidized biochar; c) Biotic control: 120 mL of medium containing 3.5 mM K¹⁵NO₃-inoculated with 1% (v/v) culture without biochar; d) Abiotic control: 120 mL of sterile medium containing 3.5 mM ¹⁵NO₃-and 0.5 g of reduced biochar without bacteria. The reactors were purged with grade 5 ¹⁴N₂ to remove H₂ from the glovebox atmosphere. Reactors were covered with aluminum foil to prevent phototrophic activities and were shaken at 100 rpm. Samples were withdrawn at different elapsed times. The ¹⁴N mass that was carried over from the seed culture was ~6 μmol or <1% of the total N, and hence did not measurably affect the ¹⁵N content (>97%) in each bioreactor.

<u>Analyses</u>. Perchlorate, chloride, and nitrate were analyzed using a Metrohm Eco ion chromatogram (IC) equipped with a Metrosep Supp 5-100/4.0 anion column. The eluent solution used was HCO₃⁻/CO₃²⁻ (1.0 mM/3.2 mM) and the regenerant solution was 0.1 mM H₂SO₄. Elution times were 3.67 min, 6.8 min, and 34 min for chloride, nitrate, and perchlorate, respectively. Ammonium was analyzed by the salicylate method (Hach Method 10031) and measured using a Vernier LabQuest 2 UV-vis spectrophotometer (Vernier, OR). Chlorate was detectable but never observed above the detection limit during experiment, suggesting chlorate was biodegraded faster than perchlorate.

 15 N₂ mass was quantified using an Agilent 6890N gas chromatograph (GC) coupled to an Agilent 5973 mass selective detector (MS) (Santa Clara, CA). Gas samples (50 μL) were withdrawn from reactor headspace and injected into the GC-MS using a 250-μL gas syringe with a side port needle. The GC was equipped with an Agilent 19091P-Q03 capillary column and the carrier gas was grade 5 helium at a flow rate of 1.6 mL/min. The temperature of the injector and oven were 250°C and 35°C, respectively, and the run time was 1 min. Selective ion monitoring (SIM) was used to scan only m/z 28, 29, and 30 (i.e., 14 N₂, 14 N- 14 N, and 15 N₂) to maximize the sensitivity of quantification. The retention time for N₂ was 0.49 ± 0.01 min.

5.3.2 RESULTS and DISCUSSION

As shown in Figure 5-7, perchlorate was removed minimally over 4 days without microorganisms or reduced biochar. In the presence of reduced biochar, perchlorate was consumed rapidly in the first 24 h, with concomitant production of chloride. Specifically, 1.55 mM and 2.80 mM perchlorate were reduced with 1 g and 2 g of RedBc, respectively, yielding almost quantitative amounts of chloride (1.52 and 3.0 mM). Doubling the mass of reduced biochar not only doubled the initial rate of perchlorate reduction, from 0.049 to 0.082 mM/h, but also the total amounts of perchlorate removed and chloride formed. The chlorine mass balance remained roughly constant throughout the incubation.

Assuming that the diminishing activities toward the end of the incubation was due to depletion of readily microbially available electrons in Rogue biochar, and given that 8 electrons are required to convert a perchlorate into chloride, the bioavailable ESC of Rogue biochar can be calculated to be 1.19 ± 0.05 mmol e⁻/g. That is, each gram of fully reduced Rogue biochar provided approximately 1.2 mmoles of electrons to reduce ~ 150 µmoles of perchlorate to chloride.

Given that the total (chemically accessible) ESC of Rogue biochar was 6.78 mmol e⁻/g (Table 5-3), the portion of stored electrons in Rogue biochar that were microbially accessible is about 18%. This fraction is comparable to that (19%) observed for Soil Reef biochar and the iron-reducing bacterium *Geobacter metallireducens* (Saquing et al., 2016). Determining the portion of the total ESC that is accessible to microbes would be useful for designing stormwater treatment systems for removing perchlorate and other reducible contaminants (e.g., chlorinated solvents and munitions constituents) of interest to DoD.

Results of microbial nitrate reduction are shown in Figure 5-8. Without reduced biochar, nitrate reduction was minimal, presumably due to traces of electron donors carried over from the seed culture via inoculation. In contrast, nitrate was consumed completely over 13 days in the presence of reduced biochar (panel a), and ¹⁵N₂ was produced concomitantly during the same period (panel b). The ¹⁵N mass balance was obtained based solely on ¹⁵NO₃⁻ and ¹⁵N₂ (panel c), whereas little NH₄⁺ was produced throughout the experiment. Comparing the results to the abiotic and biotic controls, we estimated approximately 90% of the 0.43 mmol of ¹⁵NO₃⁻ was reduced with biochar as an electron donor and 10% with residual electron donors in the inoculum. Saquing et al. (2016)¹⁴ observed that the bacterium *Geobacter metallireducens* converted nitrate into NH₄⁺ quantitatively using biochar as an electron donor. In contrast, our results here suggest that (1) the ability to utilize biochar as an electron donor is likely widespread in soil, not specific to *Geobacter* species, and (2) reduced biochar can promote microbial conversion of nitrate to the harmless nitrogen gas (i.e., autotrophic denitrification) rather than to the toxic NH₄⁺. These findings are encouraging and may represent a novel approach to address nitrate contamination.

Figure 5-7. Microbial reduction of perchlorate with chemically-reduced biochar as the electron donor.

Reduction with a) 1 g and b) 2 g of biochar added. RedBc and OxBc represent reduced and oxidized biochar, respectively. Mass balance = $[ClO_4^-] + [Cl^-]$. Error bars represent one standard deviation based on duplicates

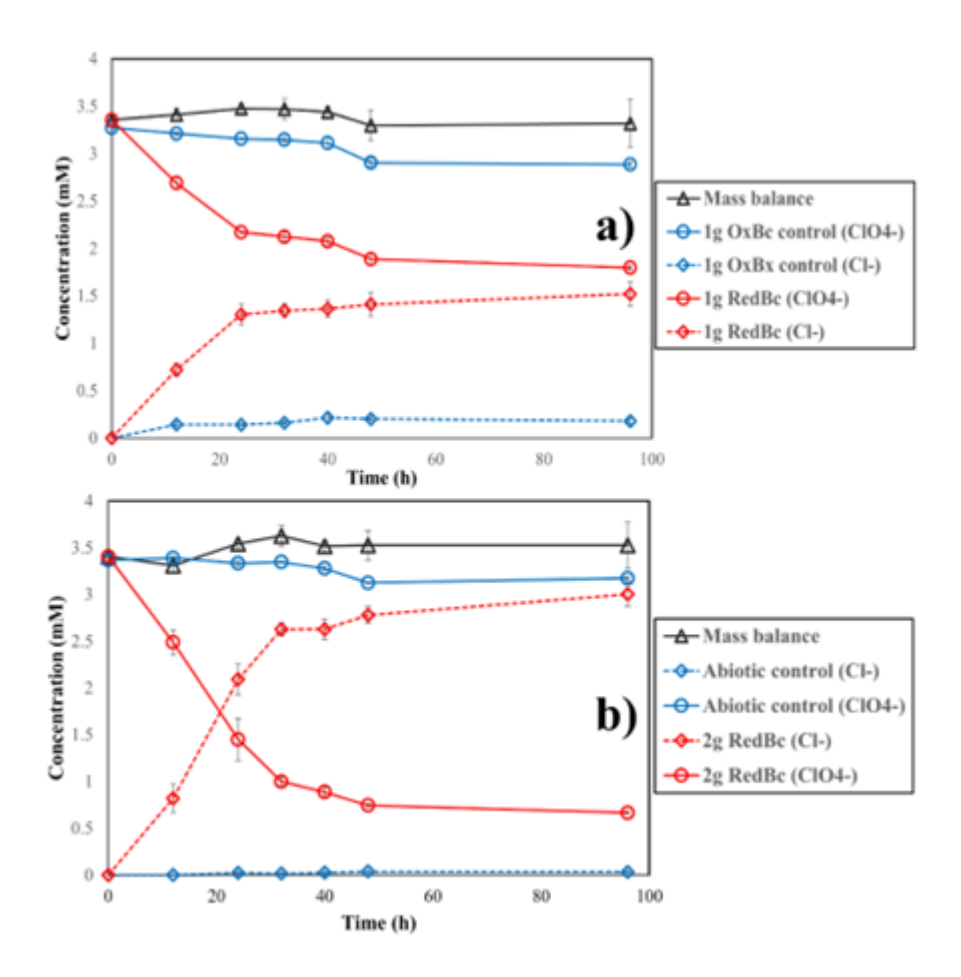
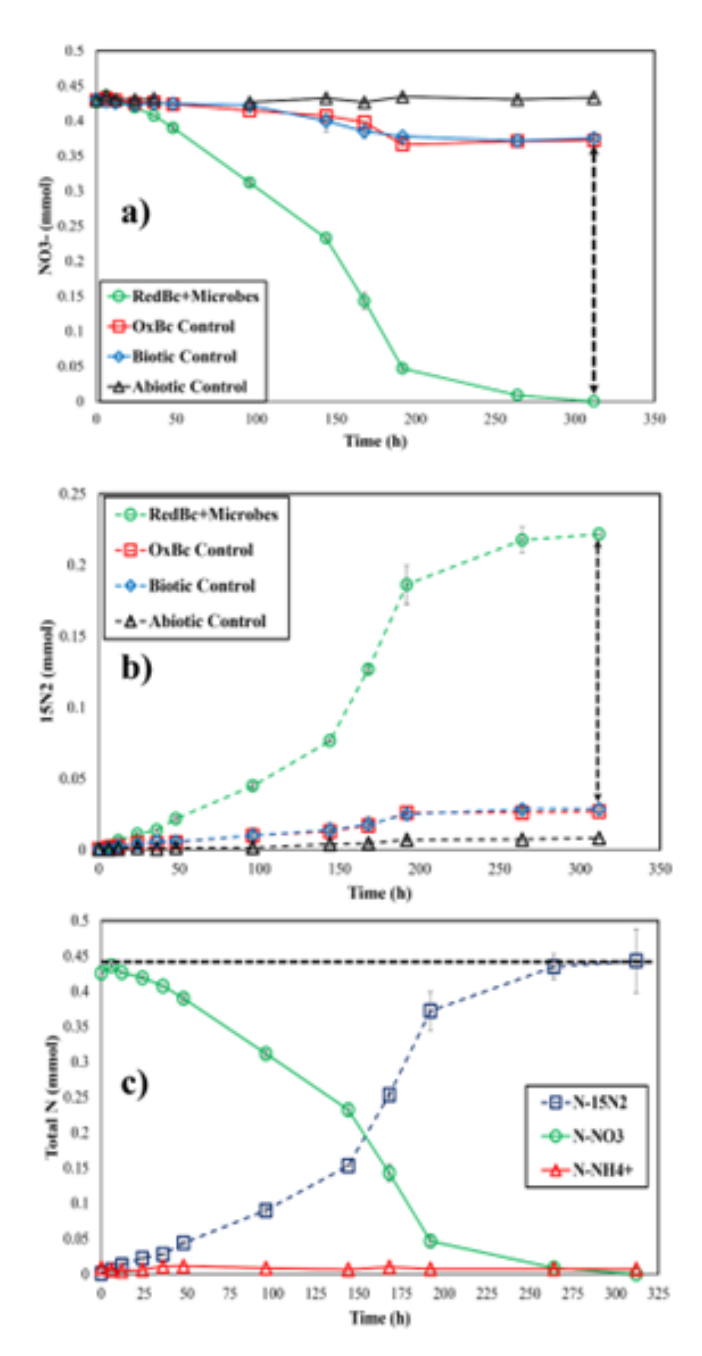


Figure 5-8. Microbial reduction of nitrate with chemically-reduced biochar as the electron donor.

a) Microbial reduction of $^{15}NO_3^-$ using reduced biochar as an electron donor with b) concomitant production of $^{15}N_2$. c) Nitrogen mass balance was established based solely on $^{15}NO_3^-$ and $^{15}N_2$, whereas NH_4^+ formation was negligible. Error bars represent one standard deviation based on duplicate reactors.



5.4 Microbial Regeneration of Reduced Biochar for Perchlorate Reduction

The results above demonstrate that reduced biochar can directly react with the NTO, DNAN, and RDX as well as indirectly reduce perchlorate and nitrate through naturally occurring microbes. However, for biochar to serve as a long-lasting redox buffer and electron donor to continually degrade energetic compounds in a stormwater treatment system, its ESC needs to be rechargeable *in situ*. Preferably this would occur through microbial oxidation of common fermentation products, such as acetate and hydrogen, that are common in soil and other anoxic systems. It was hypothesized that (1) biochar's ESC can be recharged microbially under anoxic conditions, and (2) microbially reduced biochar can serve as an electron donor to support perchlorate reduction.

The ability of biochar to abiotically reduce NTO repeatedly via *chemical* regeneration of its ESC has been demonstrated in our previous work (Xin et al., 2022). Here, the ability of *microbial* regeneration of reduced biochar was examined to sustain perchlorate reduction.

5.4.1 METHODS

Bio-reduction of Biochar. Bio-reduction of biochar was investigated using a wastewater culture form the Aberdeen Wastewater Treatment Plant (MD) as a seed culture, air-oxidized wood biochar as an electron acceptor, and one of the three electron donors: acetate, formate, and H₂. All three electron donors are common intermediates/products in anaerobic microbial systems. These donors also have different redox potentials (–0.291 V, –0.432 V, and –0.414 V for acetate, formate, and H₂, respectively) and thus may be able to drive biochar reduction to different extents. Bioreactors were prepared in quadruplicate 155-mL serum bottles containing 2 mL of sludge culture, 1 g of air-oxidized biochar, and 6 mM acetate, 25 mM formate, or 55 mL of H₂ gas. The different amounts of electron donors were chosen to give approximately the same total amount (4.4–5.0 mmol) of electrons. The background medium was the same for all three experiments and contained the following per liter: 0.4 g of MgCl₂·6H₂O, 0.113 g of CaCl₂·2H₂O, 0.027 g of NH₄Cl, 2.971 g of KH₂PO₄·H₂O, 1.9081 g of Na₂HPO₄·2H₂O, 1 mL of vitamin solution, and 1 mL of trace element solution. The pH was adjusted to 6.5 initially and was buffered with 30 mM phosphate.

To monitor microbial activities and establish electron balance, production of CH₄ and CO₂ from fermentation and anaerobic respiration were measured periodically during the incubation. Fifty μ L of gas from bioreactor head space was withdrawn using a 250- μ L gas-tight syringe equipped with a Mininert valve and was injected into a gas chromatograph with a mass-selective detector (Agilent 5890N GC–5973N MSD).

EDC Measurement. The electron accepting capacity (EAC) of the air-oxidized and deoxygenated biochar, as well as biochar samples collected from bioreactors at the end of the incubation, were measured via redox titration with titanium(III) citrate (-0.36 V vs. the standard hydrogen electrode [SHE] at pH 6.4) as a reductant, following the method developed by Xin et al., (Xin et al., 2019; Xin et al., 2021). Briefly, EAC was quantified based on the cumulative oxidation of Ti(III) by biochar over time, as measured by the UV-vis absorption at 400 nm. For air-oxidized virgin biochar, the EAC was equal to the ESC of the biochar for the redox potential (EH) range between -0.36 to +0.81 V vs. SHE; i.e., in the EH range between the Ti(IV)/Ti(III) and O₂/H₂O couples. EAC measurements were repeated using different masses of biochar prepared in duplicate with control and blank (no biochar) to ensure the ESC was constant and independent of the biochar mass used.

<u>Perchlorate Reduction by Bio-reduced Biochar</u>: The biologically reduced biochar recovered from the bio-reduction experiment was thoroughly washed with anaerobic 1% Tween 80 solution for 20 min on an orbital shaker at 300 rpm to remove attached cells and biomolecules. Batch perchlorate reduction experiments were conducted in an anaerobic glove box (98.0±0.5% N₂, 2.0±0.5% H₂, Coy, MI) using 100-mL serum bottles containing 50 mL of 2.75 mM NaClO₄ in 30 mM phosphate buffer (pH 6.47 ± 0.13). The background medium in all bioreactors included (per liter) 0.027 g of NH₄Cl, 2.971 g of KH₂PO₄·H₂O, 1.9081 g of Na₂HPO₄·2H₂O, 1 mL of vitamin solution, and 1 mL of trace element solution. To study ClO₄⁻ reduction, 0.5 g of microbially reduced biochar from acetate-, formate-, and H₂-amended bioreactors were added to separate vials prepared in triplicate. Control and blank reactors were included that contained air-oxidized biochar (0.5 g), chemically reduced biochar (0.3 g), no biochar, and no inoculum. All vials were purged with N₂ for 10 minutes to remove H₂ in the headspace prior to perchlorate addition. Samples (0.1 mL) were collected at different times, diluted 10 times with deionized water, and passed through a 0.22-µm PTFE syringe filter. The filtrates were analyzed for ClO₄⁻ and its reduction product Cl⁻ using a Metrohm Eco Ion Chromatograph (IC) equipped with a Metrosep A Supp 5-100/4.0 anion column. The total volume of samples taken from any single vial accounted for less than 10% of the total solution volume.

5.4.2 RESULTS and DISCUSSION

Figure 5-9 shows the production of CH₄ and CO₂ during biochar incubation with acetate, formate, or H₂ as an electron donor. All three electron donors were provided in stoichiometric excess to ensure that biochar was charged to the maximum extent possible in each case. As a result (of the excess electron supply), CH₄ was produced in all reactors, presumably after the bioavailable EAC of the biochar had been exhausted (Xin et al., 2023). CO₂ was produced sooner than CH₄ with both acetate and formate, suggesting anaerobic oxidation of these electron donors coupled to biochar respiration dominated and outcompeted methanogenesis in the early times (Xin et al., 2023). We suspect H₂ was similarly oxidized preferentially by biochar-respiring autotrophs, although this could not be confirmed due to the lack of CO₂ production in H₂-fed reactors. Nonetheless, the facts that (1) CH₄ was produced at approximately the same time with all three electron donors, and (2) less CH₄ was formed with H₂ than with acetate and formate, suggest that a significant portion of the H₂ added was microbially oxidized with biochar as an electron acceptor.

As shown in Figure 5-10(a), the amount of Ti(III) consumed (i.e., electrons transferred from Ti(III) to biochar) was proportional to the mass of biochar used. The EAC of the virgin biochar could be determined from the slope of the linear correlation to be 4.79 ± 0.06 mmol/g. Figure 5-10(b) shows that the EACs of surfactant-washed biochar samples retrieved from the bioreactors amended with acetate, formate, and H₂ as electron donor were 2.51, 2.25, and 1.42 mmol/g, respectively. These data suggest that 48% (2.28 mmol/g, acetate), 53% (2.54 mmol/g, formate) and 70% (3.37 mmol/g, H₂) of the original EAC of the biochar had been utilized by the mixed culture in each case. While the data is preliminary and more studies are needed, the different extents of biochar reduction by the same seed culture utilizing different substrates suggest that microbial charging of biochar is, at least in part, thermodynamically rather than sterically controlled, and thus can vary with the redox property of the electron donor.

The ability of the three microbially reduced biochars to support perchlorate reduction was then assessed. As shown in Figure 5-11, no perchlorate consumption or chloride production occurred without either microbes or biochar. In contrast, perchlorate was removed, and chloride was formed concomitantly, when a bio-reduced biochar was amended. The biochar (0.5 g each) retrieved from the acetate, formate, and H_2 reactors could reduce ClO_4^- by 0.56, 0.58, and 0.81 mM, respectively, corresponding to 0.72, 0.74, and 1.04 mmol of electrons transferred to perchlorate per gram of biochar. The extent of perchlorate reduced (i.e., the amount of electrons transferred) is consistent with the extent of biochar reduction; i.e., $H_2 >$ formate \geq acetate. Dividing the amount of electrons consumed by the electron content of the corresponding bio-reduced biochar (i.e., 2.28 mmol/g for acetate, 2.54 mmol/g for formate, and 3.37 mmol/g for H_2), we found that 32% (= 0.72/2.28), 29% (= 0.74/2.54), and 31% (= 1.04/3.37), respectively, of the electrons in the bio-reduced biochar were utilized for perchlorate reduction. The reason for the roughly constant (\sim 30%) electron utilization rate, regardless of the electron donor used to do the charging, is unclear and will require additional studies.

In summary, our results show that biochar, as a microbially accessible electron storage medium, can be biologically (re)charged through anaerobic oxidation of common electron donors including acetate, formate, and hydrogen. Microbial charging can partially refill the ESC of biochar and restore its ability to reduce perchlorate. In biochar-amended stormwater treatment systems, acetate, formate, and H₂ can be produced *in situ* through biodegradation of complex organic substrates or biopolymers (e.g., wood chips and peat moss). This may continually recharge biochar and sustain its capacity to support the reduction of perchlorate and other energetic compounds and oxyanions in surface runoff. The results support our hypotheses and illustrate the potential utility and benefits of incorporating biochar for stormwater treatment in military ranges.

Figure 5-9. Microbial methanogenesis and respiration using oxidized biochar as an electron acceptor.

Production of (a) CH₄ and (b) CO₂ during incubation with 1 g of air-oxidized biochar as an electron acceptor and acetate, formate, or H₂ as an electron donor. (c) Total gas production and (d) CH₄/CO₂ ratios were calculated using data from panels (a) and (b). Error bars represent one standard deviation based on quadruplicate reactors.

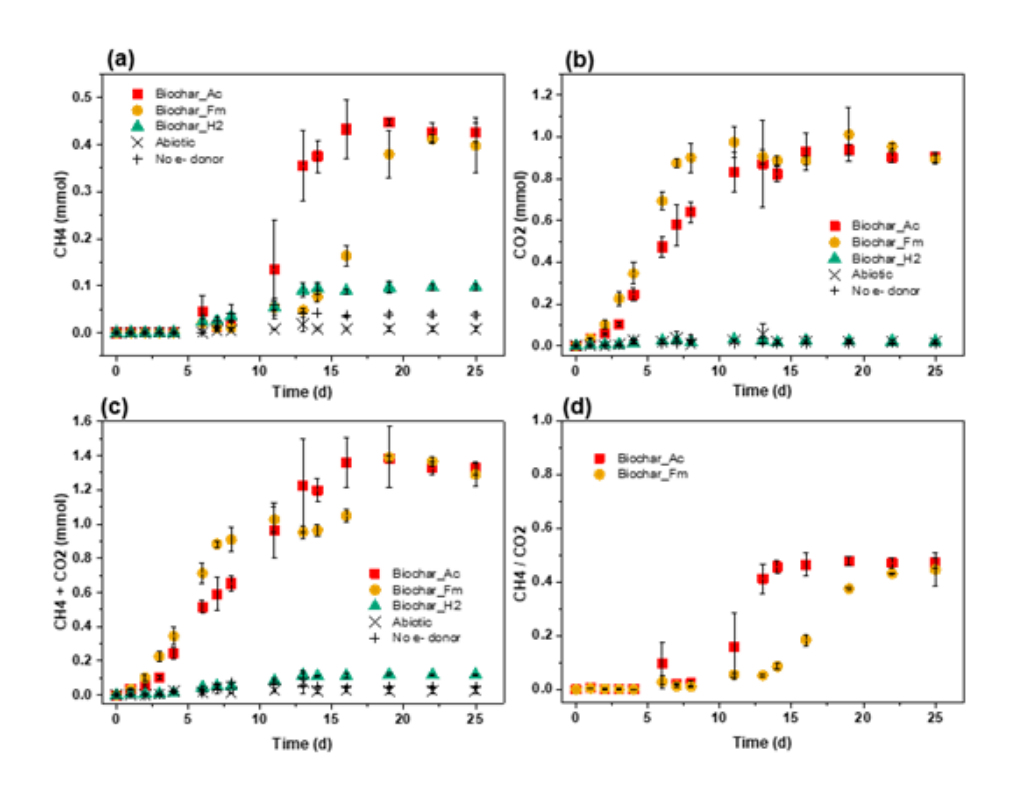
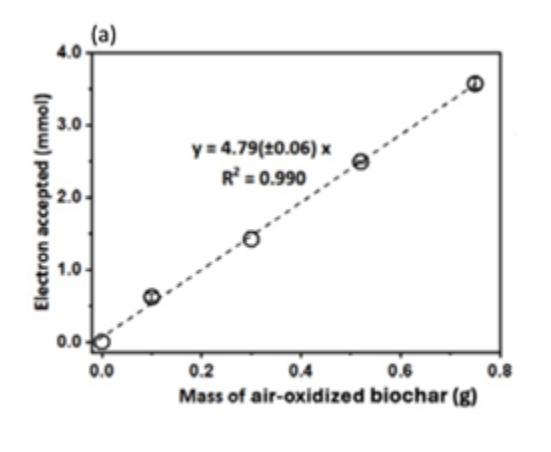


Figure 5-10. Measured electron accepting capacity (EAC) of biochar after microbial reduction.

(a) The EAC of air-oxidized biochar measured by redox titration with Ti(III) citrate was 4.79 ± 0.06 mmol/g. (b) The EACs of biochar samples retrieved from bioreactors amended with acetate, formate, and H₂ as an electron donor were 2.51, 2.25, and 1.42 mmol/g, respectively.



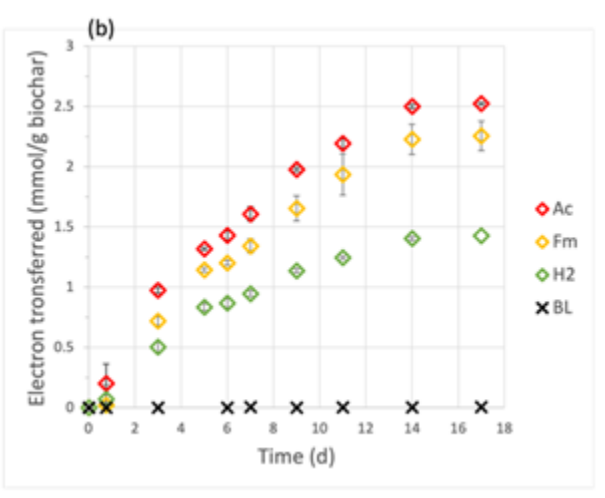
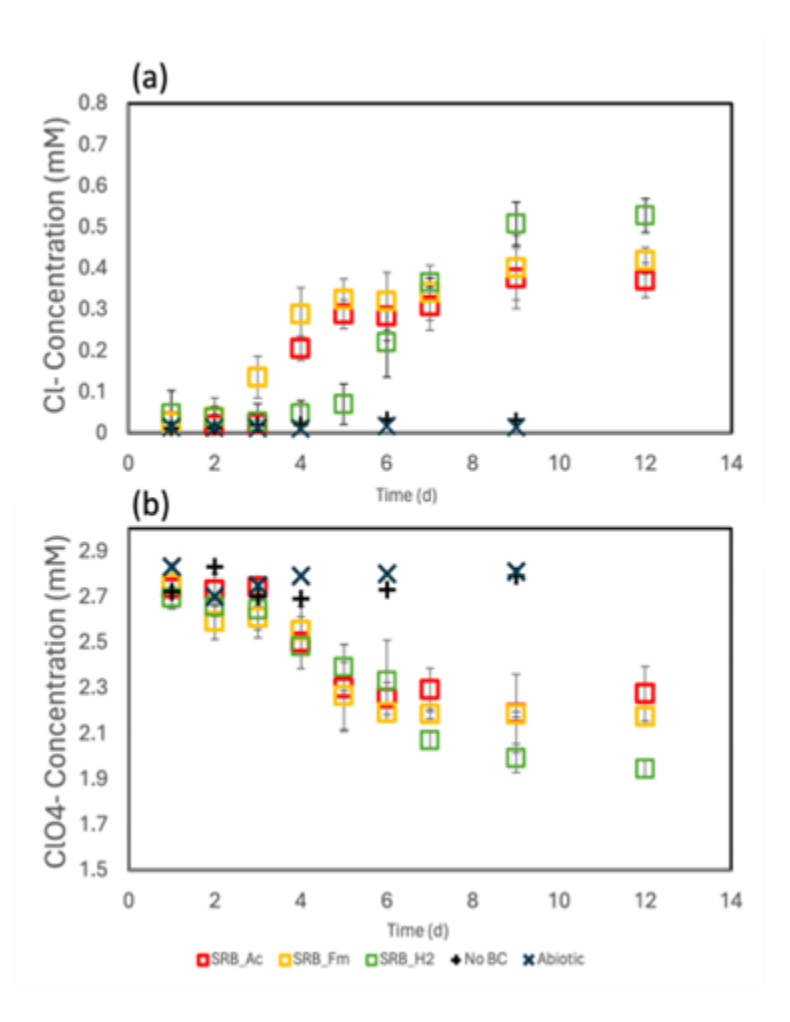


Figure 5-11. Microbial perchlorate reduction with microbially reduced biochar as an electron donor.

Error bars represent one standard deviation from triplicate reactors.



REFERENCES

- Aeschbacher, M., Sander, M., Schwarzenbach, R.P., 2010. Novel electrochemical approach to assess the redox properties of humic substances. Environmental Science & Technology 44, 87-93.10.1021/es902627p.
- Aeschbacher, M., Vergari, D., Schwarzenbach, R.P., Sander, M., 2011. Electrochemical analysis of proton and electron transfer equilibria of the reducible moieties in humic acids. Environmental Science & Technology 45, 8385-8394.10.1021/es201981g.
- Arthur, J.D., Mark, N.W., Taylor, S., Šimůnek, J., Brusseau, M.L., Dontsova, K.M., 2018. Dissolution and transport of insensitive munitions formulations IMX-101 and IMX-104 in saturated soil columns. The Science of the total environment 624, 758-768.10.1016/j.scitotenv.2017.11.307.
- Bernstein, A., Ronen, Z., Gelman, F., 2013. Insight on RDX degradation mechanism by *Rhodococcus* strains using ¹³C and ¹⁵N kinetic isotope effects. Environ Sci Technol 47, 479-484.
- Cao, X., Pignatello, J.J., Li, Y., Lattao, C., Chappell, M., Chen, N., Miller, L., Mao, J., 2012. Characterization of wood chars produced at different temperatures using advanced solid-state ¹³C NMR spectroscopic techniques. Energy & Fuels 26, 5983-5991.10.1021/ef300947s.
- Cárdenas-Hernández, P.A., Anderson, K.A., Murillo-Gelvez, J., Di Toro, D.M., Allen, H.E., Carbonaro, R.F., Chiu, P.C., 2020. Reduction of 3-nitro-1,2,4-triazol-5-one (NTO) by the hematite–aqueous Fe(II) redox couple. Environ Sci Technol 54, 12191-12201.10.1021/acs.est.0c03872.
- Cárdenas-Hernández, P.A., Hickey, K., Di Toro, D.M., Allen, H.E., Carbonaro, R.F., Chiu, P.C., 2023. Linear free energy relationship for predicting the rate constants of munition compound reduction by the Fe(II)–hematite and Fe(II)–goethite redox couples. Environ Sci Technol 57, 13646-13657.10.1021/acs.est.3c04714.
- Cornelissen, G., Gustafsson, Ö., Bucheli, T.D., Jonker, M.T.O., Koelmans, A.A., van Noort, P.C.M., 2005. Extensive sorption of organic compounds to black carbon, coal, and kerogen in sediments and soils: Mechanisms and consequences for distribution, bioaccumulation,

- and biodegradation. Environmental Science & Technology 39, 6881-6895.10.1021/es050191b.
- Dontsova, K., Taylor, S., Pesce-Rodriguez, R. 2018. Dissolution of NTO, DNAN and Insensitive Munitions Formulations and Their Fates in Soils. ER-2220. https://sepub-prod-0001-124733793621-us-gov-west-1.s3.us-gov-west-1.amazonaws.com/s3fs-public/project_documents/ER-2220_Final_Report.pdf.
- Klüpfel, L., Keiluweit, M., Kleber, M., Sander, M., 2014. Redox properties of plant biomass-derived black carbon (Biochar). Environmental Science & Technology 48, 5601-5611.10.1021/es500906d.
- Lee, K.-Y., Chapman, L.B., Cobura, M.D., 1987. 3-Nitro-1,2,4-triazol-5-one, a less sensitive explosive. J Energ Mater 5, 27-33.10.1080/07370658708012347.
- Liang, J., Olivares, C., Field, J.A., Sierra-Alvarez, R., 2013. Microbial toxicity of the insensitive munitions compound, 2,4-dinitroanisole (DNAN), and its aromatic amine metabolites. J Hazard Mater 262, 281-287. https://doi.org/10.1016/j.jhazmat.2013.08.046.
- Menezes, O., Yu, Y., Root, R.A., Gavazza, S., Chorover, J., Sierra-Alvarez, R., Field, J.A., 2021. Iron(II) monosulfide (FeS) minerals reductively transform the insensitive munitions compounds 2,4-dinitroanisole (DNAN) and 3-nitro-1,2,4-triazol-5-one (NTO). Chemosphere 285, 131409.https://doi.org/10.1016/j.chemosphere.2021.131409.
- Mukherjee, A., Zimmerman, A.R., Harris, W., 2011. Surface chemistry variations among a series of laboratory-produced biochars. Geoderma 163, 247-255.https://doi.org/10.1016/j.geoderma.2011.04.021.
- Murillo-Gelvez, J., Hickey, K., Di Toro, D.M., Allen, H.E., Carbonaro, R.F., Chiu, P.C., 2023. Electron transfer energy and hydrogen atom transfer energy-based linear free energy relationships for predicting the rate constants of munition constituent reduction by hydroquinones. Environ Sci Technol 57, 5284-5295.10.1021/acs.est.2c08931.
- Oh, S.-Y., Cha, D.K., Chiu, P.C., 2002. Graphite-mediated reduction of 2,4-dinitrotoluene with elemental iron. Environ Sci Technol 36, 2178-2184.10.1021/es011474g.

- Oh, S.-Y., Cha, D.K., Kim, B.J., Chiu, P.C., 2005. Reductive transformation of hexahydro-1,3,5-trinitro-1,3,5-triazine, octahydro-1,3,5,7-tetranitro-1,3,5,7-tetrazocine, and methylenedinitramine with elemental iron. Environ Toxicol Chem 24, 2812-2819.10.1897/04-662R.1.
- Oh, S.-Y., Chiu, P.C., 2009. Graphite- and soot-mediated reduction of 2,4-dinitrotoluene and hexahydro-1,3,5-trinitro-1,3,5-triazine. Environ Sci Technol 43, 6983-6988.
- Oh, S.-Y., Son, J.-G., Chiu, P.C., 2013a. Biochar-mediated reductive transformation of nitro herbicides and explosives. Environ Toxicol Chem 32, 501-508.
- Oh, S.-Y., Son, J.-G., Hur, S.H., Chung, J.S., Chiu, P.C., 2013b. Black carbon–mediated reduction of 2,4-dinitrotoluene by dithiothreitol. J Environ Qual 42, 815-821.https://doi.org/10.2134/jeq2012.0411.
- Pennington, J.C., Brannon, J.M., 2002. Environmental fate of explosives. Thermochemica Acta 384, 163-172.
- Prévoteau, A., Ronsse, F., Cid, I., Boeckx, P., Rabaey, K., 2016. The electron donating capacity of biochar is dramatically underestimated. Scientific Reports 6, 32870.10.1038/srep32870 https://www.nature.com/articles/srep32870#supplementary-information.
- Saquing, J.M., Yu, Y.-H., Chiu, P.C., 2016. Wood-derived black carbon (biochar) as a microbial electron donor and acceptor. Environmental Science & Technology Letters 3, 62-66.10.1021/acs.estlett.5b00354.
- Selwyn, L., Tse, S., 2008. The chemistry of sodium dithionite and its use in conservation. Studies in Conservation 53, 61-73.10.1179/sic.2008.53.Supplement-2.61.
- Tong, Y., Berens, M.J., Ulrich, B.A., Bolotin, J., Strehlau, J.H., Hofstetter, T.B., Arnold, W.A., 2021. Exploring the utility of compound-specific isotope analysis for assessing ferrous iron-mediated reduction of RDX in the subsurface. Environ Sci Technol 55, 6752-6763.10.1021/acs.est.0c08420.
- Xiao, F., Pignatello, J.J., 2015. π^+ – π Interactions between (hetero)aromatic amine cations and the graphitic surfaces of pyrogenic carbonaceous materials. Environmental Science & Technology 49, 906-914.10.1021/es5043029.

- Xiao, X., Chen, B., 2017. A direct observation of the fine aromatic clusters and molecular structures of biochars. Environmental Science & Technology 51, 5473-5482.10.1021/acs.est.6b06300.
- Xin, D., Barkley, T., Chiu, P.C., 2020. Visualizing electron storage capacity distribution in biochar through silver tagging. Chemosphere 248, 125952.https://doi.org/10.1016/j.chemosphere.2020.125952.
- Xin, D., Girón, J., Fuller, M.E., Chiu, P.C., 2022. Abiotic reduction of 3-nitro-1,2,4-triazol-5-one (NTO) and other munitions constituents by wood-derived biochar through its rechargeable electron storage capacity. Environmental Science: Processes & Impacts 24, 316-329.10.1039/D1EM00447F.
- Xin, D., Li, W., Choi, J., Yu, Y.-H., Chiu, P.C., 2023. Pyrogenic black carbon suppresses microbial methane production by serving as a terminal electron acceptor. Environmental Science & Technology 57, 20605-20614.10.1021/acs.est.3c05830.
- Xin, D., Saha, N., Reza, M.T., Hudson, J., Chiu, P.C., 2021. Pyrolysis creates electron storage capacity of black carbon (biochar) from lignocellulosic biomass. ACS Sustainable Chemistry & Engineering 9, 6821-6831.10.1021/acssuschemeng.1c01251.
- Xin, D., Xian, M., Chiu, P.C., 2019. New methods for assessing electron storage capacity and redox reversibility of biochar. Chemosphere 215, 827-834.https://doi.org/10.1016/j.chemosphere.2018.10.080.
- Xin, D.H., Xian, M.H., Chiu, P.C., 2018. Chemical methods for determining the electron storage capacity of black carbon. Methodsx 5, 1515-1520.
- Xu, W., Dana, K.E., Mitch, W.A., 2010. Black carbon-mediated destruction of nitroglycerin and RDX by hydrogen sulfide. Environ Sci Technol 44, 6409-6415.
- Zhang, Y., Xu, X., Cao, L., Ok, Y.S., Cao, X., 2018. Characterization and quantification of electron donating capacity and its structure dependence in biochar derived from three waste biomasses.

 Chemosphere 211, 1073-1081.https://doi.org/10.1016/j.chemosphere.2018.08.033.

- Zhang, Y., Xu, X., Zhang, P., Ling, Z., Qiu, H., Cao, X., 2019. Pyrolysis-temperature depended quinone and carbonyl groups as the electron accepting sites in barley grass derived biochar. Chemosphere 232, 273-280. https://doi.org/10.1016/j.chemosphere.2019.05.225.
- Zhu, D., Kwon, S., Pignatello, J.J., 2005. Adsorption of single-ring organic compounds to wood charcoals prepared under different thermochemical conditions. Environmental Science & Technology 39, 3990-3998.10.1021/es050129e.

6. Column Study Evaluation of Combined Sorption/Biodegradation of Legacy and Insensitive Munition Energetics

Hypothesis 6: Bioaugmentation with know explosive degrading bacterial cultures can enhance the degradation of legacy and insensitive munitions constituents in surface runoff.

6.1 METHODS

6.1.1 Chemicals and media

Sources of energetic compounds, peat moss, pine shavings, and the synthesis of cationized pine shavings were described previously (Fuller et al., 2022). Ground oyster shell flour (Southside Plants LLC, Santa Rosa Beach, FL, USA), chunk oyster shell (Four Winds Trading, Seymour, TN, USA), and soft wood-based biochar (Char Bliss, Plantonix LLC, Ashland, OR, USA) were purchased via Amazon (Seattle, WA, USA). Information on PHB, PCL, and BioPBS is shown in Table 4-1 of section 4. All other chemicals were reagent grade or higher. The artificial surface runoff (ASR) solution and Hareland's basal salts medium (BSM) were described previously (Hareland et al., 1975; Fuller et al., 2022).

6.1.2 Column setup and packing

A schematic and photograph of the column setup is shown in Figure 6-1. All column parts were PVC, polypropylene, polystyrene, or stainless steel. The influent lines consisted of FEP tubing (1/16" ID x 1/8" OD; Altaflow LLC, Sparta, NJ, USA) inside the influent reservoir in direct contact with the energetics-amended ASR solution, and FEP-lined Tygon® tubing (1/8" ID x 1/4" OD; Saint Gobain Performance Plastics, Akron, OH, USA) between the reservoir and the pump, and between the pump and the column inlet. Norprene® tubing was used in the pump heads (Masterflex® L/S 13; VWR, Radnor, PA, USA), and between the column outlet and the fraction collector (Masterflex® L/S 14).

The composition of the columns during the sorption experiment are shown in Figure 6-2. The materials were added in small portions (3-5 g), packing each portion firmly with a plastic rod, until the indicated mass was reached. Washed silica sand (<1000 μ m, >500 μ m) (Agsco Corp, Pine Brook, NJ, USA) was packed in and topped with two stainless steel screens (pore size: 380 μ m above 150 μ m). Borosilicate glass beads (5 mm) (Fisher Scientific, Somerville, NJ, USA) were added and the top column fitting was screwed on until secured.

The composition of the columns during the sorption-biodegradation experiments are shown in Figure 6-3. Columns were packed as follows: The bottom (inlet) of each columns received 5 g of dry CAT pine as the first component, which was compacted firmly with a plastic rod. For each column, air dry peat moss (7.1 g) was combined in a glass jar with ground oyster shell (2.8 g) and chunk oyster shell (2.1 g), which provided good neutralization of the peat acidity, and buffered the column pore water to a circumneutral pH. The peat/oyster shell mixture was combined with 10 g of energetics-free air dry soil from an east coast DoD testing range and mixed on a roller for five minutes to homogenize. Sterile range soil was used for the mix for columns 1 and 2, which was prepared by autoclaving on three consecutive days for 1 hour, followed by drying in an over at 105°C overnight. The peat/soil mixture was packed as is above the CAT pine in column 1 in 5.5 g portions. After each portion was added, the material was compacted firmly with a plastic rod. For

columns 2, 3, and 4, each 5.5 g portion of the peat/soil mixture were first mixed with 0.25 g each of polyhydroxybutyrate (PHB), polycaprolactone (PCL), and polybutylene succinate (BioPBS) before packing into the columns. This process was repeated four times until all the peat/soil (plus biopolymer for columns 2, 3, and 4) were packed. For column 4, the peat and soil layer was overlain with a layer of 1 g of coarse biochar ($<1000 \, \mu m$, $>212 \, \mu m$). As with the sorption columns, silica sand and glass beads were added, and the top fitting was screwed on until secured. After packing, the side port fittings were inserted.

During these experiments, the column designations are as follows:

Column 1 (C1) – Sorption Only – Cationized pine and peat moss acting as sorbents. Minimal biological activity from any indigenous microorganisms in the peat moss using the peat moss as a carbon source. No added biopolymer carbon source.

Column 2 (C2) – Sorption Plus – Cationized pine and peat moss acting as sorbents. Minimal biological activity from any indigenous microorganisms in the peat moss. Biopolymer carbon source added may have supported slightly higher biological activity than Col 1. Biopolymer carbon source may also contribute somewhat to sorption.

Column 3 (C3) – Sorption/Biodegradation - Cationized pine and peat moss acting as sorbents. Biopolymer carbon source added. Aerobic and anaerobic cultures added to the column to promote the degradation of perchlorate and explosives, including:

Aerobic RDX degrader pure cultures (KTR9, DN22)

Aerobic NQ degrader pure culture (NQ5)

Anoxic RDX degrader pure culture (Ps I-C)

Aerobic and anaerobic mixed cultures from a dual MBR system treating explosives + perchlorate (Fuller et al., 2023)

Column 4 (C4) – Sorption/Biodegradation Plus - Cationized pine and peat moss acting as sorbents. Biopolymer carbon source added. Aerobic and anaerobic cultures added as in Col 3. Biochar added to effluent end of column as a polishing step as a sorbent/abiotic reductant/electron storage material.

6.1.3 Column operation

Once the columns were packed, a flow of ASR was initiated at approximately 4 ml/h to saturate the materials, in an upflow direction (e.g., column inlet at bottom of column). The influent reservoir was continuously stirred, with automatic addition of 0.05 N NaOH as needed to maintain the pH at ~6.4 S.U. For the sorption-biodegradation experiments, the dissolved oxygen (DO) and oxidation-reduction potential (ORP) of the influent was also monitored. Effluent from each column was directed to tubes in a SuperFracTM fraction collector (Pharmacia Biotech AB, Uppsala, SWEDEN) equipped with adapters to allow collection from two separate columns. For the sorption-biodegradation experiments, the effluent passed through acrylic flow cells equipped with ORP probes prior to going to the fraction collector, with Norprene® Masterflex L/S 14 tubing between the column outlet and the flow cells. Influent and effluent samples were analyzed for anions, and once the influent and effluent chloride concentrations were approximately equal, a

chloride tracer test was initiated. The tracer solution consisted of 200 mg/L chloride (as NaCl) in ASR, and at least 100 ml of tracer solution was injected into the columns before switching the influent back to ASR only.

Upon completion of the tracer test, the feed was switched to ASR amended with all the energetics. For the sorption only experiment, the nominal concentrations of all six organic explosives and perchlorate was 1 mg/L, whereas the explosives and perchlorate were at nominal concentrations of 10 mg/L (except for HMX, which at \sim 2 mg/L) for the sorption-biodegradation experiments. The higher concentrations were done to assure that any metabolites produced would be at detectable levels, as well as to accelerate target compound breakthrough slightly, thus shortening the duration of the experiments.

Columns 3 and 4 during the sorption-biodegradation experiments were also bioaugmented with energetic degrading bacterial cultures after the tracer test was completed. The pure cultures (DN22, KTR9, NQ5, I-C) were grown in their appropriate media, concentrated by centrifugation, and washed twice in phosphate buffer. The mixed cultures were collected from the anaerobic and aerobic MBRs (Fuller et al., 2023), concentrated by centrifugation, and resuspended in a small volume of the original MBR solution. Aliquots of DN22, KTR9, NQ5, I-C, and the aerobic MBR culture were combined in ASR, each at a final optical density at 600 nm (OD₆₀₀) of 1, and 2 ml of the mix cultures was injected into the lower side port of columns 3 and 4. Similarly, aliquots of I-C and the anaerobic MBR culture were combined to and OD₆₀₀ of 1 and 2 ml was injected into the upper side port of columns 3 and 4.

Effluent fractions volumes were recorded by weight. Fraction subsamples were collected for energetics, metabolites, and anions as previously described (Fuller et al., 2022). Selected fractions were used to monitor effluent pH and total organic carbon (TOC).

The sorption experiment was performed over 169 days (excluding the tracer test), with an evaluation of energetics desorption starting at 91 days by a switch to energetic-free ASR. The sorption-biodegradation experiment was performed twice, with durations of 115 days and 118 days, respectively, and desorption was not evaluated due to time constraints.

At the end of the second sorption-biodegradation experiment, additional testing was done with Columns 3 and 4 to assess the cause of the decline in energetics removal. Specifically, experiments were conducted to assess whether the slow increase in the effluent concentrations of the energetics was the result of loss of microbial activity due to cell viability (e.g., death of the degradative organisms) or due to depletion of utilizable carbon to support the degradative process.

The first stage involved a very low feed of fructose added to the upper side port of the columns, immediately below the "anoxic" zone of the columns. The feed was composed of 5 g/L of fructose, which was added using a syringe pump at a rate of 70 μ L/h, which gave a calculated final concentration of 100 mg/L entering the columns, assuming good mixing. Collection and analysis of effluent fractions continued, and the effluent ORP was monitored. The feed was continued for approximately 20 PV, at which time it was turned off and the columns were allowed to reequilibrate based on column effluent energetics concentrations and ORP monitoring, which required approximately 7 PV.

The fructose feed was then redirected to the lower side port of the columns, which was within the aerobic/oxic zone, using the same fructose concentration. The feed was continued for approximately 15 PV, with monitoring of the effluent energetics concentrations and ORP.

Lastly, fresh bioaugmentation with strain NQ5 was performed via the lower side port of the columns, and the fructose feed was continued for an additional 20 PV, at which time the experiment was terminated. This was done to examine if NQ removal by the columns could be revived.

6.1.4. Analytical

Analytical methods for explosives, metabolites, perchlorate, anions, and TOC were previously published (Fuller et al., 2022; Fuller et al., 2023).

6.1.5. Data analysis for the column sorption experiment

The chloride tracer data was used to calculate the pore volume (PV) for each column based on the volume at which the effluent concentration (C) of chloride was equivalent to 50% of the influent concentration (C₀) of chloride. All effluent data is presented using the cumulative PV as the x-axis. The dispersity (D) was calculated by curve fitting the chloride data according to the method of Kato et al. (Kato et al., 2021), derived from van Genuchten and Parker (van Genuchten and Parker, 1984), using the iterative Levenberg-Marquardt curve fitting algorithm of the graphing software KaleidaGraph (v4.5, Synergy Software, Reading, PA).

The apparent sorption capacity of the target compounds was assessed by applying the the equation (modified from (Chowdhury et al., 2015)):

$$q_{org50} = PV_{50} * C_0 / M \tag{1}$$

where q_{org50} (mg/g) was the absorption capacity at 50% breakthrough of the specific energetic compound, PV_{50} (L) was the total volume of spiked artificial surface runoff ASR that had passed through the column at the time of 50% breakthrough of the specific energetic compound, C_0 (mg/L) was the concentration of the specific energetic compound in the spiked influent ASR, and M(g) is the mass of the sorbent material (peat moss or CAT pine).

The sorption capacity of the peat and CAT pine for the target compounds was also evaluated by modeling the breakthrough curves for each energetic in the three columns using the Thomas column adsorption kinetic model. The Thomas column adsorption kinetic model can be expressed as (Aminul Islam, 2022):

$$\ln(C/C_0 - 1) = (K_T * q_0 * M) / (Q - K_T * C_0 * t)$$
(2)

where C and C_{θ} (mg/mL) were the effluent and influent concentrations of the target compound at any given time, K_T was the Thomas constant (mL/min/mg), q_{θ} (sometimes referred to as q_{max}) was the maximum sorption capacity (mg/mg), M was the sorbent mass (mg), Q was the volumetric flow rate (mL/min), and t was time (min). Equation 2 was rearranged to get:

$$C/C_0 = 1 / (1 + \exp(K_T * ((q_0 * M) / (Q - C_0 * t))))$$
(3)

Making the following substitutions,

```
y = C/C_0

x = t

a\# = q_0 * M/Q

b = C_0 (of each target compound)
```

the equation was rewritten as:

$$y = 1 / (1 + (\exp(K_T * (a\# - b * x))))$$
(4)

In this form, the equation was processed using KaleidaGraph (v4.5), solving for K_T to achieve the lowest sum of the squared error between the experimental breakthrough curve data and the equation result for each timepoint in the breakthrough curve.

Once a value for a# was obtained, the sorption capacity was calculated as:

$$q_0 = a\# * Q / M$$

The retardation factor (R), defined as the transport of the target compound relative to that of the conservative tracer, was also calculated for all the compounds. The reference point was designated as the time when the target compound (or tracer) had reached 50% of the influent concentration $(C/C_0 = 0.5)$, and was chosen for the calculations because TNT effluent concentrations never reached influent concentrations. The retardation factor was PV_{50} of the target compound divided by the PV_{50} of the tracer for each column. For comparison, R values were also calculated based on the PV_{50} of the tracer in the control column, given that the chloride did not act as a perfect conservative tracer in the columns containing CAT pine due to chloride interaction with the anion-sorbing material.

6.1.6. Data analysis for column sorption-biodegradation experiments

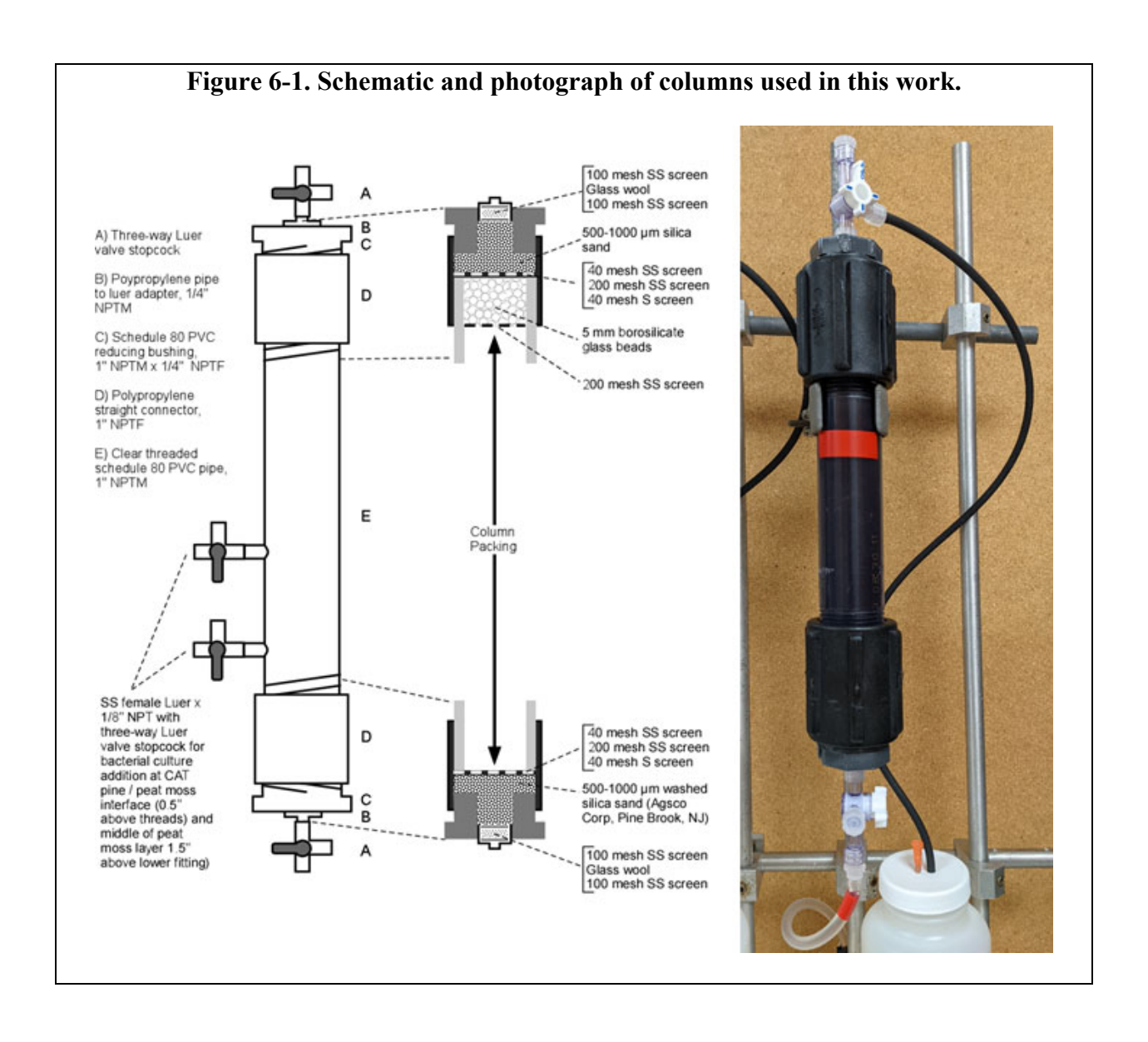
The column pore volumes were calculated using the chloride tracer data as described above.

The total mass of energetics removed (M_{REM}) by sorption (columns 1 and 2) and sorption plus biodegradation (columns 3 and 4) after 100 PV of energetics-amended ASR has passed through the column was also calculated by integrating breakthrough curves as follows.

The total mass (M_{INi}) of a given energetic that entered the column at pore volume i was calculated by multiplying the fraction volume at pore volume i (V_i) by the corresponding influent concentration, C_{0i} , of each energetic compound at pore volume i. The total mass (M_{OUTi}) that exited the column was similarly calculated by multiplying V_i by the corresponding effluent concentration, C_i , of each energetic compound at pore volume i. Fractions for which there was not a corresponding measured influent or effluent concentrations were multiplied by the previous measured concentration, e.g., if the fraction at pore volume i had a corresponding measured energetic concentration (C_{0i}) or C_i , but the fraction at at pore volume i +1 did not, then the

concentration for the fraction at pore volume i was multiplied by the volume of the fraction at pore volume i+1.

Given the low variability of the influent concentrations, and the relative slow changes in the effluent concentrations, the pore volume water was transiting from the influent reservoir and reaching the fraction collector was ignored. M_{REM} is was calculated by subtracting M_{OUTi} from M_{INi} for each pore volume i, and M_{REM} was calculated by summing the resulting M_{REM} values were summed from i=1 to i=1 the pore volume when C reached C_0 . If C did not reach C_0 by 100 PV, then the sum from 1=1 to 100 was calculated.



Col 1 Peat Moss	Col 2 Peat Moss	Col 3 Peat Moss		То	tal mass	(g)
+ Native Pine	+ CAT Pine	+ CAT Pine		Col 1	Col 2	Col 3
radive i me			Sand	10	10	10
	Mixed	Layered	Peat Moss	20	20	20
			Native Pine	2		
Sand/Glass Beads	Sand/Glass Beads	Sand/Glass Beads	CAT Pine	-	2	2
Peat Moss + Native Pine	Peat Moss + CAT Pine	Peat Moss				
		CAT Pine				

C1 Sorption	C2 "Sorption	C3 Sorption +	C4 Sorption +			Total m	nass (g)	
Only"	Plus"	Biodegradation	Biodegradation		C1	C2	C3	C4
	Added effect	Added effect of	Added effect of	Sand	2	2	2	-
	of Biopolymer	Biopolymer +	Biopolymer +	Biochar	-	-	-	1
		Inocula	Inocula + Biochar	Peat + Oyster Shell (5:3.5 w:w)	12	12	12	12
Sand/	Sand/	Sand/	Sand/ Glass Beads	Sterile Soil	10	10	-	-
Glass Beads	Glass Beads	Glass Beads	Biochar	Soil		-	10	10
Peat + Oyster Shell + Sterile Soil	Peat + Oyster Shell + Sterile Soil +	Peat + Oyster Shell + Soil + Biopolymers + ANOXIC	Peat + Oyster Shell + Soil + Biopolymers + ANOXIC	Biopolymer (PHB, PCL, BioPBS, 1:1:1, w.w)		1.5	1.5	1.5
Sterile Soil	Biopolymers	Inocula	Inocula	CAT Pine	5	5	5	5
CAT Pine	CAT Pine	Peat + Oyster Shell + Soil + Biopolymer + AEROBIC Inocula CAT Pine	Peat + Oyster Shell + Soil + Biopolymer + AEROBIC Inocula CAT Pine	ANOXIC inocula Anaerobic Mi Pure culture AEROBIC inocu Aerobic MBR Pure cultures Pure cultures	BR mix I-C (RI Ia mix c KTR9	ulture , DN22		RDX)

6.2 RESULTS and DISCUSSION

6.2.1. Column sorption experiment

The pH of the influent was controlled at approximately 6.3 S.U. The effluent from C1 remained subneutral for the duration of the experiment (Figure 6-4), while the effluent pH of C2 and C3 were initially around 6 S.U., then declined to around the same value as C1. This reflected the long term impact of the acidity of the peat moss.

Full breakthrough curves for energetics are shown in Figure 6-5, and plots focused on the sorption and desorption phases are shown in Figure 6-6. Additional plots showing the energetics breakthrough relative to the tracer for each column are presented in Figure 6-7.

The retardation factors (relative to the tracer) for all the target energetics in the different columns are shown in Table 6-1, calculated when each compound had reached a C/C₀ of 0.5. NTO and ClO4- were retarded relative to the chloride tracer when CAT pine was present, with the greatest retardation factors observed with the CAT pine as a single layer beneath the peat (3.3 and 7.0, respectively). For HMX, RDX, TNT, and DNAN, the high retardation factors were observed in the control column containing peat plus unmodified pine shavings. Slightly lower retardation of these compounds was observed in the columns containing CAT pine, likely due to their lack of sorption onto the CAT pine. NQ exhibited a slight degree of retardation in the control column which also was reduced in the columns with the CAT pine.

The apparent sorption capacity of the peat derived from the column experiment data using Equation 1 above are shown in Table 6-2. The sorption capacity values for the peat were quite comparable to the batch values for HMX, RDX, TNT, and DNAN (within 1.5- to 5-fold). Batch peat testing indicated a higher capacity for TNT than for DNAN, but the column testing would indicate similar peat capacities for both aromatic explosives. The columns study also indicated very low sorption capacity of NQ, NTO, and ClO4- in the column testing, matching what was seen in the batch testing (e.g., no significant sorption; insufficient data to generate a good Freundlich or Langmuir model fit).

With CAT pine, the column sorption capacity for NTO and ClO₄⁻ were on the order of 8- and 23-fold lower than calculated from the batch study data. This is not totally unexpected. The batch testing had a fixed concentration of competing anions, and it was demonstrated that increased competing anions results in decreased NTO (and by analogy, ClO₄⁻) removal by CAT pine. During the column study, there was a continuous feed of competing anions in the ASR, so the overall apparent sorption capacity of the CAT pine for the target compounds was reduced. The columns more closely represent real environmental conditions, so these sorption capacities are likely more reliable. However, as these columns did not explicitly include any biological processes, the biological component of an actual passive biofilter would also likely be removing several of the competing anions (e.g., NO₃⁻, SO₄²-) via nitrate and sulfate reduction, respectively. This will be explored in the next set of column experiments.

The sorption capacity for the target compounds was also explored by modeling the breakthrough curves using the Thomas model. All the model fits had r² values greater than 0.98. As seen in Table 6-3, the results of this modelling were in good agreement with the values obtained using Equation 1 above. Sorption capacity of peat for HMX, RDX, TNT, and DNAN were 1.5- to 6.5-fold lower than the batch isotherm estimates, but CAT pine sorption capacity for NTO and ClO₄ were somewhat higher, and only 5.5-fold and 15-fold lower than batch estimates.

Combining the Thomas model sorption capacities, estimates of the mass of explosives detected in Dahlgren surface runoff, and some conservative safety factors, these data indicate that the mass of passive biofilter material required to essentially sorb all the dissolved explosives is on the order of 1500 kg peat, plus 200 kg CAT pine (Table 6-4). This equates to a volume around the size of a small moving van (6' x 8' x $11' = \sim 500$ cu ft), which is reasonable for a surface runoff treatment system. Additionally, this does not take into account the added benefits of the abiotic and biotic degradation that would be included in the final technology, which may decrease the size estimate.

Table 6-1. Retardation factors (R) for all energetics in the three columns.

	R Factor usi	ng control	chloride tra	cer			
	HMX	RDX	TNT	NQ	NTO	DNAN	CIO4
Peat+Pine	13.3	7.0	41.3	1.7	1.1	36.7	1.0
Peat+CAT Pine Mix	12.1	4.9	37.2	1.6	1.6	30.7	2.6
Peat+CAT Pine Layered	12.7	7.5	38.7	1.8	3.3	36.0	7.0
	R Factor usi	r					
	HMX	RDX	TNT	NQ	NTO	DNAN	CIO4
Peat+Pine	13.3	7.0	41.3	1.7	1.1	36.7	1.0
Peat+CAT Pine Mix	9.6	3.9	29.5	1.2	1.3	24.3	2.1
Peat+CAT Pine Layered	8.8	5.2	26.6	1.3	2.2	24.8	4.8

Table 6-2. Calculated sorption capacity for all energetics based on batch and column experiments at 50% breakthrough.

	mg/g peat						
	HMX	RDX	TNT	NQ	NTO	DNAN	CIO4
Batch Sorption Freundlich qe1	0.08	0.11	1.64	-	-	0.61	-
Batch Sorption Langmuir qe1	0.08	0.07	2.45	-	-	0.58	-
Peat+Pine	0.06	0.03	0.48	0.02	0.01	0.46	0.00
Peat+CAT Pine Mix, q _{org50}	0.06	0.02	0.45	0.02	0.02	0.40	0.01
Peat+CAT Pine Layered, q _{org50}	0.06	0.04	0.46	0.02	0.04	0.45	0.02
	mg/g CAT F	Pine					
					NTO		CIO4
Batch Sorption Freundlich qe1	-	-	-	-	1.52	-	2.24
Batch Sorption Langmuir qe1	-	-	-	-	1.61	-	2.50
Peat+CAT Pine Mix, q _{org50}	-	-	-	-	0.13	-	0.06
Peat+CAT Pine Layered, q _{org50}	-	-	-	-	0.24	-	0.16

¹ Fuller ME, Farquharson EM, Hedman PC, Chiu P. 2022. Removal of munition constituents in stormwater runoff: Screening of native and cationized cellulosic sorbents for removal of insensitive munition constituents NTO, DNAN, and NQ, and legacy munition constituents HMX, RDX, TNT, and perchlorate. Journal of Hazardous Materials 424:127335.

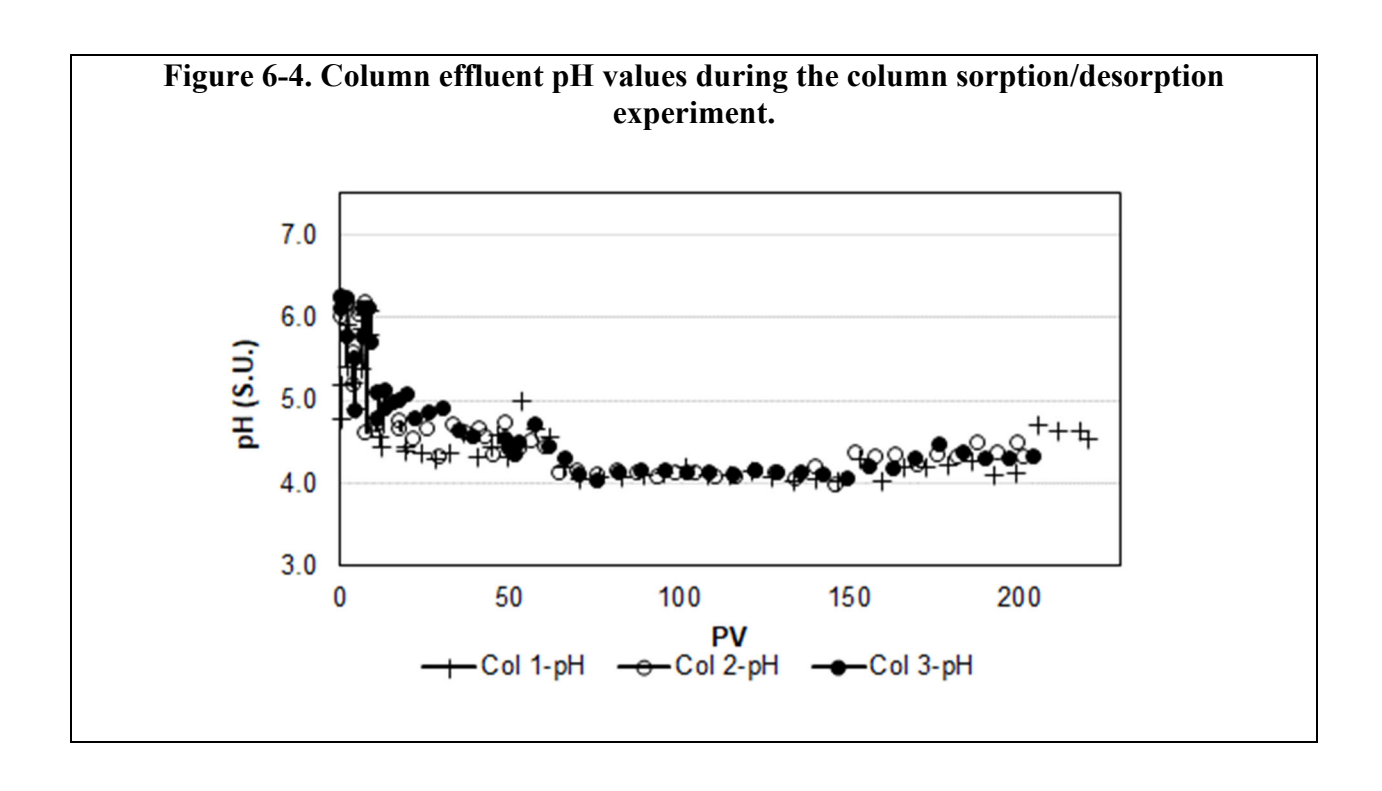
Table 6-3. Calculated sorption capacity for all energetics based on batch and column experiments and the Thomas column adsorption kinetic model.

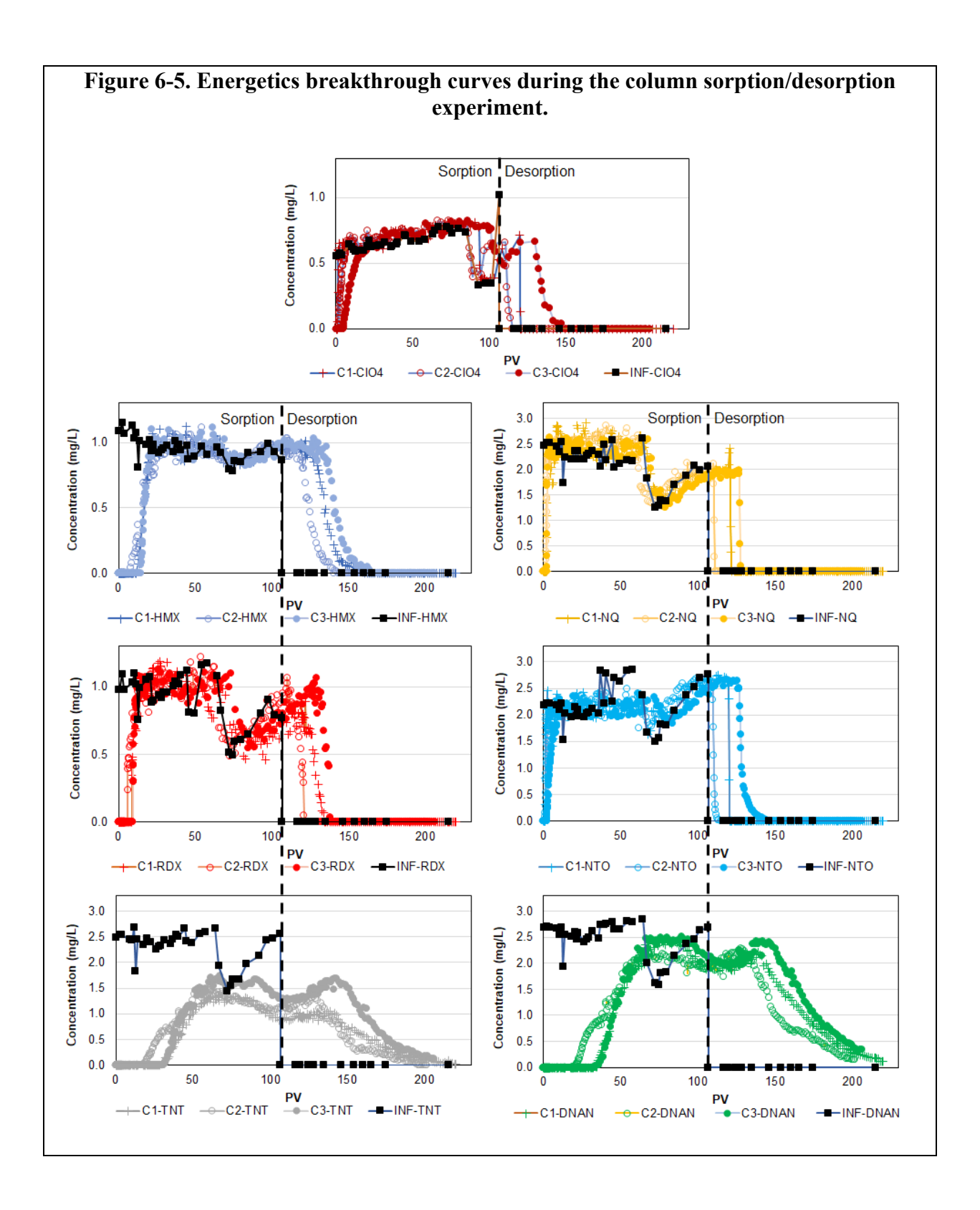
	mg/g peat						
	HMX	RDX	TNT	NQ	NTO	DNAN	CIO4
Batch Sorption Freundlich qe1	0.08	0.11	1.64	-	-	0.61	-
Batch Sorption Langmuir qe1	0.08	0.07	2.45	-	-	0.58	-
Peat+Pine Mix, q ₀ Thomas Model	0.05	0.03	0.40	0.02	0.01	0.45	0.00
Peat+CAT Pine Mix, q ₀ Thomas Model	0.06	0.03	0.36	0.02	0.02	0.41	0.01
Peat+CAT Pine Layered, q ₀ Thomas Model	0.06	0.03	0.36	0.02	0.04	0.45	0.02
	mg/g CAT	Pine					
					NTO		CIO4
Batch Sorption Freundlich qe1	-	-	-	-	1.52	-	2.24
Batch Sorption Langmuir qe1	-	-	-	-	1.61	-	2.50
Peat+CAT Pine Mix, q ₀ Thomas Model	-	-	-	-	0.20	-	0.10
Peat+CAT Pine Layered, q ₀ Thomas Model	-	-	-	-	0.37	-	0.23

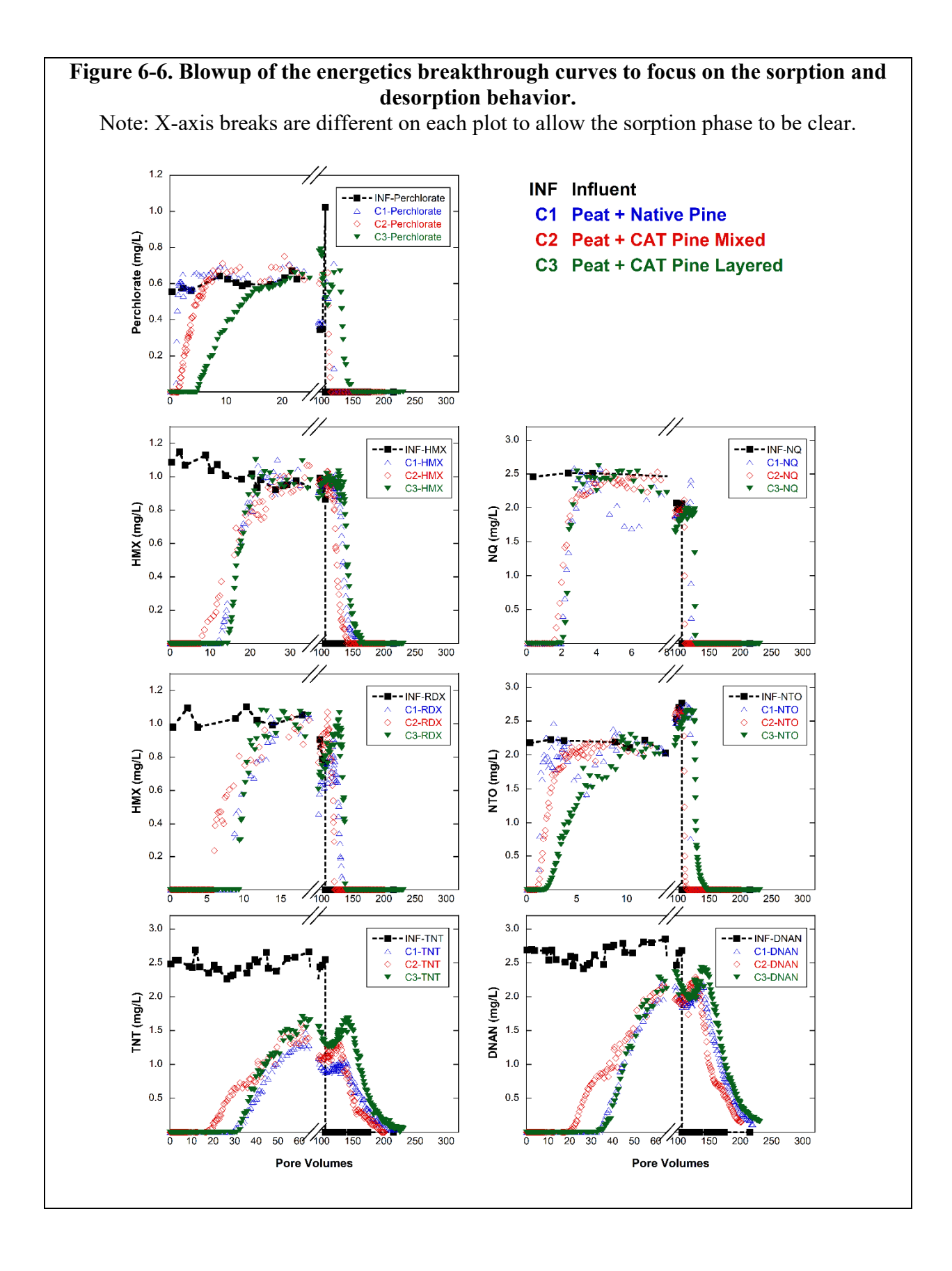
¹Fuller ME, Farquharson EM, Hedman PC, Chiu P. 2022. Removal of munition constituents in stormwater runoff: Screening of native and cationized cellulosic sorbents for removal of insensitive munition constituents NTO, DNAN, and NQ, and legacy munition constituents HMX, RDX, TNT, and perchlorate. Journal of Hazardous Materials 424:127335.

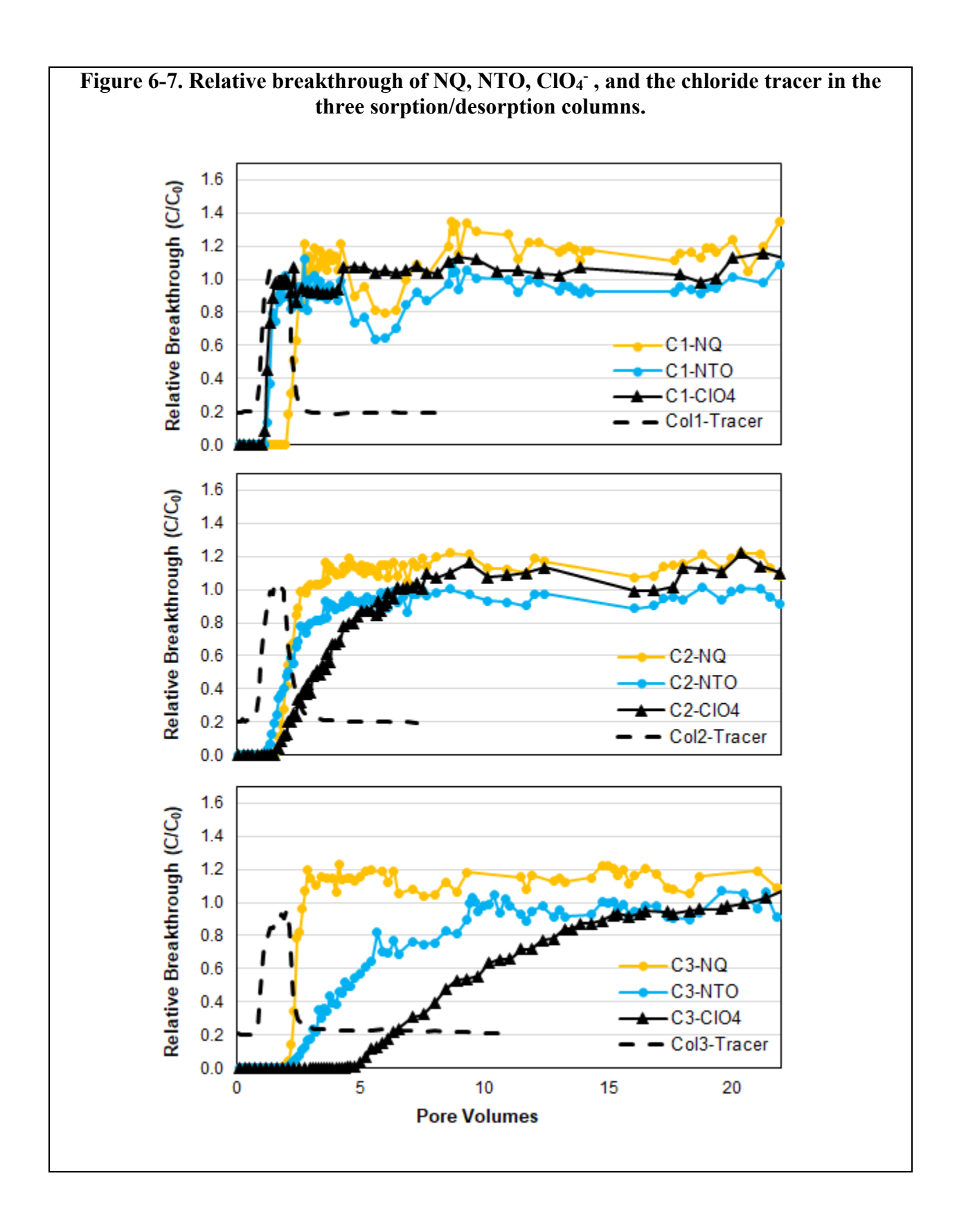
Table 6-4. Preliminary mass and volume sizing for a passive biofilter to treat NSWC Dahlgren surface runoff based on maximum sorption capacity from sorption-only column experiment and runoff characterization.

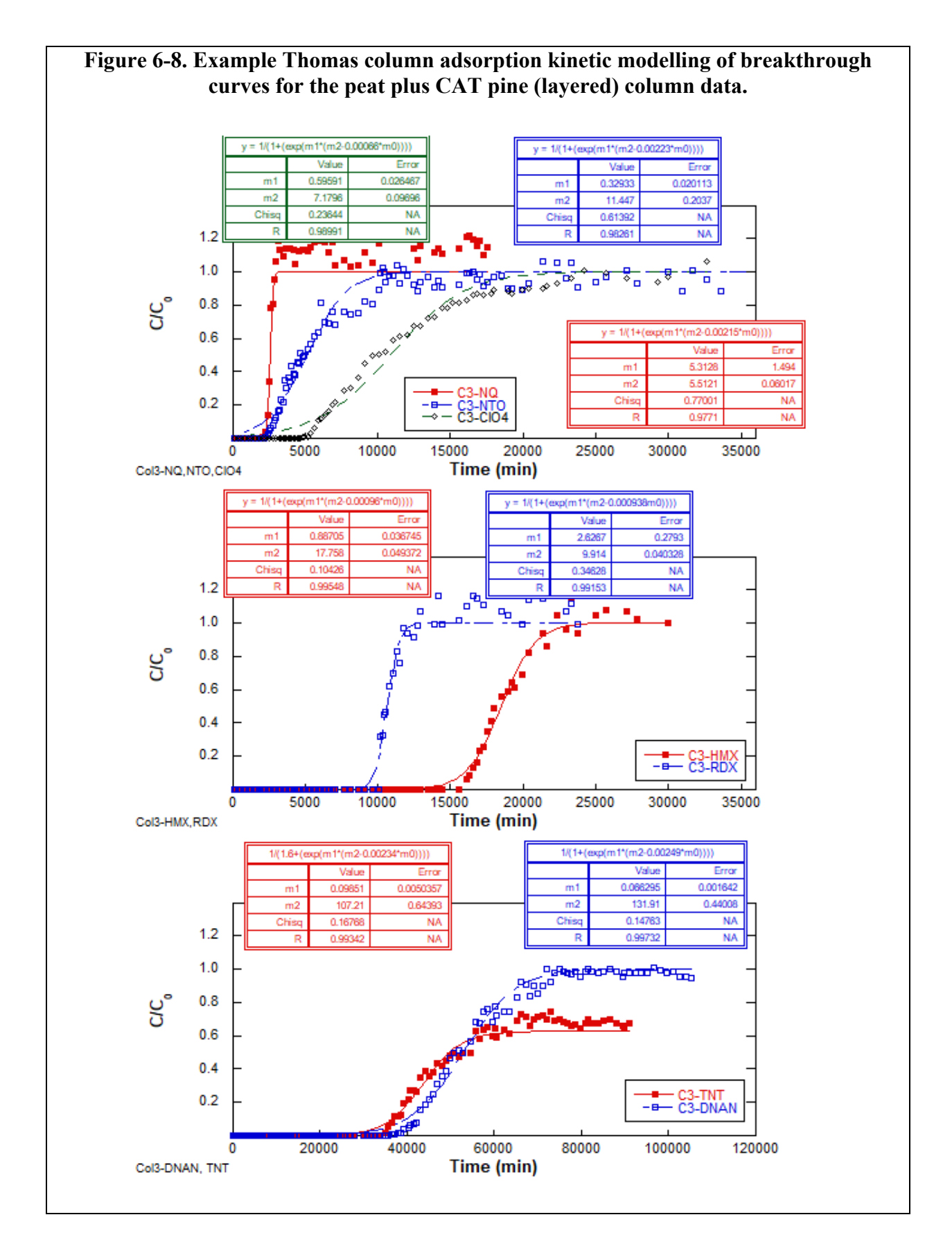
	Average m	aximum so	orption capa	acity (q ₀ , n	ng/kg)		
	HMX	RDX	TNT	NQ	NTO	DNAN	CIO4
Peat	57	32	376	18		435	
CAT Pine					285		163
Estimated mass in runoff based on NSWC Dahlgren samples (mg)	837	429					289
Assumed same order of magnitude for undetected explosives (mg)			500	500	500	500	
Safety Factor	100	100	100	100	100	100	100
Mass of explosives in runoff needing removal (mg)	83700	42900	50000	50000	50000	50000	28900
	Minimum	mass of me	edia require	d (kg)			
	HMX	RDX	TNT	NQ	NTO	DNAN	CIO4
Peat	1477	1324	133	2708		115	
CAT Pine					175		177
Max mass required (kg)	2708						
Max mass excluding NQ (kg)	1477						
Peat dry bulk density (kg/m3)	100	100	100	100	100	100	100
Biobarrier volume (m3)	15	13	1	27	2	1	2
Max volume required (m3)	27						
Max volume excluding NQ (m3)	15						
Biobarrier volume (cu ft)	522						











6.2.2. Column sorption-biodegradation experiments Column Experiment 1

Figure 6-9 presents the influent and effluent pH and ORP, the influent DO, and the effluent TOC during the first column sorption-biodegradation experiment.

The influent pH averaged 6.5 ± 0.1 S.U. due to proper operation of the pH controller. The column effluents were generally around 8 S.U. This indicated that the oyster shell added as a buffering agent to counteract the acidity of the peat worked very well.

The influent remained aerobic/oxygenated (DO = 5.8 ± 0.3 mg/L) and at a positive redox (209 \pm 15 mV) throughout the experiment. The column effluent ORP varied between the columns.

Redox decreased for C1 over the course of the experiment, but remained positive. C2 also decreased, but went negative for a short period between 30 and 50 PV before returning to low positive values for the remainder of the experiment. The ORP decreases in these two columns is attributed to low level biological activity of the native peat moss microbial community, with some utilization of the biopolymer carbon source in C2.

Summary breakthrough curves are presented in Figure 6-10, and detailed analysis is provided below.

Influent and effluent perchlorate is shown in Figure 6-11. Perchlorate exhibited relatively fast breakthrough in the uninoculated C1 and C2. The delay of perchlorate elution from these two columns can mostly be attributed to the effects of the CAT pine. C4 effluent demonstrated a slow increase in perchlorate starting around 30 PV, while no perchlorate was observed in the C3 effluent for the duration of the experiment. Perchlorate is quite readily biodegraded under anoxic conditions, so the enhanced removal of perchlorate in the inoculated C3 and C4 was expected. The only difference between C3 and C4 is the presence of biochar in C4. The biochar would not be expected to impact perchlorate removal in the bulk of the column, as it is at the top of the column near the effluent. Therefore, the reason for the difference in perchlorate removal dynamics between these biologically active columns is not readily apparent.

Legacy explosive (HMX, RDX, TNT) concentrations in the influent and column effluents is shown in Figure 6-12. C1 and C2 effluent concentrations generally reflect removal by sorption as was observed in the previous set of column experiments. The slightly elevated concentrations of HMX in the C1 and C2 effluent compared to the influent was attributed to matrix interference during analysis. However, for all three explosives, there appeared to be more removal, and a slightly slower increase in effluent concentrations in C2 compared to C1. This may be due to some additional sorptive losses of HMX, RDX, and TNT because of the added biopolymers, as these materials were observed to sorb explosives during batch testing. The difference in removal may also reflect some biodegradation of these explosives was being supported by the biopolymers, or even by the peat. The lower ORP in C2 would also facilitate biodegradation of these compounds, although the timing of when C2 ORP dropped to negative values does not completely aligned with when the divergence between C1 and C2 was observed. Effluent HMX and RDX concentrations

reached close to the influent concentration, while TNT concentrations appeared leveled off at about 55% of the influent concentration, indicating that we had not reached the sorptive capacity by the end of the experiment, or that there was a small amount of ongoing biological activity transforming / degrading the TNT.

In contrast, biological active C3 and C4 explosives removal was much greater than uninoculated C1 and C2, and C3 was slightly greater than C4. HMX, remained below the influent concentration for most of the experiment in both C3 and C4, with slightly lower concentrations in C3 by the end of the experiment. C3 data also seemed to indicate that biological HMX transformation / degradation was initially lower than in C4, but increased at around 15 PV. Also, with the exception of an early pulse of RDX in C3, the effluent concentration of RDX from both C3 and C4 remained below detection until the end of the experiment. TNT removal was also very similar for both C3 and C4.

The RDX metabolite NDAB was detected in the all the column effluents over the course of the experiment, with higher detections at the beginning of the experiment, and slightly decreasing concentrations over time (Figure 6-13). NDAB is indicative of aerobic RDX degradation, and is produced by the two RDX degrading pure cultures added to C3 and C4. NDAB can also be produced from RDX under microaerophilic conditions by some bacteria (Fuller et al., 2010), and has been observed as a byproduct of aerobic HMX biodegradation by some microbes and/or their enzymes (Nagar at al., 2018; Bhushan et al., 2003). Essentially stoichiometric conversion of the influent HMX+RDX to NDAB was observed after 20 PV.

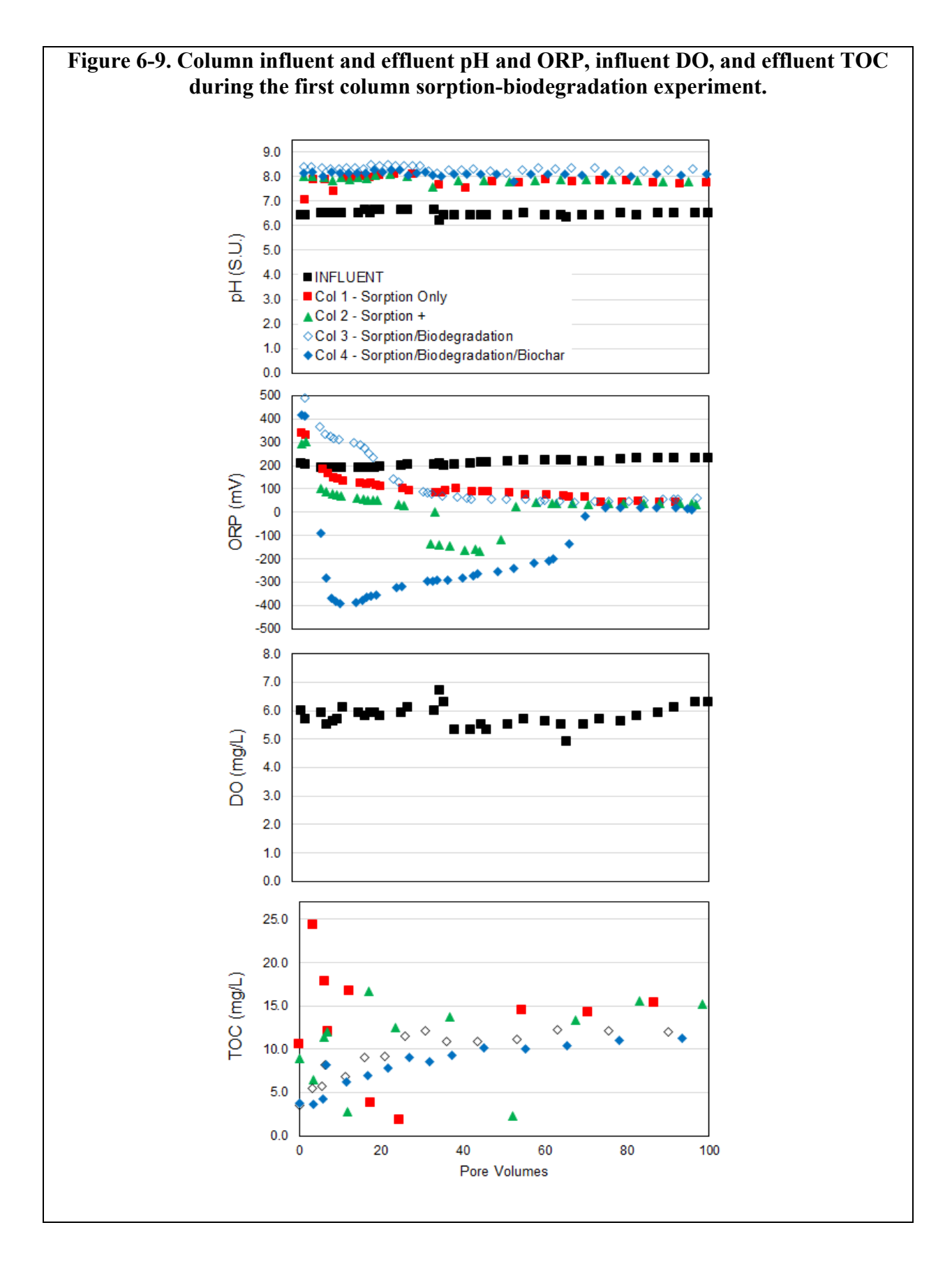
Two TNT breakdown products, 4-amino-2,6-dinitrotoluene (4-AM-2,6-DNT) and 2-amino-4,6-dinitrotoluene (2-AM-4,6-DNT), were also detected at low concentrations in the column effluents (Figure 6-14). The maximum combined 4-AM-2,6-DNT and 2-AM-4,6-DNT was less than 10% (molar basis) in C1 and C2, 25% in C3, and ~15% in C4. These compounds are the first products generated when TNT undergoes reductive transformation, and can occur even under bulk aerobic conditions by some microorganisms (Fuller et al., 1997). As with NDAB, non-stoichiometric transformation of TNT to 4-AM-2,6-DNT and 2-AM-4,6-DNT was observed, indicating some degree of further degradation or sorption of these compounds.

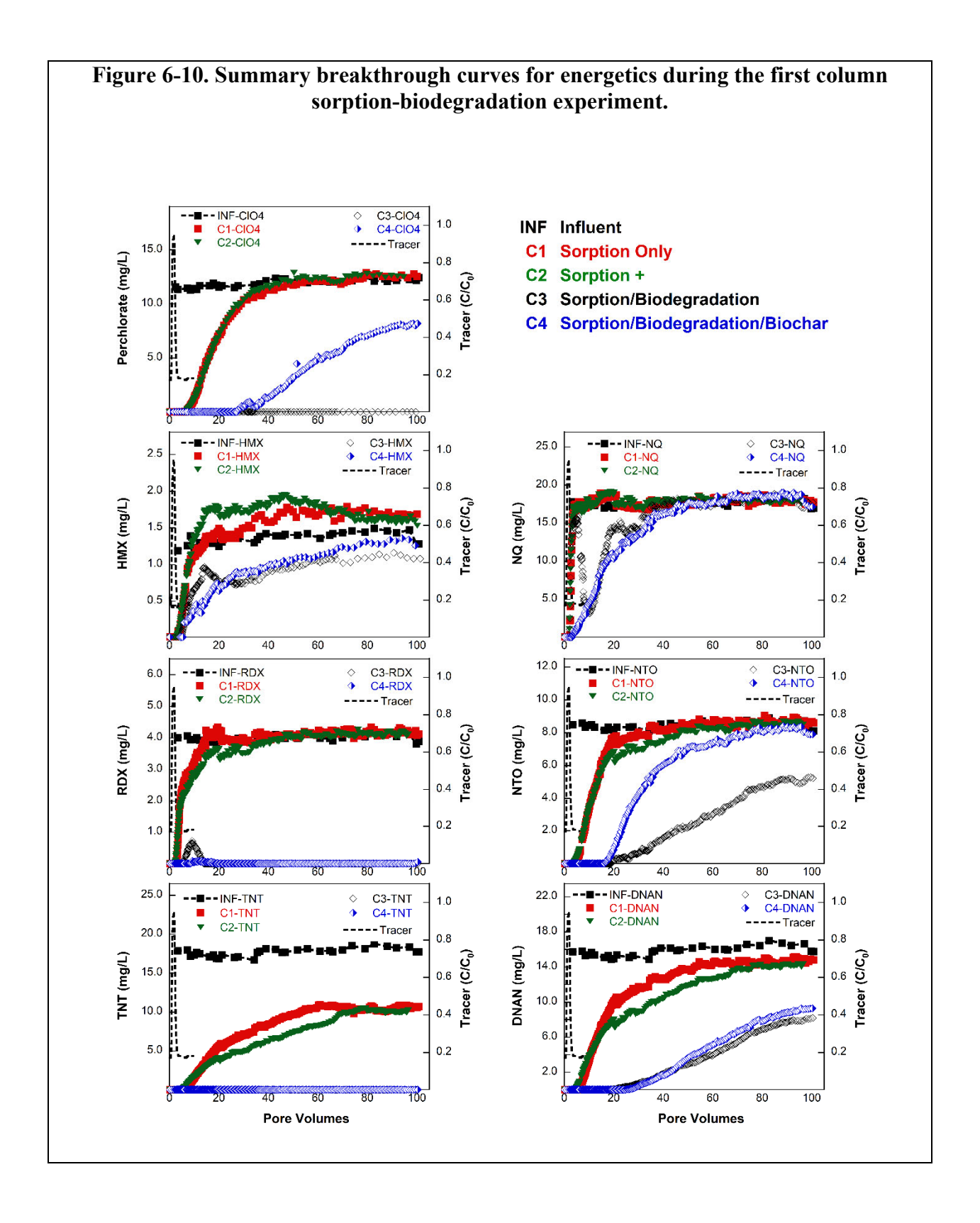
Influent and effluent concentrations of insensitive explosive (NQ, NTO, DNAN) are shown in Figure 6-15. NQ quickly eluted from C1 and C2, reaching the influent concentration within 5 PV, and was attributed to minimal sorptive removal, as observed during the previous column experiment. Inoculated C3 exhibited an early pulse of NQ up to concentrations close to that in the influent, then exhibited a very large decrease in concentration, followed by a slow rise, approaching the influent concentration by 40 PV (Figure 6-16). This was attributed to a rapid onset of NQ biodegradation in C3, likely by the pure aerobic NQ degrading culture added to the column, NQ5, or by the NQ degrading organisms in the anaerobic mixed culture. In contrast, NQ in C4 effluent slowly rose, reaching the influent concentration at around 40 PV. The reason for the difference in NQ breakthrough between C3 and C4 was not readily apparent, as the only difference was the presence of biochar at the effluent end of C4. However, since the capacity of biochar for NQ is not very high, the difference probably reflects variations in the biotic activity of the columns, rather than an abiotic reaction.

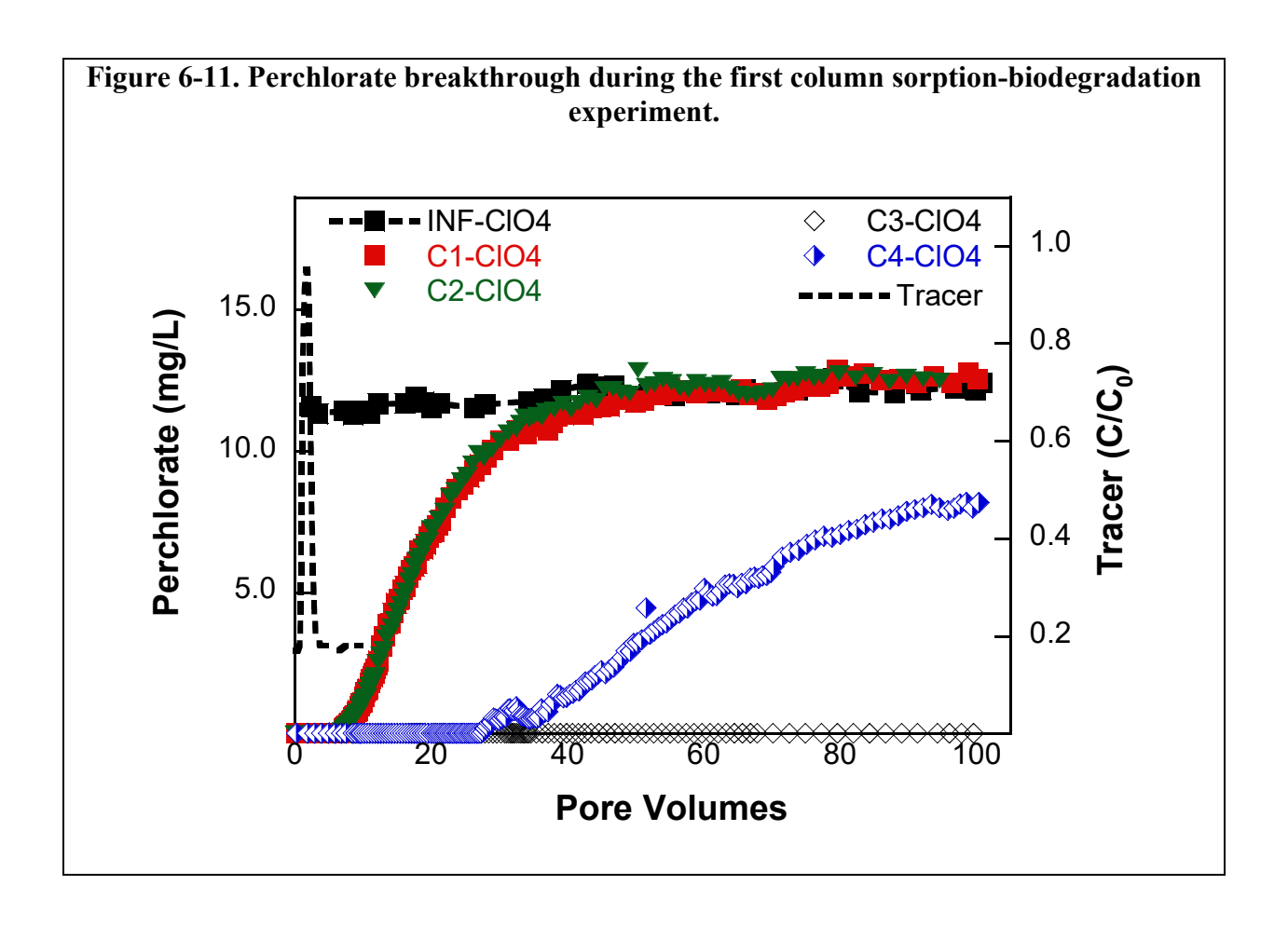
NTO and DNAN elution from uninoculated C1 and C2 were similar, although C2 exhibited slightly better removal of both compounds. This was similar to what was observed for legacy explosives, and may also be attributed to some amount (or a greater amount) of biodegradation in C2 compared to C1. In contrast to TNT, C1 and C2 effluent DNAN concentrations leveled off at around 90% of the influent concentration.

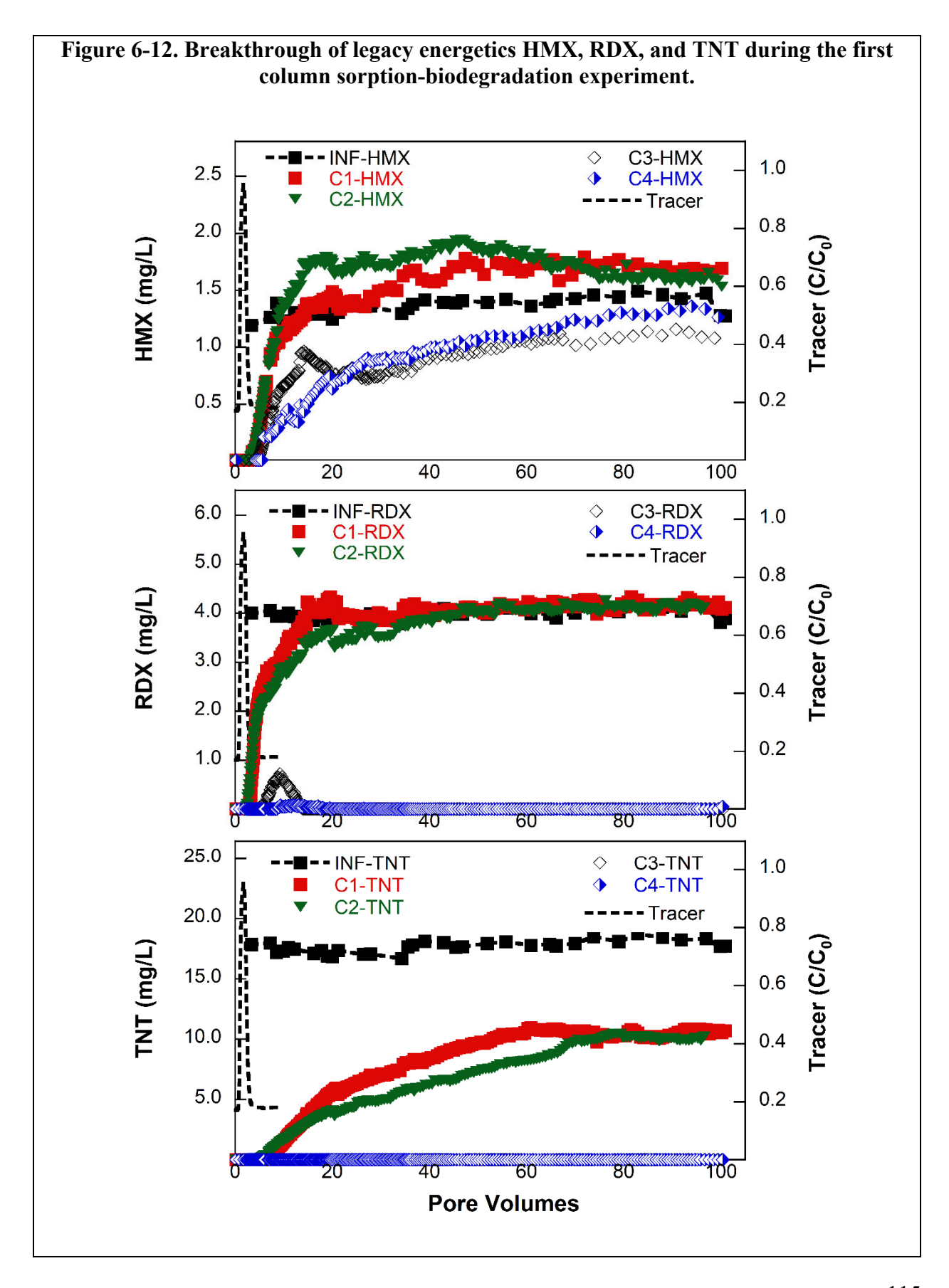
In C3 and C4, the timing of breakthrough of NTO was similar, but the rate of increase in the effluent concentrations was much slower in C3 than in C4. This is likely due to more biodegradation in C3 compared to C4. Similarly, there was slightly more DNAN removal in C3 than in C4 (similar to TNT), again probably due to more biodegradation.

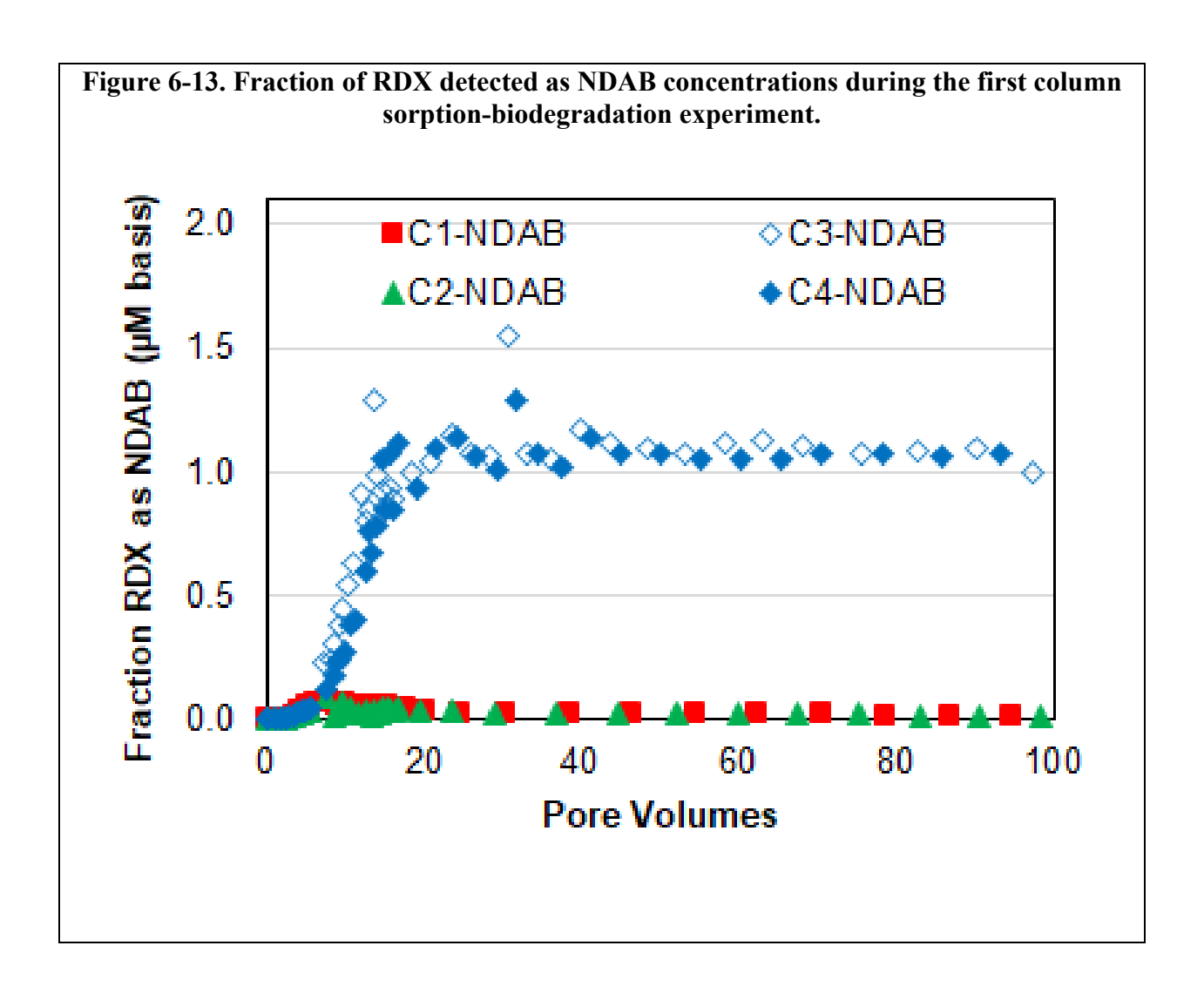
Due to co-eluting interferences in the column effluent, the detection of the NTO breakdown product ATO was not possible. The DNAN breakdown product 2-amino-4-nitroanisole (2-ANAN, or MENA) was detected in all the column effluents (Figure 6-17). The highest concentrations were observed in C3 (maximum at ~38% of influent DNAN on a molar basis), with C1, C2, and C4 at 7 to 10%. The effluent 2-ANAN concentrations all decreased after their respective peaks, indicating that 2-ANAN was either no longer being produced, or that it was being further degraded.

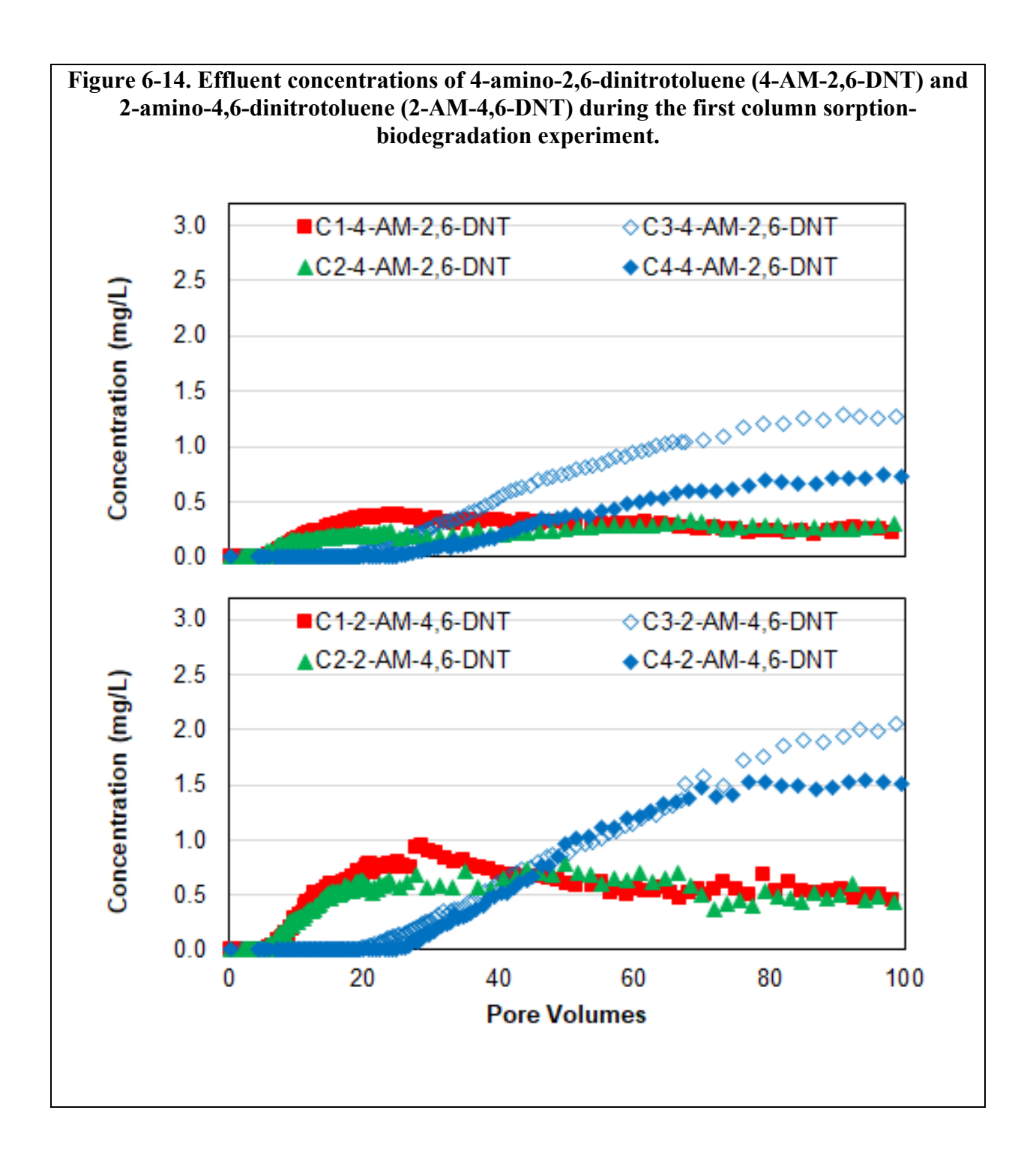


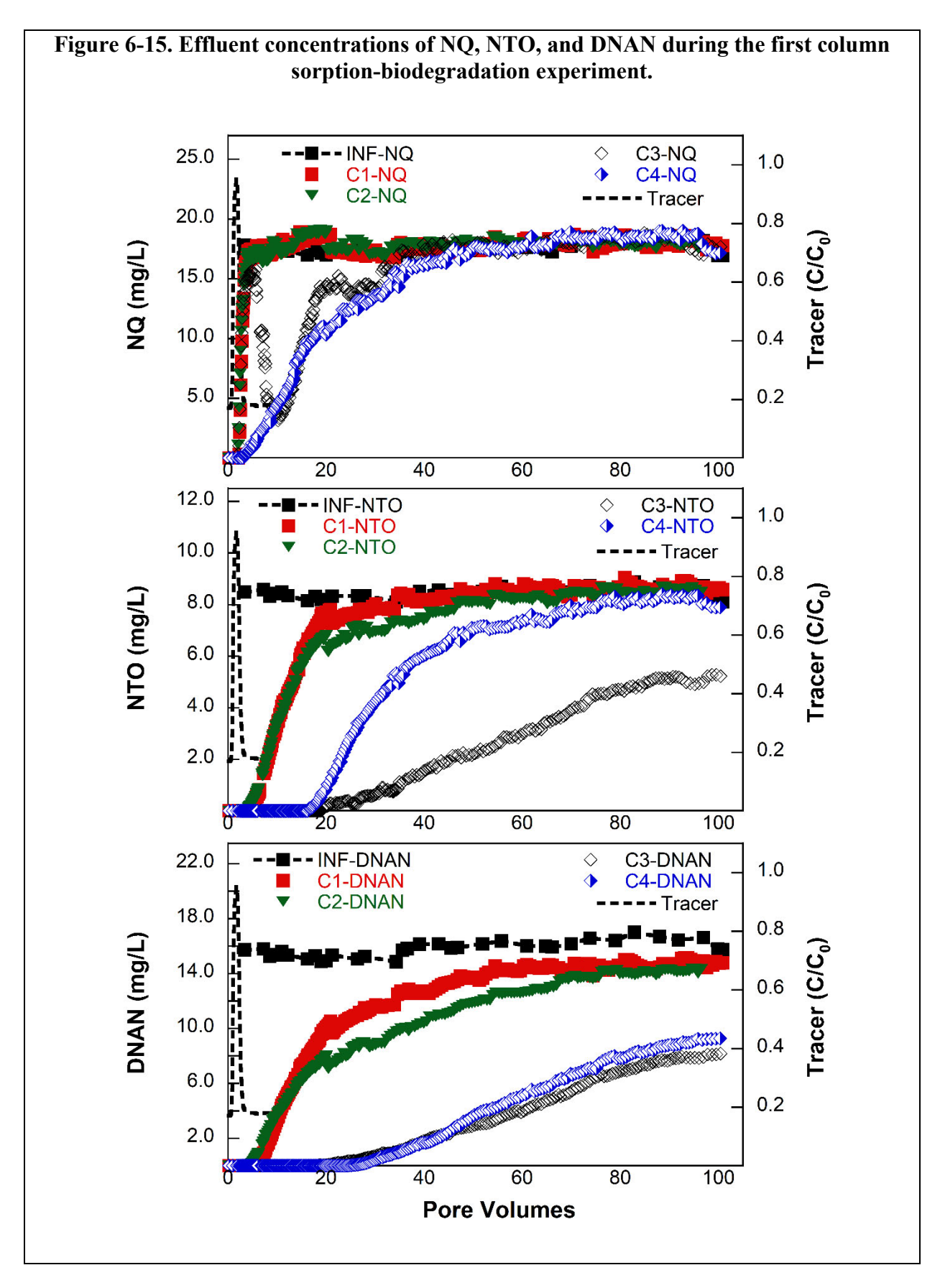


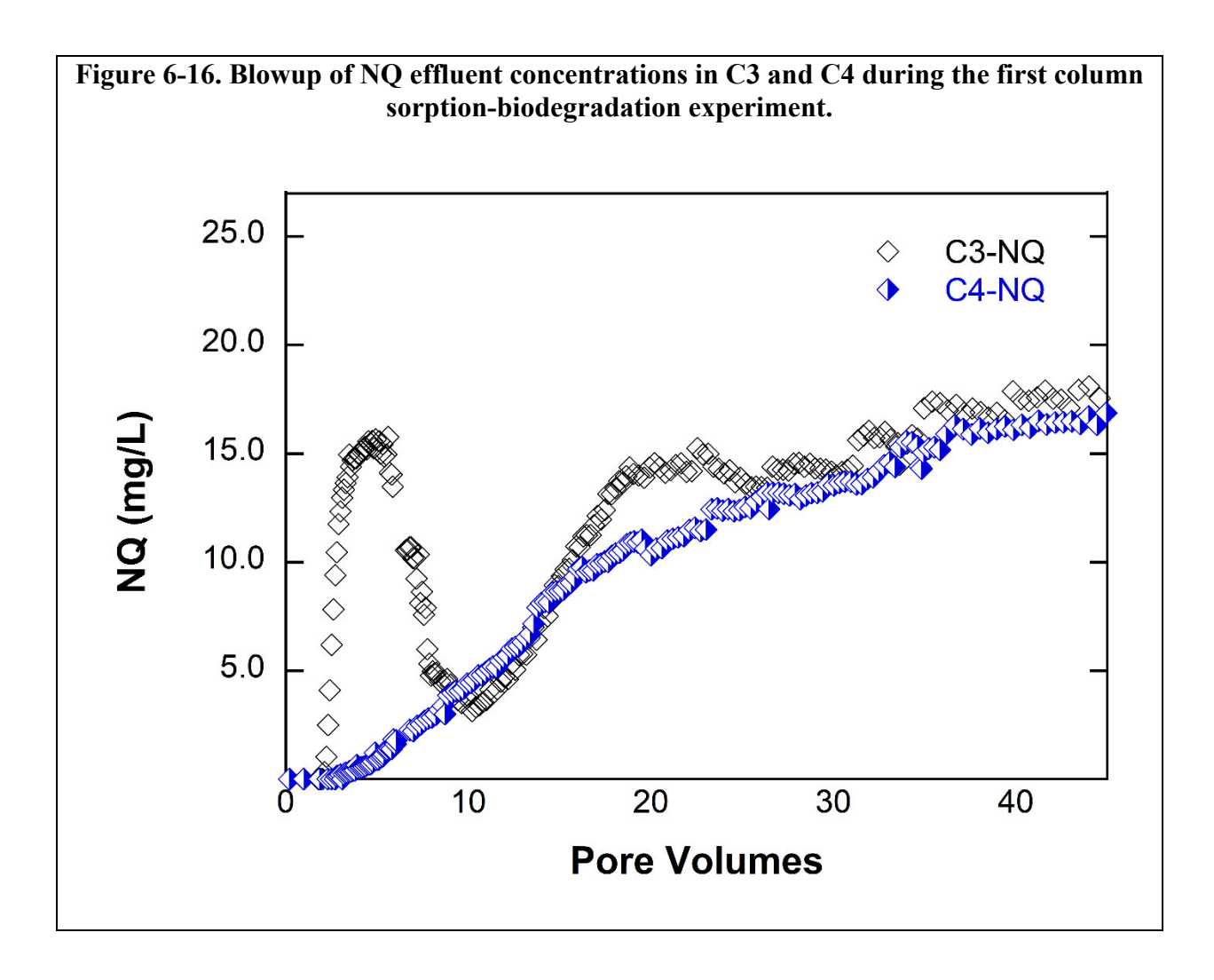


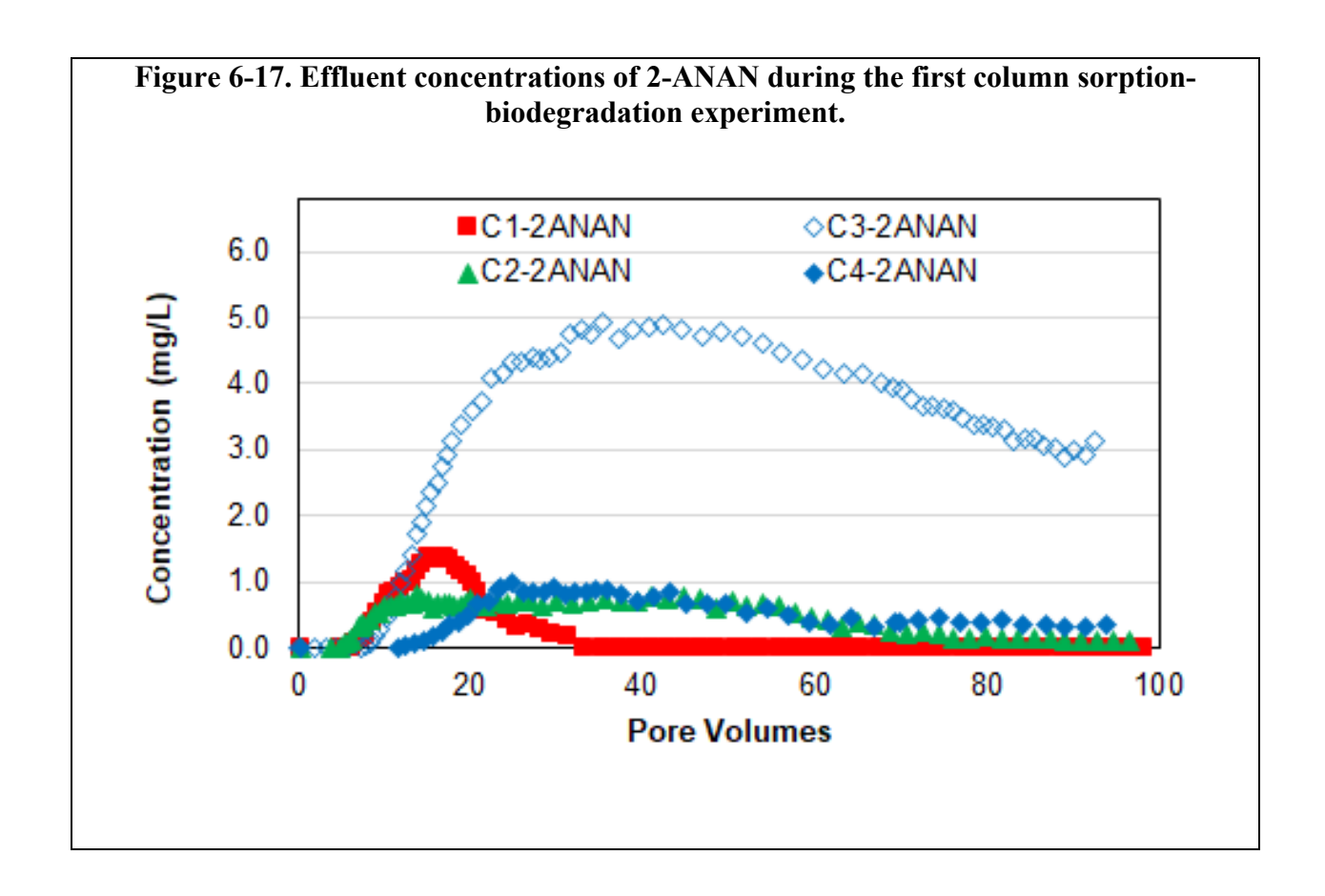












Column Experiment 2

The influent and effluent pH and ORP, and the influent DO during the first experiment are shown in Figure 6-18.

As seen in the first experiment, the pH controller maintained the influent at 6.4 ± 0.1 S.U. and the column effluents were all generally around 8 S.U. This indicated that the oyster shell added as a buffering agent to counteract the acidity of the peat worked very well. The influent remained aerobic/oxygenated (DO = 6.5 ± 0.5 mg/L) and at a positive redox (227 ± 12 mV) throughout the experiment.

The column effluent ORP variation between the columns was lower than observed during the first experiment, and ORP values generally remained more positive at around +50 mV for the majority of the experiment. This is somewhat interesting, given that the assumed higher microbial activity in columns C3 and C4 would have been expected to result in lower (negative) effluent ORP values.

However, as is seen below, the higher effluent ORP did not result in any apparent reduction in energetics biodegradation.

Summary breakthrough curves are presented in Figure 6-19, and detailed analysis is provided below, with specific attention to comparison between the first and second experiments

The breakthrough of ClO₄⁻ followed a similar pattern as observed during the first sorption-biodegradation column experiment (Figure 6-20). Removal of ClO₄⁻ in C1 and C2 was attributed to sorption by the CAT pine, while significant biodegradation was observed C4, and essential no ClO₄⁻ was observed in the effluent of C3 over the entire course of the experiment. The timing of the ClO₄⁻ breakthrough from C4 was approximately 20 PV later during the second experiment compared to the first experiment, which may indicate sustained biological degradation.

The breakthrough of HMX followed the same pattern as observed during the previous sorption/biodegradation column experiment (Figure 6-21), with the apparent effluent concentrations from C1 and C2 being elevated above the influent concentration due to matrix interferences during analysis. There was also indications of some HMX biodegradation in C3 and C4, although activity seemed lower than observed during the first sorption-biodegradation experiment.

For RDX, the same pattern was observed in C3 and C4 during the second experiment as was observed in the first experiment (Figure 6-22). Namely, there was a short appearance of RDX in the effluent of C3 (without biochar) early on, which then decreased to below detection. After this initial elution, the effluent RDX from C3 and C4 (with biochar) have remained below the detection limit. As postulated previously, it is believed that this result reflects a delay in the initiation of robust RDX biodegradation. The biochar in C4 served as a buffer for the RDX that was not yet being biodegraded, either via sorption or abiotic degradation, leading to no detections in the effluent. The stoichiometric transformation of RDX to NDAB was also similar in both experiments, indicative of almost full degradation of RDX in the aerobic zone (Figure 6-23).

The behavior of TNT during the first and second experiment was quite similar (Figure 6-24), with complete or near complete TNT removal for the duration of the experiment in C3 and C4. The production and elution of only two TNT breakdown products, 4-AM-2,6-DNT and 2-AM-4,6-DNT, was also comparable between the two experiments, albeit the maximum concentrations observe red in C4 effluent were slightly lower during the second experiment (Figure 6-25). This could indicate less overall production or further metabolism of these compounds, or more sorption or sequestration by the column media.

The elution of NQ during the second experiment was also similar, although not identical to, that observed during the first experiment (Figure 6-26). In C3, the same fast rise and fall of NQ was observed, indicative of a delay in robust NQ biodegradation activity. This was followed by a slow rise in effluent NQ from C3. These features were not observed in C4, which was attributed to the biochar acting as a sorption "buffer". One key difference between the two experiments was that the breakthrough of NQ in C4 was approximately 12 PV later during the second experiment compared to the first experiment. The reason for this is not clear at this time.

During both experiments, NQ removal in the inoculated columns was observed to increase initially, then decrease as the experiment continued. This would seem to indicate that NQ biodegradation by strain NQ5 had stopped or slow considerably. NQ5 uses NQ as a sole nitrogen source when supplied with a carbon source. It is possible that NQ5 was only able to utilize a small portion of the slow release PHB and BioPBS biopolymers that were added to the columns. This could be due to either an inherent limit on NQ5's ability to degrade all the biopolymer present. However, a more likely explanation is that NQ5 was unable to compete with the RDX degraders (specifically DN22 and KTR9), which also use the biopolymers as a carbon source. Additional small scale experiments are being considered to investigate this further, examining the effects of a higher initial mass of biopolymer, as well as the presence/absence of the RDX degrading cultures.

The breakthrough of NTO in C3 and C4 were essentially reversed in the second experiment compared to the first experiment (Figure 6-27). The biochar in C4 appeared to cause NTO to elute roughly twice as slowly during the second experiment compared to the first experiment. This delay effect was similar to what was observed for NQ. As observed in the first experiment, the concentration of NTO in the effluent of C4 surpassed that in C3 at later PV.

There was a decrease in the timing of DNAN breakthrough by about 10 PV in C4 during the second experiment compared to the first experiment (Figure 6-28). Overall, slightly less DNAN breakthrough was observed by the end of the second experiment compared to the first experiment from both C3 and C4. This is comparable to what was observed with NQ. Additionally, as with the first experiment, the only DNAN breakdown product detected was 2-ANAN (Figure 6-29). During the second experiment, the maximum 2-ANAN eluting from C3 was lower, while the maximum eluting from C4 was higher.

Upon starting and stopping each fructose addition to columns C3 and C4 during the latter phase of the experiment, the column effluent ORP values decreased and increased, respectively (Figure 6-30). These ORP trends were indicative of microbial activity increasing and decreasing in response to the added carbon, and meant that the microbial biomass in the columns was carbon limited.

The effluent concentrations of energetics also decreased and increased in the same general pattern as the ORP (Figure 6-31). This confirmed that the reason for less removal of these compounds by the columns over time was most likely due to limitations in labile carbon. All the energetics responded to the added carbon in terms of increase biodegradation. NQ degradation appeared to predominantly respond to fructose addition to the anoxic zone, and bioaugmentation with fresh NQ5 culture did not stimulate more NQ removal. This would indicate that long term removal of this compound is mainly the result of anoxic biodegradation, and that degradation by NQ5 under aerobic conditions may not be able to be sustained. Additionally, HMX biodegradation increased in response to fructose in column C3, but no response to fructose was seen in C4. Given that the effluent HMX concentrations in C4 also appeared to be above the influent concentrations, it is possible that the response in column C4 was masked by the analytical interferences.

Sorption-Biodegradation Column Performance

The total mass removed during both sorption-biodegradation column experiments was calculated for each energetic, as shown in Figure 6-32. The mass removal by combined sorption-biodegradation was calculated relative to the removal by sorption alone based on column C1 data (Figure 6-33). On an absolute basis, the biologically active columns removed more than the sorption-only column. On a relative basis, removal of energetics by combined sorption-biodegradation was ~2-fold higher for TNT, and around 20- to 25-fold higher for RDX, with the other energetics between these values. This clearly demonstrated the added benefit of biodegradation over just sorption. For NQ (in both experiments) and HMX (in the second experiment), there was also an indication that the inclusion of biochar increased mass removal.

The sorption capacity (q_0) for the target compounds calculated for the data from the sorption-only column (C1) of each experiment using the Thomas model are presented in Table 6-5, and the values derived from the sorption-only experiment are shown for reference. All the model fits had r^2 values greater than 0.90, except for NQ ($r^2 = 0.83$), and the relative error of the estimates averaged $1.8 \pm 0.8\%$ of the calculated value. The q_0 values for peat and CAT pine were all higher during the sorption-biodegradation experiments, which was attributed to the higher influent concentrations used during these latter experiments compared to the sorption-only experiment (Samarghandi et al., 2014; Kulkarni et al., 2018). The q_0 values for each energetic in the first versus the second sorption-biodegradation experiment varied from around 5% for TNT and ClO₄ to 25 to 45% for HMX, RDX, NTO, DNAN, and NQ. As these values were calculated based on the sorption-only column data which was not bioaugmented nor contained slow-release carbon sources biopolymers, and the experiments were run under identical operational parameters, so the variation must reflect inherent variation of the peat and CAT pine materials.

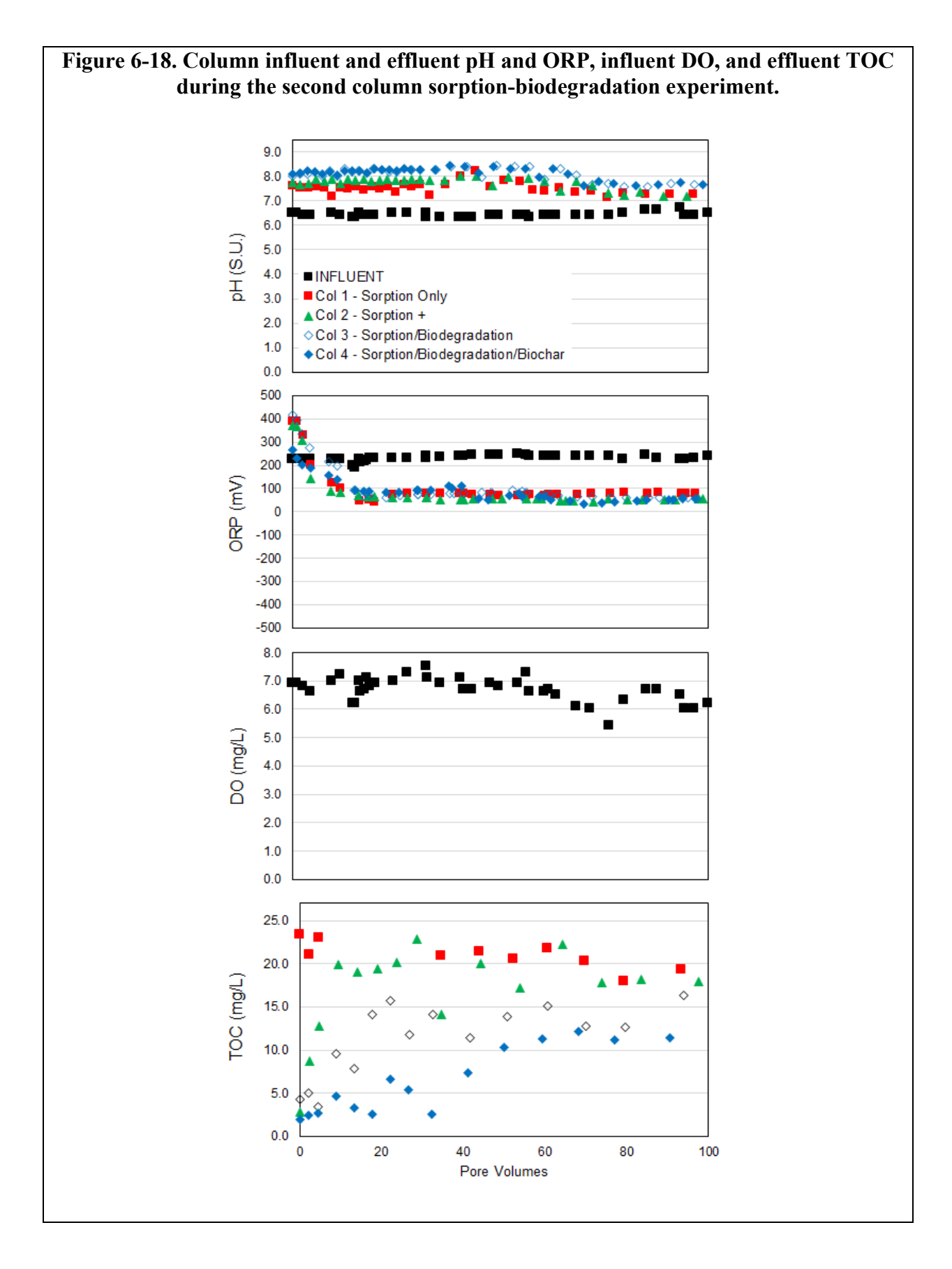
Combining these revised Thomas model sorption capacities, an estimate of the size of biofilter system needed to treat NSWC Dahlgren surface runoff was generated (Table 6-6). This estimate is approximately 40% of the preliminary estimate (e.g., 200 vs. 500 cu ft). This assumes that higher concentrations of energetics are in the runoff, which is possible, but not probable, based on the results of actual surface runoff characterization in Section 2.

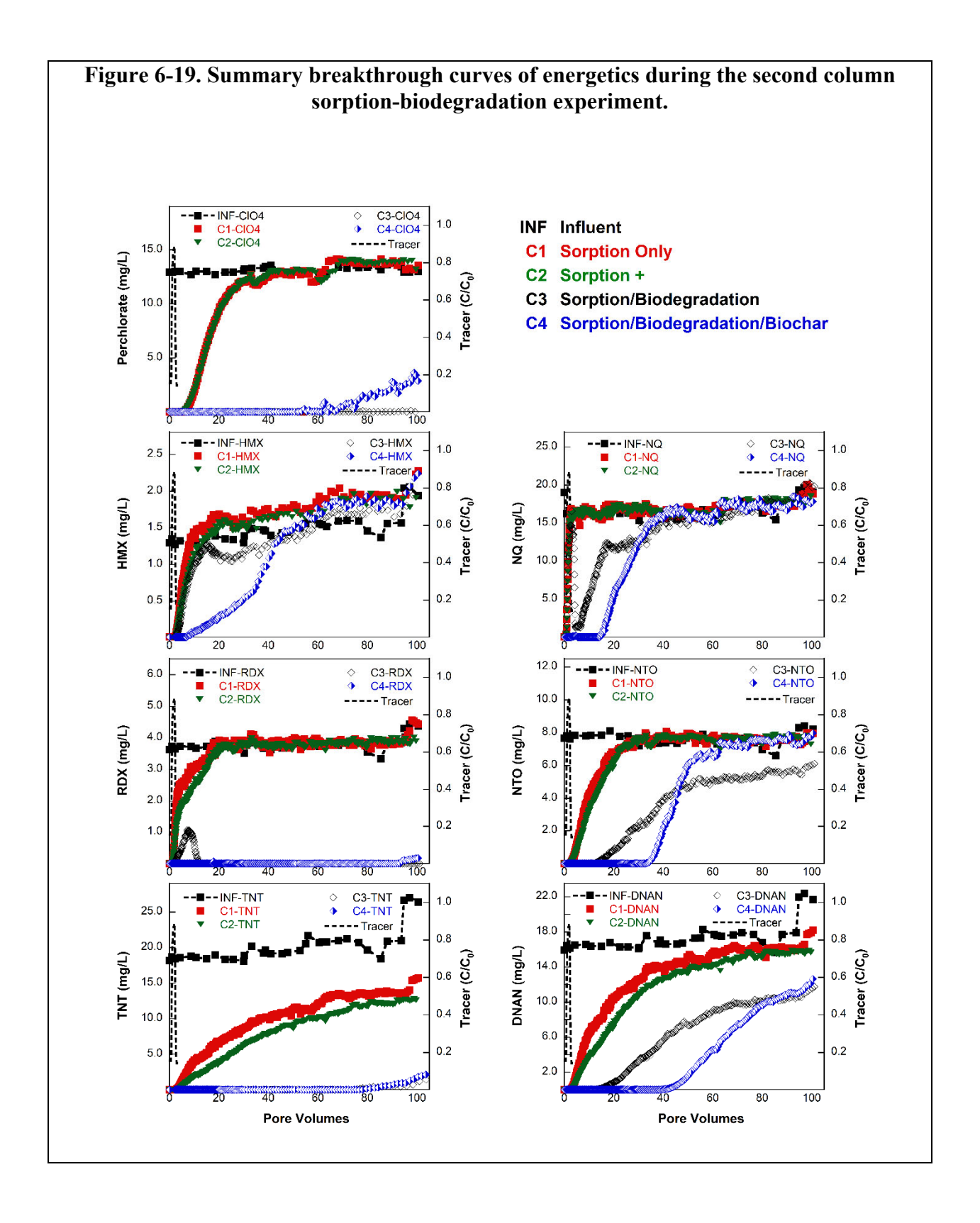
Table 6-5. Comparison of sorption capacities (q_{θ}) for energetics from the sorption-only experiment versus the sorption-only column (C1) during the sorption-biodegradation experiments.

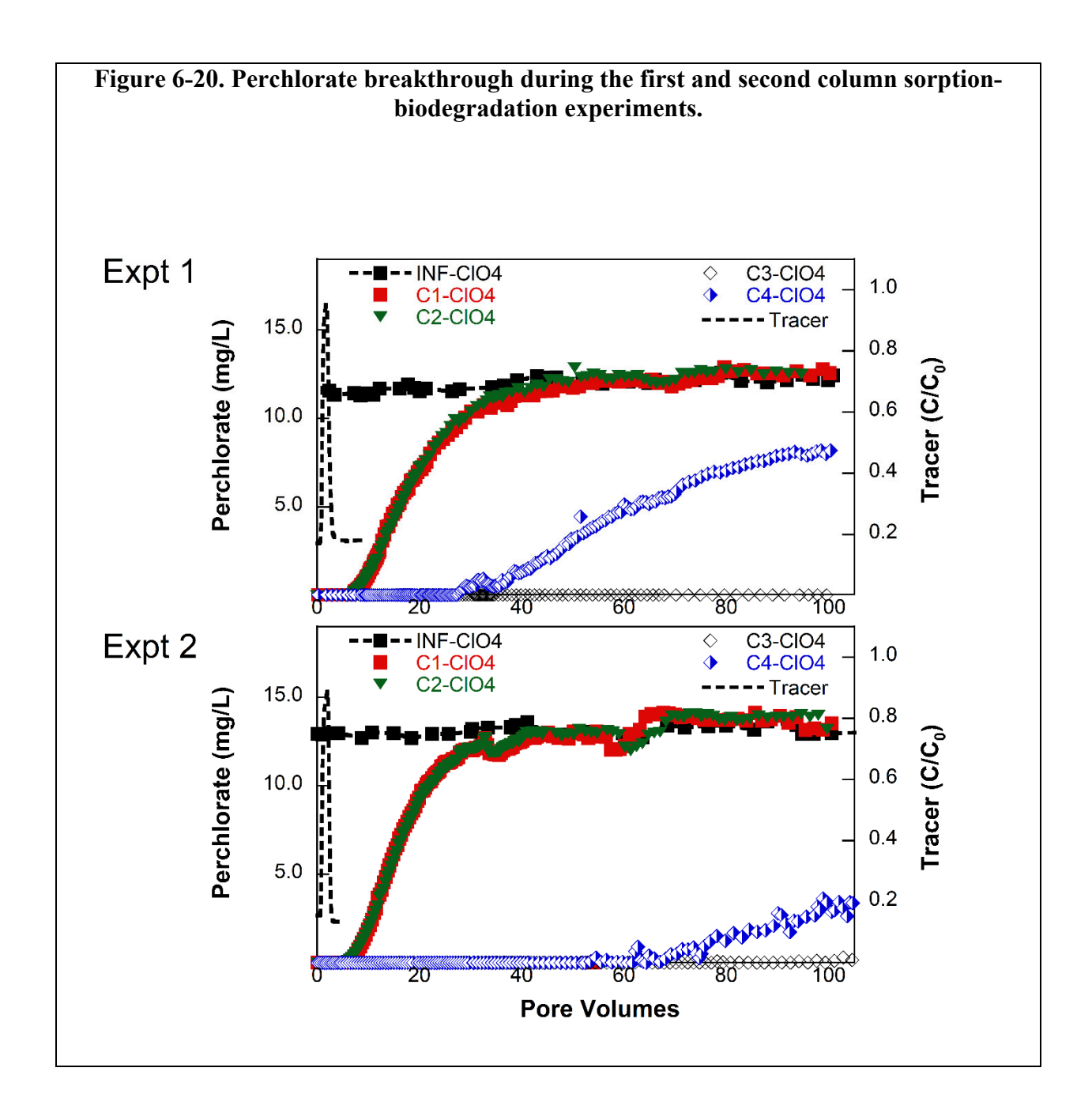
		$q_0 \text{ (mg/g)}$	Peat)1					
Experiment	Column	HMX	RDX	TNT	NQ	NTO	DNAN	CIO4
Sorption Only	Peat+Pine	0.05	0.03	0.40	0.02	-	0.45	-
	Peat+CAT Pine (mixed)	0.06	0.03	0.36	0.02	-	0.41	-
	Peat+CAT Pine (layered)	0.06	0.03	0.36	0.02		0.45	-
Sorption-Biodegradation 1	Sorption Only (C1)	0.13	0.23	5.16	0.25		1.92	-
Sorption-Biodegradation 2	Sorption Only (C1)	0.17	0.18	5.45	0.14		2.75	-
		q ₀ (mg/g	CAT Pi	ne) ¹				
						NTO		CIO
Sorption Only	Peat+CAT Pine (mixed)	-	-	-	-	0.20	-	0.10
	Peat+CAT Pine (layered)	-	-	-	-	0.37	-	0.23
Sorption-Biodegradation 1	Sorption Only	-				1.95	-	3.42
Sorption-Biodegradation 2	Sorption Only		-	-	-	1.44	-	3.67

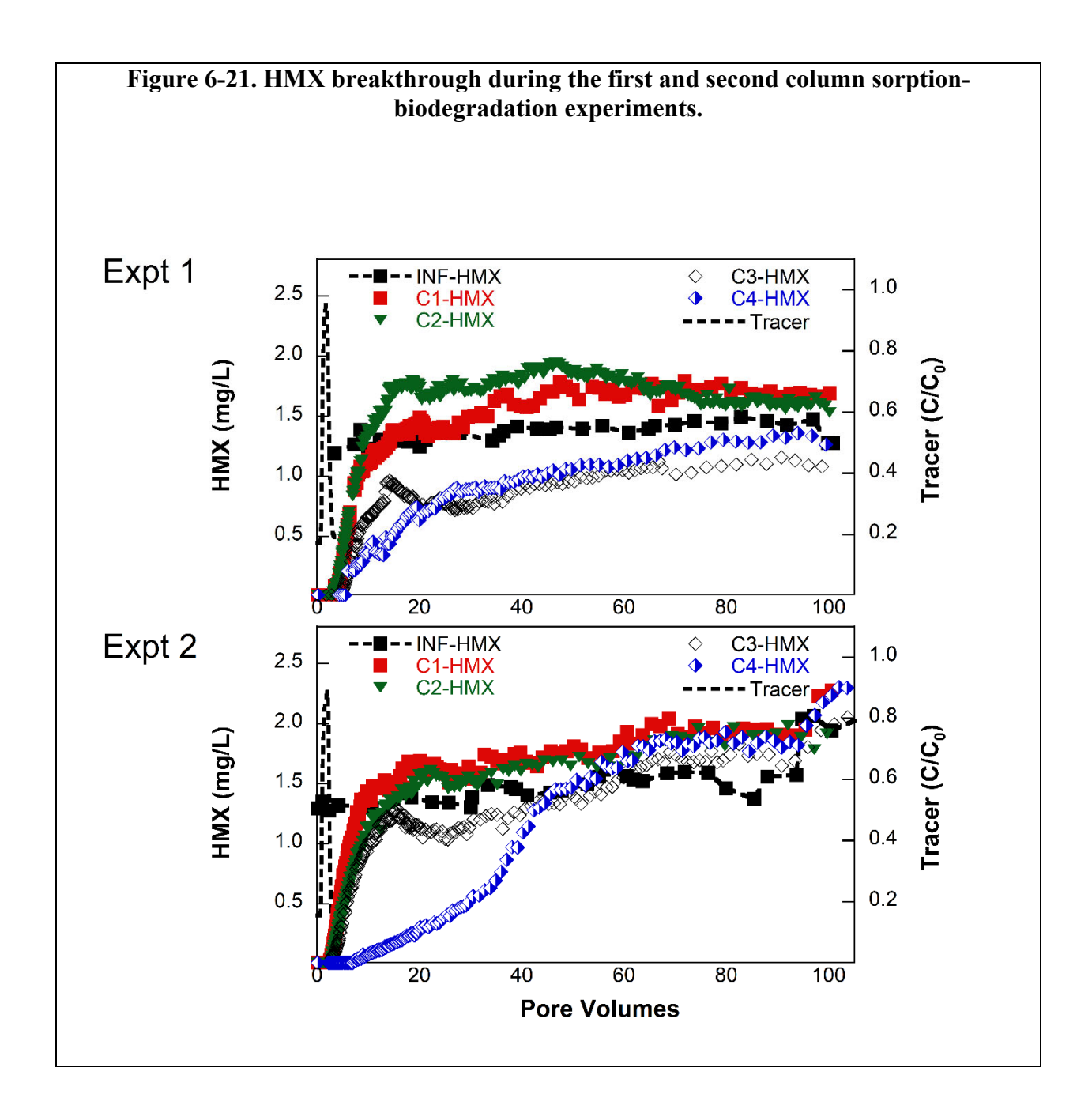
Table 6-6. Revised mass and volume sizing for a passive biofilter to treat NSWC Dahlgren surface runoff based on sorption-only derived from maximum sorption capacity from sorption-only column (C1) during sorption-biodegradation experiments.

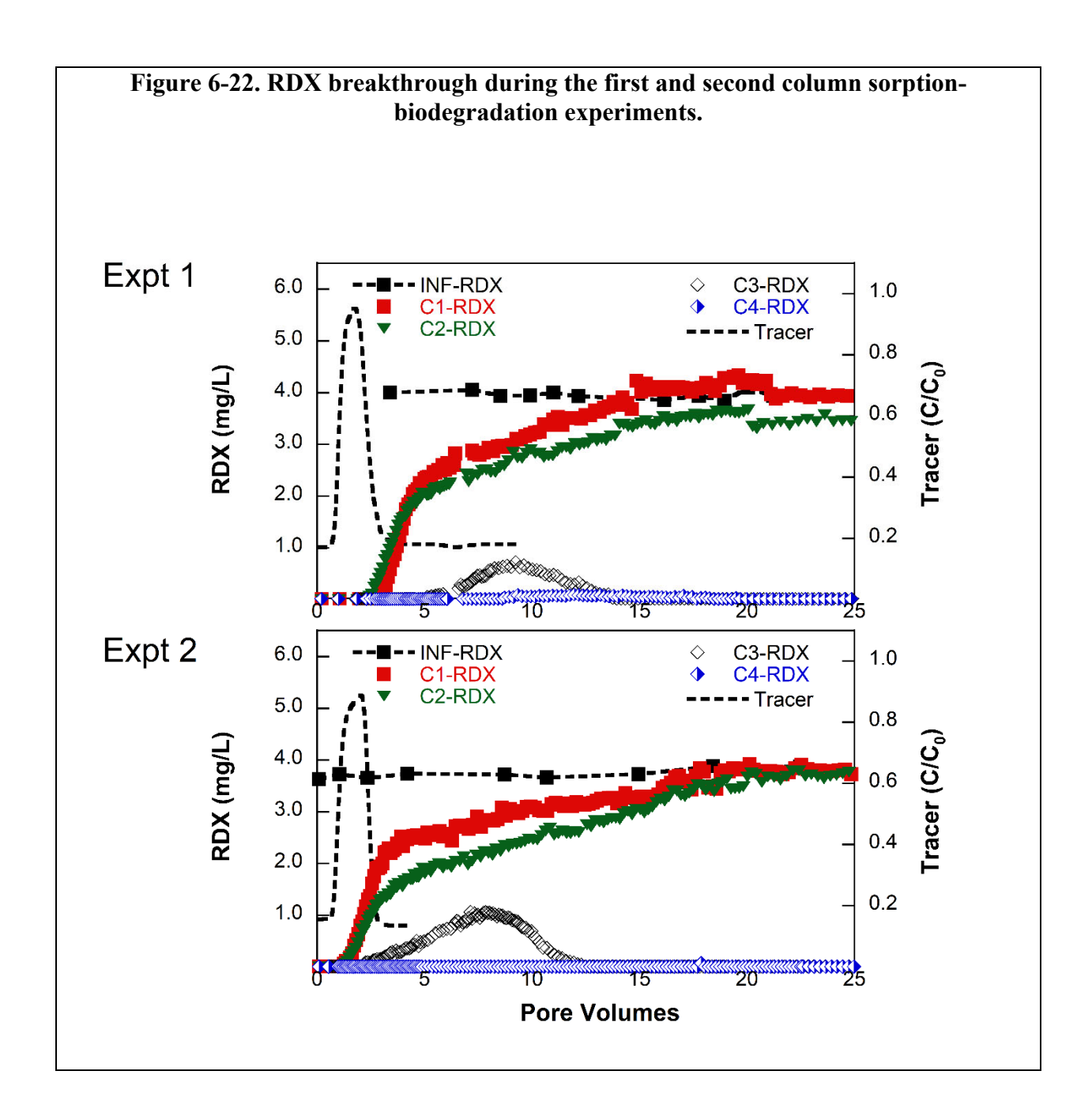
	Maximum	sorption ca	pacity (q ₀ .	mg/kg)			
	HMX	RDX	TNT	NQ	NTO	DNAN	CIO4
Peat	172	227	5451	252		2752	0.0.
CAT Pine			0.0.		1946	2.02	3668
Estimated mass in runoff based on NSWC Dahlgren samples per event (mg)	837	429					289
Assumed same order of magnitude for undetected explosives (mg)			500	500	500	500	
Safety Factor	100	100	100	100	100	100	100
Mass of explosives in runoff needing removal per event (mg)	× 4/1101	42900	50000	50000	50000	50000	28900
	Minimum r	mass of me	dia require	d (kg)			
	HMX	RDX	TNT	NQ	NTO	DNAN	CIO4
Peat	487	189	9	199		18	
CAT Pine					26		8
Max mass required (kg)	487						
Max mass excluding NQ (kg)							
Peat dry bulk density (kg/m3)	100	100	100	100	100	100	100
Biobarrier volume (m3)		2	0	2	0	0	0
Max volume required (m3)	5						
Max volume excluding NQ (m3)	5						
Biobarrier volume (cu ft)	172						
Biobarrier volume excluding NQ (cu ft)	172						

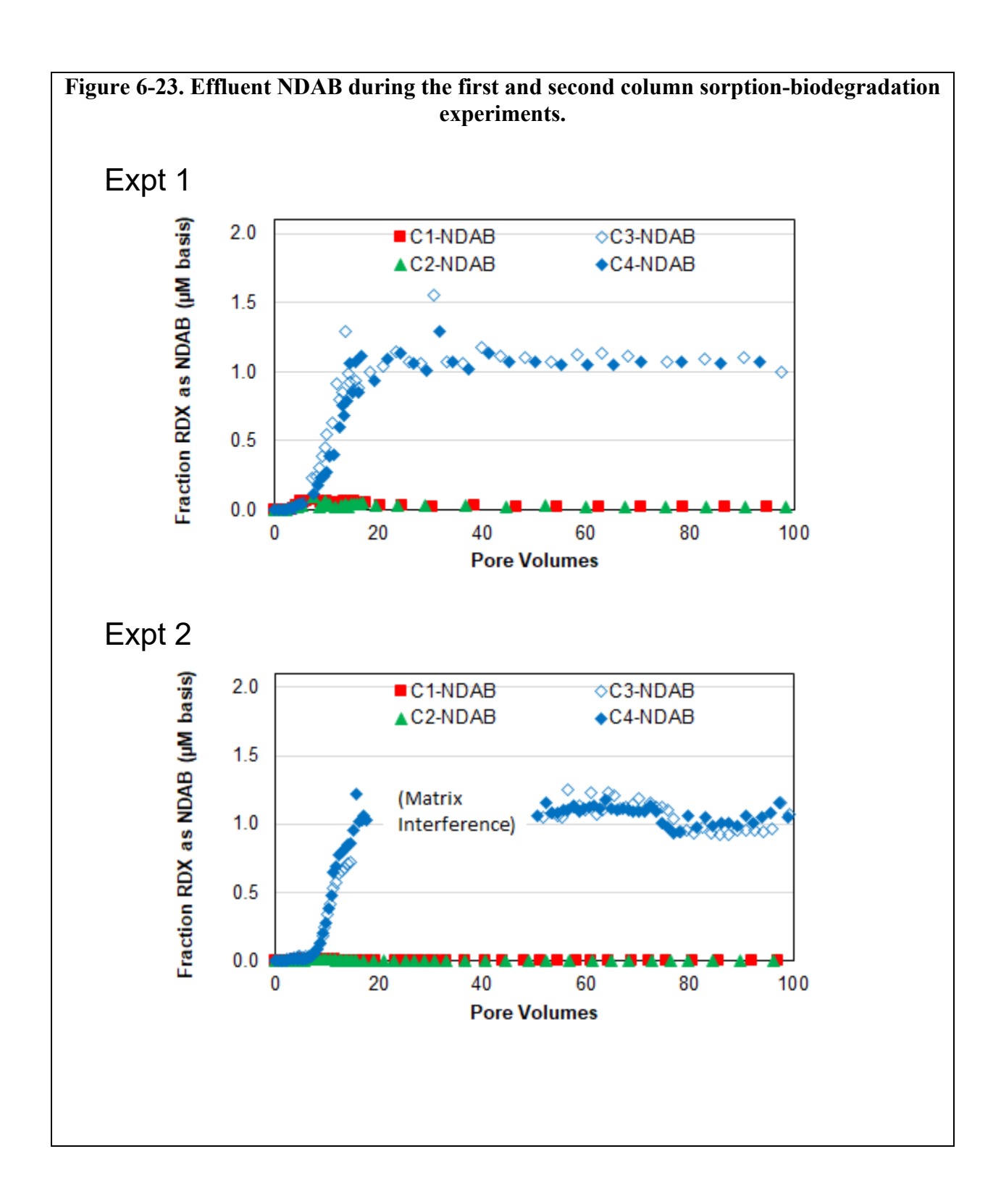


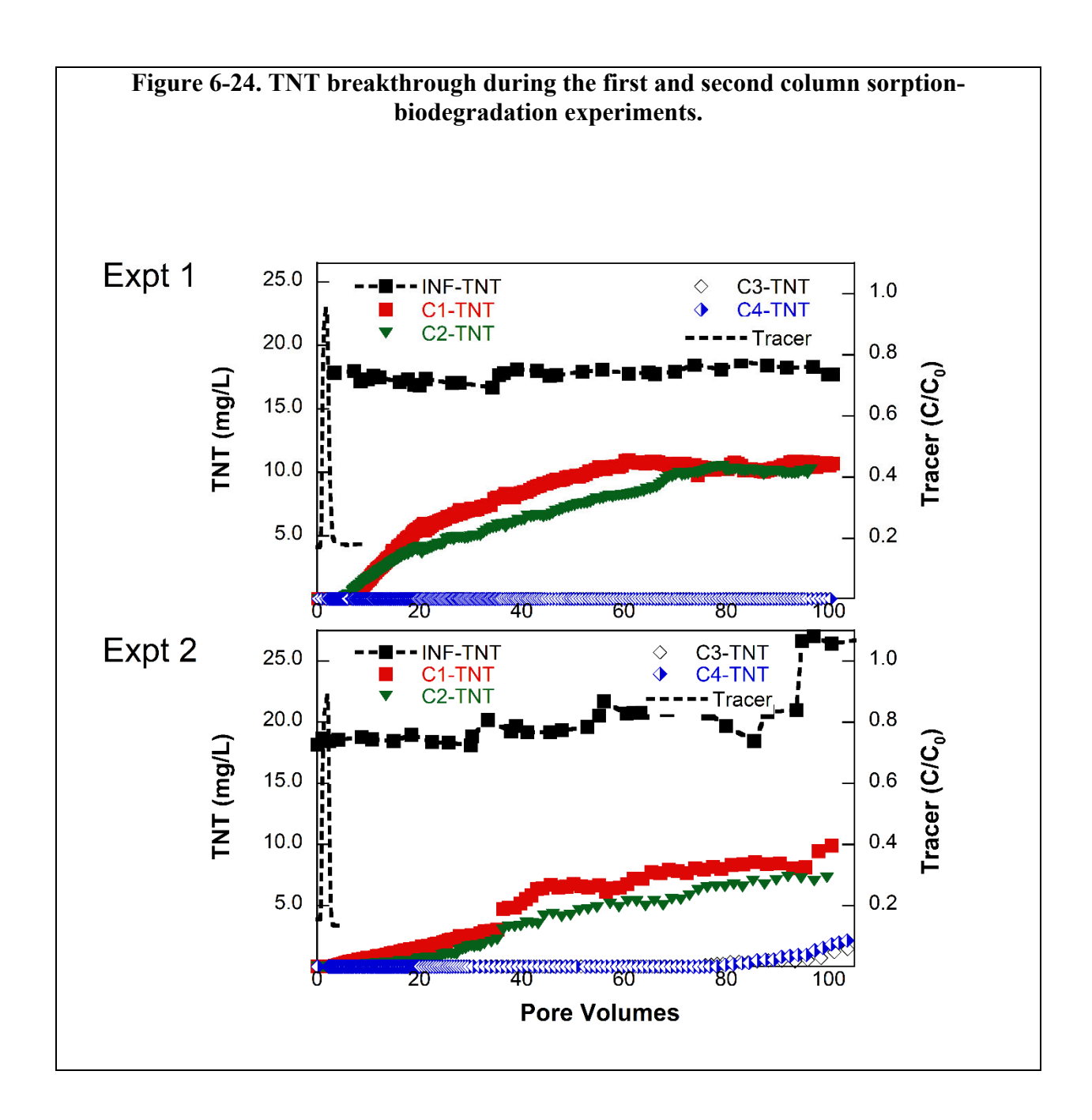


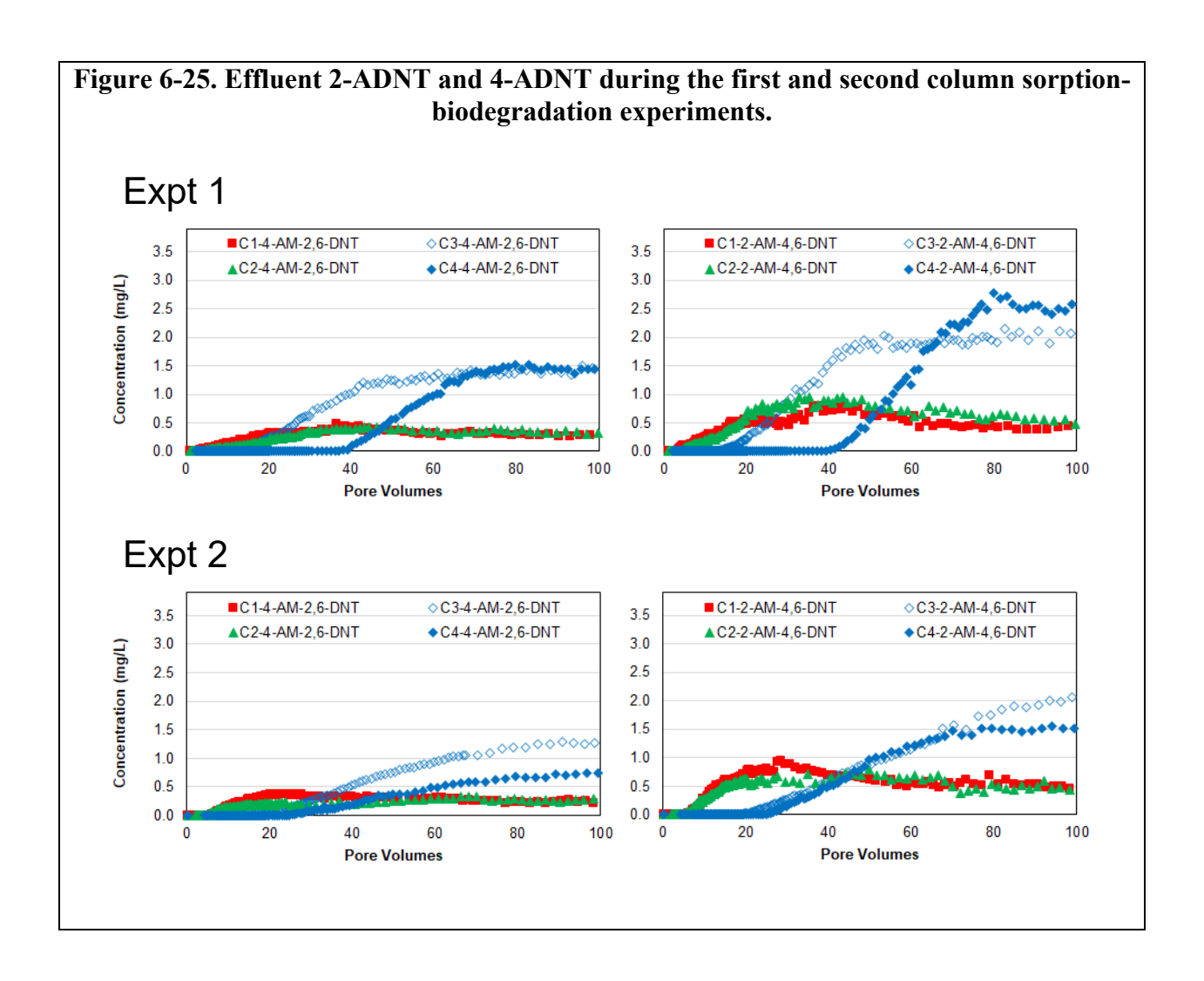


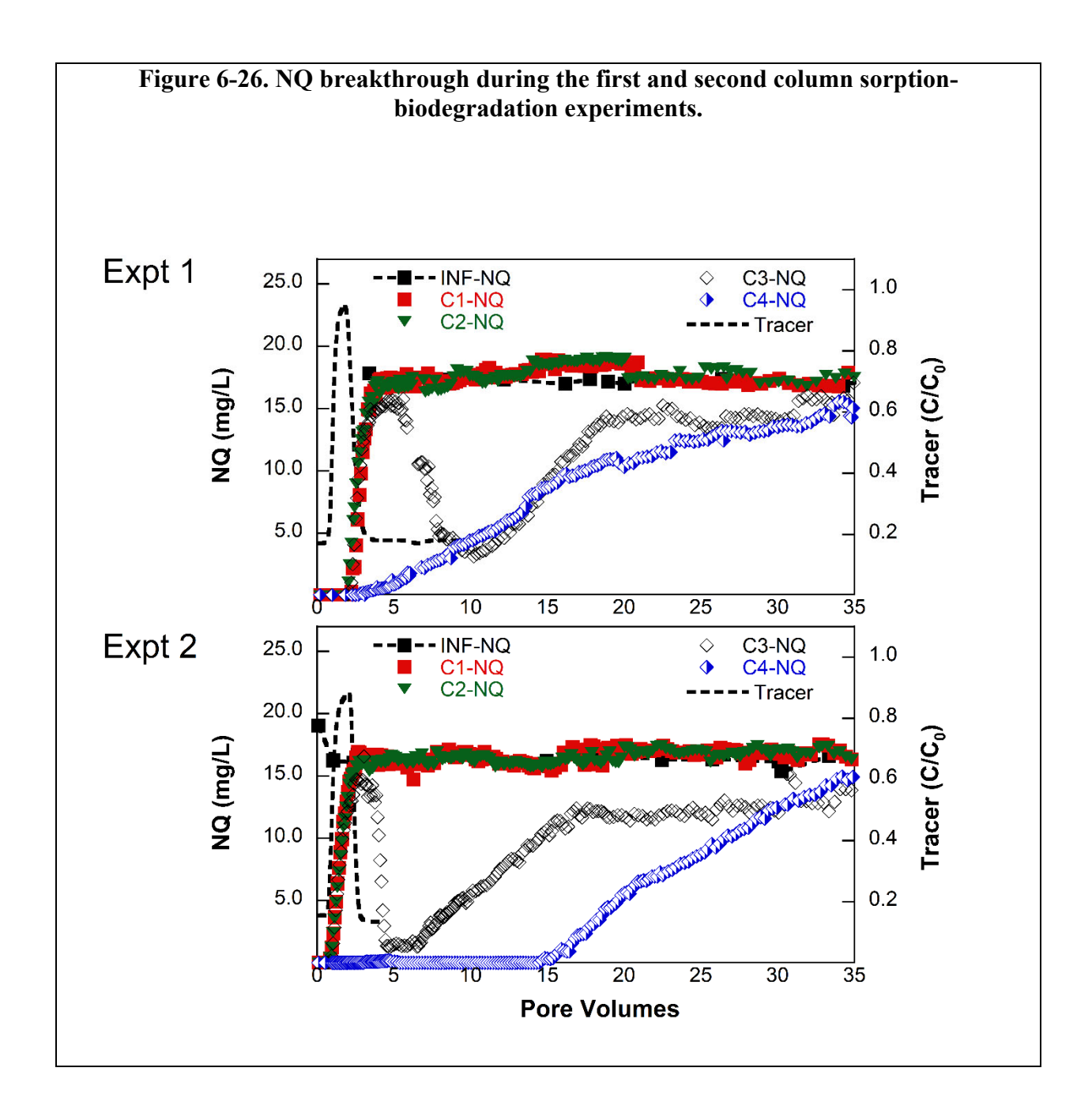


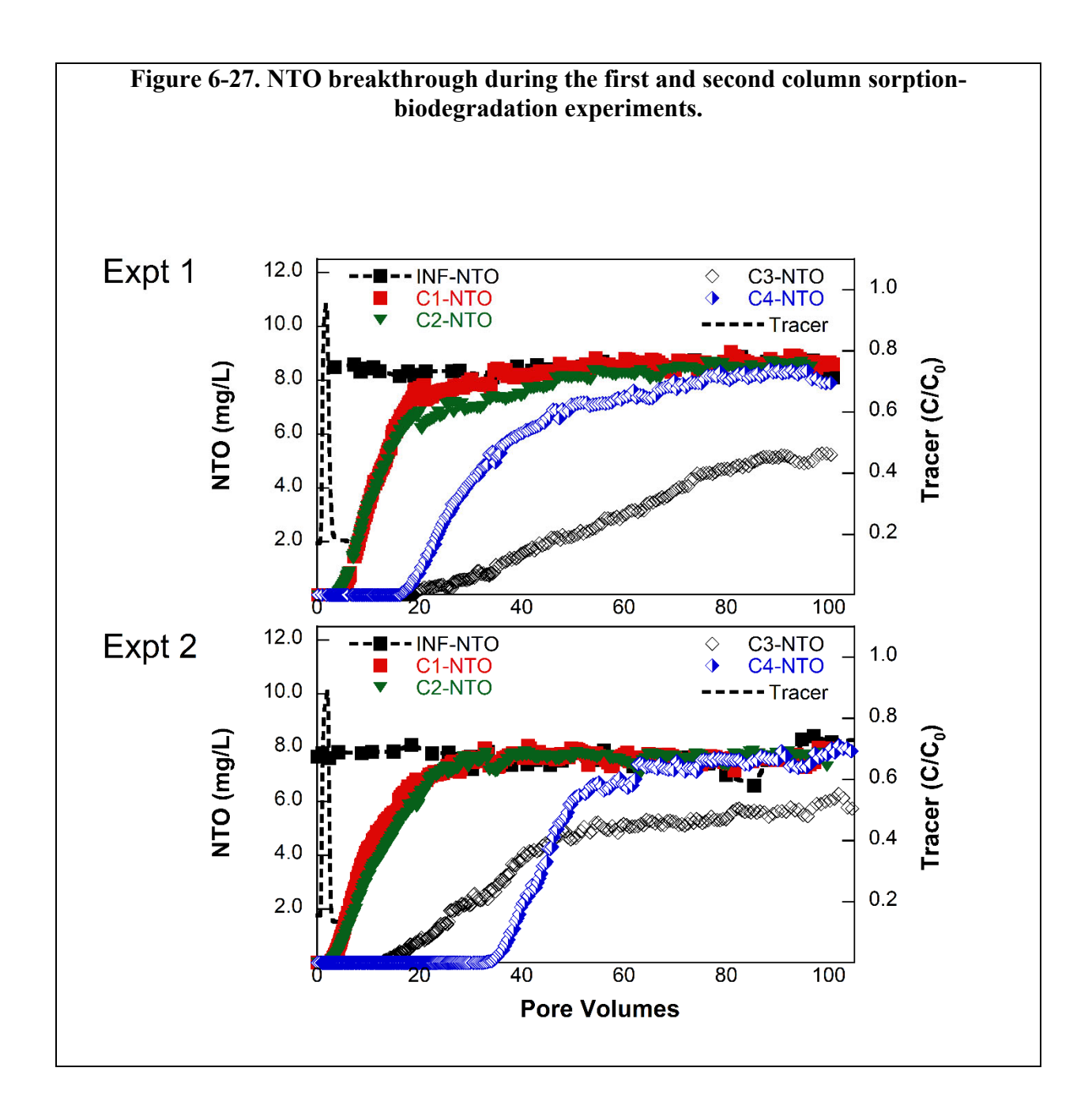


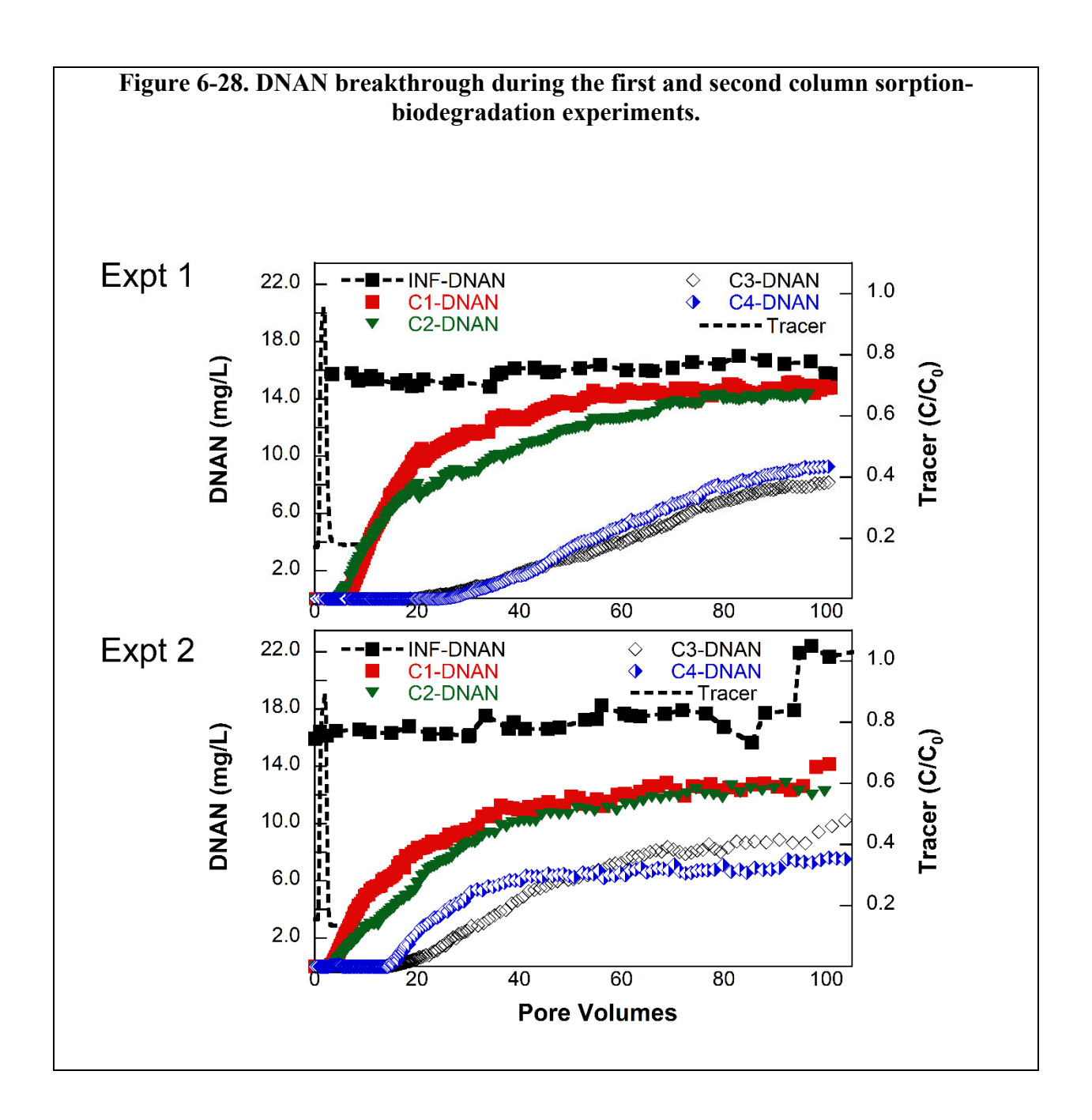


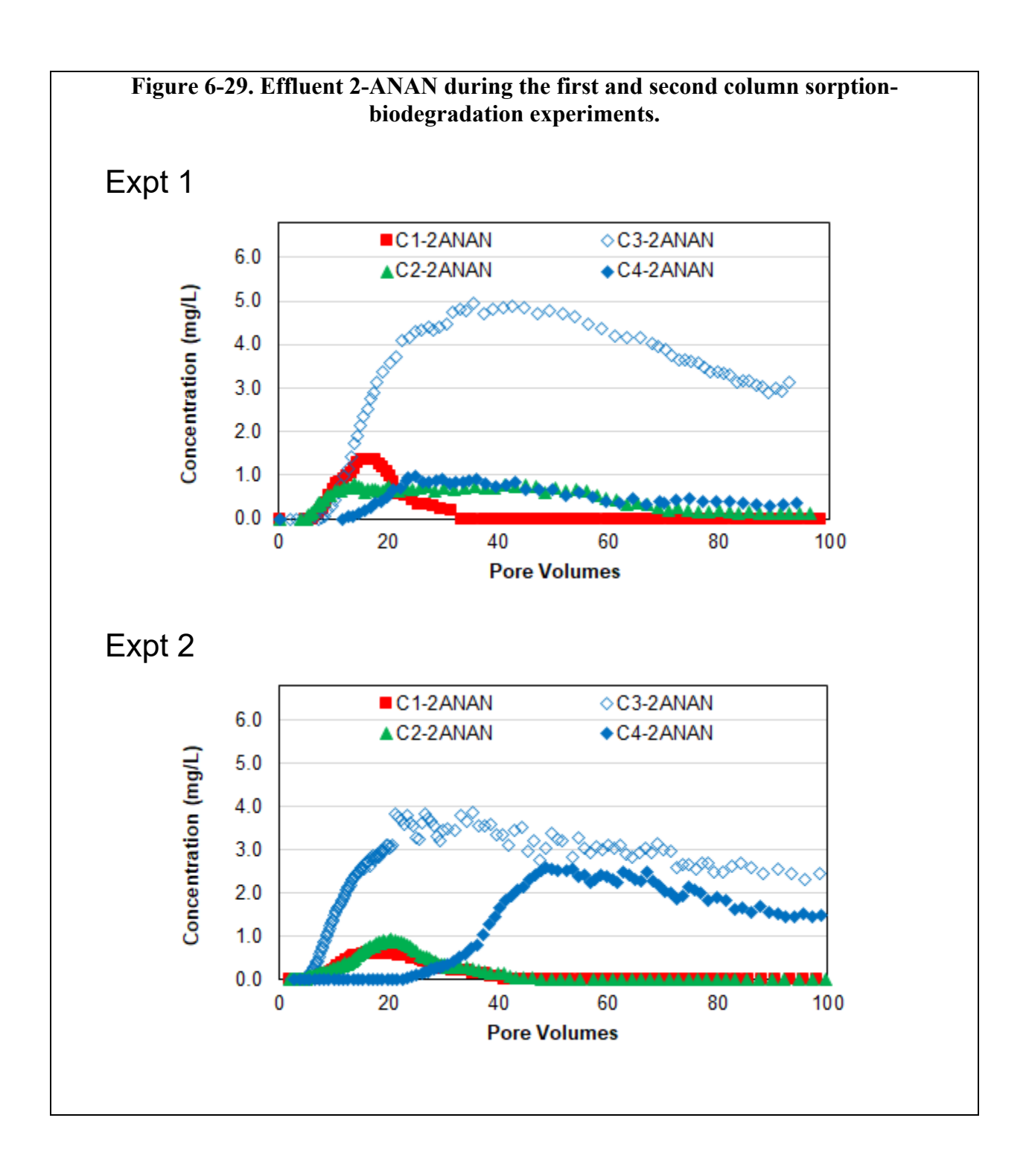












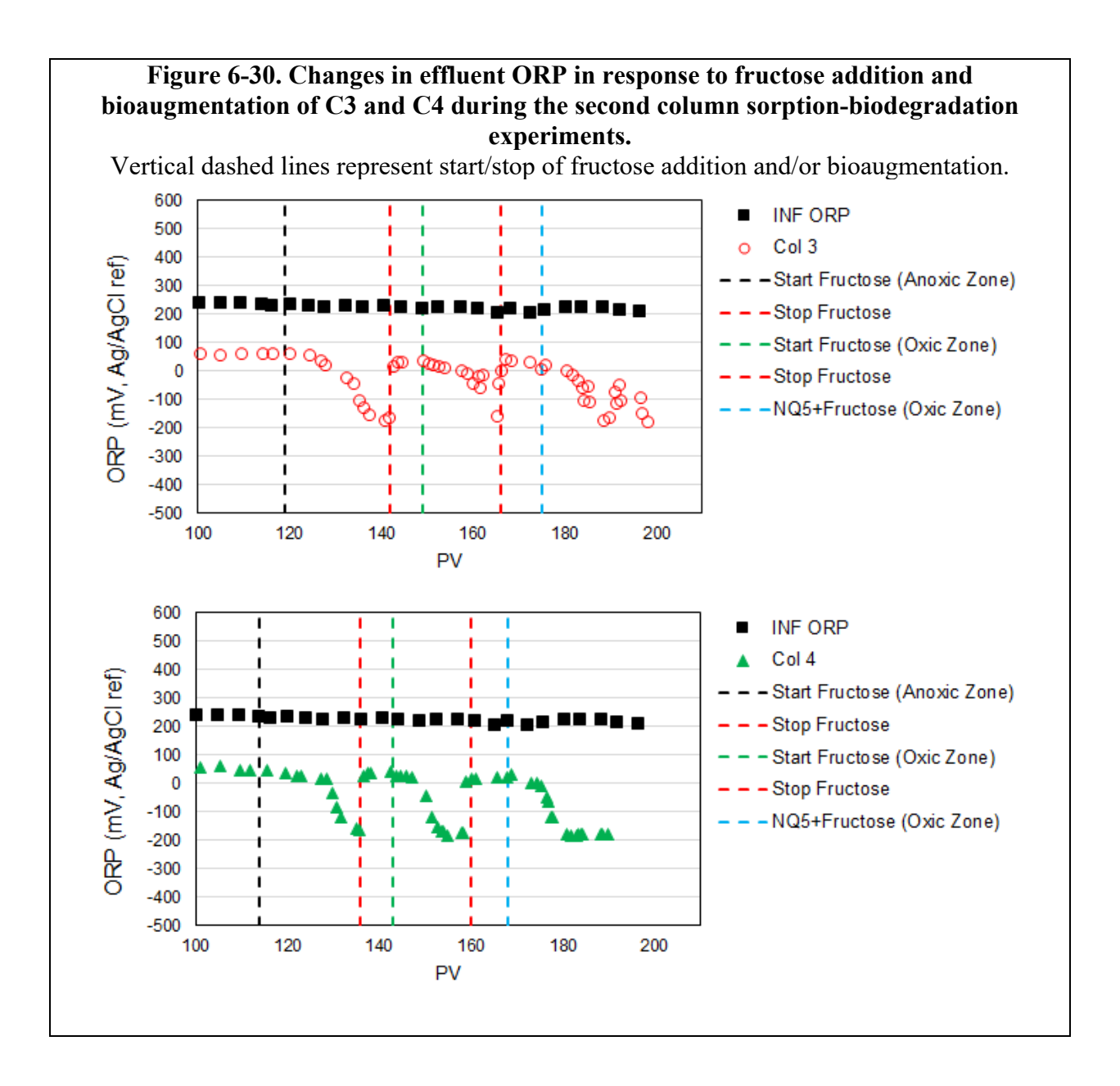
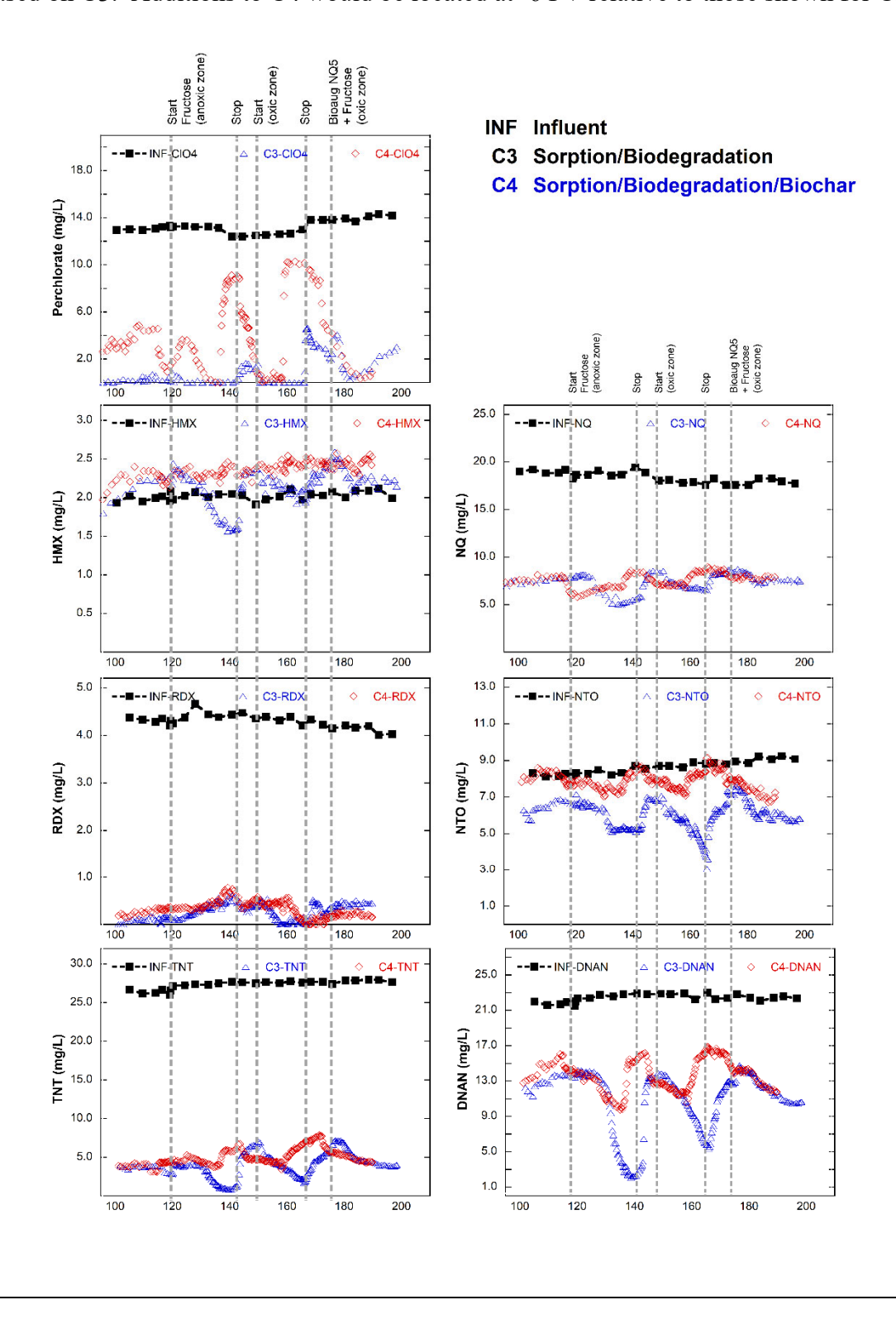
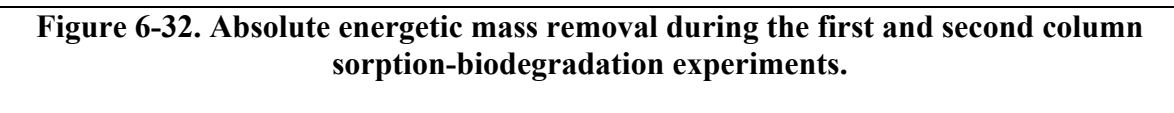
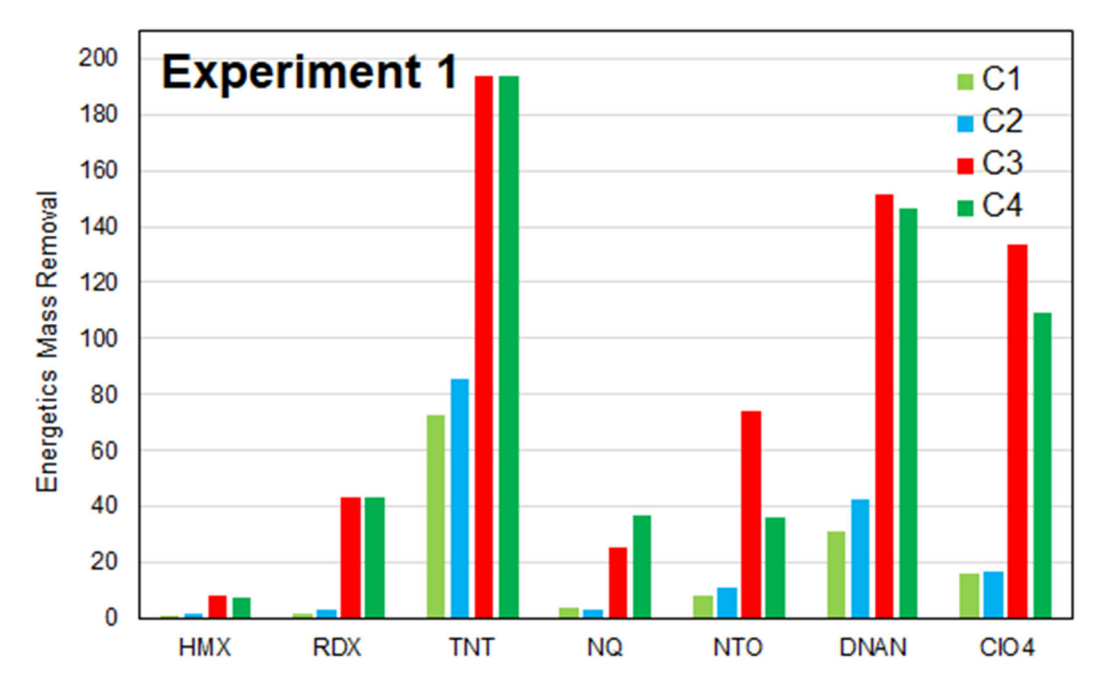


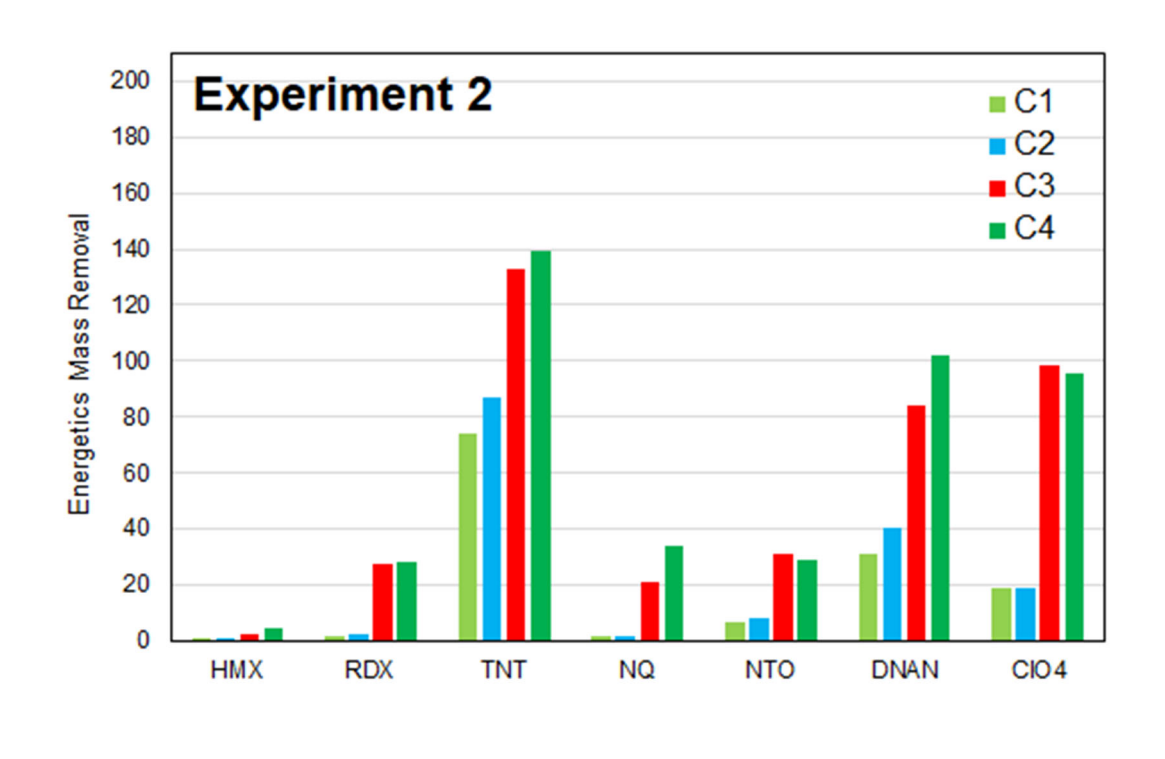
Figure 6-31. Effluent energetics concentrations in response to fructose addition and bioaugmentation during the second column sorption-biodegradation experiment.

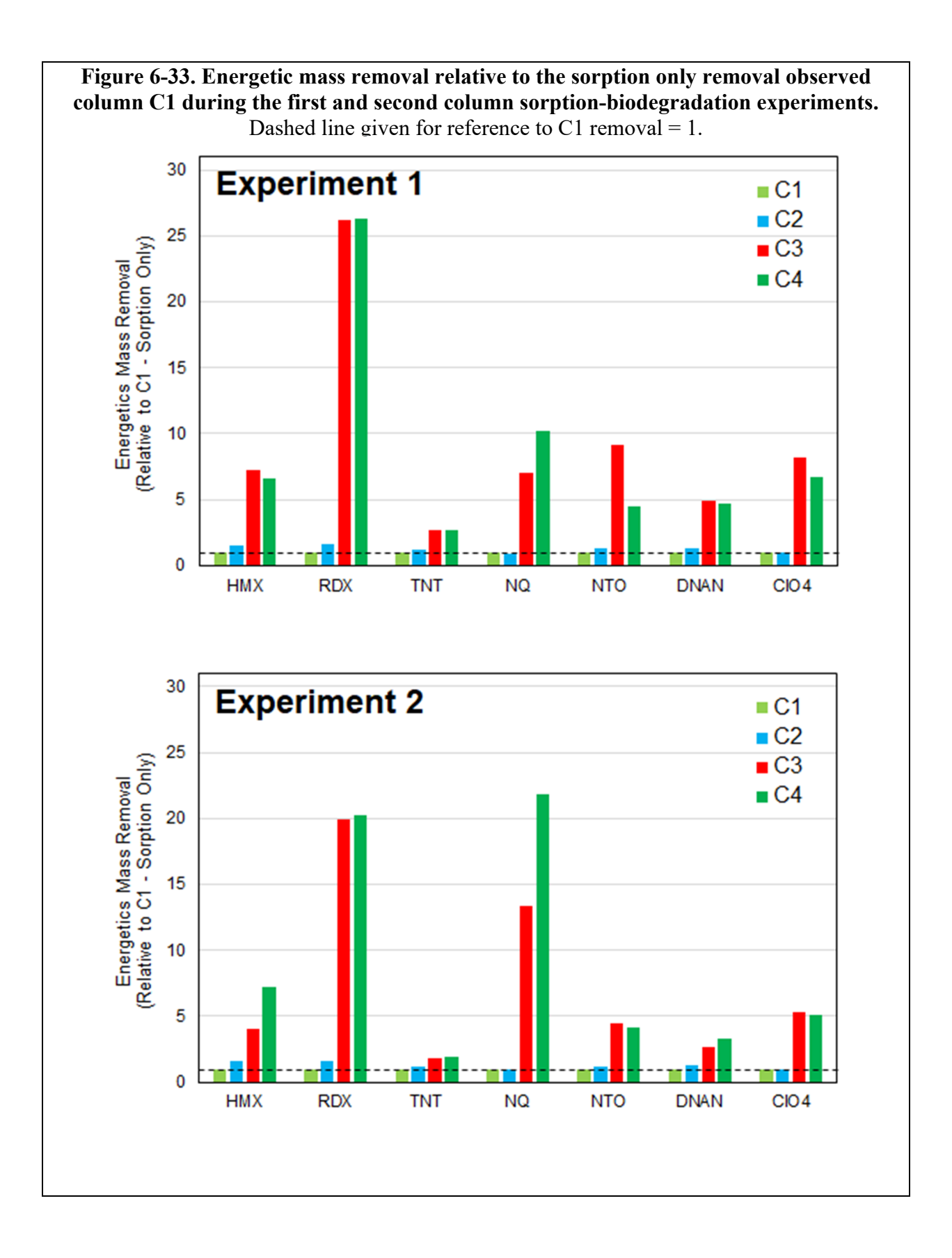
Vertical dashed lines represent start/stop PV of fructose addition and/or bioaugmentation based on C3. Additions to C4 would be located at -6 PV relative to those shown for C3.











6.3 CONCLUSIONS

Overall, both column experiments demonstrated the added benefit of inoculation with explosives degrading cultures, as well as slow-release biopolymer carbon sources, over just pure sorption approaches. As discussed above, the total energetics mass removed was 2- to over 20-fold higher (in the bioaugmented columns compared to sorption alone.

The added benefit of biochar was mixed. Biochar appeared to act as sorption "buffer" for RDX, preventing RDX breakthrough until RDX biodegradation had been established. Biochar also had a similar effect on HMX and NQ breakthrough, delaying the breakthrough compared to the column without biochar. No effects of biochar on TNT breakthrough were observed, and effects on DNAN breakthrough were not seen during the first experiment, and were minimal during the second experiment (e.g., slight reduction in time of first breakthrough, but lower effluent concentrations as latter times). Interestingly, as ClO₄- would not be expected to interact with biochar, its breakthrough timing was reduced, but its final effluent concentrations were significantly higher in the column with biochar compared to the column without biochar.

REFERENCES

- Aminul Islam, M., 2022. Nonlinear Thomas column adsorption model fitting in origin. Aminulchem

 [https://www.youtube.com/watch?v=6sDm94pMyKE&list=PLxbTf96DhNSRtUvA0lZC 706OK0WwfpCku&index=19).
- Chowdhury, Z.Z., Hamid, S.B.A., Zain, S.M., 2015. Evaluating design parameters for breakthrough curve analysis and kinetics of fixed bed columns for Cu(II) cations using lignocellulosic wastes. BioResources 10, 732-749.
- Fuller, M.E., Farquharson, E.M., Hedman, P.C., Chiu, P., 2022. Removal of munition constituents in stormwater runoff: Screening of native and cationized cellulosic sorbents for removal of insensitive munition constituents NTO, DNAN, and NQ, and legacy munition constituents HMX, RDX, TNT, and perchlorate. J Hazard Mater 424, 127335.https://doi.org/10.1016/j.jhazmat.2021.127335.
- Fuller, M.E., Hedman, P.C., Chu, K.-H., Webster, T.S., Hatzinger, P.B., 2023. Evaluation of a sequential anaerobic-aerobic membrane bioreactor system for treatment of traditional and insensitive munitions constituents. Chemosphere 340, 139887. https://doi.org/10.1016/j.chemosphere.2023.139887.
- Hareland, W.A., Crawford, R.L., Chapman, P.J., Dagley, S., 1975. Metabolic function and properties of 4-hydroxyphenylacetic acid 1-hydroxylase from *Pseudomonas acidovorans*. J Bacteriol 121, 272-285.
- Kato, T., Gathuka, L.W., Okada, T., Takai, A., Katsumi, T., Imoto, Y., Morimoto, K., Nishikata, M., Yasutaka, T., 2021. Sorption-desorption column tests to evaluate the attenuation layer using soil amended with a stabilising agent. Soils and Foundations 61, 1112-1122.https://doi.org/10.1016/j.sandf.2021.05.004.
- Kulkarni, S.J., Mishra, A., Patil, S., Uphale, K., 2018. Modeling of breakthrough curves for removal of chromium from waste water. International Journal of Advanced Research in Chemical Science 5, 29-40.
- Samarghandi, M.R., Hadi, M., McKay, G., 2014. Breakthrough curve analysis for fixed-bed adsorption of azo dyes using novel pine cone—derived active carbon. Adsorption Science & Technology 32, 791-806.10.1260/0263-6174.32.10.791.

van Genuchten, M.T., Parker, J.C., 1984. Boundary conditions for displacement experiments through short laboratory soil columns. Soil Science Society of America Journal 48, 703-708. https://doi.org/10.2136/sssaj1984.03615995004800040002x.

7. Conclusions and Recommendations

The key findings of this project were as follows:

- Low and sporadic detectable concentrations of energetic compounds were detected in surface runoff from an active range. No heavy metals were detected above drinking water standards. No potential non-energetic munition constituents (plasticizers, waxes, binders) were detected in surface runoff samples.
- A new methods to remove perchlorate and NTO from contaminated water using cationized cellulose materials was developed and evaluated, with cationized pine shavings demonstrating the best removal.
- Multiple biodegradable plastic polymers were identified and demonstrated to be able to serve as slow-release carbon sources which support energetic compound biodegradation.
- Biochar was shown to remove energetic compounds by sorption (DNAN, RDX, NQ), chemical reduction (NTO, DNAN, RDX), or microbial reduction (perchlorate), and its reductive capacity can be regenerated in situ. Due to the multiple mechanisms involved, for best performance, biochar should be incorporated based on the target pollutant(s) and soil redox conditions.
- Column experiments demonstrated that the combination of sorption and biodegradation resulted in robust removal and transformation of dissolved energetics.

The results of this project lay the foundation for a passive, sustainable surface runoff treatment technology, and should be demonstrated at the pilot scale at an appropriate field site, specifically:

- The "trap" component of the technology utilizing peat moss and cationized pine shavings would be relatively robust for all the target energetics except NQ. The relative placement of the sorbent media, as well as the mass of media, may need some additional testing to optimize sorptive removal of the energetics based on characterization of the energetics in the runoff at a given site.
- The "treat" component of the technology using a mixed inoculum, combined with the natural inoculation of the treatment media via exposure to the surface runoff, is expected to be effective for all of the energetics, especially for RDX, TNT, DNAN, and perchlorate. The biological removal of HMX, NTO, and NQ was demonstrated to be affected by the presence of labile carbon at longer timeframes of column operation. This is expected to be mitigated by the addition of more of the biodegradable biopolymer carbon sources in the system.
- The development and production of the custom inoculants would not be a major hindrance to the use of the technology. Companies such as Aptim have the experience and industrial infrastructure to address this issue. We also have archived the anaerobic and aerobic MBR biomass which was used as the main mixed inoculum for the column studies, and the other pure cultures are also archived. These can be used as a starting point for fresh inoculum for further development and optimization of the technology, e.g., at pilot or field scale.

• The mix of energetics in the runoff at a given site may require some fine tuning of the sorbent mix or inocula to achieve the most efficient treatment.

Based on the results obtained during the project, the following recommendations would be offered for follow-on efforts:

- A more comprehensive survey of energetics in stormwater runoff at testing and training ranges should be done at several different sites. The data from this project indicate that low concentrations of energetics in stormwater runoff can be present, and given the volume of runoff, the total mass releases may be of concern. It would also be advisable to include some modeling efforts to attempt to identify the main factors controlling the presence of energetics.
- Related to the first point, it would be recommended to perform additional studies on the fate of the energetics in runoff once the water has entered the receiving body.
- The technology developed during this project should undergo evaluation at the field-scale at a site with documented sustained concentrations of energetics in stormwater runoff. This should also include evaluation of the scale-up of the cationization process for production of the CAT pine sorbent material using existing textile industry infrastructure.
- NQ proved to be the most recalcitrant energetic, exhibiting the least removal over the duration of the column experiments compared to the other energetics. More efforts focused on effective sorbents for this compound, or on identifying more robust biodegradative cultures, is warranted. These efforts would not only benefit the technology developed during this project, but also the overall NQ remediation area. In parallel, some effort should be directed at understanding the potential extent of NQ contamination at DoD sites, so that the relative risk and focus on NQ remediation can be correctly assessed.

APPENDIX A: Supporting Data:

All relevant data included in the main text.

APPENDIX B: List of Scientific/Technical Publications

- Fuller, M.E., Farquharson, E.M., Hedman, P.C., Chiu, P., 2022. Removal of munition constituents in stormwater runoff: Screening of native and cationized cellulosic sorbents for removal of insensitive munition constituents NTO, DNAN, and NQ, and legacy munition constituents HMX, RDX, TNT, and perchlorate. J Hazard Mater 424, 127335. https://doi.org/https://doi.org/10.1016/j.jhazmat.2021.127335.
- Xin, D., Giron, J., Fuller, M.E., Chiu, P.C., 2022. Abiotic reduction of 3-nitro-1,2,4-triazol-5-one (NTO), DNAN, and RDX by wood-derived biochars through their rechargeable electron storage capacity. Environmental Science: Processes & Impacts 24, 316-329. https://doi.org/https://doi.org/10.1039/D1EM00447F.
- Fuller, M.E., Thakur, N., Hedman, P.C., Chiu, P., 2024. Combined sorption-biodegradation for removal of energetic compounds in stormwater runoff. J Hazard Mater (in preparation).
- Li, W., Giron, J., Fuller, M.E., Chiu, P.C., 2024. Microbially-reduced biochar as an electron donor for nitrate and perchlorate bio-reduction. Environ Sci Tech (in preparation).

APPENDIX C: SPE Protocols

SPE PROTOCOL FOR EPA 8330 EXPLOSIVES AND DNAN

Revised 01/23/20

PREPARE MATERIALS:

You will need clean, small glass tubes to collect the SPE eluent able to hold 12 ml of solvent (usually 16 mm x 100 mm). These can be prepared by either baking the tubes at 550°C overnight or rinsing well with LC/MS GRADE ACETONITRILE. The baking method is preferred as many tubes can be prepared at once.

After the tubes are cleaned, you may also want to mark the outside of each tube to approximately indicate the 1 ml mark, which will allow the drying of the SPE extract to be more easily monitored

Prepare the 3-NT recovery standard @ 20 mg/L in LC/MS GRADE ACETONITRILE.

CONDITION THE SPE TUBES:

This can be done ahead of the SPE procedure or the day of the procedure.

Open enough SPE tubes (Sigma; Supercleantm Chrom P SPE Tubes (6 ml, 250 mg, #57225-U, https://www.sigmaaldrich.com/catalog/product/supelco/57225u?lang=en®ion=US) for the samples. They come three to a pouch so you may have some left in the last pouch, if so, tape the opening closed to try to keep the tubes fresh. Label the SPE tubes.

Remove the tube rack from inside the SPE Unit and place new Teflon liners in the screw valves. Place the SPE tubes on the unit and close the screw valves.

Place a glass microfiber filter inside the SPE tube on top of upper frit. The filter must be extracted with the SPE tube to elute anything bound to it.

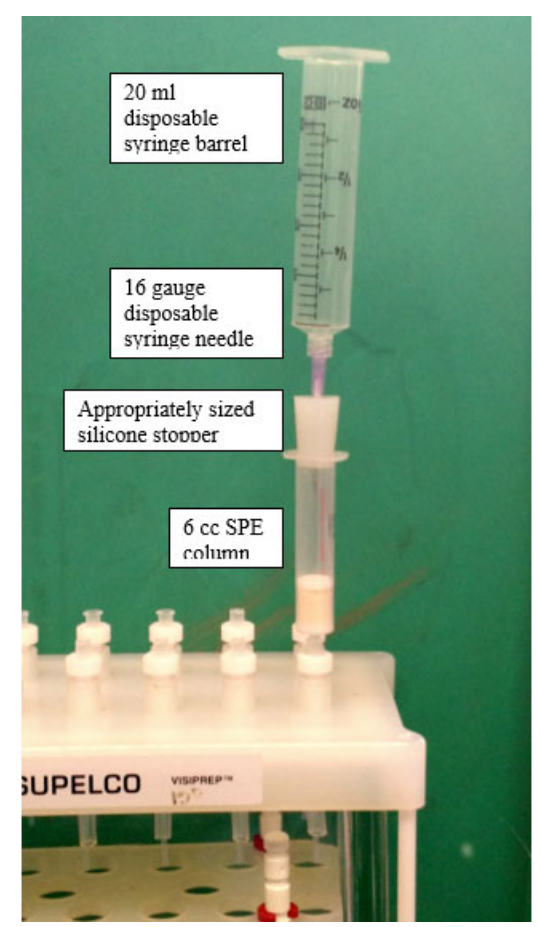
Your SPE setup will include the vacuum manifold and a vacuum line, with a large vacuum-resistant (or vacuum-rated) reservoir (several liters) for liquid waste in between.

If you have a very small volume of sample for SPE, then use the SPE tube adaptor as seen in photo below. Use whatever size disposable syringe you need to accommodate your sample volume. We have used up to 50/60 ml syringes before, although that sometimes makes accessing the valves under the SPE tubes cumbersome and there is a danger of tipping/spilling. Usually better to use something like a 20 ml syringe and just add sample in several portions.

Then follow these steps to condition the adaptor + SPE tube assembly:

1) Add 30 mL of LC/MS GRADE ACETONITRILE to the top syringe, crack the seal of the stopper to allow it to run into the SPE tube to a depth of ~1/2" and push the stopper back down (if the valve is closed the LC/MS GRADE ACETONITRILE will not drip into the glass basin). Repeat until all syringes have 30 mL of LC/MS GRADE ACETONITRILE.

- 2) Open each valve ½ turn until the LC/MS GRADE ACETONITRILE starts to drip into the basin then shut the valves and leave all closed for one minute. This is done to saturate the resin. After the minute is up, open all the valves and let gravity pull the LC/MS GRADE ACETONITRILE through the SPE tube BUT CLOSE THE VAVLES WHEN THE LC/MS GRADE ACETONITRILE REACHES THE TOP OF THE RESIN (do not allow the resin to get dry).
- 3) Now add 25 mL of NANOPURE/HIGH PURITY water to each syringe and crack the stopper seal to fill the tube with water. Next open all valves ½ turn and the gravity fed water will rinse off the LC/MS GRADE ACETONITRILE from the resin (however, it is said the LC/MS GRADE ACETONITRILE inside the resin facilitates explosives absorption).
- 4) Add another 25 mL of NANOPURE/HIGH PURITY water to the upper syringes before they run out (50 mL water rinse). Keep your eye on the remaining water and when the upper syringe is empty but the tube is full, shut the valve and remove the syringe/stopper. If the



water in the tube is low you can add more water to fill it to within $\frac{1}{4}$ " of the top, BUT NEVER LET THEM GO DRY.

LOADING THE EXPLOSIVES/DNAN ONTO THE SPE TUBES:

- 1) Remove the samples from the refrigerator the day before the procedure and allow to warm to RT.
- 2) NOTE: If you are doing quantitative analysis, add the internal recovery standard to samples now. Otherwise, you can skip this step.
 - a) Label a 2 mL HPLC vial "3-NT Recovery Std"
 - b) Add 500 μ L of NANOPURE/HIGH PURITY water and 450 μ L of LC/MS GRADE ACETONITRILE to the vial and mix.
 - c) Add 50 uL of the 20 mg/L 3-NT recovery standard to the vial (NOTE: This assumes a 1 mL final SPE extract volume. Adjust accordingly based on 50 µL per 1 mL final SPE extract volume after dry-down.)
 - d) Add 50 uL of the 20 mg/L 3-NT recovery standard to each sample bottle (AGAIN, assuming a 1 mL final SPE extract volume)
 - e) Mix each sample well.
- 3) Weigh and record the starting weight of each sample (bottle + cap + sample).

- 4) Make sure the vacuum is off and the valves under each SPE tube are closed
- 5) Connect the a new silicone stopper / FEP tubing assembly to each SPE tube. Place the other end of the tubing into the respective sample bottle.
- 6) While holding the SPE tube static, turn the knurled knob/shut off valve ½ turn to open the valve without turning the SPE tube/transfer tube. Repeat for all SPE tubes. Turn on a vacuum and attach the vacuum line from the carboy to the SPE unit WITH THE VACUUM VENT OPEN (near the vacuum line and vacuum gauge). Slowly close the vacuum vent until you suck sample from their bottles and into the SPE tube. Adjust the vacuum vent until you get the desired flow through the SPE tubes of 5-10 mL/min.
- 7) NOTE: When you get the initial sample passing through all the SPE tubes, their flow rates will differ (sometime significantly). If you have one that is markedly slower, open the SPE tube valve another ½ turn and see if it helps. If it didn't fix the problem, tighten the SPE valves to all the other tubes until they are similar to the slow one. Now adjust the vacuum vent a little (increasing the vacuum) until all tubes appear to be dripping evenly (again, target is 5-10 mL/min flow rate through the SPE tubes).
- 8) The SPE tubes will get dirty and start to drip slower (hopefully all tubes at the same rate) throughout the process. Flow can be increased by closing off the vacuum vent or opening up the SPE valves. Replace the glass microfiber filter as needed, but retain all the filter for the elution step.
- 9) After all the sample has been passed through the SPE tubes, remove the silicone stopper / FEP tubing assembly.
- 10) Open all SPE valves to one turn to create the greatest vacuum, and pull air through the tubes to dry for at least one hour.
- 11) Weigh and record the ending weight of each bottle + cap.

ELUTION OF THE EXPLOSIVES FROM THE SPE TUBES:

- 1) Replace all Teflon liners with new ones and close the SPE valves.
- 2) Position the precleaned glass tubes in the rack in the SPE manifold.
- 3) Attach the now dry SPE tubes to the unit and pack in any glass microfiber filters used to trap solids.
- 4) Add 6 mL of LC/MS GRADE ACETONITRILE to all tubes. Open the SPE valves ½ turn to allow gravity to saturate the resin with LC/MS GRADE ACETONITRILE (occasionally you will need to pull a little vacuum to get the LC/MS GRADE ACETONITRILE started) then shut the SPE valves for one minute. Open the SPE valves 1 turn and allow the LC/MS GRADE ACETONITRILE to pass through the SPE tubes and into the test tubes.
- 5) Just before the first 6 mL runs out add 6 mL more to each tube (DO NOT LET THE RESIN GO DRY), for a total of 12 ml.

6) After all the LC/MS GRADE ACETONITRILE has stopped dripping, gradually open the vacuum . As the tubes slow their dripping, increase the vacuum (but no more than 20" Hg).

CONCENTRATION OF THE SPE EXTRACT (this refers to the Visi-Dry process; ignore if you do some other process):

- 1) Carefully transfer the full test tubes from the SPE unit to a temporary rack and set aside.
- 2) Remove the SPE manifold cover and replace with the drying attachment.
- 3) Place the test tubes into the drying unit and start the flow of nitrogen. We actually pass the nitrogen through a coil immersed in almost boiling water to warm it up and enhance the solvent evaporation.
- 4) Watch the volumed in each tube carefully. When the bottom of the extract meniscus gets near to the 1 mL mark on the test tube (hopefully its less than 1 mL), use a 2 mL sterile, individually wrapped, glass pipette to SLOWLY pull the sample from the tube. Transfer the extract to a 2 mL screw cap sample vial.

Phenomenex Strata X-A SPE protocol for NTO

6 cc column
500 mg packing P/N 8B-S123-HCH
https://www.phenomenex.com/products/part/8b-s123-hch?fsr=1

NOTE: Here were our NTO recoveries in different matrices. Best recovery appeared to be in "clean" water/low salt background. Low pH should be neutralized base or buffer, but not too high overall salt molarity in final solution (e.g., do what it takes to get to pH 6-7, but don't overbuffer).

		SPE	SPE
	рН	%Capture	%Recovery
A NanoPure Water	3.6	100	79
B Acidified & Neutralized PO4 Buffer	7.1	78	62
C Acidified & Neutralized NaOH	7.1	98	78
D Artificial Groundwater (AGW)	4.6	100	80
E 1/10 Basal Salts Medium (BSM)	7.0	100	90
F Methanotroph Medium (MM)	5.7	99	79

NOTES:

Solution B - dropped to pH 2.1 with 1:1 HCl (=17%), then neutralized with 6 N phosphate buffer

Solution B SPE %Recovery increased to 79% when adjusting for the lower %Capture, e.g. there was less to recover.

Solution C - dropped to pH 2.1 with 1:1 HCl (=17%), then neutralized with 1/200 BSM P-Buffer + 5 N NaOH

1. Conditioning

- a. 2 x 5 mL LC/MS grade methanol (allow first aliquot to mostly drain before adding second)
- b. 2 x 5 mL NanoPure water (allow first aliquot to mostly drain before adding second)

2. Loading

a. Pass sample thru SPE tube to allow flow at approx. 10 mL/min, under vacuum. Smaller volume samples can be done using the SPE adapter setup.

NOTE: On initial testing, you may want to collect the "waste" effluent from the SPE tubes in clean glass containers and then analyze it to make sure the NTO is being effectively capture by the SPE process. In other words, place glass bottles/vials under the SPE tubes to collected the effluent, rather than just allowing it to go to the waste reservoir.

Once you have shown that NTO is captured well from a given matrix, then further samples can be processed without collecting the waste effluent.

3. Dry under vacuum minimum 10 minutes

4. Elution

a. 10 mL 2% (v:v) hydrochloric acid (HCl) in LC/MS grade methanol
 Make by diluting the ~37% concentrated HCl solution accordingly
 54 mL 37% HCl + 946 mL LC/MS MeOH = 1 L of 2% HCl MeOH
 108 mL "" + 1892 mL ""

NOTE: On initial testing, you may want to collect the first 10 mL elution, then do a second 10 mL elution with the same solution to make sure the NTO is being effectively recovered from the SPE packing. In other words, do 2 elutions for each SPE tube, <u>Make</u> sure the resin does not dry out between the two elution steps.

Once you have shown that NTO is recovered well, then further samples can be processed only a single elution.

5. Concentration

- a. Evaporate solvent to ~1 mL under warm nitrogen gas
- b. Transfer to a clean HPLC via a clean glass pipet.